



Process-based modelling of the St Lucia Estuary

*Morphodynamic response of the inlet due to dredge spoil removal and
re-linkage of Mfolozi River*

Master of Science Thesis

J. Hoek

Delft, October 2017

Process-based modelling of the St Lucia Estuary

*Morphodynamic response of the inlet due to dredge spoil removal and
re-linkage of Mfolozi River*

By
Jordi Hoek

in partial fulfilment of the requirements for the degree of
Master of Science
in Hydraulic Engineering

at the Delft University of Technology,
to be defended publicly November 6th, 2017 at 16.00

In cooperation with Deltares (Delft, the Netherlands) and the University of KwaZulu-Natal (Durban,
South Africa)

Graduation committee:

Prof. Dr. Ir. S.G.J. Aarninkhof (Technical University Delft)
Dr. Ir. D.J.R. Walstra (Technical University Delft and Deltares)
Ir. A.P. Luijendijk (Technical University Delft and Deltares)
Dr. Ir. B.C. van Prooijen (Technical University Delft)
Prof. Dr. Ir. D. Stretch (University of KwaZulu-Natal)

Picture on the front-page was taken in Maphelane, South Africa by Jordi Hoek. ©all rights reserved.



Preface

This thesis is my graduation work for the Master of Science in hydraulic engineering at the Technical University of Delft. It is the final part at which my student life comes to an end. In this chapter I would like to thank several people who made it possible for me to write this thesis.

First of all I would like to thank my graduation committee from TU Delft: Prof. Stefan Aarninkhof, Dirk-Jan Walstra, Arjen Luijendijk and Bram van Prooijen. Our meetings were very helpful for my progress and brought up many new ideas. I am very thankful for the flexibility I have been given, which made it possible to do a lot of my work in South Africa. Special thanks to Dirk-Jan Walstra who was my daily supervisor and helped me at defining my graduation topic. Dirk-Jan made it possible to work at Deltares, which was of real help and meeting so many other graduate students. Thanks to Arjen Luijendijk who was available for great support with the modelling in Delft3D.

Spending five months in South Africa was a wonderful experience within my research. I would like to thank Prof. Derek Stretch, Katrin Tirok, Ooma Chetty and Aline Cotel for the warm welcome and unconditional support in Durban. I got to visit the iSimangaliso Wetland Park and St Lucia Estuary which are truly magnificent. I want to thank Bronwyn James and Mike Udal for giving me information about the GEF-project and showing me the construction site.

Thanks to all graduate students at Deltares for the nice coffee breaks and discussions about our graduation work. The discussions gave insight and new ideas for my thesis.

Last, but not least, I would like to thank my family. My parents and brother who supported me during my graduating time and have always motivated me.

Jordi Hoek

Delft, 25th of October 2017

Abstract

The St Lucia Estuary is Africa's largest estuarine system and part of the iSimangaliso Wetland Park, which was listed as South Africa's first World Heritage Site in December 1999. The St Lucia Estuary is connected upstream to Lake St Lucia and downstream it flows into the Indian Ocean. The St Lucia Estuary is located at a wave dominated coast and experiences a micro-tidal regime. Along the coast of South Africa about 70% of the estuaries do not have a permanently open link to the sea, i.e. they are temporarily open/closed estuaries (TOCEs). TOCEs are mainly regulated by the amount of river flow entering the estuary. The connection to the Indian Ocean is of vital importance for the St Lucia Lakes as many marine species use the estuary as breeding ground and migrate between the estuary and ocean. Anthropogenic impacts and fresh water reductions have altered the natural system. The mouth of the St Lucia Estuary is unstable and has been closed for longer periods in the last century. The closure of the mouth is mainly caused by human interventions. Separating the Mfolozi River in the 1950's from the St Lucia Estuary has altered the system the most. The drought period ranging from 2002 has drastically affected the St Lucia System as a whole with the desiccation of 90% of the lakes, reaching the all-time low. The management authorities had to take action and research supported by the Global Environment Facility (GEF) which started in 2009 showed re-linkage of the Mfolozi River is the preferred solution to bring fresh water to the St Lucia System.

This MSc study was initiated to investigate the effects of re-linkage of the Mfolozi River and dredge spoil removal from the estuary on the tidal inlet. The main focus is on the closure times of the inlet, the transition between an open – and closed inlet, and the multi-year morphological development of the inlet. Two different scenarios, before – and after removal of the dredge spoil, are simulated in the process-based model Delft3D. In both scenarios the river discharge from the Mfolozi River is varied from 0 to 30 m³/s. The model is forced with a reduced wave climate and simulated during neap –, mean –, and spring tidal range.

The computed morphological development at the inlet shows similar behaviour as observed. Model calibration is done quantitatively on hydrodynamics and qualitatively regarding morphodynamics. In the initial situation without river discharge the inlet closes after 156 and 22 days while forced continuously with mean – and neap tidal range respectively. In March 2007 the inlet breached by Cyclone Gamede and closed naturally after 175 days during a neap tide.

The results from the scenarios are studied regarding morphological development, empirical relationships from Bruun (P/M ratio) and O'Brien (A-P Relationship), closure times and cross-sectional evolution of the inlet. The morphological development of the inlet does not show significant changes after and before removal of the dredge spoil. Three main types of morphological behaviour are observed in the model (Figure a.1); (1) a locationally stable and intermittently closing inlet, (2) a migrating inlet in northern direction due to spit formation at the updrift side and erosion at the downdrift side of the inlet, and (3) migration of the inlet in southern direction due to deposition of river sediments and increased ebb flows causing erosion at the updrift side and accretion at the downdrift side. Generally an increase in tidal range changes the behaviour from 1 to 2 and an increase in river flow changes the behaviour from 2 to 3. According to Duong (2015) inlets can be classified as unstable, intermittently closing or migrating, when P/M ratios are below 10. The model results correspond to literature and the St Lucia inlet behaves as an unstable inlet.

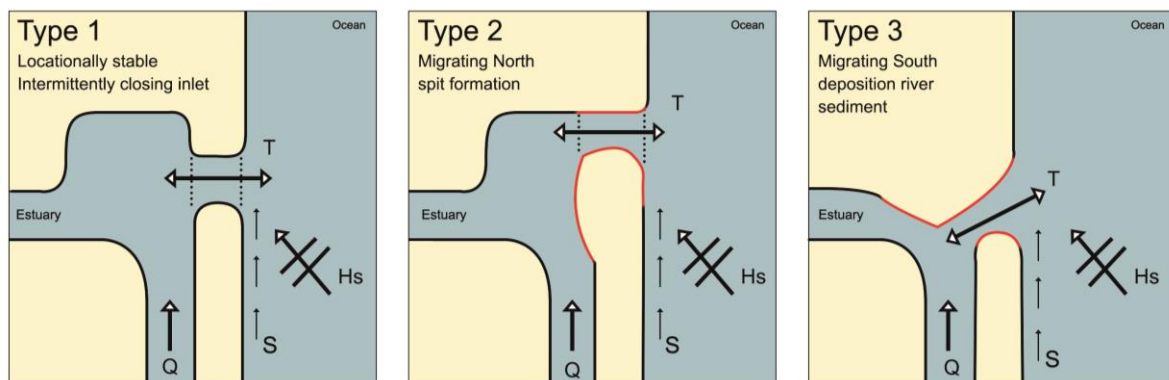


Figure a.1: Types of morphological behaviour inlet; type 1 occurs during low tidal ranges and no river discharge, type 2 occurs with increased tidal flows and type 3 with increased river discharge

An analysis of the A-P Relationship by O'Brien shows the system is closer to stable equilibrium after re-linkage of the Mfolozi River. Removal of the dredge spoil from the St Lucia Estuary does not create a stable system. The closure times of the inlet do not change significantly due to the dredge spoil removal and are almost the same as in previous scenario, after re-linkage of the Mfolozi River. However, the river discharge from the Mfolozi River has a large effect; reducing the closure times from 50% with no river flow to 11%, 6% and 3% during the winter – ($2 \text{ m}^3/\text{s}$), drought – ($5 \text{ m}^3/\text{s}$) and summer period ($14 \text{ m}^3/\text{s}$) respectively. The cross-sectional evolution of the inlet shows no exact transition point of inlet closure, but a clear trend is visible in all scenarios. During low wave action the cross-sectional area of the inlet decreases slightly. The smaller waves lead to a net onshore sediment transport in cross-shore direction. High wave action causes an increase in longshore sediment transport and spit formation, which results in closure of the inlet in several occasions. In case the inlet remains open the larger waves erode the coast and lead to widening of the inlet. After re-linkage of the Mfolozi River the inlet remains flood dominant; during the winter and drought period the flood flows are higher than the ebb flows. In the summer period the flood flows are approximately equal to the ebb flows. Simulations with the mean annual runoff ($30 \text{ m}^3/\text{s}$) result in higher ebb flows than flood flows. This shows the inlet is only dominated by ebb flows during river floods. Hinwood et al. (2012) analysed tidal estuaries to investigate dominance of tidal and fluvial flows. The average size of the cross-sectional area from the computed St Lucia inlet, ranging from 60 to 270 m^2 , indicates dominance by tidal flows. The river flow is very important in maintaining an open inlet; however tidal flows dominate the morphological development of the inlet.

The results from this study show re-linkage of the Mfolozi River lead to an inlet that remains open for majority of the time leading to a connection between the St Lucia Estuary and the Indian Ocean. This can make the St Lucia Estuary and Lake System a breeding ground for many marine species as it was before. The removal of dredge spoil however does not seem to be very effective. The closure times of the inlet barely change and the inlet re-imports most of the sediments. It is advised to limit the amount of dredge spoil removal, because the estuary will return to its equilibrium state.

Contents

1	Introduction	1
1.1	Rationale of study	1
1.2	Research questions	3
1.3	Approach	4
1.3.1	Literature study	4
1.3.2	Wave climate reduction	4
1.3.3	Setup and calibration of Delft3D model	4
1.3.4	Analyse and compare results from scenarios	4
1.4	Thesis outline	4
2	St Lucia Estuary	7
2.1	Area description	7
2.2	Flow regimes	7
2.3	Historic overview	8
2.4	Present stage	10
2.5	Hydrodynamics	13
2.5.1	Tide	13
2.5.2	Waves	15
2.5.3	Rivers	17
2.6	Sediment transport	19
2.7	Tidal inlet theory	21
2.7.1	Inlet stability	21
2.7.2	Empirical relationships determining inlet stability	23
2.7.3	Previous modelling	25
2.8	Conclusion	26
3	Methodology	27
3.1	Scenarios	27
3.2	Delft3D Model	28
3.2.1	Grid & Bathymetry	28
3.2.2	Flow module	29
3.2.3	Wave module	30
3.3	Wave climate reduction	31
4	Calibration	35

4.1	Tidal forcing only.....	35
4.2	Time-varying wave climate	38
4.2.1	Mean tidal range	38
4.2.2	Neap tidal range.....	40
4.2.3	Spring tidal range	42
4.3	Conclusions	43
5	Results.....	45
5.1	Scenario A: Re-linkage Mfolozi River	45
5.1.1	Mfolozi River with discharge of 2 m ³ /s (Winter)	45
5.1.2	Mfolozi River with discharge of 5 m ³ /s (Drought)	50
5.1.3	Mfolozi River with discharge of 14 m ³ /s (Summer)	54
5.1.4	Mfolozi River with discharge of 30 m ³ /s (Mean Annual Runoff)	59
5.2	Analysis scenario A.....	64
5.2.1	Morphological development.....	64
5.2.2	Closure times	64
5.2.3	A-P Relationship	66
5.2.4	Wave dominant system	67
5.3	Scenario B: Dredge spoil removal	68
5.3.1	Future state, Q = 0 m ³ /s (No river flow).....	68
5.3.2	Future state, Q = 2 m ³ /s (Winter)	74
5.3.3	Future state, Q = 5 m ³ /s (Drought)	79
5.3.4	Future state, Q = 14 m ³ /s (Summer).....	83
5.3.5	Future state, Q = 30 m ³ /s (MAR).....	88
5.4	Analysis scenario B.....	93
5.4.1	Morphological development.....	93
5.4.2	Closure times	94
5.4.3	A-P Relationship	95
6	Discussion.....	97
6.1	Delft3D model setup	97
6.2	Forcing of the model.....	97
6.2.1	Wave climate	97
6.2.2	River flow	97
6.3	Process-based model	98
7	Conclusion.....	101

7.1	Closure time of the inlet	101
7.2	Exact transition point inlet.....	102
7.3	Morphological development	102
7.4	Wave dominated system	103
8	Recommendations	105
8.1	Further research	105
8.2	Suggestion management	105
	Bibliography	107

Appendix

A.	Theoretical background	2
B.	Wave climate reduction	6
C.	Calibration	10
D.	Results	14
E.	Photos site visit St Lucia Estuary	15
F.	List of symbols	17

1 Introduction

1.1 Rationale of study

Around the world there are many different kinds of coastal systems. All of these coastal systems behave differently and are governed by different processes. Tidal inlets are one of these coastal systems. A tidal inlet is an opening in the shoreline that provides a connection between the ocean and tidal creeks, bays or lagoons. This thesis is focused on the St Lucia Estuary in South Africa, located in the South African province KwaZulu-Natal approximately 230 kilometres north from the city Durban. The St Lucia Estuary is connected upstream to Lake St Lucia and downstream it flows into the Indian Ocean. It is Africa's largest estuarine system and part of the iSimangaliso Wetland Park, which was listed as South Africa's first World Heritage Site in December 1999. The location of the study is given in Figure 1.2 on the next page.

The St Lucia Estuary is a very dynamic system and has been subject to many changes in the past. Over the past century fresh water reductions and anthropogenic impacts have altered the natural functioning of the system (Lawrie & Stretch, 2011a). The mouth of the St Lucia Estuary is unstable and has been closed for longer periods in the last century. The closure of the mouth is mainly caused by human interventions. Separating the Mfolozi River in the 1950's from the St Lucia Estuary has altered the system the most. The Mfolozi River is the largest of the five main rivers entering the system and accounts for 60% of the freshwater inflows into Lake St Lucia's system.

During the period from 2002 until 2012 the riverine flow from the other four catchment areas was limited and there was almost no inflow from the ocean due to the closure of the mouth. The severe drought caused extreme saline conditions in the lake that harmed the fauna and flora and led to temporary disappearance of more than 90% of St Lucia's water area (Whitfield & Taylor, 2009). The desiccation of the St Lucia System is clearly visible in Figure 1.1. In 2009 the iSimangaliso Wetland Park Authority received a grant of 9,000,000 USD from the Global Environment Facility (GEF). The GEF project was initiated to bring fresh water into the St Lucia System. To prevent further damage it was agreed that the Mfolozi River should join the St Lucia Estuary once again, like in the period before 1952 when there was a combined mouth in a natural state. The dredge spoil which has been dumped between the St Lucia inlet and the Mfolozi River over a timespan of 40 years is removed in order to enhance flows from the Mfolozi River to the St Lucia Lakes.



Figure 1.1: Effects of drought in St Lucia South Lake (Times Live, 2016)

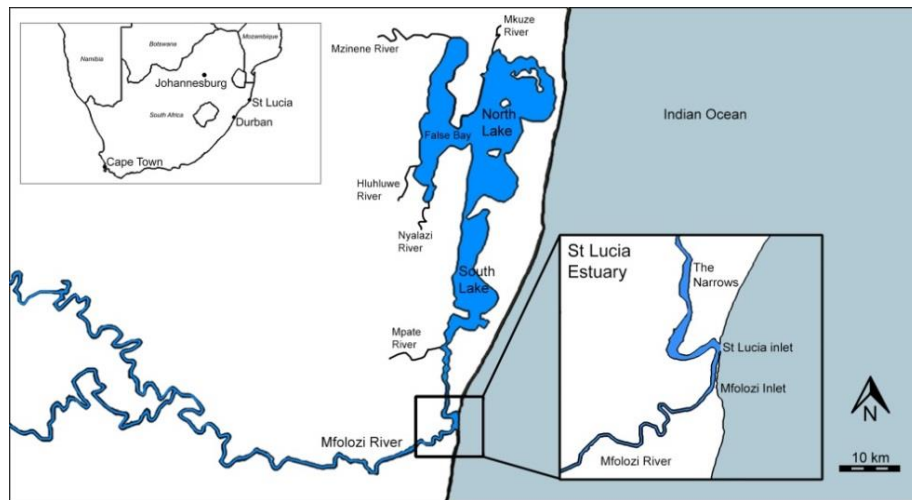


Figure 1.2: Location study area: St Lucia Estuary

The current remediation works are done in order to create a natural system that was present before the human interventions in the 1950's. In the past human interventions caused dramatic changes to the system. In order to restore the St Lucia Estuary, so it can live up to its potentials as the first World Heritage site from South Africa, management of the system had to change. Re-linkage of the Mfolozi River and removal of the dredge spoil will re-create the natural system. With a natural system it is meant that no interventions are made to the system; e.g. breaching of the mouth, maintaining certain water levels, dredging of the inlet, etc.

A better understanding of the physical processes at the mouth will improve future management decisions that need to be taken. The effects of re-linkage of the Mfolozi River and the dredge spoil removal on the St Lucia inlet have not been investigated yet. The connection to the Indian Ocean is of vital importance for the St Lucia Lakes as many marine species use the estuary as breeding ground and migrate between the estuary and ocean. Determining the closure time and transition between an open/closed inlet will give more insight into the inlet stability and the future development of the St Lucia Estuary. The closure times of the different interventions, re-linkage of the Mfolozi River and removal of the dredge spoil, are investigated. The transition point at which the St Lucia inlet will close or stay open will be studied. Several empirical relationships are found in literature, which describe the stability of inlets. In this thesis the Escoffier diagram, the ratio by Bruun and the A-P relationship are used.

The process-based model Delft3D is used to model the morphological development of the St Lucia inlet. The South African coast is highly energetic with relatively high wave action resulting in temporarily open/closed estuaries. Delft3D is able to simulate the wave forcing which leads to more accurate results compared to the empirical relationships. The highly energetic wave climate along the coast causes a flood dominant behaviour in most estuaries. The previous closures of the St Lucia inlet indicate this behaviour. River flow enhances ebb dominance and re-linkage of the Mfolozi River will decrease the flood dominant behaviour of the system. The relative importance of the Mfolozi River is investigated with respect to tidal or fluvial dominance of the inlet.

1.2 Research questions

The main objective is to investigate the effects of relinking the Mfolozi River and removal of the dredge spoil on the inlet. This leads to the main research question: what is the effect of re-linking the Mfolozi River and removal of the dredge spoil on the morphodynamic behaviour of the inlet?

The main research objective will be addressed by answering the following sub-questions:

1. What is the influence of the different interventions on the closure times of the inlet?
2. What is the exact transition point at which the St Lucia mouth will close or stay open?
3. Is there a significant change in morphological development after removal of the dredge spoil compared to the initial situation?
4. Is the inlet after re-linkage of the Mfolozi River dominated by tidal or fluvial flows?

Sub-question 1: Closure time of the inlet The St Lucia inlet is a vital connection between the Indian Ocean and the St Lucia Lake System. First of all it is important as many species use the estuary as breeding ground and migrate between the estuary and ocean. Secondly, the inflow of water from the ocean decreases the chance of desiccation of the lakes. In this report the effect of re-linkage of the Mfolozi River and the dredge spoil removal is investigated. With respect to the closure times of the inlet it is expected that both measures have a positive effect on the closure times. The river flow causes higher velocities through the inlet channel; leading to a more stable inlet that closes less often. The removal of the dredge spoil increases the tidal prism, causing the flow velocities through the inlet to increase as well. Both of the interventions will be compared with the existing situation, before any interventions is made.

Sub-question 2: Exact transition point inlet The inlet is a complex part of an estuarine system. It is investigated if there is a specific location at which the St Lucia inlet will close. The cross-sectional area is influenced by many specific parameters such as significant wave height, river flow, longshore sediment transport, cross-shore sediment transport, tidal range, etc. Empirical relationships by Escoffier, Bruun and O'Brien are used to investigate the stability of the inlet.

Sub-question 3: Morphological development The removal of dredge spoil in the St Lucia Estuary is a large remediation project where 1,300,000 m³ of sediments are removed from the estuary. The previous closures of the St Lucia inlet indicate the flood dominant behaviour of the estuarine system. The South African coast is highly energetic and wave action is relatively high resulting in temporarily open/closed estuaries. The dredge spoil removal increases tidal prism and area of the estuary which influences the opening times of the inlet. It is investigated if the removal of dredge spoil results in an inlet that has a stable equilibrium, which results in longer opening times of the mouth and does not re-import all sediments that are removed due to its flood dominant character. The process-based program Delft3D is used to simulate the wave forcing which is not taken into account by empirical relationships.

Sub-question 4: Wave dominated system The morphological development of an estuary depends on the local wave – tidal climate. Previous research has shown the St Lucia Estuary has a flood dominant character due to the high wave action present along the South African coast. Deltas can be distinguished between river-dominated, tide-dominated and wave dominated. In this report it is investigated if the inlet is dominated by tidal flows or fluvial flows.

1.3 Approach

In this section the approach for this thesis is explained. The methodology is used to answer the research questions. The following research activities are part of the methodology:

1. Literature study
2. Wave climate reduction
3. Setup and calibration of Delft3D model
4. Analyse and compare scenarios from Delft3D

1.3.1 Literature study

The St Lucia System is analysed. In order to understand the reason behind the desiccation of the lakes the major anthropogenic interventions are studied in a historical overview. The hydrological and morphological properties of the estuary are investigated which will be used to calibrate the model. The possible closure mechanisms of inlets are studied, which is used to evaluate the qualitative behaviour when calibrating the model. Finally several empirical relationships regarding inlet stability are explained, which will be used when comparing results from the Delft3D simulations.

1.3.2 Wave climate reduction

The wave climate of KwaZulu-Natal is analysed in order to reduce the wave climate. Wave recordings from Richards Bay are used to create bivariate histograms for the significant wave height and period. This data is used to create a reduced wave climate consisting of 10 wave conditions which have equal contribution to the total longshore sediment transport. The reduced wave climate is used as wave forcing in Delft3D.

1.3.3 Setup and calibration of Delft3D model

The process-based model Delft3D is used in order to simulate the behaviour of the St Lucia inlet. Delft3D consists of several modules of which Delft3D-Flow, Delft3D-Wave and Delft3D-Mor are used in this model. The St Lucia Estuary is a complex estuarine system, which means the setup of the model is important. The purpose of calibrating the model is to represent features observed in reality as best as possible. The model has to work properly before other scenarios are simulated. The model is calibrated quantitatively on tidal prism and longshore sediment transport. The model is calibrated qualitatively in cross-shore direction in order to maintain an equilibrium beach width.

1.3.4 Analyse and compare results from scenarios

Several scenarios are simulated in Delft3D in order to answer the research questions. The morphological development from the St Lucia inlet will be studied due to re-linkage of the Mfolozi River and removal of the dredge spoil. The closure times of the inlet are investigated and the cross-sectional area of the inlet over time is studied. A comparison with empirical relationships from literature is made in order to validate the results. The results and observations from the simulations are used to give answer to the research questions.

1.4 Thesis outline

In chapter 2 an analysis of the St Lucia System is made. A description of the area is given, major anthropogenic interventions are described and the hydrological and morphological properties of the estuary are analysed. The methodology is explained in chapter 3. The wave climate is investigated and a reduced wave climate for the St Lucia coast is made. The reduced wave climate consists of 10

wave conditions and is derived from bins with approximately equal weight. The parameters used in Delft3D are explained in chapter 3. The calibration of the model is given in chapter 4. The initial scenario, before any interventions, is calibrated in this chapter. The model is calibrated on longshore sediment transport, cross-shore sediment transport, migration of the inlet, peak flows through the inlet and the tidal prism. In chapter 5 the results of the scenarios are given and analysed. In chapter 6 the results and setup of the model are discussed. The main findings and conclusion of the research are listed in chapter 7. Finally, recommendations are given in chapter 8 about possible further research of the St Lucia Estuary and advice regarding future management of the system.

2 St Lucia Estuary

2.1 Area description

The St Lucia Estuary is part of a larger system, the iSimangaliso Wetland Park, and it is the largest estuarine system of Africa. At the north side the estuary is connected to the St Lucia Lakes with the Narrows, a 20 km long very shallow tidal channel of approximately 1 m deep. Downstream the estuary is connected to the Indian Ocean with the presence of an open inlet. The St Lucia Lake has five catchment areas, namely, the Mfolozi, Mzinene, Hluhluwe, Nyalazi and Mkhuze rivers. From these areas the Mfolozi River contributes the largest freshwater inflow into the system. The St Lucia inlet is situated at 28° 38' South 32° 42' East.

As mentioned before the St Lucia system is part of the iSimangaliso Wetland Park. The name iSimangaliso translates to miracle and wonder and originates from Zulu, which describes the uniqueness of this site. The St Lucia Estuary was ranked 5th out of South Africa's 250 estuaries regarding their size, type and biogeographical zone, habitats and biota (Turpie, et al., 2002). The St Lucia estuarine system accounts for 60% of South Africa's total estuarine area and over 80% of the estuarine area of the southern African sub-tropical region. It is one of the most important nursery ground for juvenile marine fish and prawns along the east coast.

2.2 Flow regimes

The flow regime in the St Lucia Estuary depends on multiple factors. It is mainly influenced by the discharge from the Mfolozi River, discharge from the Lakes and the state of the mouth, whether it is open or closed. Four different states can be recognized in the system:

- a) A closed mouth state with the presence of higher water levels in the Mfolozi River compared to the St Lucia Estuary. This will lead to water flowing from the Mfolozi River into the St Lucia Estuary and further northwards to the Lakes.
- b) A closed mouth combined with a water level in the Mfolozi River and St Lucia Estuary that is similar. This state will lead to rising water levels which backs up into adjacent land until the inlet breaches.
- c) An open mouth combined with higher water level in the Mfolozi River compared to the St Lucia Estuary. In this state the river flow from the Mfolozi River will be split into two different directions; part of the discharge will flow northwards to the Lakes and part will divert into the sea.
- d) An open mouth with the presence of similar water levels in the Mfolozi River and the St Lucia Estuary. In this final state both water discharge from St Lucia Estuary and the Mfolozi River enter the sea directly.

In Figure 2.1 the four different flow regimes are given. The flow regimes can change from one state to another. For example, when water levels in St Lucia Estuary are low and the inlet is closed water from the Mfolozi River will flow in northern direction to the Lakes (state a). Once water levels have reached a certain limit the discharge from the Mfolozi River to the St Lucia Lakes will decrease and water backs up into adjacent land (state b). This will continue until the inlet breaches and in this state water will flow into the sea from both the Mfolozi River and the St Lucia Estuary (state d).

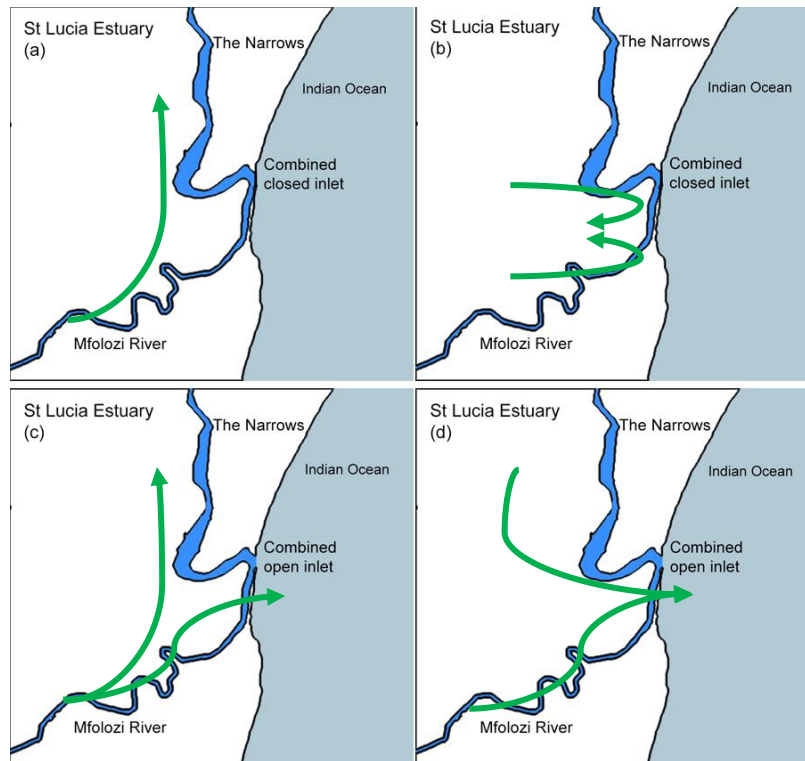


Figure 2.1: Flow regimes St Lucia Estuary: (a) closed inlet and low lake water levels, (b) closed inlet and backing-up of water into adjacent land, (c) open inlet combined with high river discharge from Mfolozi River, (d) open inlet combined with both river discharge from St Lucia Lakes and Mfolozi River

2.3 Historic overview

The St Lucia estuarine lake has gone through many changes in the last century. Over the years park authorities changed and so did their policy on the iSimangaliso Wetland Park. In this paragraph the main stages of the St Lucia Estuary are given.

Before 1952 the system was in a natural state. The Mfolozi River and St Lucia Estuary had a combined inlet. During this period the mouth was open during the majority of the time and there was no active control. During wet periods when fresh water inflow from the rivers was maximal, most of the discharge from the Mfolozi River entered St Lucia Bay and then passed out to the sea on ebb tide. With the start of a dry period the mouth would tend to close and the Mfolozi River was diverted into the St Lucia system. Freshwater inputs replaced most of the water lost by evaporation and the probability of occurrence of extreme hypersalinity in the system was low (Taylor, 1993). At the end of a drought period river flows would increase and water levels would gradually rise and backup into adjacent swamps. The berm that had formed across the St Lucia mouth would breach when the water levels reached approximately 3 to 3.5 m above mean sea level (Huizinga & Niekerk, 2005).

Around the 1920s sugar cane farming started in the Mfolozi floodplain and wetlands. To prevent the farmland from flooding parts of the Mfolozi River and surrounding streams were excavated and canals were constructed. This resulted in higher flow velocities and higher sediment budgets in the river. Without these interventions this area used to behave as a buffer layer, capturing sediment and releasing relatively sediment-free water downstream of the swamps. In the drought of the 1950s the

whole mouth area became silted up, completely blocking both the St Lucia and Mfolozi systems from the sea. To prevent farmland from flooding by backing-up Mfolozi River water a canal was dredged to discharge river water into the ocean (Kriel, 1966).

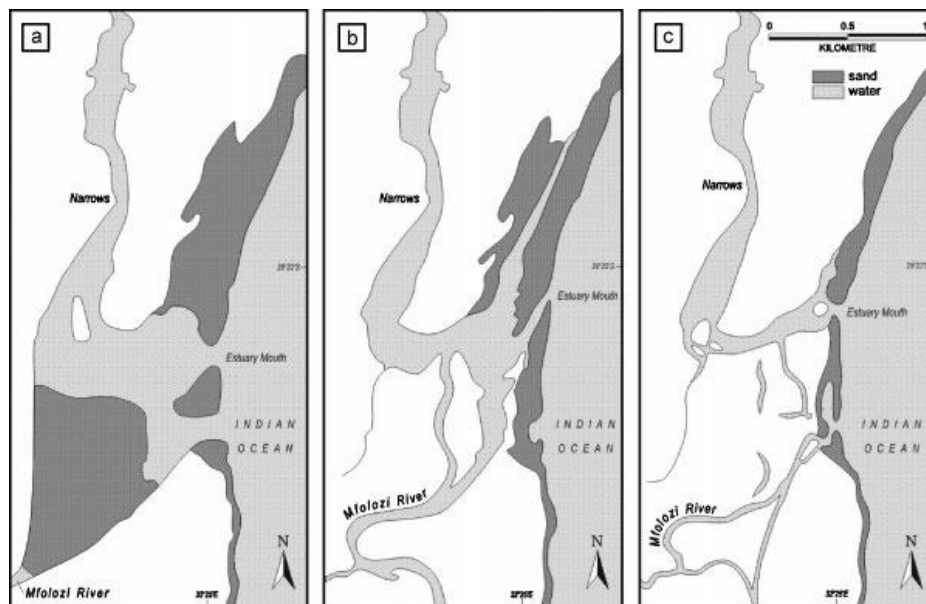


Figure 2.2: Configuration of the St Lucia mouth region in (a) 1883/4 (modified from Metheven, (b) 1937 and (c) 1966 (source aerial photography; Chief Directorate Surveys and Mapping, South-Africa) (Whitfield & Taylor, 2009)

The authorities opted for a different policy after recognizing the threat of siltation in the mouth and decided to separate the Mfolozi River from the St Lucia Estuary. During the period from 1952 until 2002 the policy changed to active manipulation of the system with two separate mouths continuously open, as a consequence a continuous dredging programme was established. In

Figure 2.2 the change in configuration of the St Lucia mouth is visible from the period 1883 until 1966. At the banks of the St Lucia mouth hard structures were constructed in order to stabilize the mouth. The desired effects of self-scouring were not achieved and the mouth closed during every dry period. In 1984 all of these structures, together with the dredger, were washed away by Cyclone Domoina and were never replaced (Heerden & Swart, 1986).

In the past many droughts have been recorded and can last for many years. The drought from 1967 to 1972 was particularly long and severe. At the start of this drought the St Lucia mouth closed, but according to the policy it was artificially dredged open. During most of this period all rivers entering St Lucia stopped flowing and water lost from the surface area through evaporation was replaced by seawater inflow. The seawater was likely to carry a high content of sediments and caused sedimentation in the lower regions of the estuary. Evaporation and the constant inflow of seawater led to an increase in salinity. This caused severe damage to the system; shoreline vegetation was killed causing extensive erosion, animals had difficulties finding drinking water and food (Whitfield & Taylor, 2009). The most recent drought occurred from 2001 until 2012. To prevent extreme salinity conditions as in the drought from 1967 to 1972 the management policy changed. The decision was taken not to actively manipulate the St Lucia mouth. At the start of this drought period the mouth closed and the rivers entering St Lucia were dry for most of this time. The salinity levels were less

compared to the severe drought in the 1970s which was mainly because of the closed mouth. However, during 2005 and 2006 the condition of the lake has become worse with less than 10% of the normal lake water area being present in July 2006 (Whitfield & Taylor, 2009). In March 2007 the mouth was breached by Cyclone Gamede, which allowed sea water to enter the St Lucia system for a period of 175 days before the mouth closed naturally. The inflow of salt sea water caused salinity levels to rise significantly and made the system more vulnerable to future droughts.



Figure 2.3: Photo of the Mfolozi River and St Lucia mouth region showing main management interventions: (a) weak link at Mfolozi Mouth and Indian Ocean, (b) back channel and (c) construction wall (Whitfield & Taylor, 2009)

As the drought continued the park authorities decided different measures were necessary to prevent further degradation of St Lucia. The interventions are given in Figure 2.3. The intervention existed of (a) a weak link at the Mfolozi Mouth and Indian Ocean in order to release pressure during floods. At (b) a back channel was created from the Mfolozi River into the St Lucia Estuary. This channel diverts Mfolozi winter low-flows into the St Lucia Estuary. During low flows the river contains less sediment. Last part of this measure was the construction of a wall (c) to prevent Mfolozi River from moving into St Lucia Estuary.

The construction of the back channel has proven to be effective and authorities are satisfied with current results. The inflow from the fresh water through the back channel has showed the importance of Mfolozi River. The Mfolozi Mouth effectively closed after this intervention was applied and salinity levels declined in the St Lucia Estuary. However, the limited inflow did not prevent occurrence of hypersalinity in the Lakes.

2.4 Present stage

Due to the severe drought periods and anthropogenic effects that led to desiccation of 90% of the Lakes it was necessary to find a solution to bring fresh water into the St Lucia System. In 2009 the iSimangaliso Wetland Park Authority has been awarded a Grant of 9,000,000 USD from the Global Environment Facility through the World Bank. The GEF project, P086528, is named: "Development, empowerment and conservation in the iSimangaliso Wetland Park (Greater St Lucia) and surrounding region". Part of this grant is used for consulting services, under the iSimangaliso GEF Project Component 1, to study: 'Analysis of alternatives to determine the most feasible solution to the hydrological issues of the Lake St Lucia estuarine system.'

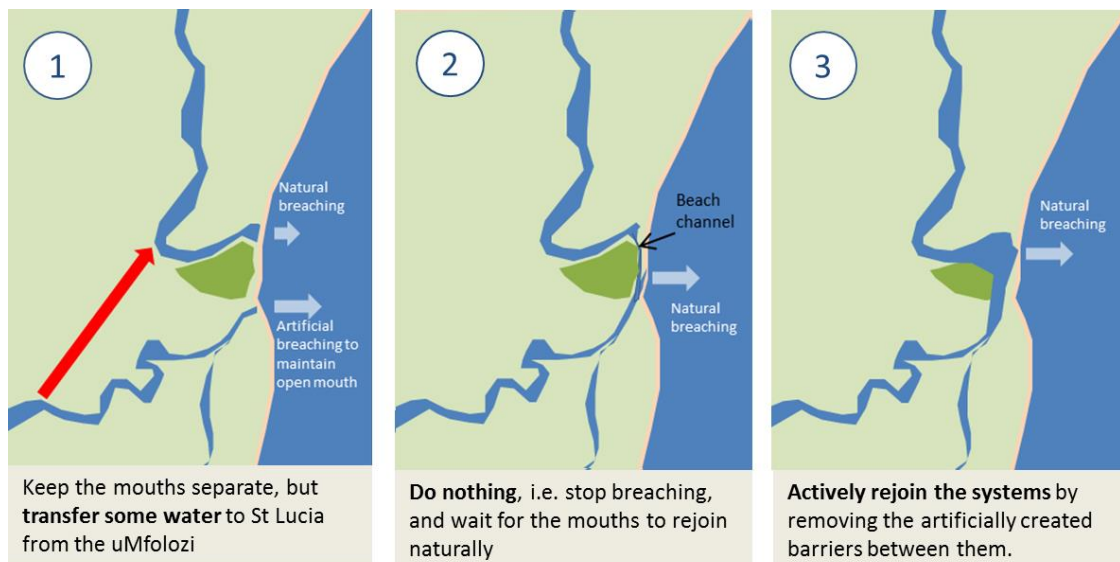


Figure 2.4: Schematic diagram of the three options considered in this study to restore the hydrodynamic functioning of the system (Clark, et al., 2014)

Four different management scenarios have been modelled in order to determine the most feasible solution (Clark, et al., 2014). The process based model MIKE21 developed by IHE has been used for these simulations. The simulations focussed on bringing fresh water into the St Lucia System. The first three scenarios are visible in Figure 2.4.

- “Separate mouths + water transfers” - maintaining separate uMfolozi and St Lucia mouths as in the past, but facilitating water transfers from the uMfolozi River into the lakes via constructed channels or pipelines.
- “Do nothing” - no further interventions in the mouth area (including cessation of breaching of the uMfolozi) with the expectation that the mouths will join naturally in time
- “Common mouth” - interventions to actively facilitate the re-joining of the uMfolozi with the St Lucia system and allowing the common mouth to operate as naturally as possible including closure during low flow periods.
- “Common mouth + conservation” – as above, but also including implementation of conservation actions to increase protection of utilised species

The research showed re-linkage of the Mfolozi River is the preferred solution to bring fresh water to the St Lucia System (Sobrevila, 2017). The last option “Common mouth + conservation” is the most feasible option to restore the natural system. A one dimensional model was used to investigate the mouth state, tidal prism, water level, salinity, and suspended sediments. The fourth option had the greatest positive impact on mouth dynamics (projected to be open for 72% of the time), which corresponds to findings by Lawrie and Stretch (2011b) that showed a combined St Lucia/Mfolozi mouth would be predominantly open for about 70% of the time.

In order to re-link the Mfolozi River to the St Lucia estuarine system it is necessary to remove the artificially created barrier located between them. Numerical 2D simulations indicated that successfully restoring the natural hydrodynamic functioning of the system would require removal of majority of the dredge spoil that has been deposited in the area between St Lucia and the Mfolozi

mouths. Several photographs made during the site visit on the 15th of March 2017 are shown in Appendix E. The photos give a good impression of the scale of the project.



Figure 2.5: Dredges spoil areas to be removed by contractors (iSimangaliso, 2017)

The dredging works started in early 2016 and consisted of removal of 100,000 m³ of dredge spoil, which is a portion of section A as indicated in Figure 2.5. The removal of material in section A has already shown positive impacts to the system. In February 2016 due to droughts only 10% of the Lake's surface area was covered by water, while in November 90% of the Lake's surface area was covered due to good inflows from the Mfolozi River. On the 5th of January 2017 the iSimangaliso Wetland Park signed two new contracts, with T&T Marine (Pty) Ltd and Scribante Africa Mining (Pty) Ltd, after receiving additional funds from the World Bank to restore Africa's largest estuarine lake. Until June 2017 two contractors will be on site to complete Phase B, which is a further removal of 1.1 million cubic metres of dredged spoil (iSimangaliso, 2017).

The main idea about the dredging activities is recreating the natural system that occurred in the period before 1952. In Figure 2.6 the changes to the St Lucia Estuary are visible that occurred due to deposition of the dredge spoil between the Mfolozi River and St Lucia. The yellow part corresponds to Section A from Figure 2.5.

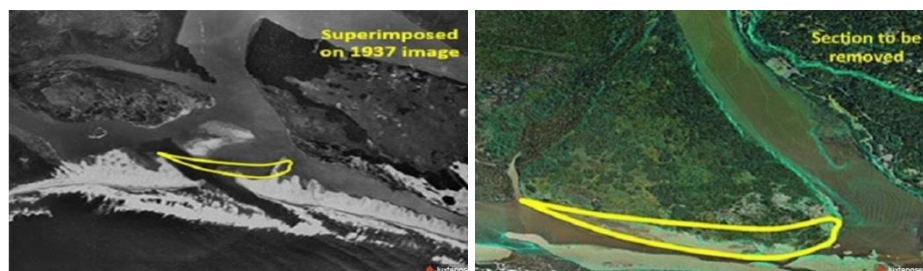


Figure 2.6: Evolution of St Lucia Estuary from 1937 up to 2013 (iSimangaliso, 2016)

The modelling done by Anchor Environmental Consultants did not contain inlet morphodynamics and offshore boundary conditions. The effects of waves, tides, currents, longshore and cross-shore sediment transport have not been implemented in the models. This thesis focusses on the physical processes at the inlet that arise due to re-linkage of the Mfolozi River and the removal of the dredge spoil.

2.5 Hydrodynamics

The St Lucia Estuary is located at a wave dominated coast and experiences a micro-tidal regime. The sediment transport along the coast is influenced by these factors. In general inlets experiencing a micro-tidal regime in combination with a high energetic wave climate are prone to closure. Along the coast of South Africa about 70% of the estuaries do not have a permanently open link to the sea, i.e. they are temporarily open/closed estuaries (TOCEs) (Stretch & Zietsman, 2015). TOCEs are mainly regulated by the amount of river flow entering the estuary, which is primarily governed by the catchment size and rainfall. Hayes (1979) and Davis and Hayes (1984) distinguish tidal inlets into five different classes depending on their tidal range and wave energy. The hydrodynamic classification of the St Lucia inlet is wave-dominated with a mean tidal range of 1.33 m and a significant wave height of 1.60 m.

2.5.1 Tide

Tidal waves are the largest waves present on earth. The tide is generated by the mutual gravitational attraction of the earth and the moon and the earth and the sun. The frequencies are governed by the movements of earth, moon and sun and are mainly diurnal and semi-diurnal and not continuous as with wind waves. Due to a daily fall and rise in water level the part of the coastal profile that is attacked by waves changes during the tidal cycle; at high tide waves will attack a more shoreward portion of the profile than at low tide (Bosboom & Stive, 2015). At estuaries the fall and rise in water level (respectively emptying and filling of the basin) result in large tidal currents that help maintaining an open inlet.

The tidal waves are influenced by the Coriolis force which results in a direction of motion to the left in the southern hemisphere. The air and water currents are moving clock-wise, from south to north along the coast. Schumann (2013) investigated sea level variability in South African estuaries. In South Africa propagation of the tide generally occurs as barotropic Kelvin waves in a west to east direction, with an amphidromic point situated in the Southern Ocean. Such waves have their crests lying perpendicular to the coast, with maximum amplitudes at the coast, decreasing offshore according to the local Rossby radius of deformation. Most of the South African estuaries have a shallow nature and tidal exchanges tend to be flood dominant. Ebb dominance requires relatively deep mouth channels. In flood dominant estuaries the flood flow is shorter but more intense than the ebb flow. As the flood currents are generally stronger than the ebb-tidal currents there is an import of sediments in the estuary. In the area of KwaZulu-Natal longer-period oceanic fluctuations are much lower, and this results in muted estuarine responses. It seems like river inflow and mouth spits play an import part in estuarine levels.

Three tidal regimes are distinguished around the world: micro-, meso- and macro-tidal. The mean spring tidal range is respectively less than 2 m, 2 to 4 m or larger than 4 m. The tidal character along the coast of St Lucia is semi-diurnal and it experiences a micro-tidal regime. The average tidal range at spring tide is about 2.1 m and 0.5 m at neap tides (Perissinotto, Stretch, & Taylor, 2013) (Moerland, 2013). In Figure 2.7 the tidal data at Richards Bay is given. The graph gives a tidal record of the past 19 years indicated by the orange dots. Following the tidal record the spring -, mean - and neap tidal range are equal to 1.84 m, 1.33 m and 0.51 m respectively.

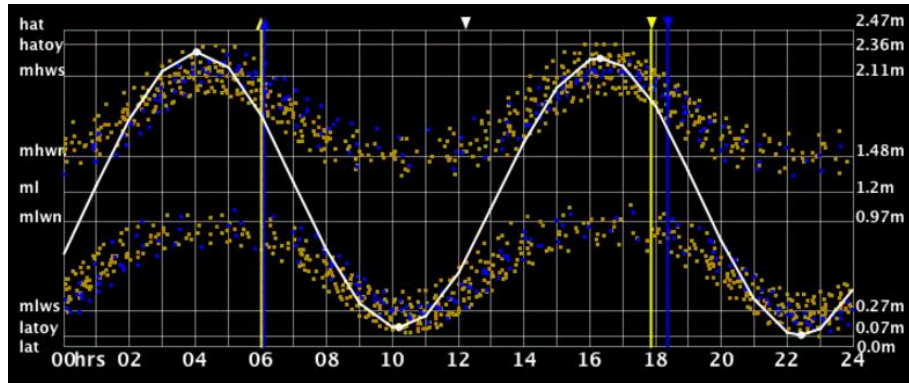


Figure 2.7: Tidal record at Richards Bay on 28-3-2017 (SANHO, 2017). Orange dots show recorded high and low tides of the year. Blue dots show predicted high and low tides of the year. White line shows tide on the 28th of March 2017. Vertical yellow and blue line show sunrise/ –set and moonset/ –rise respectively.

The tidal prism is defined as the volume of water that flows in or out through the inlet during one tidal cycle. Field measurements done by Lawrie et al. (2011c) during a 6-month period in 2007, together with data from Hutchinson (1974), indicate that St Lucia Estuary has a tidal prism of approximately 500,000 to 1,500,000 m³ depending on the tidal cycle and mouth conditions. The observations are summarized by Chrystal & Stretch (2014) and given in Table 2.1. The measurements in 2007 were done after the St Lucia berm was breached by storm waves. The lake water levels were very low due to the drought period that occurred since 2002. In March 2007 the mouth was breached by Cyclone Gamede, which allowed sea water to enter the St Lucia system for a period of 175 days before the mouth closed naturally. The positive net volume that is observed is caused by the low water levels in the lakes. The positive net tidal prism contributes to a flood dominant system, thus importing sediments. The tidal range in the estuary is clearly dampened with the average ratio of estuary range compared to sea equal to 0.39. Measurement on the 14th of July 1972 shows a net volume of 1,786,167 m³ was flushed from the estuary into the ocean. This can be explained by heavy rainfalls and rising water levels after the end of the drought period occurring from 1967 to 1972.

Table 2.1: Tidal observations at St Lucia Estuary

Date	Tidal stage	Peak flows (m ³ /s)		Volume (m ³)		Net volume (m ³)	Tidal range (m)		Estuary range/ sea range
		Flood	Ebb	Flood	Ebb				
20/04/2007	Spring	131.0	68.0	1,600,000	1,333,668	266,332	1.80	0.70	0.39
25/05/2007	Neap	48.7	24.8	851,397	332,996	518,401	0.53	0.23	0.44
28/05/2007	Mid	57.8	24.4	822,890	445,099	377,881	1.19	0.28	0.23
31/05/2007	Spring	63.9	25.6	965,566	454,445	511,121	1.45	0.32	0.22
22/06/2007	Neap	49.7	30.9	495,003	594,964	-99,960	0.80	0.27	0.34
11/07/1972	Spring	187.0	115.0	2,067,179	1,829,419	237,760	1.67	0.87	0.52
12/07/1972	Mid	176.0	100.0	1,887,813	1,586,904	300,909	1.74	0.85	0.49
13/07/1972	Mid	150.0	91.0	1,338,517	1,495,033	-106,516	1.63	0.72	0.44
14/07/1972	Mid	105.0	147.0	1,198,524	2,984,691	-1,786,167	1.49	0.63	0.42

2.5.2 Waves

The coast along the St Lucia Estuary is subject to a high energetic wave climate. The wave height and wave direction are the main drivers of beach evolution and spit formation. The main driving force of the longshore current velocity is by breaking waves which approach the coast at an angle. This longshore current induces longshore sediment transport.

Three different sources for storm waves can be distinguished at the coast of KwaZulu-Natal (Corbella & Stretch, 2012b). Storm waves are generated by cold fronts, tropical cyclones or cut-off lows. Cold fronts move from west to east and occur closer to the beach. Cold fronts have generally smaller wave heights and wave periods with southern direction. Tropical cyclones are generated in the Mozambique Channel and produce north-easterly swells. However, tropical cyclones are rarely responsible for extreme waves along the coast of KwaZulu-Natal. Cut-off lows are generated further offshore than cold fronts and have relatively higher wave heights and wave periods. Storm waves generated by cut-off low pressure systems have the largest influence on morphodynamic processes along the beach of KwaZulu-Natal.

Wave data has been analysed by Corbella and Stretch (2014). Wave data has been measured at Richard Bay which is the nearest measure station to St Lucia, about 60 km away. Richard Bay has directional data recorded by a directional GPS 3D buoy (1997 – 2002) and a directional Waverider buoy (2002 – 2013). Comparison of both data sets has shown similar directional spectra, so it is acceptable to combine the data sets into a 16-year record. The variability in energy is largest in summer and spring due to the absence of large swell waves (low frequencies) in these periods and the presence of south-westerly and north-easterly winds (high frequencies). Autumn and winter show less variability in energy distribution due to the presence of more south-easterly winds during these months. The most wave energy is present in winter and mainly focused from southeast direction.

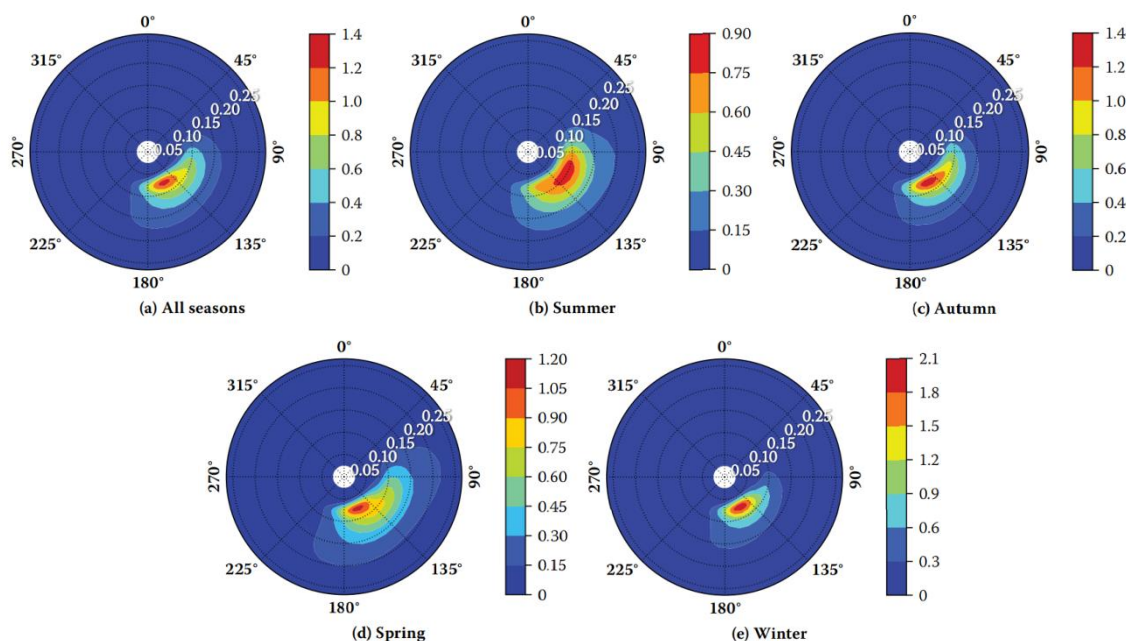


Figure 2.8: Richards Bay's averaged seasonal distribution where (a) is the entire data set, (b) is summer, (c) is autumn, (d) is spring and (e) is winter (Corbella & Stretch, 2014)

Table 2.2: Summary of Wave statistics from Richards Bay wave records (1997-2013)

	Median			Mean			99 th percentile	
	Hs	Tp	θ	Hs	Tp	θ	Hs	Tp
Full	1.49	11.1	147	1.60	11.0	139	3.43	16.6
Summer	1.42	10.0	134	1.51	10.2	133	3.01	15.5
Autumn	1.46	11.7	145	1.59	11.4	139	3.61	16.6
Winter	1.50	11.9	151	1.66	12.5	145	3.57	18.1
Spring	1.57	10.5	147	1.66	10.6	139	3.39	16.6

Extreme wave events are also investigated and show a similar distribution as the averaged seasonal distribution. In literature it is generally agreed that a storm wave event is specified at significant wave height larger than 3.5 m (Corbella & Stretch, 2012b). The energy distribution is bimodal with two storm components, one from approximately 100 degrees and the other from 150 degrees. Large storm events are not evenly distributed and most storm events are clustered in groups. This has a large effect on the response of the beach, because the beach has less time to restore after the first storm event. The storm events with wave heights larger than 3.5 m occur most frequently in winter, followed by spring. The occurrence of these waves is five times higher during winter compared to summer (Olij, 2015). The occurrence of storm events with wave heights more than 2.5 m is twice as much during winter than in summer. It can be concluded that the occurrence of large wave events is not evenly distributed over the seasons.

In Table 2.2 the wave statistics of the Richards Bay wave climate are given. For the full wave climate the mean wave condition has a significant wave height $H_s=1.60\text{m}$, a peak period $T_p=11.0\text{s}$ and direction $\theta=139^\circ$. The orientation of the coast at the St Lucia Estuary is approximately 28° E of true N (Perissinotto, Stretch, & Taylor, 2013). The mean angle of incidence at the coast is 21° , equal to the difference of the mean wave direction with respect to the normal to the coastline ($28^\circ + 90^\circ = 118^\circ$). The angle of incidence influences the amount of longshore sediment transport. The maximum transport occurs at an angle of incidence equal to around 45° (Bosboom & Stive, 2015).

The mean wave heights during winter (1.51m) and spring (1.66m) are larger than during summer (1.51m) and autumn (1.51m). The mean wave periods are largest during winter (11.4s) and autumn (11.4s) followed by spring (10.6s) and summer (10.2s). The mean wave direction comes from south-eastern direction where the largest angle with respect to the normal of the coastline is found in winter. The median wave heights and periods correspond to the mean wave values. The longer periods during winter and autumn suggest that more swell waves are present during this period, which can be confirmed by the wave spectra visible in Figure 2.8.

Swell waves and wind waves have different propagation velocities. The deep water phase velocity is equal to $c_0 = \sqrt{gL_0 / 2\pi}$. The velocity is depended on the wave length, which results in a larger propagation speed for swell waves than shorter wind waves. The separation of the different harmonic components due to their different propagation speed is called frequency dispersion. Swell is generated in a storm in the ocean and spreads out to different locations, which is called directional dispersion. Corbella et al. (2015) analysed the link between atmospheric circulation patterns and wave spectra in order to improve wave modelling. A difference is observed in the

directional spreading of the wind waves and swell waves. The dominant wind directions are from north-east and south-west. The narrow spectrum of swell waves is due to frequency and direction dispersion. At long distances from the storm the shorter wind waves are filtered out because dissipation processes affect the shorter waves stronger.

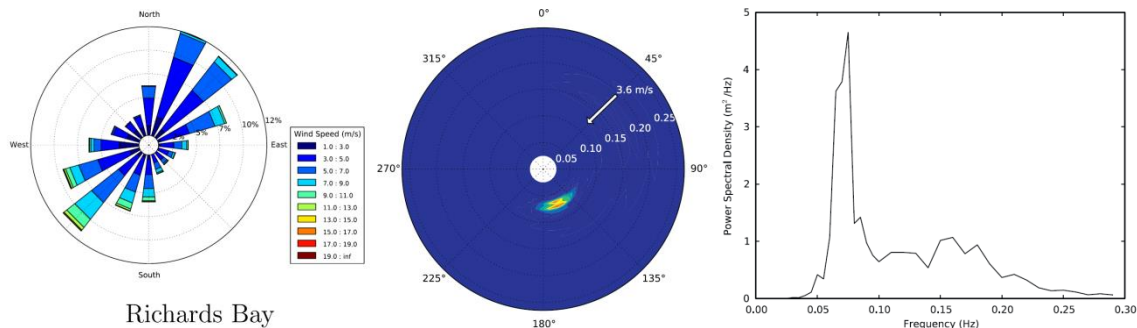


Figure 2.9: From left to right: Wind rose Richards Bay (19/08/1993-31/07/2013), directional energy spectrum, frequency spectrum

2.5.3 Rivers

In temporary open/closed estuaries (TOCEs) the open link to sea is mainly regulated by the amount of river flow entering the estuary. Inlets present in micro tidal and wave dominated regions where stream flows and longshore transport are highly seasonal, the main driving force in the flushing of an estuary is stream flow, while tidal exchange, wind and entrance channel location have minimal influence (Ranasinghe & Pattiaratchi, 1998). In the case of low riverine flows and large longshore transport the mouth will close. An increase in river flow will eventually breach the mouth, creating an open link to sea. Tidal conditions will be influenced by river flow. The tide fluctuates between high and low tide, which causes a flux of sediment import during rising tide (flood flows) and sediment export during lowering of the tide (ebb flows). Riverine flow enhances ebb flows, resulting in less sediment import in the estuaries and longer open mouth conditions.

Horrevoets et al. (2004) shows riverine flow can have large effect on tidal dampening in alluvial estuaries depending on the amount of discharge from the river. The river flow has influence on the phase lag ε that characterizes the tidal wave. The phase lag is defined by the difference between high water (HW) and high-water slack (HWS) and low water (LW) and low-water slack (LWS). During HWS and LWS the current velocities equal zero. In alluvial estuaries the phase lag is equal to 0 and $\pi/2$. It is in between the extreme situation that a tidal wave might have; a progressive wave (HW occurs at same time as maximum flow velocity, $\varepsilon = \pi/2$) or standing wave (HW and HWS occur at the same time, $\varepsilon = 0$). The river discharge influences the moments at which HWS and LWS occur; the lag between HW and HWS becomes shorter and the lag between LW and LWS becomes longer.

According to Guo et al. (2015) estuaries can be classified as tide dominated when the ratio of tidal discharge over river discharge (Q_t/Q_r) is larger than 12-15. River dominance is described by the ratio of cross-sectionally integrated flood-directed transport (S_f/S_r) in one tidal cycle. When this ratio is smaller than 1 an estuary can be classified as river dominant. Using only one ratio has limitations, because e.g. the same Q_t/Q_r ratio can be achieved by a combination of low river flow and small tide or a high river flow and strong tide, whereas sediment transport increases non-linearly with increasing river flow. The use of both Q_t/Q_r and S_f/S_r ratios will provide two dimensions to

differentiate river- and tide dominance and it indicates that the balance between the amount of water and sediment in motion is of equal importance to morphodynamics.

At the St Lucia Estuary two river discharges with major influence on the system can be distinguished. The first one is coming from the Narrows that is connected to the St Lucia Lakes and the second is the Mfolozi River that is reconnected to the St Lucia Estuary. Niekerk & Huizinga (2011) analysed the hydrological data from the Mfolozi River and its influence on the St Lucia Estuary. The Mean Annual Runoff (MAR) of the Mfolozi is estimated at $940 \times 10^6 \text{ m}^3$. Significant variations in runoff are observed between years with floods and years with droughts, but these fluctuations also occur between summer and winter. An overview of the variation in discharge from the Mfolozi River is given in Table 2.3. Runoff during floods can reach 425% of MAR while runoff during years with droughts can be 15% of MAR. In summer the runoff is approximately 47% of MAR and in winter 7% of MAR. Monthly flow volumes of $10 \times 10^6 \text{ m}^3$ is exceeded for about 80% of the time, while higher monthly flows equal to $100 \times 10^6 \text{ m}^3$ are only exceeded for 15% of the time. The Msunduzi River that is connected to the Mfolozi River is estimated at $61 \times 10^6 \text{ m}^3$, about 7% of the MAR from the Mfolozi River.

Table 2.3: Hydrological data Mfolozi River

	Runoff Mfolozi		
	MAR [m^3]	Flow [m^3/s]	% of MAR
Average	940×10^6	29.81	100
Floods	3996×10^6	126.71	425
Drought	142×10^6	4.50	15
Summer	$\sim 442 \times 10^6$	~ 14.01	~ 47
Winter	$\sim 658 \times 10^5$	~ 2.09	~ 7

Sediment loads in the Mfolozi River were measured from 1973 until 1975. The Mfolozi River carries relatively high silt loads compared to other South African rivers and shows a lot of variation in silt content. The highest values are present during the months with the strongest flows, i.e. during summer. Higher flow velocities will generally result in higher silt loads due to sediments that are brought into suspension from the river bed. In Table 2.4 sediment concentrations are given.

Table 2.4: Average sediment content measured in Mfolozi River

	Sediment content Mfolozi River	
	[mg/l]	[kg/m ³]
Autumn (April – May)	752	0.752
Winter (June – August)	78	0.078
Spring (September – October)	300	0.300
Summer (November – March)	2486	2.486

The Mfolozi River with a MAR of $940 \times 10^6 \text{ m}^3$ ($\sim 60\%$ of fresh water inputs) is of real importance to the freshwater balance of the St Lucia System. Whitfield and Taylor (2009) summarized the most important freshwater inputs within the St Lucia System. Mean annual evaporation in the lakes is equal to $-420 \times 10^6 \text{ m}^3$. Mean annual rainfall equals $+273 \times 10^6 \text{ m}^3$. The MAR of the five rivers entering the St Lucia Lakes equals $+362 \times 10^6 \text{ m}^3$ and the mean annual ground flow is equal to $+23 \times 10^6 \text{ m}^3$.

2.6 Sediment transport

Sediment transport can be separated into two parts, cross-shore sediment transport and longshore sediment transport. Cross-shore sediment transport is the sediment transport in onshore or offshore direction. Cross-shore sediment transport can be caused by undertow or rip currents along the coast. Undertow is a current flowing offshore near the seabed and driven by the cross-shore setup gradient (radiation stress). Sediment transport in cross-shore direction can also occur with severe storm events. Longshore sediment transport is the sediment transport along the coast. Long shore sediment transport is generated by oblique incident waves causing longshore currents. The breaking of waves in the surf zone causes stirring up of sediments in the water column, which are transported by the current. The amount of sediment transport depends on the angle of wave incidence with respect to shore normal. The maximum transport occurs at an angle of incidence equal to around 45° . The coastline adjacent of the St Lucia Estuary is $N28^\circ E$ orientated. The sediment consists mainly out of sand with a grain size diameter in the range of 100 – 300 microns (Wright & Mason, 1990). In Figure 2.10 it is clearly visible the beach consists out of sand and no silt is present.

The total sediment transport consists of bed load and suspended load. Bed load is the transport of sediment in a layer close to the bed at which the sediment is in contact with the bed most of the time. Suspended load transport is the transport of suspended sediments in the water column that have no contact with the bed. In literature several sediment transport formulae are known, e.g. the CERC formula (1984), Kamphuis formula (1991), Bijker formula (1971) and Soulsby – Van Rijn formula (1997).

A Lidar and Bathymetric survey of the St Lucia beach barrier and adjacent offshore areas has been performed in 2014. The average beach slope is 1/100 stretching to 2400 m offshore depth contours. The profile closure to the beach is steeper with a slope of approximately 1/50 – 1/60 (Environmental Mapping & Surveying, 2014). In Figure 2.11 bathymetric profiles of the coastline are given.

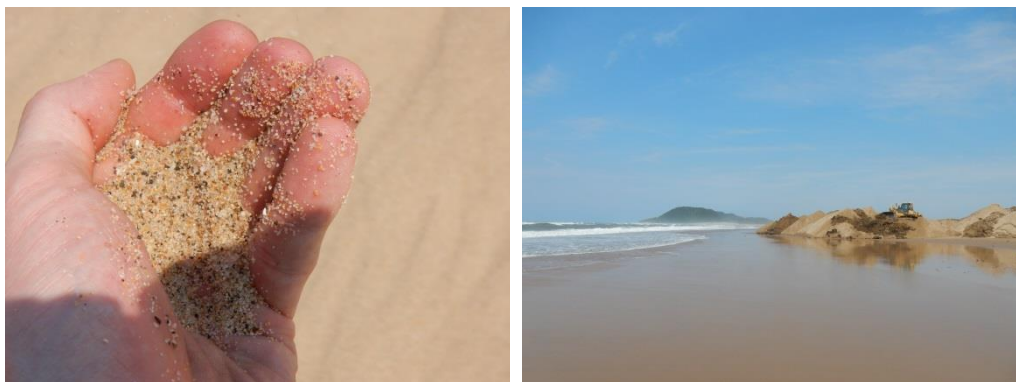


Figure 2.10: Sand particles of beach and piles of removed dredge spoil (photos taken on 15/03/2017)

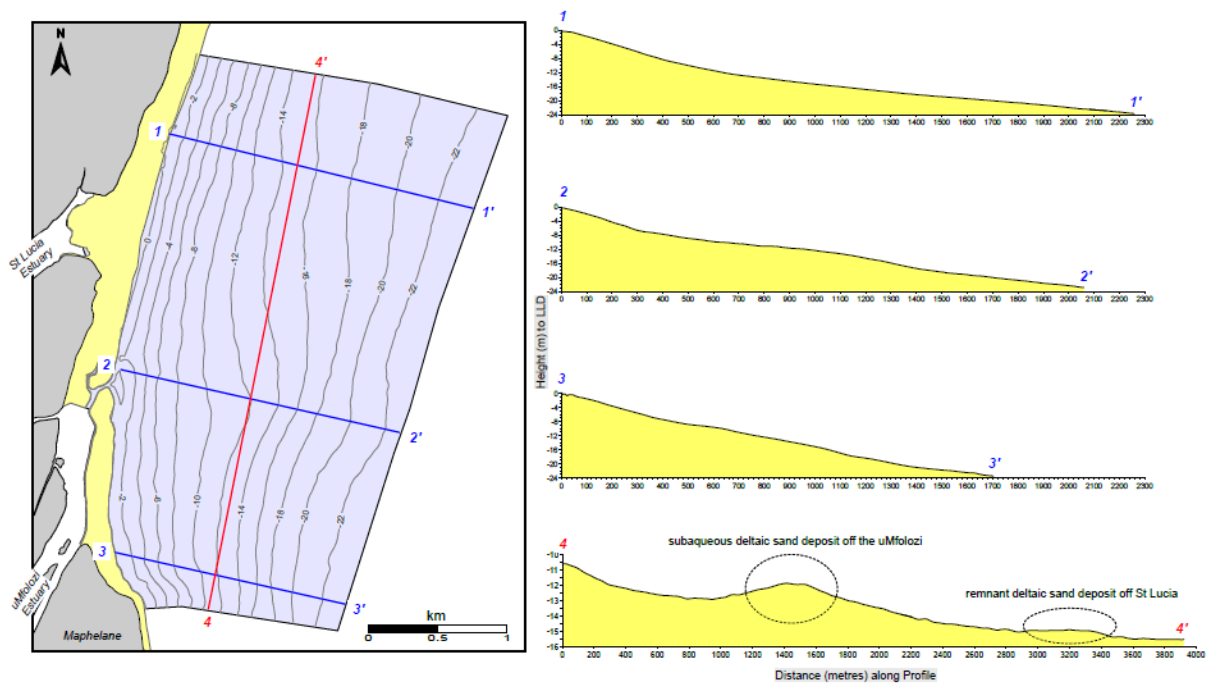


Figure 2.11: Position of offshore bathymetric Profiles 1 to 4. Profiles 1, 2 & 3 are perpendicular to coastline, whilst, Profile 4 is coast parallel (Environmental Mapping & Surveying, 2014).

Schoonees (2000) has investigated the longshore sediment transport along the South African coast. Measurements were done on three sites of which Richards Bay is nearest to St Lucia. This is the same location where the wave data is obtained from. At Richards Bay a port is located where the measurements were done. Sand was dredged at the southern side of the harbour entrance and pumped onto the northern beach. The longshore sediment transport is computed from annual beach, hydrographic surveys and the volumes of material dredged. The mean longshore transport rate equals $850,000 \text{ m}^3/\text{year}$. The annual net longshore transport rates are given in Table 2.5. The standard deviation is equal to $750,000 \text{ m}^3/\text{year}$. The coefficient of variation is relatively high, equal to 0.88, and is probably caused by inaccurate measurements and shifts in deep-sea wave direction.

Table 2.5: Annual net longshore transport rates at Richards Bay

Period	Net longshore transport rate (m^3/year)
1979/1980	1,020,000
1980/1981	830,000
1981/1982	850,000
1982/1983	2,120,000
1983/1984	1,880,000
1984/1985	1,570,000
1985/1986	-420,000
1986/1987	-260,000
1987/1988	720,000
1988/1989	1,010,000
1989/1990	-60,000
1990/1991	1,220,000
1991/1992	980,000
1992/1993	440,000

The longshore sediment transport along Richards Bay is also evaluated by Van Rijn (2013). Wave data from Corbella and Stretch (2012b) is used to compute longshore sediment transport rates. Input parameters have been varied yielding in a net longshore sediment transport rate of 450,000 to 850,000 m³/year. The computed transport rates correspond to the results by Schoonees (2000). The original Kamphuis 1991 formula performs better than the modified Kamphuis 2013 formula, resulting in a net longshore transport of 550,000 and 390,000 m³/year respectively.

2.7 Tidal inlet theory

Tidal inlets occur in different states depending on the hydraulic conditions present. As described in the previous chapter the St Lucia inlet is located along a wave dominated coast. However, once the Mfolozi River is reconnected to the St Lucia Estuary it is possible the system will be dominated by fluvial processes. Inlets are classified within three major groups, river-dominated, tide-dominated and wave-dominated. The classification of inlets is described by Bosboom and Stive (2015) and further explained in Appendix A.1.

A tidal inlet is a complex system, but can be described by three main parts. Depending on the hydraulic conditions an inlet is more developed, but it generally consists out of an ebb tidal delta, tidal gorge and flood tidal delta. The ebb tidal delta is a sand body formed seaward of the entrance channel. The tidal gorge is a narrow deep channel at the inlet entrance. The flood tidal delta is a sand body that develops in the tidal basin landward of the tidal gorge. Boothroyd (1985) described the system of a tidal system more elaborately, which can be found in Appendix A.2.

2.7.1 Inlet stability

Stability of inlets is governed by oceanic processes, such as tides, waves and mean sea level, as well as fluvial/estuarine processes like river flow. Inlet stability can refer to either locational stability or cross-sectional stability. Inlets that are locationally stable generally stay fixed in place over time; it may however be cross-sectionally stable or unstable (e.g. intermittently closing inlets). Inlet stability is primarily governed by the flow through the inlet, consisting of the tidal prism and river flow, and nearshore sediment transport around the area of the inlet.

Duong (2015) characterised small tidal inlets into three main sub-categories based on their general morphodynamic behaviour as follows:

- Permanently open, locationally stable inlets (Type I)
- Permanently open, alongshore migrating inlets (Type II)
- Seasonally/Intermittently open, locationally stable inlets (Type III)

The St Lucia inlet can be classified as Type III. Like most estuaries along the South African coast it is a temporary open/closed estuary (TOCE). However, the mouth of the Mfolozi River does migrate along the coast and can be classified as Type II. A combined mouth will result in either one of the two types depending on oceanic – and fluvial processes.

The evolution of the St Lucia Estuary from December 1984 until December 2016 can be observed in Figure 2.12. The St Lucia inlet is clearly seasonally open and locationally stable, while the Mfolozi mouth is almost permanently open and migrates along the coast. The Mfolozi mouth migrates approximately 300 to 400 meter a year in northern direction.

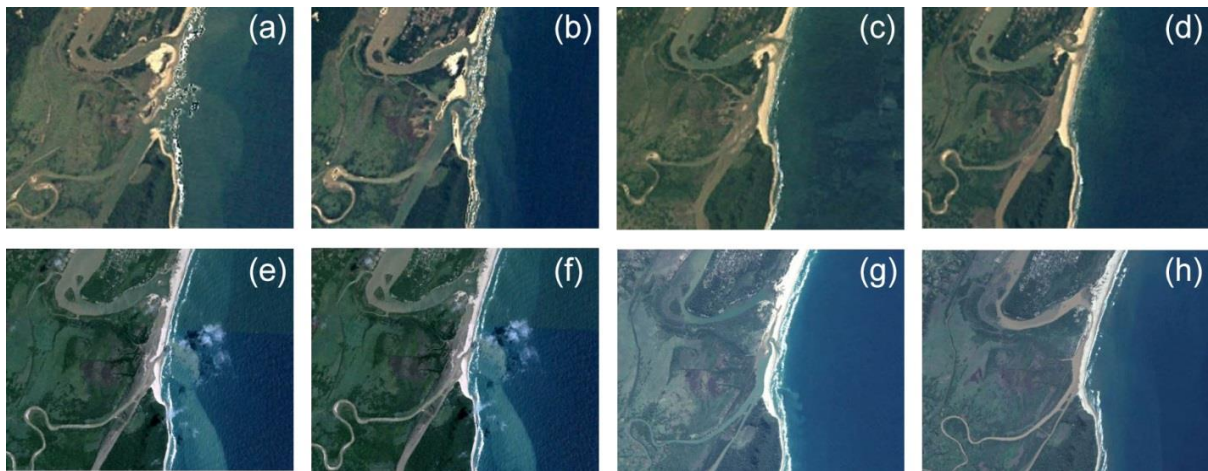


Figure 2.12: Change of St Lucia Estuary configuration in 12/1984 (a), 12/1989 (b), 12/1994 (c), 12/1999 (d), 12/2004 (e), 12/2009 (f), 12/2014 (g) and 12/2016 (h) (Google Earth, 2017).

Locationally stable inlets can either be permanently open (Type I) or seasonally open (Type III). Ranasinghe et al. (1999) described inlet closure for locationally stable inlets throughout a conceptual model. Inlet closure may occur due to longshore sediment transport on drift dominated coasts or due to onshore migration of sandbars on wave dominated coasts. These two processes of inlet closure are shown in Figure 2.13.

The first mechanism describes interaction between longshore currents and inlet currents. A shoal is formed at the updrift side of the tidal inlet, which interrupts the longshore sediment transport along the coast. The inlet currents maintain an open inlet if the current is strong enough to remove sediments deposited in the channel. When the inlet currents are weak, the shoal will form a spit across the channel that might cause complete closure of the system. The second mechanism mainly occurs in microtidal - and mesotidal environments where the inlet currents and tidal prisms are small. The inlet is only able to stay open with the presence of high river discharge or strong ebb currents due to large tidal ranges. Inlet closure is caused by swell waves that transport offshore bars to the coast when inlet currents are too small.

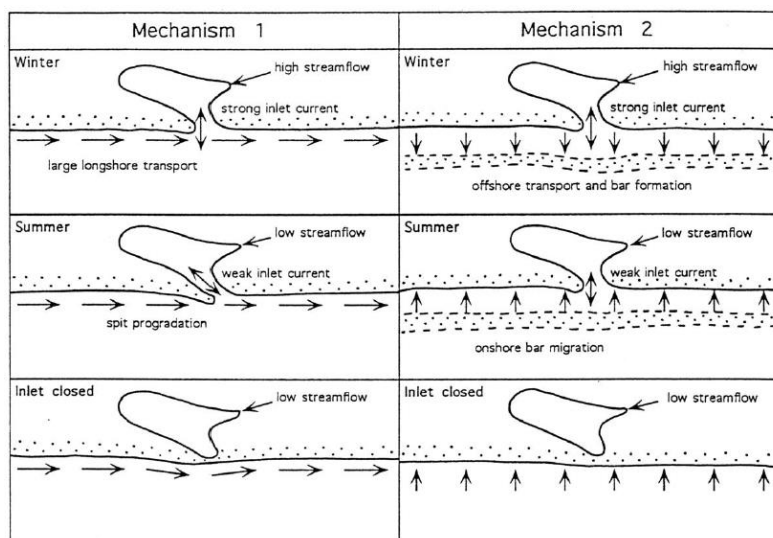


Figure 2.13: Conceptual model of inlet closure mechanisms (Ranasinghe, Pattiaratchi, & Masselink, 1999)

Permanently open, alongshore migrating inlets (Type II) are described by Davis and FitzGerald (2004) and the conceptual model is given in Figure 2.14. Longshore sediment transport induced by longshore currents leads to accumulation of sediments at the updrift side of the inlet. A reduction in channel volume causes higher flow velocities through the inlet. The tidal currents erode the downdrift side of the inlet and the inlet will migrate in downdrift direction. The migration rate depends on the longshore sediment transport, ebb tidal current velocity, river flow and composition of the channel banks. At a certain moment elongation of the inlet channel will stop due to breaching at of the updrift sand spit during extreme riverflow and/or severe storms. The new inlet will provide a shorter channel and more efficient tidal exchange. The old inlet at the downdrift side will gradually close. This process will repeat itself with the inlet migrating in the direction of the prevailing longshore sediment transport.

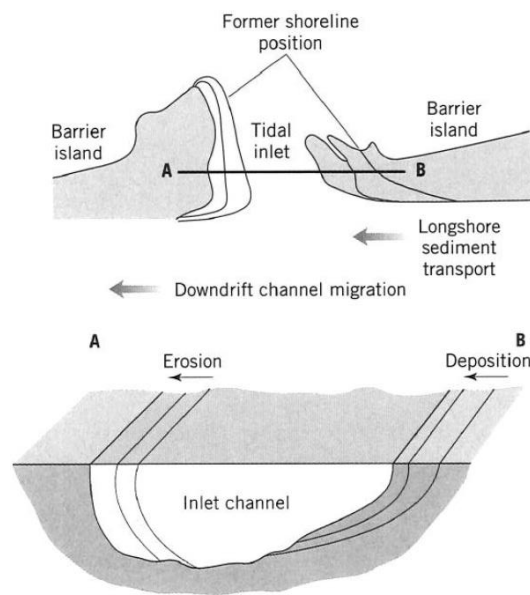


Figure 2.14: Conceptual model of inlet migration (Davis & FitzGerald, 2004)

2.7.2 Empirical relationships determining inlet stability

Several empirical relationships are derived to determine the stability of an inlet. One of the first relationships is the Escoffier diagram (Escoffier, 1940). The diagram, shown in Figure 2.15, shows a curve representing stability of an inlet where the maximum flow velocity through the inlet is plotted against the cross sectional flow area. The maximum flow velocity depends on the tidal prism, tidal amplitude and the cross-sectional area. The diagram shows two points, A and B, a unstable and

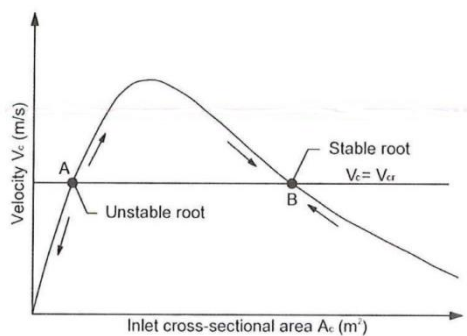


Figure 2.15: Escoffier diagram (Escoffier, 1940)

stable root respectively. If the flow velocity through the inlet is smaller than the flow velocity at point A the inlet will close. In the case of larger flow velocities than point A the inlet cross-section will grow towards and reach a stable inlet, represented by point B. The Escoffier diagram is focussed on inlet cross-sectional stability, but does not take into account locational stability.

Bruun (1978) described both the locational – and cross-sectional stability of tidal inlets. The following ratio is used to describe inlet stability (2.1):

$$r = P / M_{tot} \quad (2.1)$$

The inlet stability is described by the ratio P tidal prism ($\text{m}^3/\text{tidal cycle}$) over M_{tot} total annual littoral drift (m^3/year). The value of P / M_{tot} classifies the overall stability of an inlet as good, fair or poor. A detailed explanation of the criteria is given in Appendix A.3.

Duong (2015) has extended the classification scheme for small tidal inlets (STIs). The three different types of inlets, Type I, Type II and Type III, were modelled with the process based model Delft3D under contemporary forcing. A clear link between the STI type and ratio r was established (Table 2.6).

Table 2.6: Classification scheme for inlet Type and stability conditions (Duong, 2015)

Inlet type	$r = P / M_{tot}$	Bruun Classification
Type 1	> 150	Good
	100 – 150	Fair
	50 – 100	Fair to poor
	20 – 50	Poor
Type 2	10 – 20	Unstable (open and migrating)
Type 2/3	5 – 10	Unstable (migrating or intermittently closing)
Type 3	0 – 5	Unstable (intermittently closing)

The most widely used empirical method is probably the A-P relationship. O'Brien (1931), (1969) and Jarrett (1976) showed the cross-sectional area of an inlet is proportional to the volume of water flowing through it during half tidal cycle (tidal prism). The A-P relationship is as follows (2.2):

$$A_{eq} = C \cdot P^q \quad (2.2)$$

In which:

- A_{eq} : minimum cross-sectional area of entrance channel measured below mean sea level [m^2]
- P : spring tidal prism [m^3]
- C and q : empirical coefficients

O'Brien (1969) investigated 28 U.S. entrances and derived values for the empirical coefficients, $C = 4.69 \cdot 10^{-4}$ and $q = 0.85$. When the data was limited to 8 non-jettied entrances the empirical coefficients were equal to $C = 1.08 \cdot 10^{-4}$ and $q = 1$. The equilibrium velocity for the Escoffier curve is approximately 0.9 m/s which results in coefficients $C = 7.8 \cdot 10^{-5}$ and $q = 1$.

In previous research the effect of river flow was not – or partially taken into account. The river flow enhances ebb tidal currents and has effect on the phase leg as explained in chapter 2.5.3. Hinwood et al. (2012) analysed tidal estuaries to investigate dominance of tidal and fluvial flows. Methods of non-linear dynamics have been applied to discover and characterize a quasi-equilibrium state to which the estuary evolves over time, which is referred to as attractor. Two attractors have been identified, one in which the entrance is tidally dominated, known from field studies of tidal prism-entrance area relationships. The second, new attractor is found in which the river flow dominates the hydrodynamics but the small tidal flow dominates the evolution of the inlet. The tidal and fluvial attractors are plotted together with O'Brien's field data (Figure 2.16). A clear distinction between the tidal - and fluvial attractor is visible. The estuary dominated by tide shows larger entrance areas and higher tidal prisms compared to estuaries dominated by fluvial flows. The O'Brien data is mainly dominated by tidal flows and river flow play a small role, which can be observed by the deviation of the flow attractor from O'Brien's data. Estuaries dominated by river flow tend to have a very constricted entrance in which river flow is dominant, but the tide retains some influence.

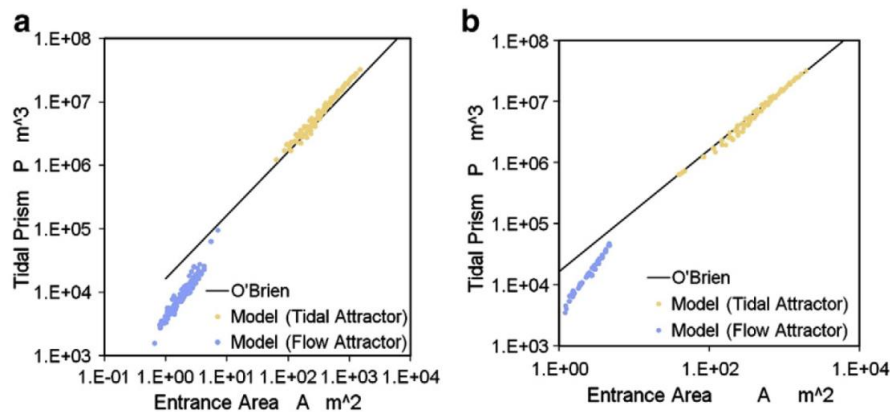


Figure 2.16: Comparison of model attractors and O'Brien field data. a) Low ocean sediment concentration; b) High ocean sediment concentration.

2.7.3 Previous modelling

Research has been done by V. Moerland (2013) who has modelled the St Lucia inlet. A schematised model of the inlet was made in the process-based program Delft3D. The research mainly focussed on determining the parameters that are of main importance in inlet closure. The parameters that were varied are the: basin width, tidal range, wave height and river discharge. In Figure 2.17 the change in bed level is visible for large basin with spring tidal range of 2 m and extreme waves of 3.5 m. From the initial state (a) the development of the flood tidal delta is clearly visible in the simulation after 300 days (b) whereas the ebb tidal delta is not present due to high waves and longshore sediment transport which wash away the bars. In few scenarios inlet closure was reproduced, however P/M ratios were a factor 10 too small compared to the theory by Bruun and the model was highly schematised. In Figure 2.17 (c) it is clearly visible that the water level in the basin is higher than the water level in the ocean. This corresponds to the flood dominant character of the South African estuaries as described by Schumann (2013). Due to wave-built sandy ridges lying parallel to the wave fronts and extending across the seaward section estuaries are separated from the sea. These barriers cause ebb-tidal flow velocities to decrease, as the flow over the sill becomes shallower. When flow is limited due to such barrier, the low tide in the sea can occur before the end of the ebb flow, and then the flood period starts again.

It can be summarized that in general higher waves will generate more longshore sediment transport that can lead to closure of the inlet. The tidal amplitude has a large influence in maintaining an open inlet, when increased the chance of closure decreases and the inlet will change from intermittently open, locationally stable inlet (Type III) to a permanently open, alongshore migrating inlet (Type II). This corresponds to the classification of inlets by Duong (2015).

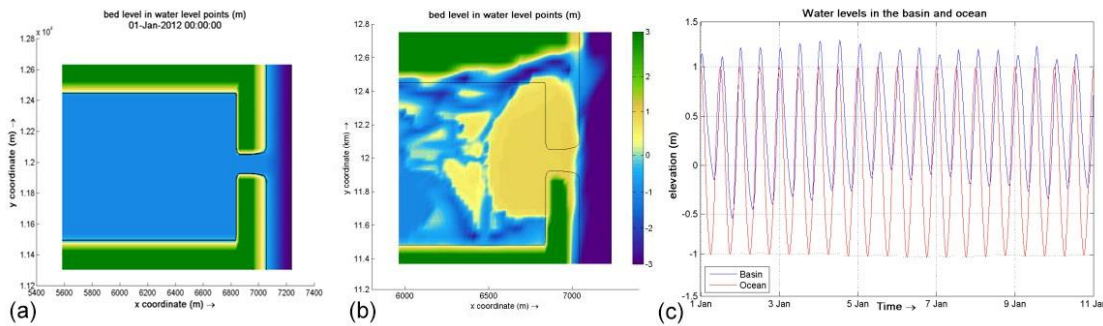


Figure 2.17: Initial bed level (a), bed level after 300 days (b), water level in basin and ocean (c) (Moerland, 2013)

2.8 Conclusion

The St Lucia Estuary has undergone major changes in the last centuries. The removal of the Mfolozi River and continuously dredging in the St Lucia Estuary were the measures with the largest impact on the system. During dry periods the consequences were the most drastic with desiccation of 90% of the St Lucia Lakes in the period from 2002 to 2012. In 2009 the GEF project started to investigate possible solutions to bring fresh water into the St Lucia Lake system. In the beginning of 2016 the dredging works started with the removal of the dredge spoil from the St Lucia Estuary and re-linkage of the Mfolozi River. In the list below properties of the St Lucia Estuary are given:

- The St Lucia Estuary behaves like most estuaries along the South African coast and can be regarded as a temporary open/closed estuary (TOCE). Previous research done by Lawrie and Stretch (2011b) showed a combined St Lucia/Mfolozi mouth would be predominantly open for about 70% of the time.
- The hydrodynamic classification of the St Lucia inlet is wave dominant with a mean tidal range of 1.33 m and a significant wave height of 1.60 m.
- The St Lucia Estuary experiences a semi-diurnal tidal regime. The mean tidal range equals 1.33 m, spring tidal range equals 1.84 m and the neap tidal range equals 0.51 m.
- The Mfolozi River with a MAR of $940 \times 10^6 \text{ m}^3$ (~60% of fresh water inputs) is of real importance to the freshwater balance of the St Lucia System.
- The average longshore sediment transport equals $850,000 \text{ m}^3/\text{year}$, but varies significantly from $420,000$ up to $2,120,000 \text{ m}^3/\text{year}$. Grain size diameters are in the range of $100\text{-}300 \mu\text{m}$.
- The St Lucia inlet can be considered as a seasonally/intermittently open, locationally stable inlet (Type III). The mouth of the Mfolozi River does migrate along the coast and can be classified as Type II (Permanently open, alongshore migrating inlets).

3 Methodology

3.1 Scenarios

The St Lucia inlet will be simulated in two different scenarios. In order to determine the effects of the dredge spoil removal and re-linkage of the Mfolozi River on the St Lucia mouth, these measures will be compared to the existing situation. The two scenarios are as follows:

Scenario A: Open inlet

The St Lucia Estuary has a connection with the Indian Ocean. The St Lucia Estuary is modelled with an open inlet in order to calibrate the model. The dredge spoil is not yet removed. The inlet has a width of 70 m. In the past the St Lucia inlet used to have a width between 50 and 100 m. The discharge from the Mfolozi River will be varied from 0, 2, 5, 14 to 30 m³/s. These river discharges corresponds to a winter season, drought period, summer season and mean annual runoff respectively.

Scenario B: Future state

The St Lucia Estuary has a connection with the Indian Ocean and the dredge spoil is removed until a depth of -0.5 m with respect to MSL. The total amount of dredge spoil that is removed equals approximately 1,300,000 m³. This is the amount that is currently removed from the St Lucia Estuary. In Appendix D photos from the remediation works are shown. The change of the St Lucia Estuary is clearly visible from the two site visits on the 15th of March and the 18th of May. The inlet width remains 70 m as in previous scenario. The discharge from the Mfolozi River will be simulated as in scenario A.

In Figure 3.1 the two scenarios are given. All scenarios have the same grid size and resolution. The bathymetry and hydrodynamics are changed for each scenario in the simulations. The depth ranges from -25 m offshore up to +12 m at the location of the dredge spoil.

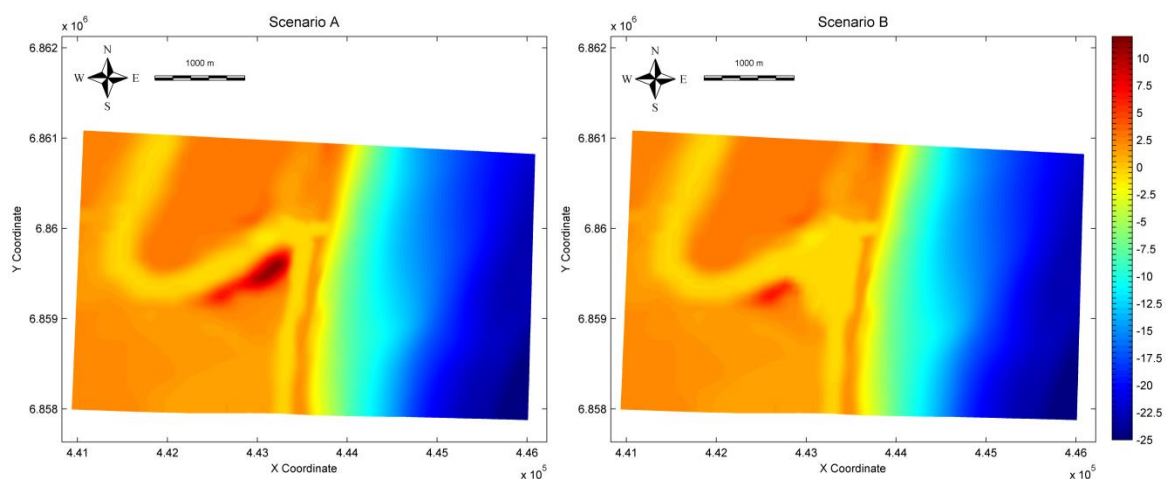


Figure 3.1: Different scenarios in shown in Delft3D including bathymetry; after re-linkage of Mfolozi River and before dredge spoil removal (scenario A) and after dredge spoil removal (scenario B)

3.2 Delft3D Model

The process-based model Delft3D is used in order to simulate the behaviour of the St Lucia inlet. Delft3D is a 3D modelling suite to investigate hydrodynamics, sediment transport and morphology as well as water quality for fluvial, estuarine and coastal environment. The software is developed by Deltares, a leading Dutch-based research institute, that focusses on areas relating to water, soil and the subsurface. Delft3D consists of several modules of which Delft3D-Flow, Delft3D-Wave and Delft3D-Mor are used in this model.

The Delft3D model is calibrated based on the tidal prism through the inlet. At first the tidal prism is computed for simulations with only tidal forcing. After this waves will be incorporated and the model will be calibrated based on longshore sediment transport and the change in morphology.

3.2.1 Grid & Bathymetry

The model uses two different grids, one grid is used for the flow module and one for the wave module, see Figure 3.2. The flow grid has a width of 5,000 m in cross-shore direction and a length of 3,000 m in alongshore direction. The grid resolution at the boundaries equals 84 x 96 m. The grid resolution increases towards the surf zone and St Lucia inlet to minimum of 20 x 22 m. The resolution is changed in steps of maximum 10% in order to have computational stability for the simulation. The grid dimensions are large enough for stability of the model and include large flow phenomena as refraction of waves. The bathymetric data is obtained from the iSimangaliso Wetland Park. Lidar and bathymetric surveys were done in August 2013 and September 2014 of the St Lucia Lakes, St Lucia Estuary, St Lucia beach barrier and adjoining offshore area (AOC Geomatics, 2013), (Environmental Mapping & Surveying, 2014).

The flow grid is nested in the larger wave grid. The wave grid has a uniform grid resolution of 200 x 200 m. The wave grid has a maximum width in cross-shore direction of 11,000 m at the southern side and has a length of 25,000 m. The grid is generated with Delft3D Dashboard and the bathymetry is obtained from General Bathymetric Chart of the Oceans, GEBCO 08.

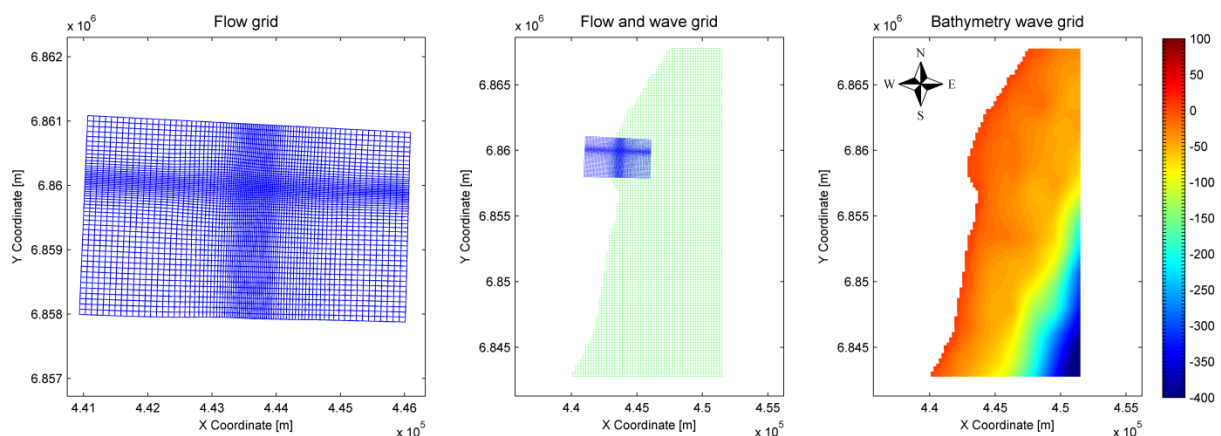


Figure 3.2: From left to right: flow grid, flow nested in wave grid and bathymetry wave grid

3.2.2 Flow module

1. Time frame

The time step of the model is 6 seconds. The time step is important to control both stability and accuracy of the model. The Courant number is a useful relation between time-step, depth and grid size, and should not exceed a value of 1 to secure a stable simulation. The Courant number can be computed as follows:

$$CFL = \frac{\Delta t \cdot \sqrt{gH}}{\Delta x} \quad (2.3)$$

When the CFL number is smaller than one the fluid particles will move from one cell to the next within one time step. In a one-dimensional model the Courant number can be computed with formula (2.3). In the area of interest, the St Lucia inlet, this would lead to a CFL number equal to approximately 0.67. The time step of 6 seconds results in a stable model, which is based on a sensitivity analyses.

The total simulation time of the model is 41.4 days of which 5 days are used as spin-up time. During the spin-up time the model runs without morphological developments. The morphological acceleration factor (morfac) is equal to 1 during the spin-up time and increased to 10 for the rest of the simulation. The coupling of the wave module to the flow module will occur every three hours. As shown by Olij (2015) in this way the wave and flow module are coupled at the highest, lowest and average water levels of the tide.

2. Boundary conditions

The flow grid has three open boundaries. At the eastern side a water level boundary condition with the tide is imposed. The northern and southern boundaries have a von Neumann water level boundary condition with a zero gradient. This boundary condition assumes there is no alongshore gradient in the water levels. This assumption can be made because the grid size is small compared to the tidal wave length.

The tidal forcing is modelled with a M2 component only, which is varied between neap-, mean- and spring tidal range. Waves breaking at the beach are influenced by the water level, thus the tide. In order to compare the different scenarios it is chosen to separately simulate the tidal ranges. The M2 component is modelled by a harmonic with similar amplitude and an adjusted period of 12 hours in Delft3D.

3. Roughness

The bed roughness is modelled by the Chézy coefficient. A Chézy value of 50 m^{1/2}/s approaches measurements the best. This is explained in more detail in chapter 4.1.

4. Viscosity

The eddy viscosity and eddy diffusivity are both set to 1 m²/s. Eddy viscosity and eddy diffusivity are parameters used to resolve dispersion and incorporate turbulence in the model. In general the eddy viscosity and eddy diffusivity are chosen between values of 1 and 10 m²/s. As shown by Olij (2015)

an increase in both eddy viscosity and eddy diffusivity results in more erosion along the coast and more intense bar forming.

5. Morphology

Several different sediment transport formulas are available in Delft3D that include currents and wave forcing. Four sediment transport formulas include both effects in Delft3D: Van Rijn formula (1993), Bijker formula (1971), Soulsby - Van Rijn formula (1997) and Soulsby formula (1997). For the case study the Van Rijn formula (1993) is used.

Delft3D has several factors to calibrate sediment transport. In this model the current related transport factors are set to 20 in order to approach longshore sediment transport measurements. The wave related factor is set to 0.31 to maintain an equilibrium beach width. The beach erodes during high wave action and accretion occurs during low wave action. The factor for erosion of dry cells is set to 0.1. Grain size diameter is chosen at 200 μm .

3.2.3 Wave module

1. Boundary conditions

The reduced wave climate is used as wave input. The wave climate is imposed at southern boundary, eastern boundary and northern boundary.

2. Wave spectrum

The directional spreading is modelled with the cosine power. Corbella & Stretch (2014) showed the wave data is best represented by this distribution. The wave spectrum is approached with a JONSWAP shape with a peak enhancement factor of 3.4.

3. Physical processes

The bore-based model of Battjes and Janssen (1978) is used to model the energy dissipation due to depth-induced breaking. The coefficient for determining the rate of dissipation is set to 1.0 and the breaker parameter equals 0.73. These are the default parameters as mentioned in the Delft3D-Wave Manual (Deltares, 2009). The bottom friction is modelled with the JONSWAP model. The bottom friction coefficient is equal to $0.067 \text{ m}^2/\text{s}^3$, which is the default value in Delft3D and appropriate for full developed wave fields near shore.

4. Various other processes

Diffraction will not be taken into account in the model. The coastline is open to sea and is not located in a shadow zone. Refraction and frequency shifts are taken into account. Refraction influences the wave direction which is one of the most important factors generating longshore transport. Whitecapping is of main importance for deep water waves when breaking due to wind forces. This process is deactivated along with wind growth in order to decrease computation time of the model. Non-linear triad interactions are also switched off since these processes are of real importance for the model results, but influence the computation time of the model.

3.3 Wave climate reduction

Input reduction is important to reduce computational time of the model. Maximum run-time is approximately 10 to 12 hours, so the wave climate should be reduced to an equivalent of 10 to 12 representative conditions. A schematisation based on the sediment transport formula from Van Rijn or Bijker will give the most accurate results, because these sediment formulae include wave angle and a broader distribution. Coastline orientation and incident wave should be included. Input reduction with bins with approximately equal weight is preferred, either derived with manual selection or coded. Choosing conditions with largest contribution does not result in an accurate representative wave climate (Walstra et al., 2013).

The wave climate of KwaZulu-Natal is analysed in order to reduce the wave climate. Wave recordings from Richards Bay are used to create bivariate histograms for the significant wave height and period, given in Table 3.1 and Table 3.2. The data is measured from February 2001 until November 2009 and contains a total of 22241 observations. The colours give attention for classes with higher frequency of occurrence.

Table 3.1: Incoming direction versus Hs bivariate histograms

Hs (m)	N	NNE	NE	ENE	E	ESE	SE	SSE	S	SSW	SW	WSW	W	WNW	NW	NNW	Total
0,0 - 0,5								0,01									0,03
0,5 - 1,0				0,13	0,74	1,45	1,96	3,58	0,56	0,01							8,43
1,0 - 1,5				0,97	5,10	9,04	8,79	19,23	2,63	0,20	0,08						46,06
1,5 - 2,0				0,63	3,28	6,63	5,46	11,57	1,78	0,50	0,10						29,95
2,0 - 2,5				0,02	0,70	1,90	1,96	4,34	1,11	0,29	0,01						10,32
2,5 - 3,0					0,18	0,45	0,64	1,60	0,44	0,05							3,36
3,0 - 3,5					0,07	0,12	0,30	0,60	0,13	0,01							1,23
3,5 - 4,0					0,03	0,05	0,14	0,21	0,05								0,49
4,0 - 4,5					0,01	0,01	0,03	0,06									0,11
4,5 - 5,0								0,01									0,02
5,0 - 5,5																	0,00
5,5 - 6,0							0,01										0,01
Total	0,00	0,00	0,00	1,75	10,12	19,65	19,29	41,21	6,71	1,07	0,19	0,00	0,00	0,00	0,00	0,00	100,00

Table 3.2: Incoming direction versus Tp bivariate histograms

Tp (s)	N	NNE	NE	ENE	E	ESE	SE	SSE	S	SSW	SW	WSW	W	WNW	NW	NNW	Total
00 - 02																	0,00
02 - 04				0,05	0,03												0,10
04 - 06				1,15	1,02	0,11	0,05	0,09	0,41	0,69	0,19						3,71
06 - 08				0,54	3,14	2,32	1,69	1,36	0,98	0,38							10,41
08 - 10				0,01	4,39	10,43	6,10	4,40	0,53								25,87
10 - 12					1,33	5,15	6,76	10,36	1,55								25,15
12 - 14					0,23	1,24	2,90	14,13	2,23								20,72
14 - 16					0,05	0,51	1,54	9,62	1,05								12,75
16 - 18						0,03	0,18	1,08	0,00								1,29
Total	0,00	0,00	0,00	1,76	10,18	19,78	19,23	41,04	6,75	1,08	0,19	0,00	0,00	0,00	0,00	0,00	100,00

The results correspond to wave data analysed in paragraph 2.5.2. The majority of waves are coming from an ESE to SSE, between 101 and 169° N. The largest fraction, 40% of the incoming waves, arrives from SSE, between 146 and 169° N. The significant wave height occurs most frequently between 1.0 and 2.0 m with a peak period of 10 – 14 s.

The wave climate will be reduced to 10 wave conditions in order to decrease computation time. The probability of wave height and relative sediment transport contribution is plotted in Figure 3.3. Waves with direction from 150°N to 160°N and corresponding wave height of 1.5 m have the highest frequency of occurrence. Longshore sediment transport is calculated with the Kamphuis 1991

formula (2.4), which has shown to be the best representation of the measured longshore sediment transport (Rijn L. v., 2013).

$$Q_t = 2.33 \rho_s / (\rho_s - \rho) (T_p)^{1.5} (\tan \beta)^{0.75} (d_{50})^{-0.25} (H_{s,br})^2 [\sin(2\theta_{br})]^{0.6} \quad (2.4)$$

In which:

- Q_t : Total sediment transport [dry mass in kg/s]
- T_p : peak wave period [s]
- $H_{s,br}$: significant wave height at breaker line [m]
- θ_{br} : wave angle at breaker line [°]
- d_{50} : median particle size in surf zone [m]
- $\tan \beta$: beach slope [-]
- p : porosity factor (=0.4) [-]

The sediment transport is mainly influenced by waves with direction from 140 – 160 °N (Figure 3.3). The wave direction is given in degrees from true North. In Appendix B the reduced wave climate is given with the wave direction with respect to the coastline. It can be observed that waves coming from an angle of 90°N have no impact on longshore sediment transport as this generates cross-shore sediment transport.

The sediment transport contribution is also calculated with the CERC formula in order to compare the results of the Kamphuis formula. The CERC formula (2.5) can be arranged to (Rijn L. v., 2002):

$$Q_{t, mass} = 0.023(1-p) \rho_s g^{0.5} (\gamma_{br})^{-0.52} (H_{s,br})^{2.5} \sin(2\theta_{br}) \quad (2.5)$$

In which:

- Q_t : Total sediment transport [dry mass in kg/s]
- $H_{s,br}$: significant wave height at breaker line [m]
- θ_{br} : wave angle at breaker line [°]
- p : porosity factor (=0.4) [-]
- ρ_s : sediment density (=2650) [kg/m³]
- γ : breaker index (=0.8) [-]

The CERC transport formula is rather crude as it does not show any influence of particle size and beach slope in the formula. According to Kamphuis (1991) the standard CERC formula ($K=0.77$) overpredicts measured transport rates considerably. This mainly holds for beaches with particle size ranging from 0.2 to 0.6 mm and beach slopes in the range of 0.01 to 0.1. The higher sediment transport contribution from the CERC transport formula is visible in Figure 3.3. Especially the higher waves are represented more in the wave climate and have a larger density. The Kamphuis formula is used to determine the reduced wave climate. The reduced wave climate is determined by manual selection of 10 bins with equal contribution.

The gross sediment transport is calculated with the reduced wave climate given in Table 3.3. The yearly sediment transport calculated with the Kamphuis formula (2.4) is equal to 3.22E+06 m³. The CERC formula (2.5) results in a sediment transport equal to 2.40E+06 m³/year.

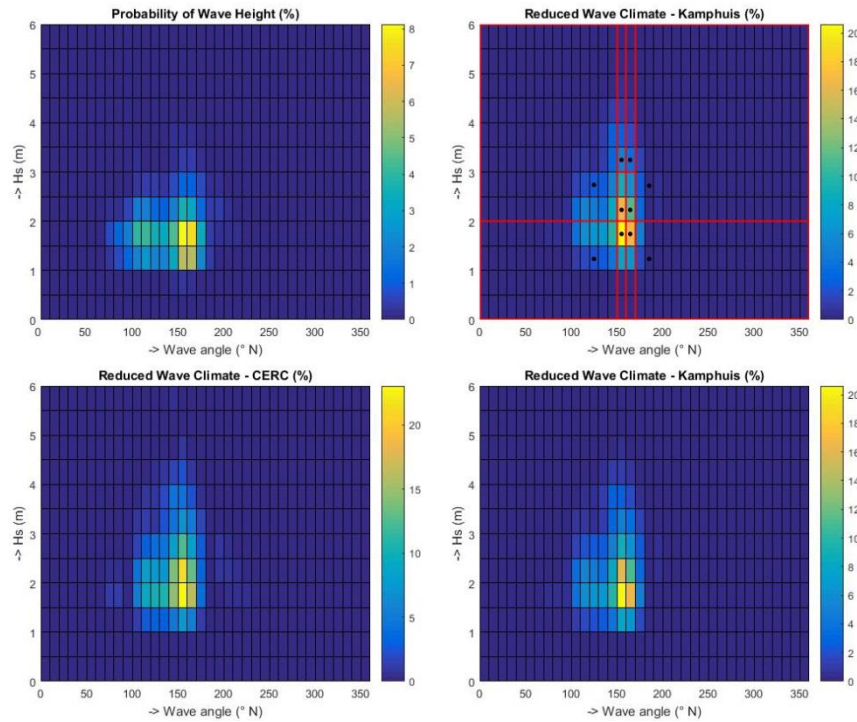


Figure 3.3: Probability of wave height (upper left), reduced wave climate (upper right) and sediment transport contribution (bottom)

The reduced wave climate consists of the following 10 wave conditions (Table 3.3):

Table 3.3: Reduced wave climate

Season	Wave condition	Hs (m)	Tp (s)	Dir [°]	Duration [days]	Morfac [-]
Summer (Nov – Mar)	1	1.5	11	160	5	10
	2	1.0	11	120	10	10
	3	2.5	11	120	0.8	10
Autumn (Apr – May)	4	1.5	11	150	5	10
	5	2.0	11	150	2	10
	6	3.0	11	150	0.4	10
Winter (Jun – Aug)	7	3.0	11	160	0.4	10
	8	2.0	11	160	2	10
Spring (Sep – Oct)	9	2.5	11	180	0.8	10
Summer	10	1.0	11	180	10	10

For stability of the model it is chosen to impose a wave angle that is slightly increasing. The significant wave height equals 1.6 m with corresponding peak period of 11.0 s. In the reduced wave climate wave heights are varied from 1.0 m to 3.0 m. The wave heights are higher during winter and autumn, while they are smaller and show more variability in direction during spring and summer. Wave periods are all set to 11.0 s, the mean peak period, in order to reduce computation time. The morphological acceleration factor (morfac) is used to simulate different time-scales between hydrodynamic and morphological developments as described by Lesser et al. (2009). The simulation time equals 36.4 days in hydrodynamic timescale which results in morphological time-scale of 364 days. The wave conditions, duration and morfac are chosen in such a way that the wave climate corresponds to Table 3.1. Further explanation is given in Appendix B.

4 Calibration

Model calibration is necessary in order to reproduce measurements and get reasonable results from the simulations. Parameters are adjusted in order to retrieve comparable results based on measured data. Scenario A is used for calibration of the model. This scenario represents the St Lucia Estuary with an open mouth configuration, no dredge spoil removed and re-linkage of the Mfolozi River.

The calibration is done in two parts. First the tide is analysed, the tidal prism and peak flows through the inlet are quantitatively calibrated to measured data. After this the model is run with tidal forcing and the reduced wave climate of 10 wave conditions to calibrate the model qualitative on inlet behaviour and quantitatively on the longshore sediment transport. The first part is simulated for a period of 30 days, a morfac of 10 and a spin-up time of 1 day. This results in a morphological time-scale of 300 days. The last part of the calibration; time-varying wave climate is simulated for 41.4 days. The spin-up time equals 5 days, which is included in the graphs that are shown in this report. The morfac is equal to 1 during the spin-up time and afterwards increased to 10 for the complete simulation time. This explained in more detail in paragraph 3.2.2.

4.1 Tidal forcing only

At first the model will be simulated with tidal forcing only. This is done to investigate if the model is able to reproduce measured data. The model is forced with a neap tidal range, mean tidal range and spring tidal range of 0.5 m, 1.3 m and 1.8 m respectively.

The parameters that are calibrated are the peak flows through the inlet and the tidal prism. The Chézy value is used to calibrate the model. The Chézy value is varied between 40 and 60 in order to optimize the model. A Chézy value of $50 \text{ m}^{1/2}/\text{s}$ approaches measurements the best. In Figure 4.1 the peak flows and water levels are given. The peak flows are around 185, 123, 41 m^3/s during flood currents and 141, 96, 35 m^3/s during ebb currents for a spring-, mean- and neap tidal range respectively. The water level in the estuary shows an elevation of 5 cm during spring tidal range.

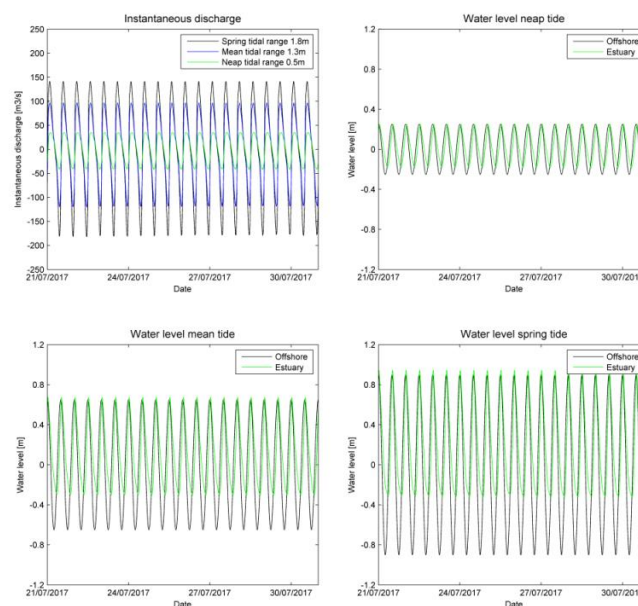


Figure 4.1: Clockwise: Peak flows through inlet and water levels during neap-, mean- and spring tidal range

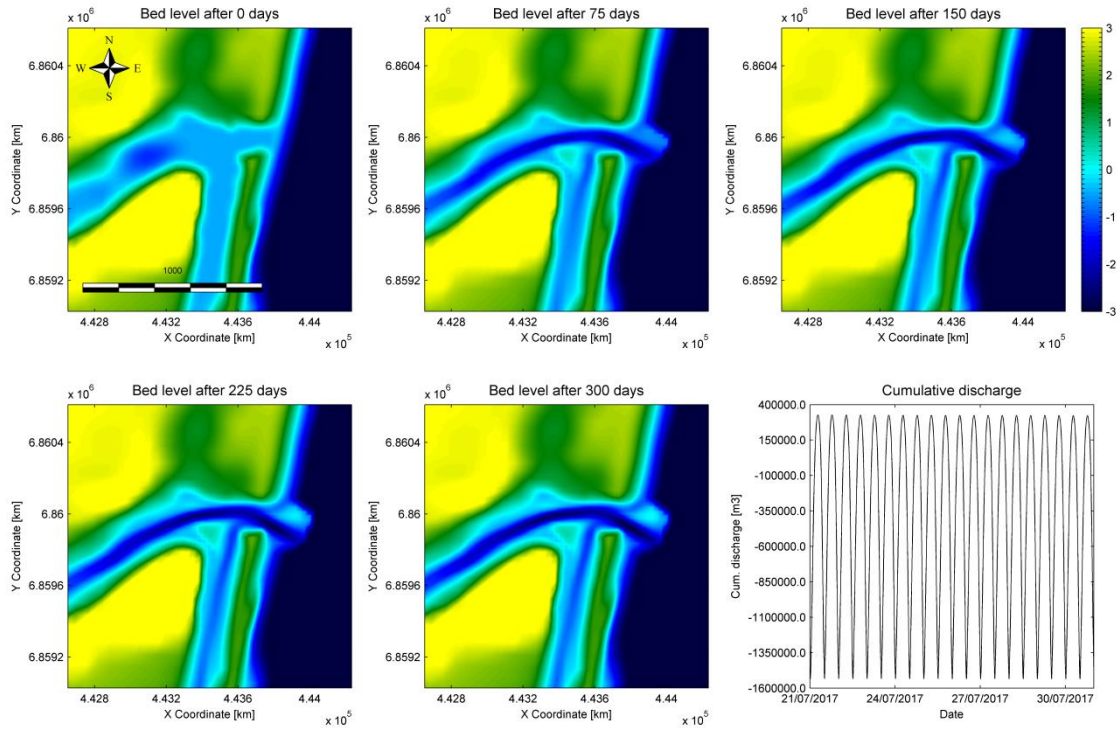


Figure 4.2: Bed level after 0 days, 75 days, 150 days, 225 days, 300 days and tidal prism for spring tidal range of 1.8 m

The change in bed level is visible in Figure 4.2. The formation of tidal flats in the flood-tidal delta is clearly visible. Two flood channels are formed; one entering the St Lucia Estuary and one towards the Mfolozi River. The tidal gorge is formed with a main ebb channel in direction of the Indian Ocean. At the northern side of the ebb-tidal delta a swash bar is formed. The tidal prism is approximately $1,860,000 \text{ m}^3$ which corresponds to measurements that have showed a tidal prism during spring tidal range of 1.6 to $2.08 \cdot 10^6 \text{ m}^3$.

In Figure 4.3 and Figure 4.4 the change in bed level and tidal prism is given for mean- and neap tidal range respectively. Both simulations show similar behaviour as the model forced with spring tidal range, however the inlets are less developed. This is observed by the flood-tidal delta, tidal gorge and ebb-tidal delta which are not as clearly visible. The tidal prism during mean tidal range is approximately $1,340,000 \text{ m}^3$. In literature the tidal prism for mean tide is around 0.8 to $1.0 \cdot 10^6 \text{ m}^3$. The tidal prism during neap tidal range equals $550,000 \text{ m}^3$, which corresponds to literature with values around $350,000$ to $800,000 \text{ m}^3$.

In Appendix C.1 the results obtained from varying the Chézy value are given. Although there are limited measurements from the St Lucia Estuary, the model reproduces the same order of magnitude of the peak flows and the flood dominant behaviour of the St Lucia Estuary is visible. This can be observed from the shorter rising water levels (flood period) and longer falling water levels (ebb period).

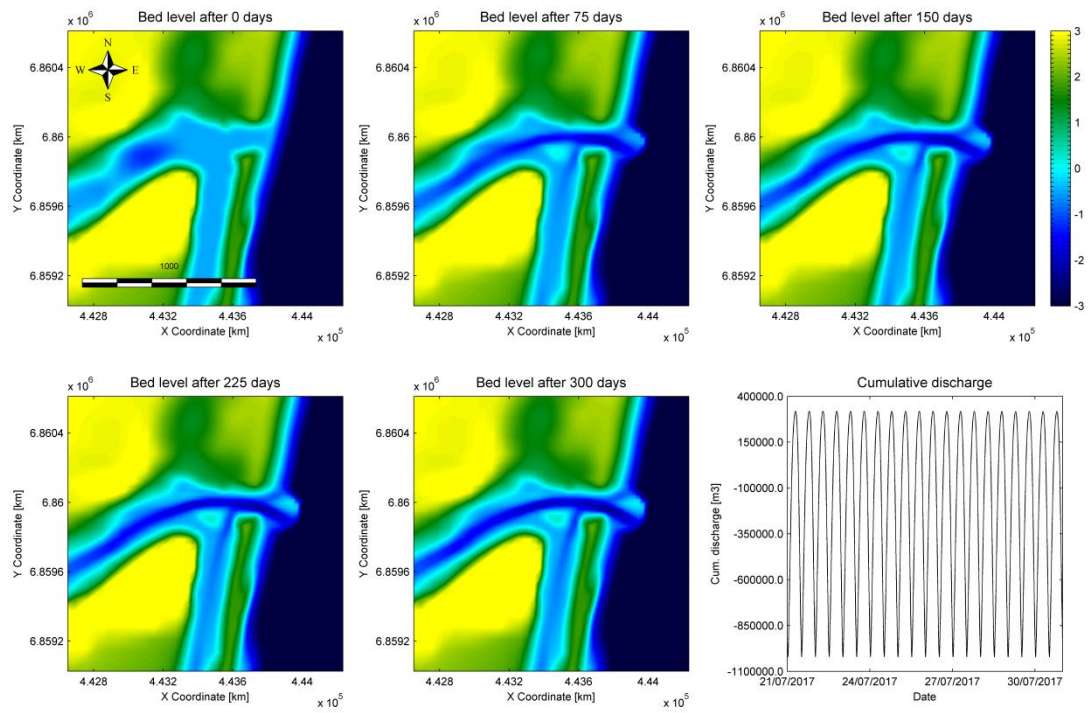


Figure 4.3: Bed level after 0 days, 75 days, 150 days, 225 days, 300 days and tidal prism for mean tidal range of 1.3 m

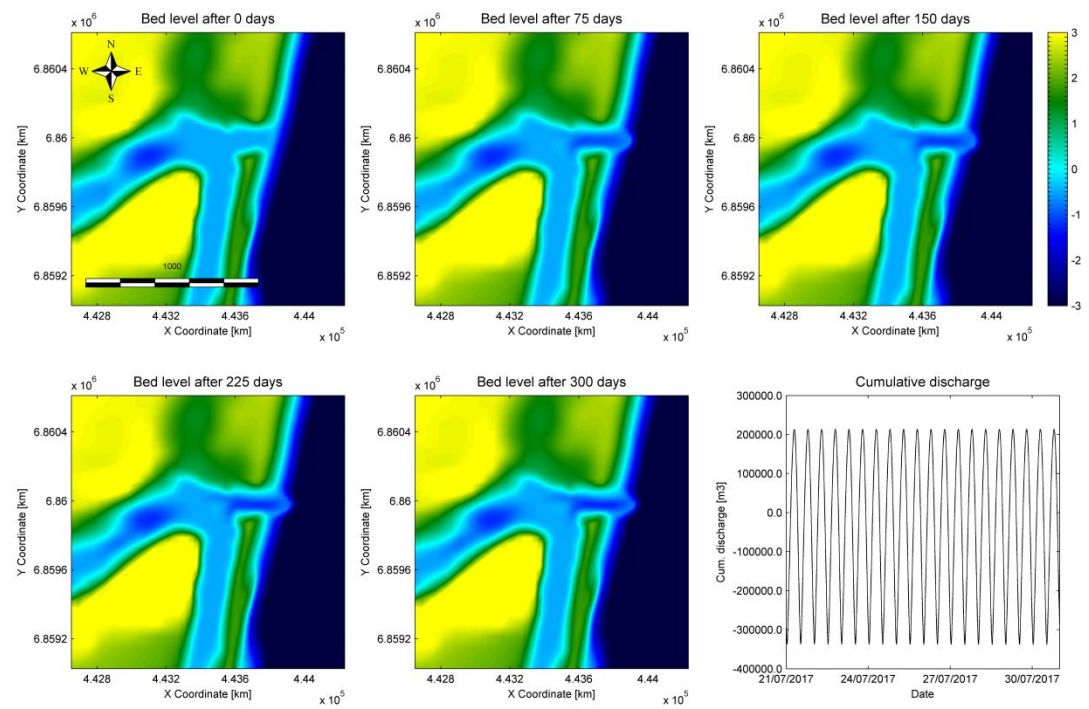


Figure 4.4: Bed level after 0 days, 75 days, 150 days, 225 days, 300 days and tidal prism for neap tidal range of 0.5 m

4.2 Time-varying wave climate

The model will be forced with the reduced wave climate as described in chapter 3.3. The wave heights are varied over the simulation period of 36.4 days. Each wave height has a different time scale in order to reproduce the frequency of occurrence of the original wave climate. A morphological acceleration factor of 10 is applied during the complete simulation. The model is simulated with a mean tidal range of 1.3 m, neap tidal range of 0.5 m and a spring tidal range of 1.8 m. The discharge from the Mfolozi River in this stage is still zero.

4.2.1 Mean tidal range

The morphological evolution of the estuary is given in Figure 4.5. After 38 days the formation of the flood tidal delta and the tidal gorge is visible. At seaward side the formation of the ebb tidal delta is not significant. The longshore transport and flood dominant system prevents the development of the ebb tidal delta. The tidal flat is increasing in size in the flood tidal delta in between two main channels heading into the St Lucia Estuary and the Mfolozi River. The estuary keeps importing sediments during the lower wave period; significant wave heights of 1.5 to 1.0 m. After 152 days the estuary almost closes as the tidal gorge has reached its maximum depth of 3.2 m (Figure 4.6). The inlet closes after 156 days, due to the longshore transport and formation of a spit at the updrift side of the inlet. The closure time approximates the real closure of the St Lucia inlet which closed after 175 days since it was breached by cyclone Gamede. The beach shows erosion at the end of the simulation, after 364 days, due to the higher wave events that start at 280 days. However, the high waves are not large enough to breach the inlet. The cumulative longshore sediment transport equals 482,000 m³/year at the southern side of the inlet and 411,000 m³/year at the northern side of the inlet. The water levels in the estuary range from a minimum of -0.2 m to 0.75 m. Water levels off shore range from -0.65 m to 0.65 m. The ratio between ocean and estuary is 0.73. Peak flows are varying from 110 to 90 m³/s during flood flows and 90 to 110 m³/s for ebb flows. The tidal prism equals approximately 1,300,000 m³. This results in a P/M ratio of 2.70. The inlet is unstable (intermittently closing) and corresponds to type 3.

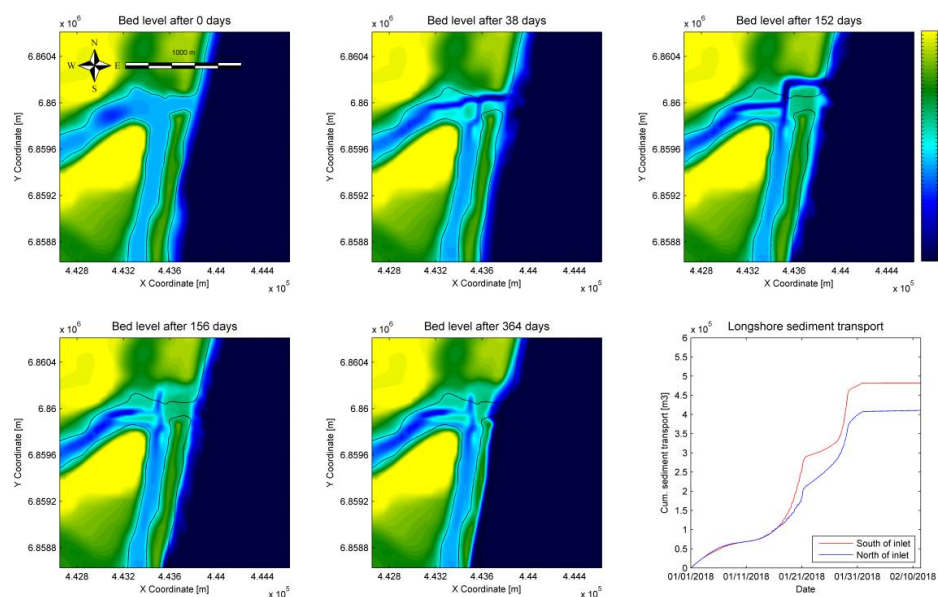


Figure 4.5: Bed level after 0 days, 38 days, 152 days, 156 days, 364 days and cumulative sediment transport along the coast for mean tidal range of 1.3 m

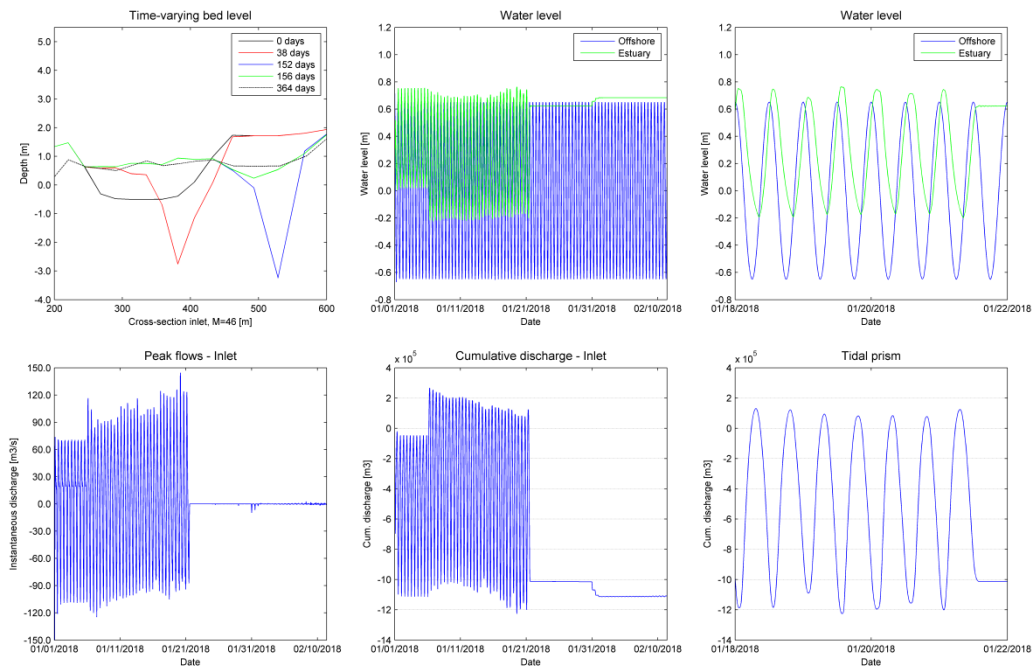


Figure 4.6: Time-varying bed level inlet, water level, detailed water level, peak flows, cumulative discharge through inlet and tidal prism for mean tidal range of 1.3 m

The water levels in the estuary and peak flows through the inlet are given in Figure 4.7. The first low water visible in the graph occurs at 20:45 and equals -0.20 m. Water levels start rising for a period of 4 hours and 15 min until a height of 0.69 m is reached at 01:00. After this water levels drop during a period of 7 hours and 50 min until a height of -0.20 m at 08:50. The first flood period visible in the graph starts after slack water occurring at 19:45. The flood period lasts until 01:03, which leads to a total flood duration of 5 hours and 18 minutes. The ebb period lasts from 01:03 until 07:46, leading to an ebb duration of 6 hours and 43 minutes.

The shorter rising periods indicate a flood dominant system. Likewise a shorter flood period is also property of flood dominant estuaries. The ebb period ends at 07:18 before the lowest water level is reached (occurs at 08:30), and then the flood period starts again. This causes the elevated water levels in the estuary. As described in chapter 2.5.1 this is a property of estuaries along the South African coast. It can be concluded that the St Lucia Estuary without river discharge is clearly flood dominant.

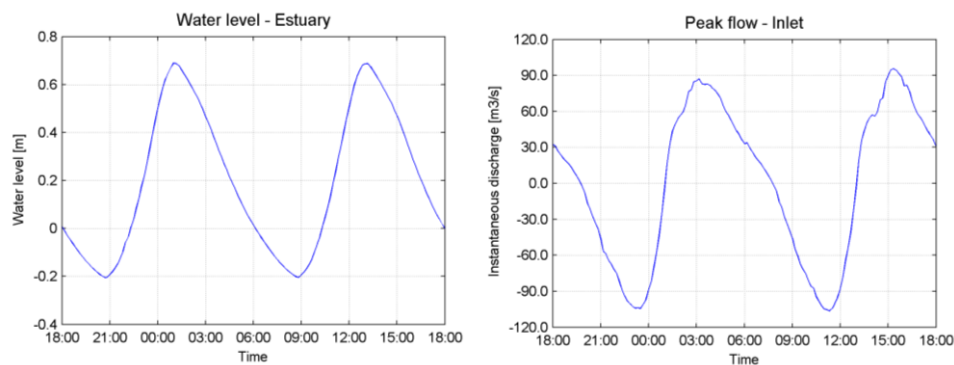


Figure 4.7: Water level and peak flows during two tidal cycles from 9/1/2018 18:00 to 10/1/2018 18:00

Currently the model is forced with a time-varying wave climate starting with smaller waves for the duration of 150 days after which larger waves start occurring during the summer season. To test the sensitivity of the model the order of occurrence is changed; the wave climate will start with higher waves and end with smaller waves. The results of this simulation are given in Appendix C.2. The beach erodes in the beginning during the presence of higher waves leading to widening of the inlet. During the simulation of 364 days the inlet stays open. Corbella and Stretch (2012a) investigated shoreline recovery from storms and they found an average recovery period of approximately 2 years. To investigate the closure times of the inlet it is preferred to start with smaller wave heights. The wave related factor is also varied to show the sensitivity of the model and the importance of this parameter to approach an equilibrium beach width.

4.2.2 Neap tidal range

The inlet is forced with a neap tidal range of 0.5 m and a time-varying wave climate. The morphological evolution of the estuary is given in Figure 4.9. After 18 days the inlet has imported a large quantity of sediments and a spit is formed at the downdrift side. The tidal gorge bends in northern direction at the ebb tidal delta, caused by the direction of the longshore transport. The tidal gorge reaches a depth of 1.6 m (Figure 4.10). The cumulative longshore sediment transport along the coast equals 472,000 m³/year at the southern side of the inlet and 381,000 m³/year at the northern side of the inlet. The difference between the northern – and southern side during neap tide is larger than during mean tide. This shows that the coastline accretes more during smaller tidal ranges. After 22 days the inlet is closed completely and until approximately 150 days the coastline accretes. The inlet closes after flood tide before the ebb tide occurs. The water levels in the estuary stay elevated at a height of 0.35 m. The higher waves during the summer season erode the beach, but the inlet remains closed with a berm height of 0.3 m above MSL. The hydrodynamic results are given in Figure 4.10. The water levels in the estuary range from -0.10 m to 0.30 m. Offshore the water levels range from -0.25 m to 0.25 m. The ratio between the oceanic tidal range and estuarine tidal range equals 0.80. Peak flows are varying from 40 to 35 m³/s during flood flows and 50 m³/s during ebb flows. The tidal prism equals approximately 580,000 m³. This results in a P/M ratio of 1.23. The inlet is unstable (intermittently closing) and corresponds to inlet type 3.

In reality the inlet closed during neap tide which can be observed in Figure 4.8. The inlet was breached in March 2007 due to a rare combination of equinox spring high tides, strong onshore winds and extreme wave heights driven by the tropical cyclone Gamede near Madagascar. The mouth remained open for a period of 6 months after it closed naturally. The model has a total closure time of 94% during the simulation forced with a neap tidal range. The low tidal range is not capable of maintaining an open inlet.

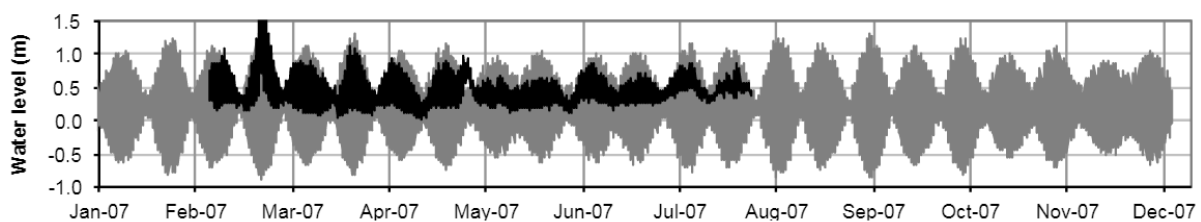


Figure 4.8: Samples of water level time series from a regional tide gauge and from a water level recorder in the St Lucia Estuary in the year 2007 (Chrystal & Stretch, 2014)

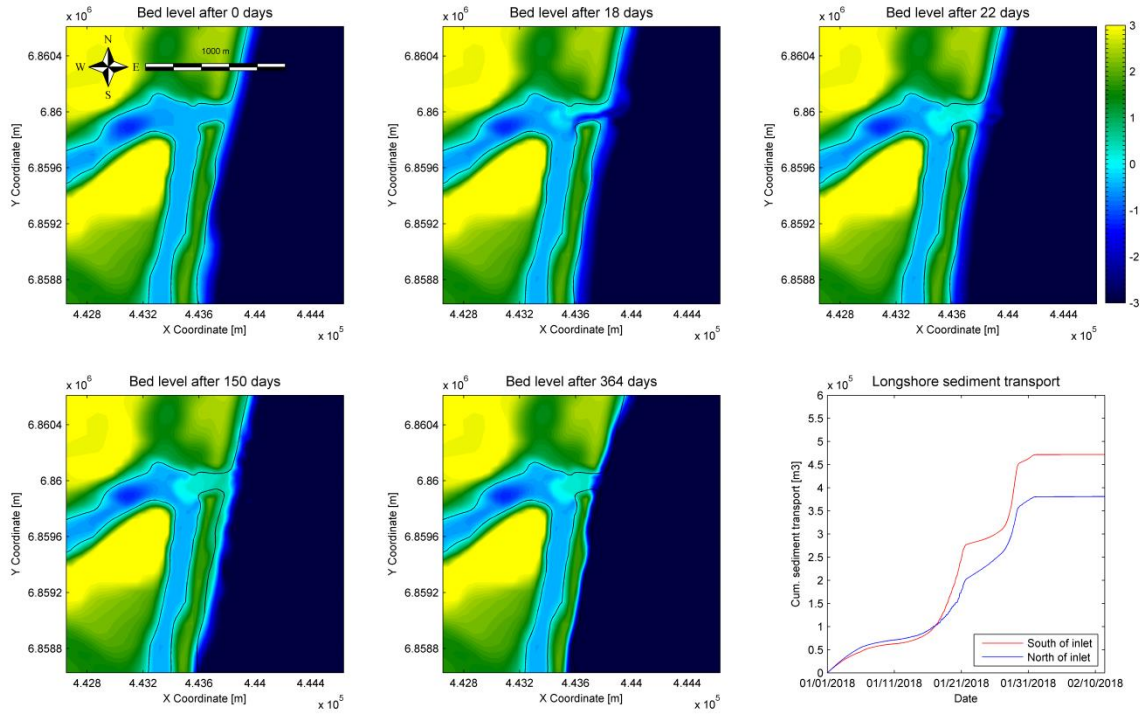


Figure 4.9: Bed level after 0 days, 18 days, 22 days, 150 days, 364 days and cumulative sediment transport along the coast for neap tidal range of 0.5 m

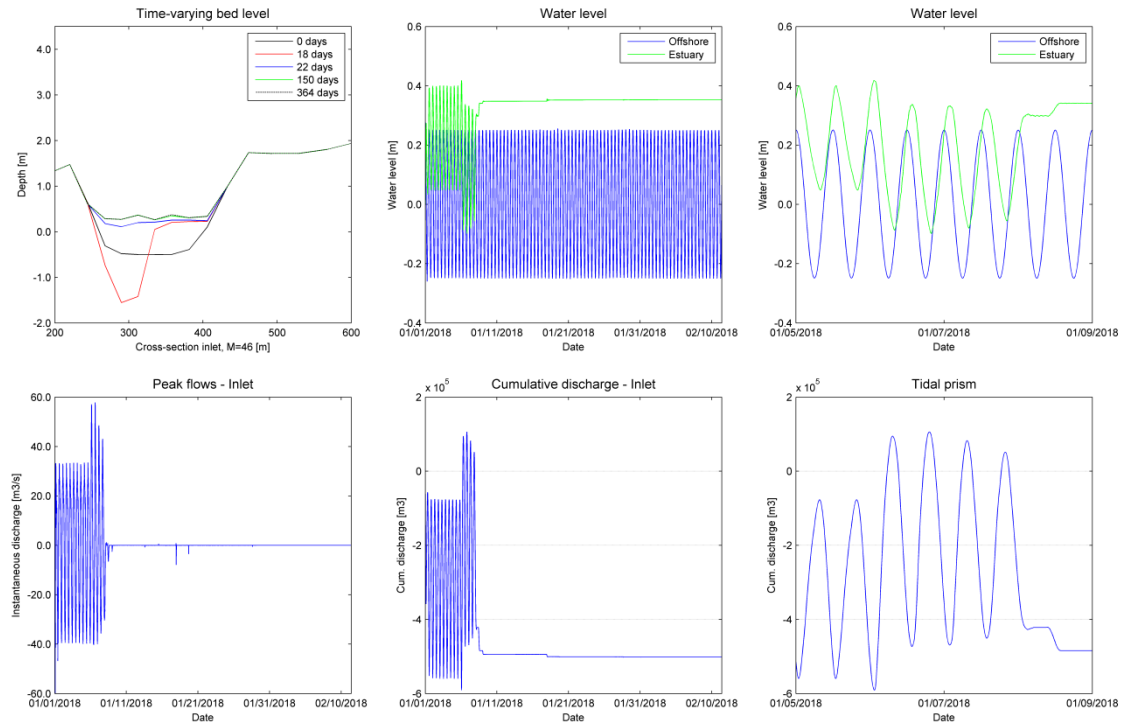


Figure 4.10: Time-varying bed level inlet, water level, detailed water level, peak flows, cumulative discharge through inlet and tidal prism for neap tidal range of 0.5 m

4.2.3 Spring tidal range

The morphological evolution of the tidal inlet during spring tidal range is given in Figure 4.11. During the complete simulation time the inlet stays open. From the start of the simulation the formation of a spit at the updrift side of the inlet is visible migrating inland of the estuary. The dredge spoil area accretes and becomes larger in size surrounded by two main channels directed towards the St Lucia Estuary and the Mfolozi River. Onwards from 92 days the inlet starts migrating further north due to the change in wave direction. The inlet migrates 390 m in northern direction (Figure 4.12). The larger waves during summer season in combination with high tidal range lead to a lot of erosion and widening of the inlet after 267 days. Until the end of the simulation smaller waves, significant wave height of 1.0 m, from an angle of 180°N result in almost no alongshore sediment transport and migration of the inlet in southern direction. The cumulative longshore sediment transport is 515,000 m³/year at the southern side of the inlet and 482,000 m³/year at the northern side of the inlet.

The hydrodynamic results are shown in Figure 4.12. The water levels in the estuary range from a minimum of -0.25 m to -0.35 m to a maximum of 1.0 m. During periods of high waves the water levels are elevated up to 1.1 m. Water levels off shore range from -0.90 m to 0.90 m. The ratio between ocean and estuary is 0.69. Peak flows are varying from 140 to 160 m³/s during flood flows and 150 to 130 m³/s for ebb flows. The tidal prism equals approximately 1,750,000 m³. This results in a P/M ratio of 3.40. This P/M ratio corresponds to an inlet type 3 that is unstable and intermittently closing. However, during the simulation the inlet does not seem to close. This might be due to high waves in combination with a spring tidal range that causes the severe erosion of the inlet; visible from the period from 202 days until 364 days where the inlet widens from 80 m to 230 m at MSL. After the summer season with high wave action the main channel from the tidal gorge increases slightly from 230 m to 250 m after the 267 days and migrates 150 m southwards towards its initial position.

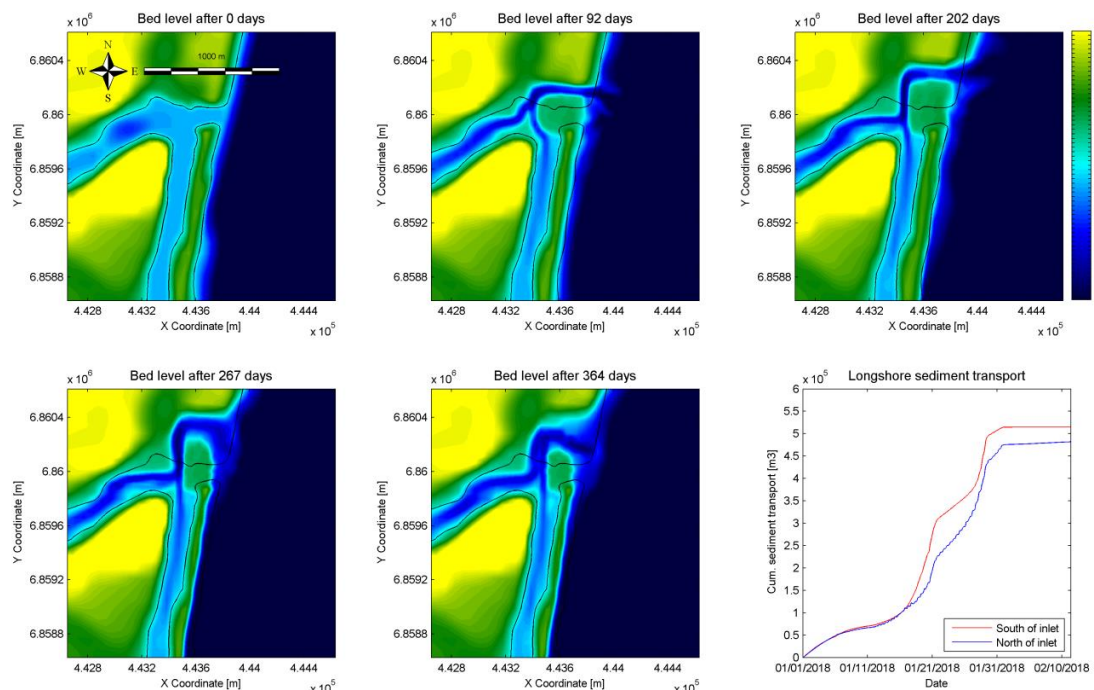


Figure 4.11: Bed level after 0 days, 92 days, 202 days, 267 days, 364 days and cumulative sediment transport along the coast for spring tidal range of 1.8 m

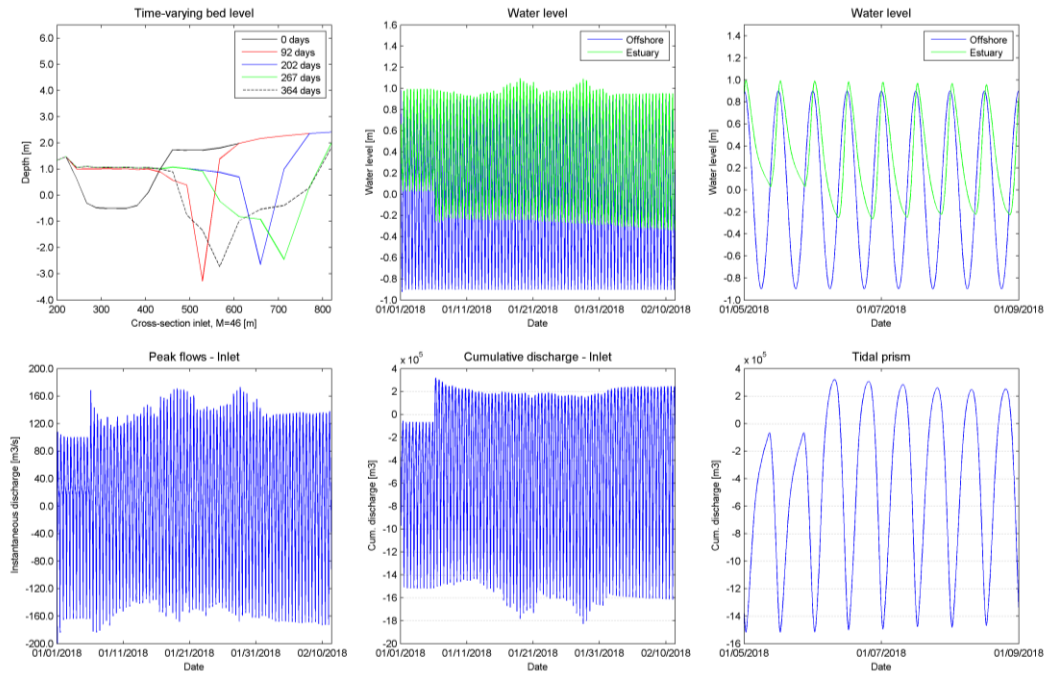


Figure 4.12: Time-varying bed level inlet, water level, detailed water level, peak flows, cumulative discharge through inlet and tidal prism for spring tidal range of 1.8 m

4.3 Conclusions

In this chapter the model is calibrated. The model is capable of reproducing measured field data and the morphological evolution of the inlet looks similar as the observed behaviour of the inlet in reality.

From the simulations with tidal forcing the following conclusions are made:

- Morphological evolution of the inlet is clearly visible during mean tidal range and spring tidal range. The development of the flood tidal delta, tidal gorge and ebb tidal delta is observed.
- Tidal prisms of the simulations during spring tidal range is 1,860,000 m³ (literature 1,6 to 2,08*10⁶ m³), during mean tidal range is 1,340,000 m³ (literature 0,8 to 1,0*10⁶ m³) and during neap tidal range 550,000 m³ (literature 350,000 to 800,000 m³).
- A Chézy value of 50 m^{1/2}/s approaches measurements the best, although the results have small variations.

The model simulations forced by the reduced wave climate give the following results:

- The current related transport factor equal to 20 does reproduce the longshore transport when the reduced wave climate is used, approximately 500,000 m³/year. The wave related factor equal to 0.31 reproduces accretion during small waves and erosion during high waves.
- The St Lucia inlet migrates 390 m northwards during spring tidal range, which is similar to observation with Google Earth of the migration of the Mfolozi mouth (300 - 400 m/year).
- The inlet closes after 156 and 22 days while forced with mean – and neap tidal range respectively. In March 2007 the inlet breached by Cyclone Gamede and closed naturally after 175 days.
- P/M ratios are 1.23, 2.70 and 3.40 for neap –, mean – and spring tidal range respectively. This corresponds to an inlet type 3 that is unstable and closes intermittently.

5 Results

5.1 Scenario A: Re-linkage Mfolozi River

In the previous chapter the model is calibrated and shows similar behaviour as the St Lucia Estuary when compared to reality. In this chapter the result of re-linkage of the Mfolozi River is investigated. The discharge of the Mfolozi River is varied from 2 m³/s to 30 m³/s. The discharge of 2 m³/s corresponds to the average discharge in winter. After this the discharge is increased to 5 m³/s which corresponds to the average discharge during drought periods. Thirdly, the discharge is simulated for the summer season where the average discharge equals 14 m³/s. Finally the river discharge is increased to 30 m³/s, which is equal to the mean annual runoff (MAR) of the Mfolozi River.

5.1.1 Mfolozi River with discharge of 2 m³/s (Winter)

5.1.1.1 Mean tidal range

The model is simulated with a river discharge of 2 m³/s from the Mfolozi River. This discharge is equal to a yearly runoff of $63.1 \cdot 10^6$ m³, which is 7% of the MAR. In previous simulation where the discharge from the Mfolozi River was zero the inlet closed after 156 days. When the Mfolozi River discharge is increased to 2 m³/s the inlet closes again after 156 days, but reopens after 21 days. The inlet closes during the first period of high wave action, significant wave heights of 2.5 m. The longshore current which increases during this period causes the narrow tidal gorge to close. The morphological evolution of the inlet is visible in Figure 5.1. At first instance two channels are present surrounding the tidal flat in the flood tidal delta. However, after 48 days the northern channel starts to accrete and eventually closes of completely. The flood tidal delta disappears and attaches to the landside. The tidal gorge migrates 90 m in southern direction due to the spit that is growing at the downdrift side of the inlet and erosion at the updrift side. The inlet is locationally stable, but widens drastically after being eroded by high wave action lasting from 208 – 264 days. The tidal gorge reaches a depth of 3.0 m and a width of 400 m (Figure 5.2). The cumulative transport along the coast equals 473,000 m³/year at the southern side of the inlet and 409,000 m³/year at the northern side.

The hydrodynamic results are given in Figure 5.2. The water levels in the estuary vary between -0.20 m to 0.70 m. During periods of high wave action water levels in the estuary rise up to 0.85 m, which is an elevation of 0.20 m compared to oceanic water levels. The offshore water levels vary between -0.65 m to 0.65 m. The ratio between the water levels in the estuary compared to ocean equals 0.69. Peak flows are varying from 120 to 90 m³/s during both flood flows and ebb flows. Due to the river discharge the tidal prism during ebb tide differs from the tidal prism during flood tide. The ebb tidal prism equals 1,450,000 m³ and the flood tidal prism equals 1,360,000 m³. This difference is almost equal to the discharge of the Mfolozi River over one tidal period, which equals 86,400 m³. The P/M ratio is equal to 3.07, which corresponds to an inlet type 3 that is unstable and intermittently closing. The tidal prism increased with 12% compared to the simulation with no discharge from the Mfolozi River. The inlet reopens after 176 days in contrast to the simulation with no river discharge. The total closure time decreased from 57% with no river discharge to 6% with a discharge equal to 2 m³/s.

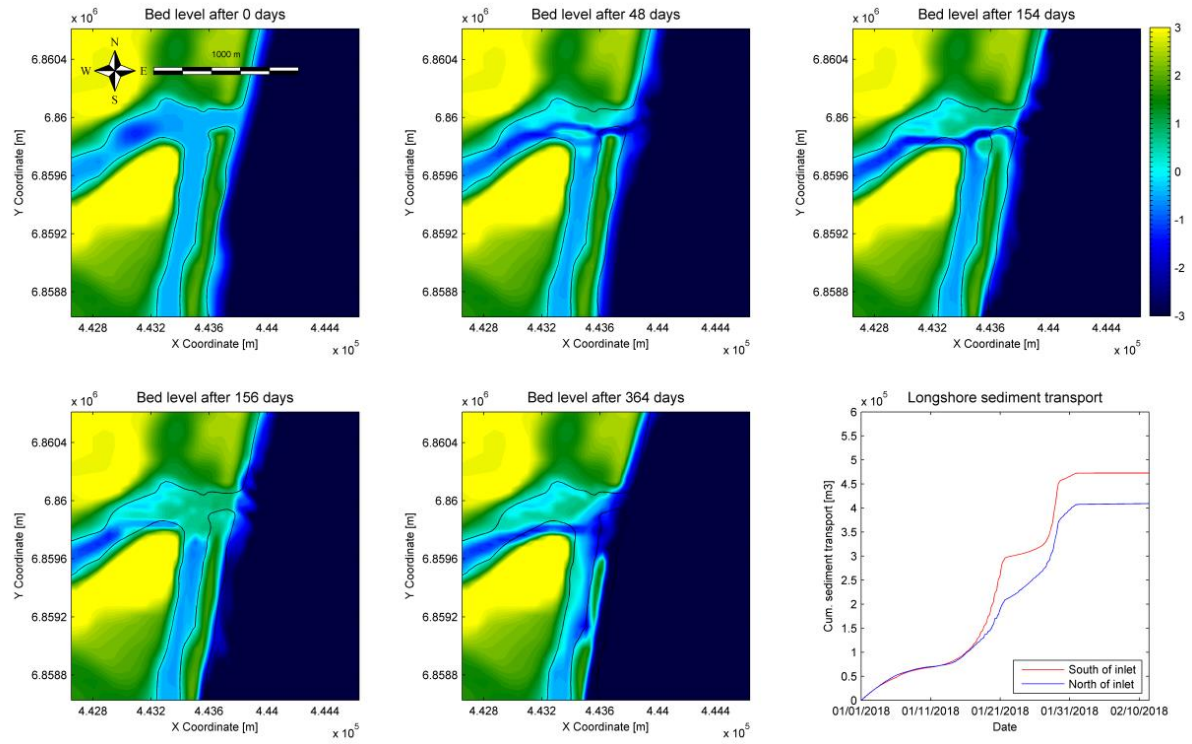


Figure 5.1: Bed level change 0 days, 48 days, 154 days, 156 days, 364 days and cumulative sediment transport along the coast for mean tidal range of 1.3 m

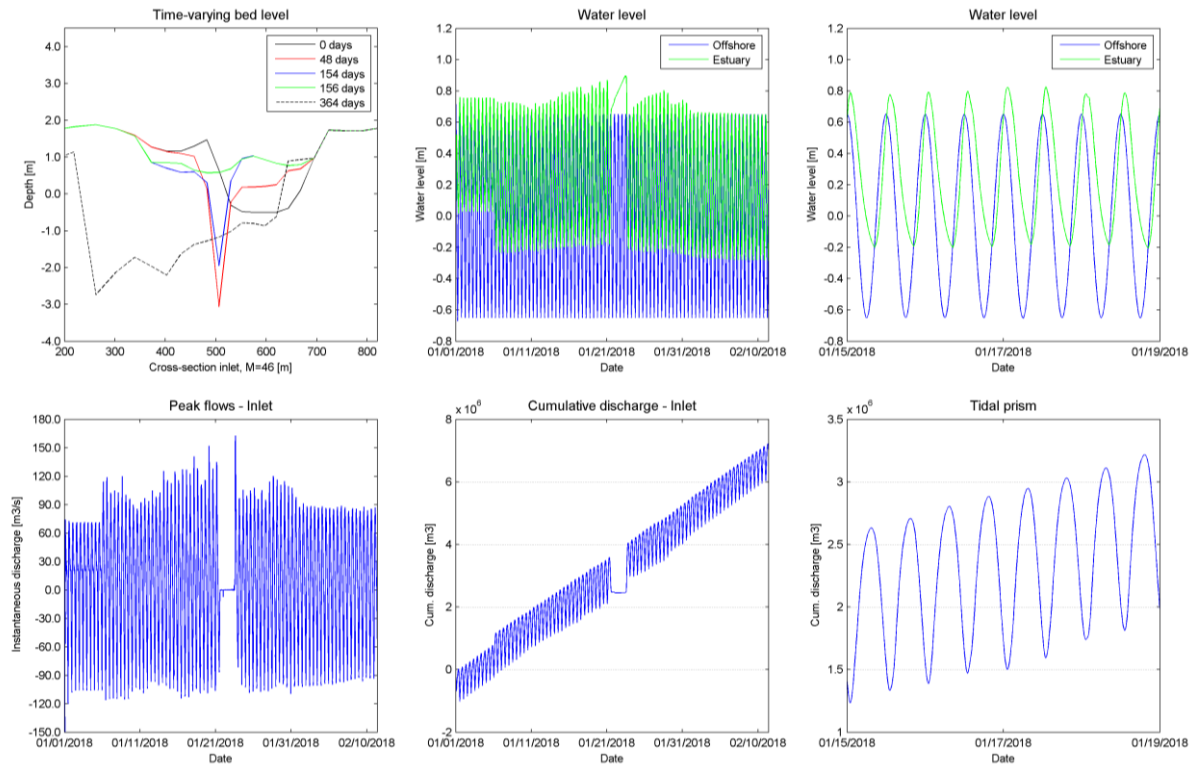


Figure 5.2: Time-varying bed level inlet, water level, detailed water level, peak flows, cumulative discharge through inlet and tidal prism for mean tidal range of 1.3 m

5.1.1.2 Neap tidal range

The morphological evolution of the inlet forced with neap tidal range and a discharge of $2 \text{ m}^3/\text{s}$ is given in Figure 5.3. In previous simulations without river discharge the inlet closed after 22 days. In this simulation the inlet closes four times during the follow periods: 51.3 – 83.8 days, 105.4 – 103.4 days, 135.8 – 164.2 days and 225 – 245 days. The inlet is closed for a total of 105.9 days. The inlet does not migrate a lot; after 93 days the mouth has migrated 50 m northwards and after one year it has moved back in southern direction 100 m with respect to its initial position. At the end of the simulation large wave action caused the inlet to breach and widen the inlet up to 160 m. The tidal gorge reaches a depth of 2.2 m after 93 days (Figure 5.4). The cumulative transport along the coast equals $466,000 \text{ m}^3/\text{year}$ at the southern side of the inlet and $367,000 \text{ m}^3/\text{year}$ at the northern side.

The hydrodynamic results are given in Figure 5.4. The water levels in the estuary vary between -0.10 m to 0.35 m . The water levels in the estuary reach 0.75 m while the inlet is closed and water from the Mfolozi River is flowing into the estuary. The offshore water levels vary between -0.25 m to 0.25 m . The ratio between the water levels in the estuary compared to ocean equals 0.90 . Peak flows are varying from $35 \text{ m}^3/\text{s}$ during flood flows and 50 to $35 \text{ m}^3/\text{s}$ for ebb flows. When the inlet breaches peak flows up to $120 \text{ m}^3/\text{s}$ are reached. Due to the river discharge the tidal prism during ebb tide differs from the tidal prism during flood tide. The ebb tidal prism equals approximately $620,000 \text{ m}^3$ and the flood tidal prism equals $510,000 \text{ m}^3$. The P/M ratio is equal to 1.33 , which corresponds to an inlet type 3 that is unstable and intermittently closing. The tidal prism increased with 7% compared to the simulation with no discharge from the Mfolozi River.

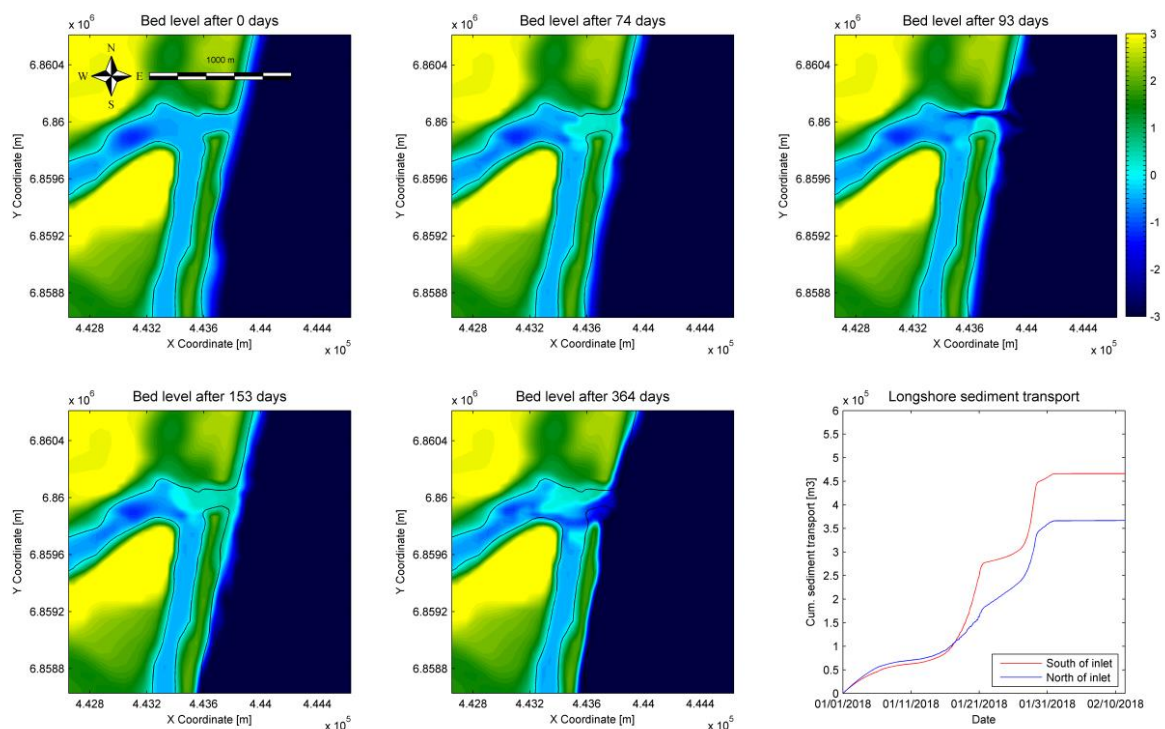


Figure 5.3: Bed level after 0 days, 74 days, 93 days, 153 days, 364 days and cumulative sediment transport along the coast for neap tidal range of 0.5 m

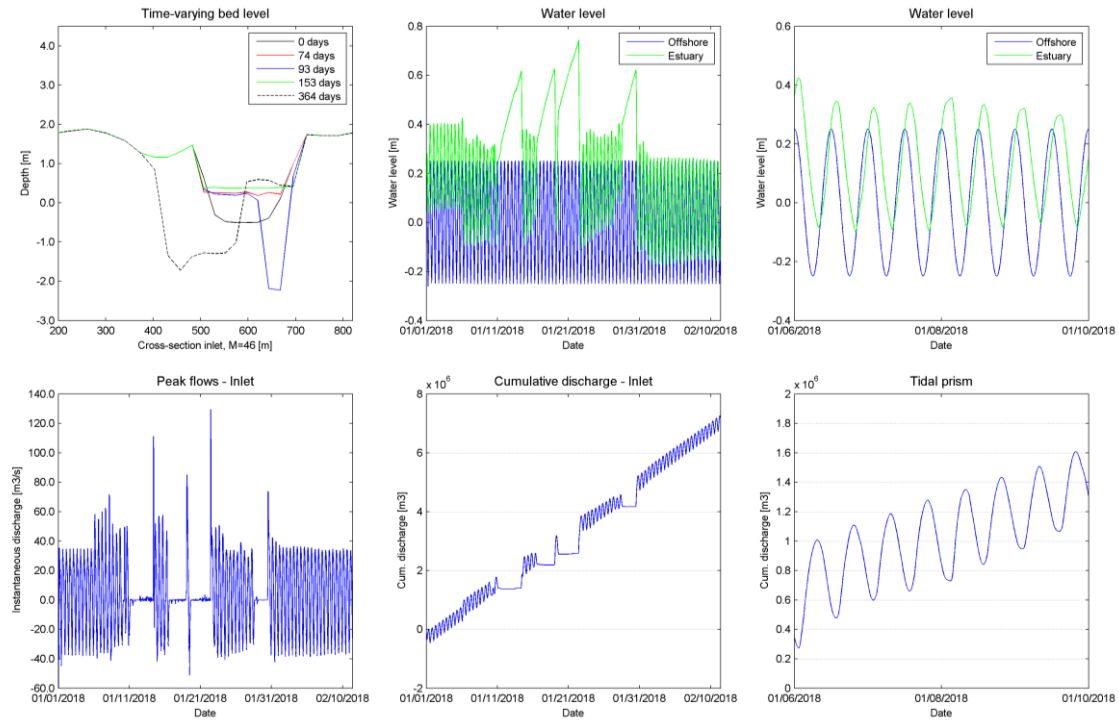


Figure 5.4: Time-varying bed level inlet, water level, detailed water level, peak flows, cumulative discharge through inlet and tidal prism for neap tidal range of 0.5 m

5.1.1.3 Spring tidal range

The morphological evolution of the inlet forced with spring tidal range and a discharge of $2 \text{ m}^3/\text{s}$ is given in Figure 5.5. In previous simulations without river discharge the inlet remained open due to the high tidal range. At first instance the inlet remains locationally stable. The formation of a spit at the updrift side of the inlet is visible migrating inland of the estuary. The dredge spoil area accretes and becomes larger in size surrounded by two main channels directed towards the St Lucia Estuary and the Mfolozi River. This behaviour corresponds to the previous simulation without river discharge. Onwards from 42 days the inlet starts migrating due to the change in wave direction. The inlet migrates 330 m in northern direction (Figure 5.6), which is less than the 390 m when no river flow was present. The larger waves during summer season in combination with high tidal range lead to a lot of erosion and widening of the inlet up to 230 m after 267 days. Until the end of the simulation smaller waves, significant wave height of 1.0 m, from an angle of 180°N result in almost no alongshore sediment transport and 150 m migration of the inlet in southern direction. The cumulative longshore sediment transport is $542,000 \text{ m}^3/\text{year}$ at the southern side of the inlet and equal to $521,000 \text{ m}^3/\text{year}$ at the northern side of the inlet.

The hydrodynamic results are given in Figure 5.6. The water levels in the estuary vary between -0.30 m to 0.95 m . The offshore water levels vary between -0.90 m to 0.90 m . The ratio between the water levels in the estuary compared to ocean equals 0.69. Peak flows are around $150 \text{ m}^3/\text{s}$ during both flood flows and ebb flows. The ebb tidal prism equals $2,010,000 \text{ m}^3$ and the flood tidal prism equals $1,820,000 \text{ m}^3$. The P/M ratio is equal to 3.71, which corresponds to an inlet type 3 that is unstable and intermittently closing. The tidal prism increased with 15% compared to the simulation with no discharge from the Mfolozi River.

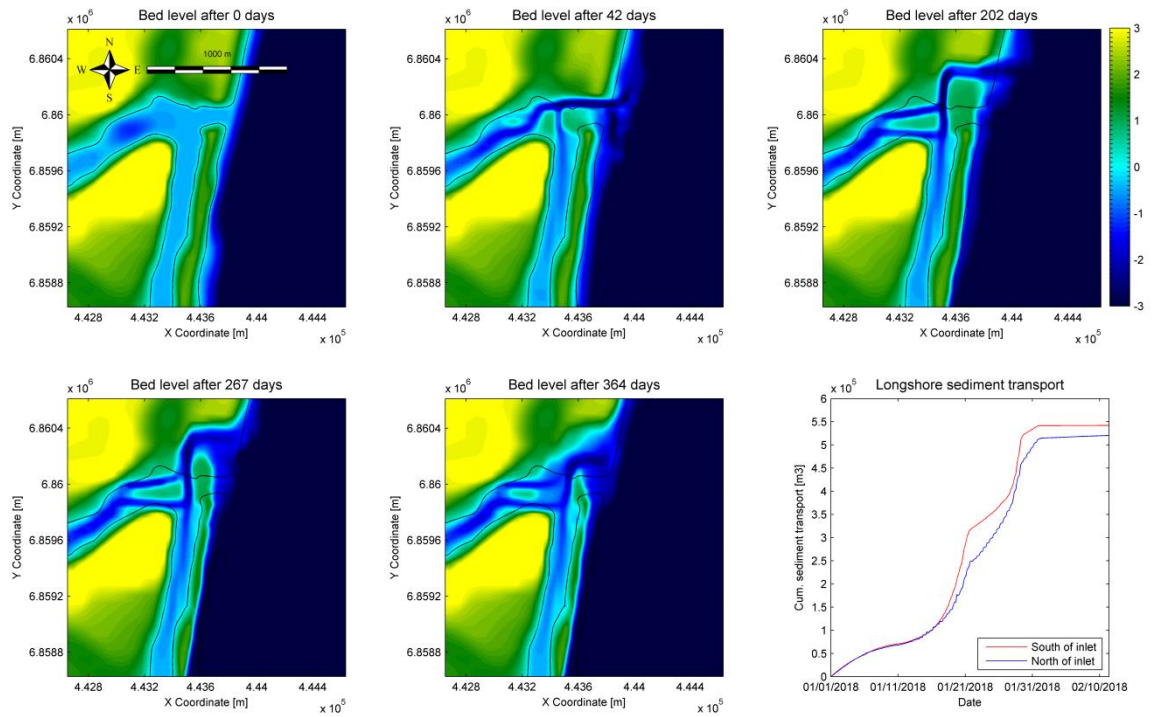


Figure 5.5: Bed level after 0 days, 42 days, 202 days, 267 days, 364 days and cumulative sediment transport along the coast for spring tidal range of 1.8 m

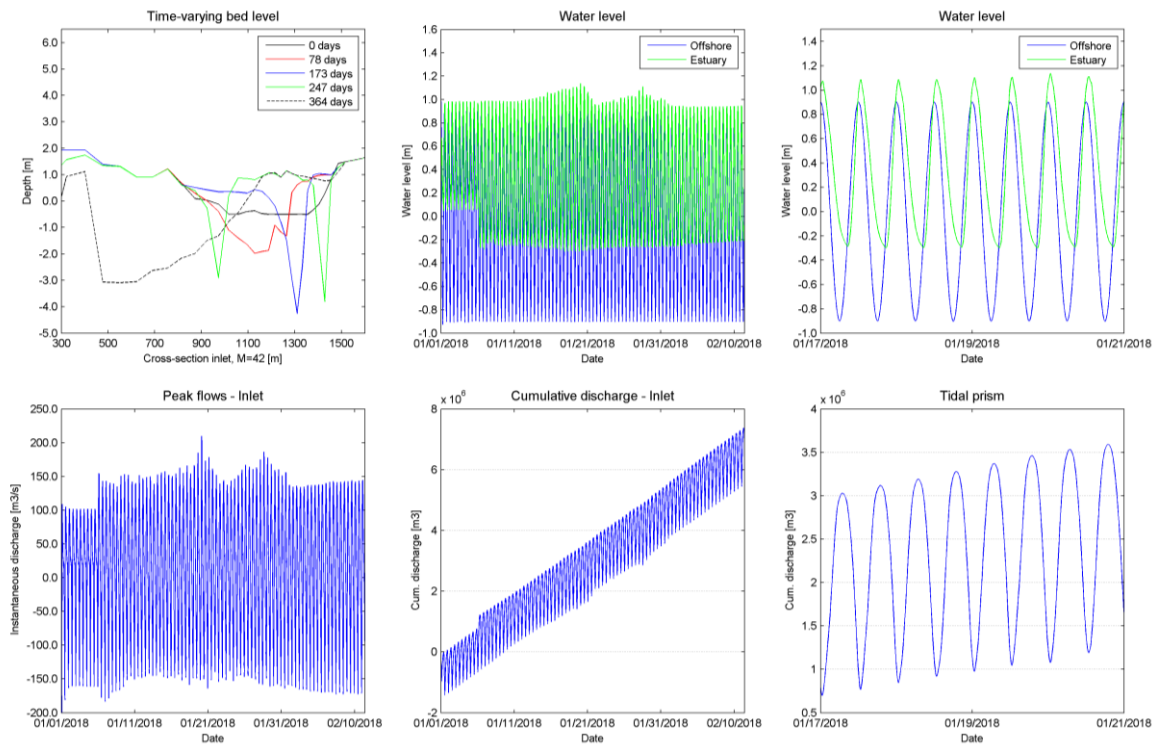


Figure 5.6: Time-varying bed level inlet, water level, detailed water level, peak flows, cumulative discharge through inlet and tidal prism for spring tidal range of 1.8 m

5.1.2 Mfolozi River with discharge of 5 m³/s (Drought)

5.1.2.1 Mean tidal range

The model is simulated with a river discharge of 5 m³/s from the Mfolozi River. This discharge is equal to a yearly runoff of $157.7 \cdot 10^6$ m³, which is 17% of the MAR. In the initial simulation where the discharge from the Mfolozi River was zero the inlet closed after 156 days. When the Mfolozi River discharge is increased to 5 m³/s the inlet closes twice, from 155.4 to 159.6 days and 160 to 160.8 days. The inlet is closed for a total duration of 5 days. The morphological evolution of the inlet is visible in Figure 5.7. At first instance two channels are present surrounding the tidal flat in the flood tidal delta. However, after 47 days the northern channel starts to accrete and eventually closes of completely. The flood tidal delta disappears and attaches to the landside. In the first 47 days the tidal gorge migrates 80 m in northern direction due to the spit that is growing at the updrift side of the inlet and erosion at the downdrift side. After reopening the inlet widens up to 380 m due to high wave action and migrates 230 m in southward direction with respect to its starting position. The tidal gorge reaches a maximum depth of 3.5 m (Figure 5.8). The cumulative transport along the coast equals 467,000 m³/year at the southern side of the inlet and 412,000 m³/year at the northern side.

The hydrodynamic results are given in Figure 5.8. The water levels in the estuary vary between -0.20 m to 0.70 m. During periods of high wave action water levels in the estuary rise up to 0.85 m, which is an elevation of 0.20 m compared to oceanic water levels. The offshore water levels vary between -0.65 m to 0.65 m. The ratio between the water levels in the estuary compared to ocean equals 0.69. Peak flows are varying from 120 to 90 m³/s for both flood – and ebb flows. The ebb tidal prism equals 1,520,000 m³ and the flood tidal prism equals 1,290,000 m³. This difference is approximately equal to the discharge of the Mfolozi River over one tidal period, which equals 216,000 m³. The P/M ratio is equal to 3.25, which corresponds to an inlet type 3 that is unstable and intermittently closing.

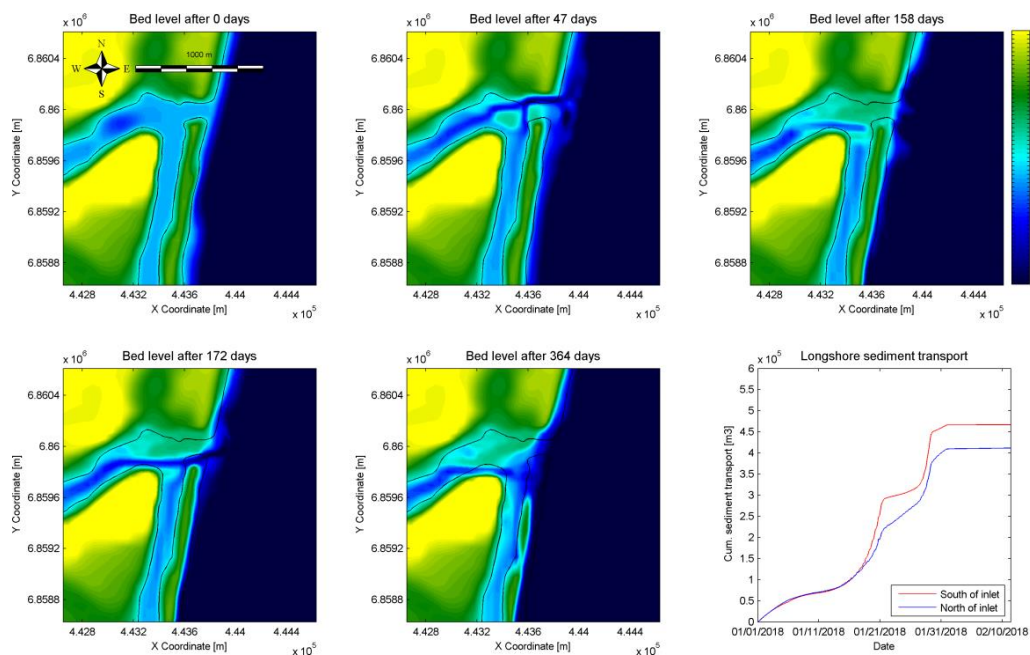


Figure 5.7: Bed level after 0 days, 47 days, 158 days, 172 days, 364 days and cumulative sediment transport along the coast for mean tidal range of 1.3 m

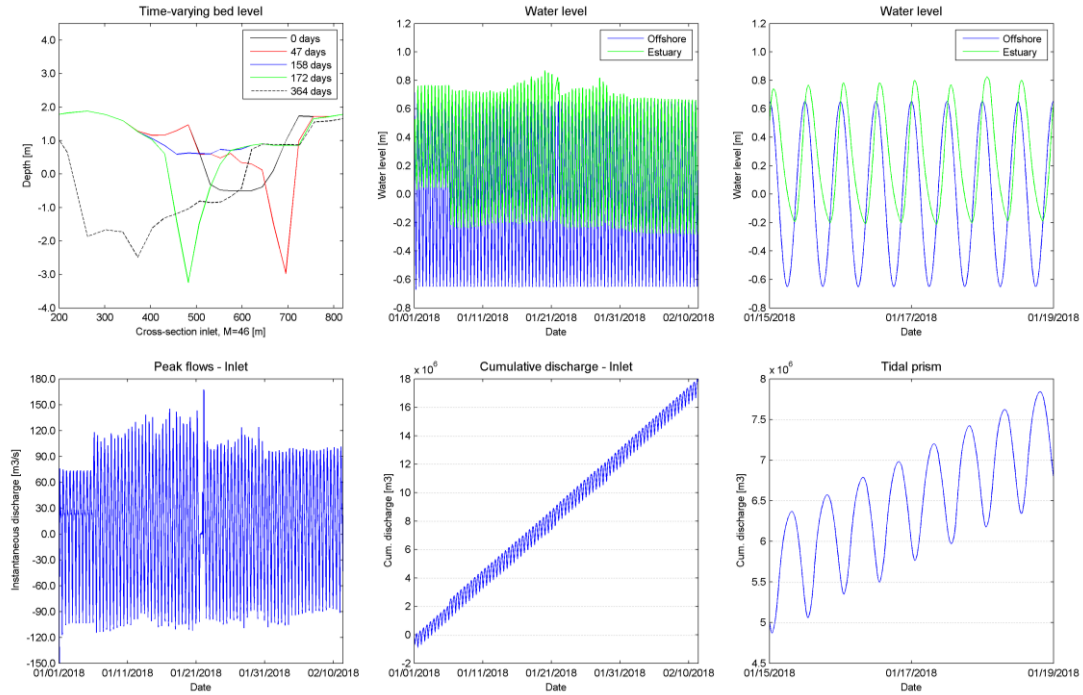


Figure 5.8: Time-varying bed level inlet, water level, detailed water level, peak flows, cumulative discharge through inlet and tidal prism for mean tidal range of 1.3 m

5.1.2.2 Neap tidal range

The morphological evolution of the inlet forced with neap tidal range and a discharge of $5 \text{ m}^3/\text{s}$ is given in Figure 5.9. In previous simulations without river discharge the inlet closed after 22 days. In this simulation the inlet closes 9 times, mainly during ebb periods, in the periods between 60.4 – 63.8 days, 65.4 – 67.1 days, 70.0 – 70.8 days, 87.9 – 91.7 days, 95.4 – 105.8 days, 130 – 139.6 days, 145.4 – 154.6 days, 225 – 227.1 days and 230 – 235.8 days. The inlet is closed for a total of 46.8 days. Water levels in the estuary built up 0.68 m due to river flow from the Mfolozi that enters the St Lucia Estuary. The inlet behaves as a type 3 inlet that is locationally stable and closes intermittently. At the end of the simulation the channel towards the St Lucia Estuary is prone to close. The tidal gorge reaches a depth of 2.6 m after 247 days (Figure 5.10). The cumulative transport along the coast equals $468,000 \text{ m}^3/\text{year}$ at the southern side of the inlet and $380,000 \text{ m}^3/\text{year}$ at the northern side.

The hydrodynamic results are visible in Figure 5.10. The water levels in the estuary vary between -0.10 m up to 0.40 m. The offshore water levels vary between -0.25 m to 0.25 m. The ratio between the water levels in the estuary compared to ocean equals 1.00. Peak flows are varying from 40 to $30 \text{ m}^3/\text{s}$ during flood flows and 60 to $40 \text{ m}^3/\text{s}$ for ebb flows with maxima of approximately $90 \text{ m}^3/\text{s}$. The ebb tidal prism equals $720,000 \text{ m}^3$ and the flood tidal prism equals $520,000 \text{ m}^3$. The P/M ratio is equal to 1.54, which corresponds to an inlet type 3 that is unstable and intermittently closing.

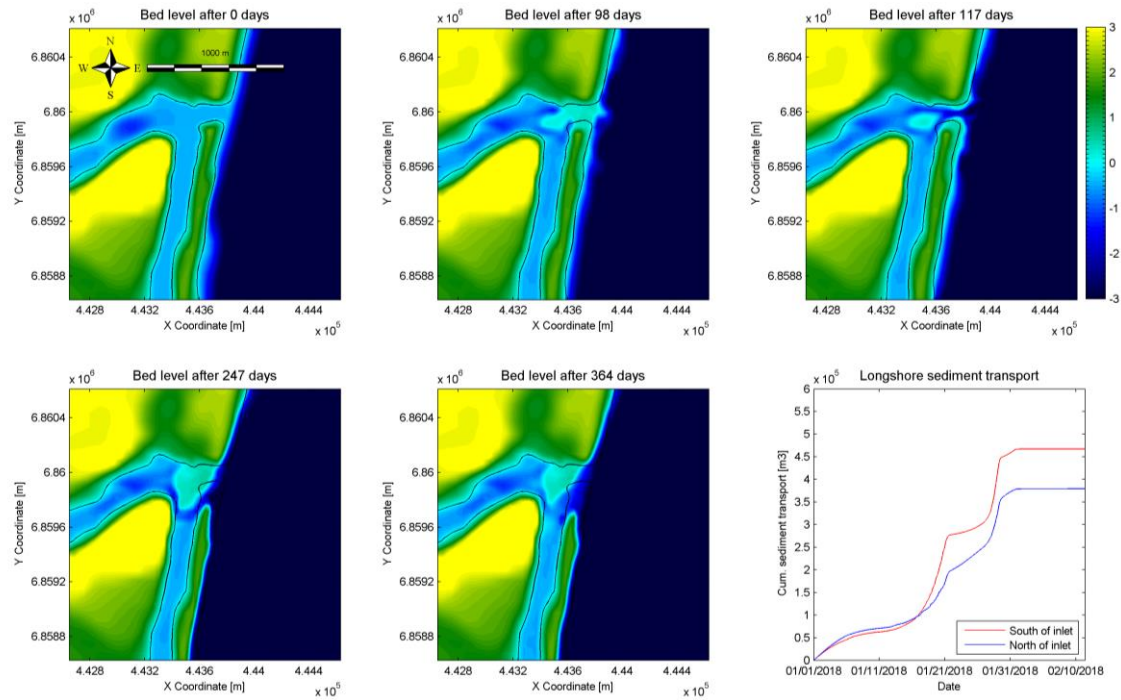


Figure 5.9: Bed level after 0 days, 98 days, 117 days, 247 days, 364 days and cumulative sediment transport along the coast for neap tidal range of 0.5 m

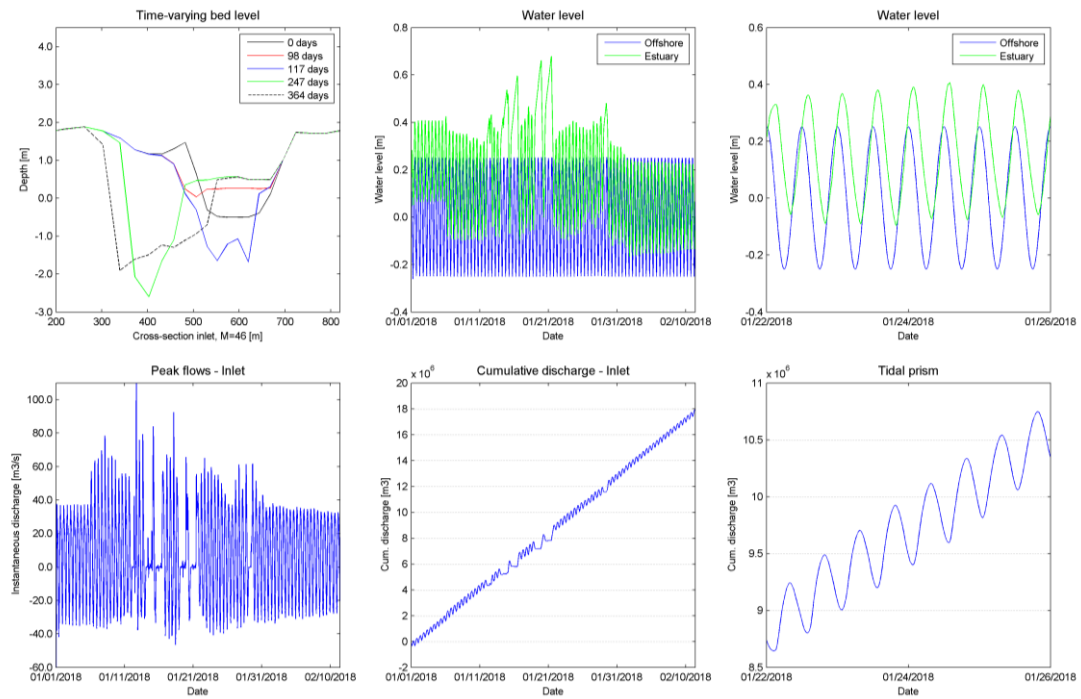


Figure 5.10: Time-varying bed level inlet, water level, detailed water level, peak flows, cumulative discharge through inlet and tidal prism for neap tidal range of 0.5 m

5.1.2.3 Spring tidal range

As in previous simulation the model is simulated with a river discharge of $5 \text{ m}^3/\text{s}$, only now with a spring tidal range of 1.8 m. The morphological evolution is visible in Figure 5.11. The estuary behaves similar as in previous simulation with a river discharge of $2 \text{ m}^3/\text{s}$. The formation of the flood tidal delta is visible in the first 149 days with two main channels flowing into the St Lucia Estuary and the Mfolozi River. The tidal flat forms onto the land of dredge spoil. The spit starts growing in northward direction for 200 m and partially moves inland. Due to the larger wave action, significant wave heights of 2.5 m, the inlet closes for a period of 15 days (from 150.8 to 165.8 days). The mouth reopens due to the large tidal range. The impact of the larger waves in combination with spring tide erodes the inlet and it widens up to 400 m at MSL (Figure 5.12). The longshore transport at the southern side of the inlet equals $558,000 \text{ m}^3/\text{year}$ and at the northern side equals $510,000 \text{ m}^3/\text{year}$.

The hydrodynamic results are given in Figure 5.12. The water levels in the estuary vary between -0.25 and -0.30 m up to 1.00 m. In the period in which the inlet is closed water levels in the estuary rise up to 1.30 m, which is an elevation of 0.40 m compared to oceanic water levels. The offshore water levels vary between -0.90 m to 0.90 m. The ratio between the water levels in the estuary compared to ocean equals 0.69. Peak flows are varying from 160 to $140 \text{ m}^3/\text{s}$ during flood flows and $140 \text{ m}^3/\text{s}$ for ebb flows with maxima of $200 \text{ m}^3/\text{s}$. The ebb tidal prism equals $1,930,000 \text{ m}^3$ and the flood tidal prism equals $1,730,000 \text{ m}^3$. The P/M ratio is equal to 3.92, which corresponds to an inlet type 3 that is unstable and intermittently closing.

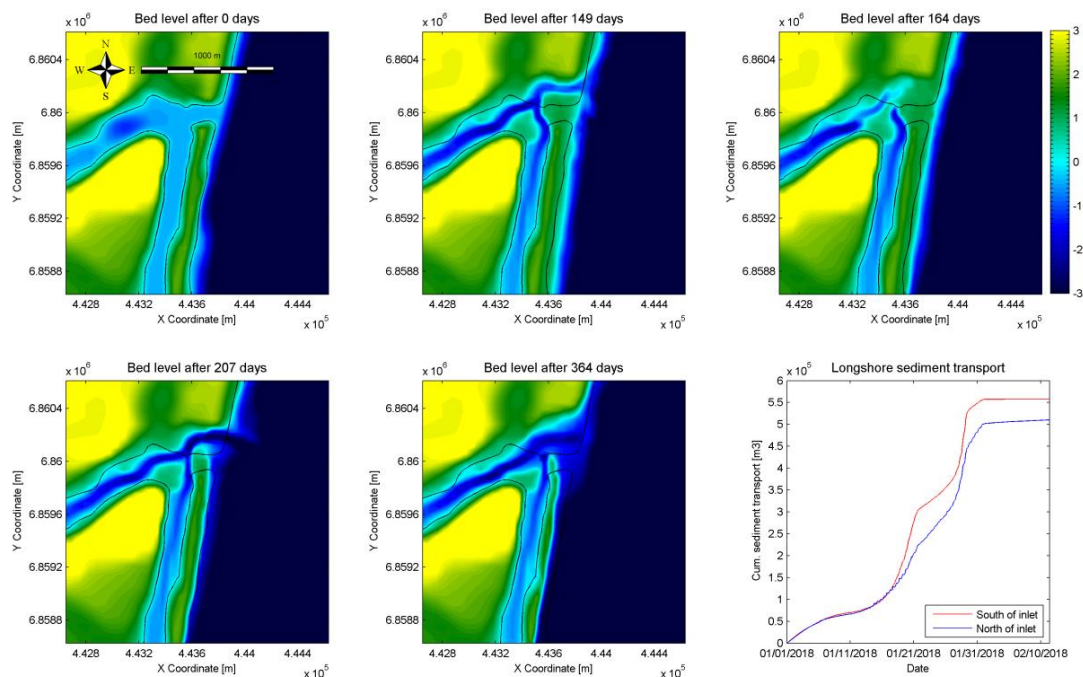


Figure 5.11: Bed level after 0 days, 149 days, 164 days, 207 days, 364 days and cumulative sediment transport along the coast for spring tidal range of 1.8 m

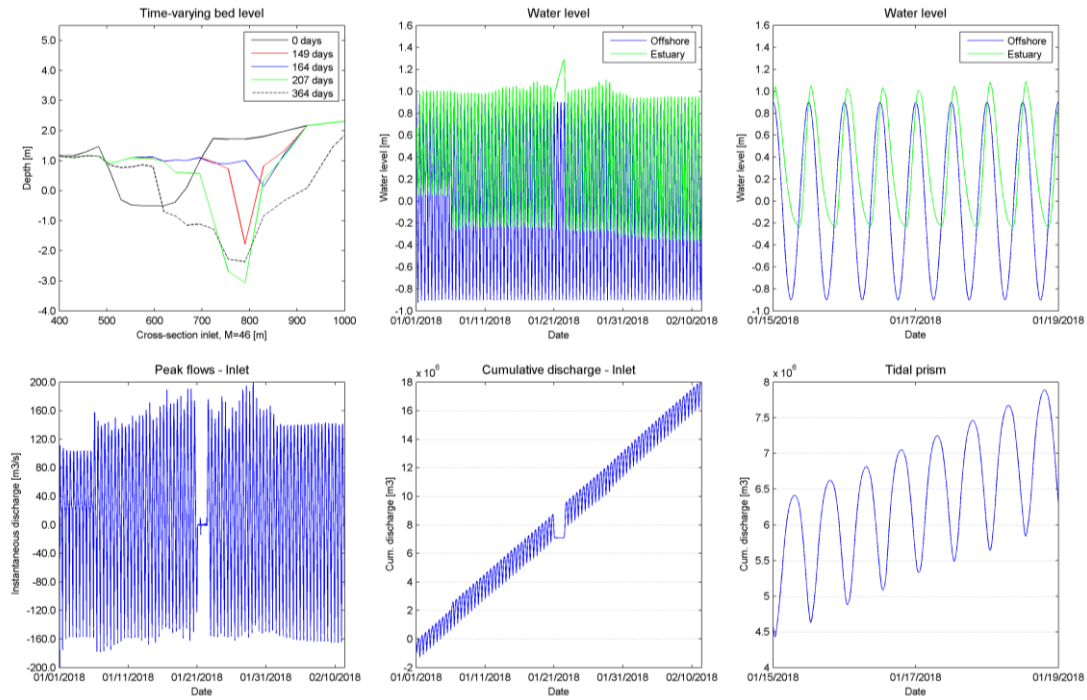


Figure 5.12: Time-varying bed level inlet, water level, detailed water level, peak flows, cumulative discharge through inlet and tidal prism for spring tidal range of 1.8 m

5.1.3 Mfolozi River with discharge of 14 m³/s (Summer)

5.1.3.1 Mean tidal range

The model is simulated with a river discharge of 14 m³/s from the Mfolozi River. This discharge is equal to a yearly runoff of $441.5 \cdot 10^6$ m³, which is 47% of the MAR. In the initial simulation where the discharge from the Mfolozi River was zero the inlet closed after 156 days. In the current simulation the inlet closes once; in between 150.4 to 151.7 days. The total closure time equals 1.3 days. The morphological evolution of the inlet is visible in Figure 5.13. The tidal gorge migrates approximately 200 m in southern direction due to sand-bypassing and accretion at the downdrift side of the inlet. At the end of the simulation time the high wave action cause widening of the inlet up to 410 m. The tidal gorge reaches depths of 3.6 m (Figure 5.14). The cumulative transport along the coast equals 470,000 m³/year at the southern side of the inlet and 415,000 m³/year at the northern side.

The hydrodynamic results are given in Figure 5.14. The water levels in the estuary vary between -0.25 m to 0.70 m. During periods of high wave action water levels in the estuary rise up to 0.90 m, which is an elevation of 0.25 m compared to oceanic water levels. The offshore water levels vary between -0.65 m to 0.65 m. The ratio between the water levels in the estuary compared to ocean equals 0.73. Peak flows are varying from 100 to 80 m³/s for flood flows and 150 to 100 m³/s ebb flows. Due to the high river discharge the ebb flows are higher than the flood flows. The ebb tidal prism equals 1,760,000 m³ and the flood tidal prism equals 1,116,000 m³. This difference is approximately equal to the discharge of the Mfolozi River over one tidal period, which equals 604,800 m³. The P/M ratio is equal to 3.74, which corresponds to an inlet type 3 that is unstable and intermittently closing.

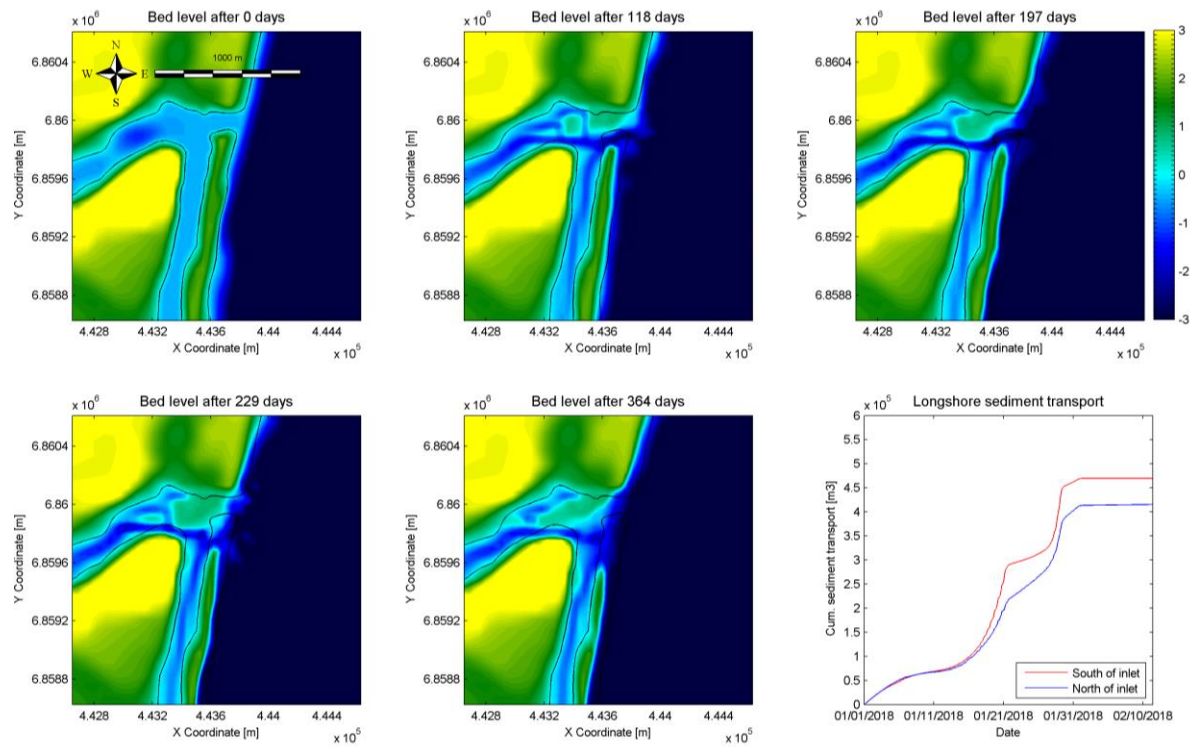


Figure 5.13: Bed level after 0 days, 118 days, 197 days, 229 days, 364 days and cumulative sediment transport along the coast for mean tidal range of 1.3 m

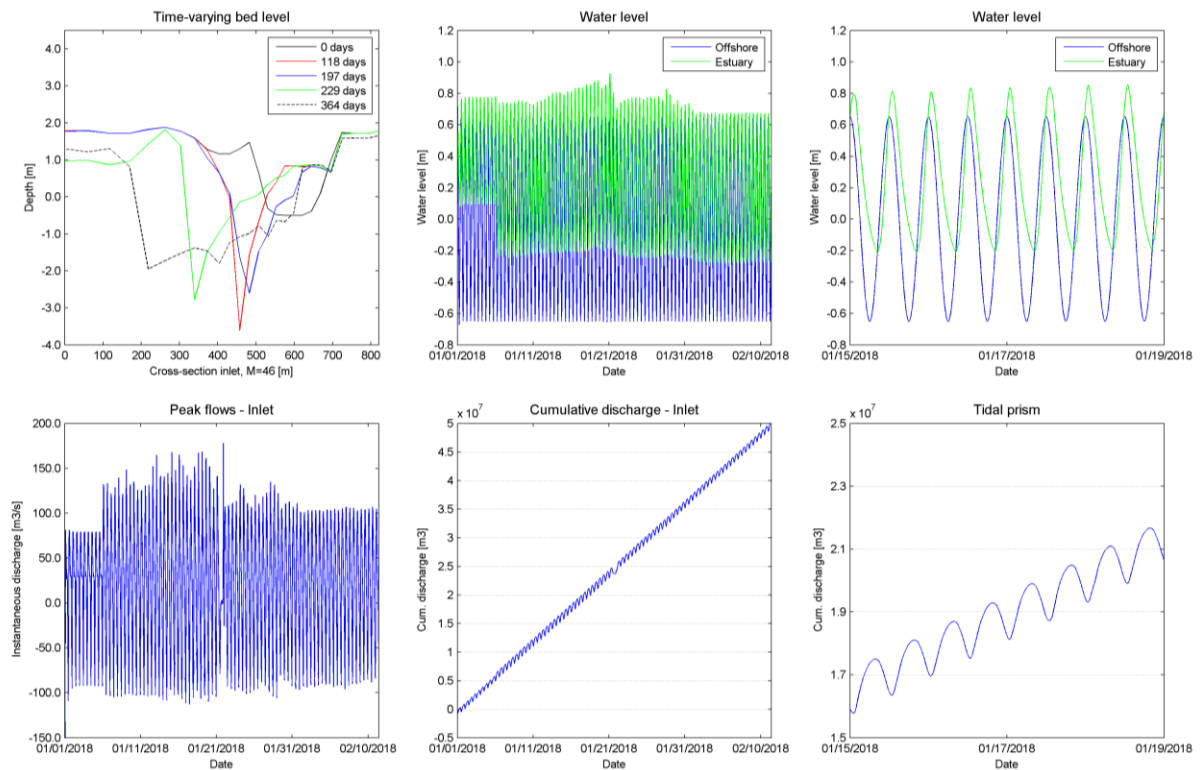


Figure 5.14: Time-varying bed level inlet, water level, detailed water level, peak flows, cumulative discharge through inlet and tidal prism for mean tidal range of 1.3 m

5.1.3.2 Neap tidal range

The morphological evolution of the inlet forced with neap tidal range and a discharge of $14 \text{ m}^3/\text{s}$ is given in Figure 5.15. In previous simulations without river discharge the inlet closed after 22 days. In this simulation the inlet closes 11 times, mainly during ebb periods, in the periods between 75.0 – 77.5 days, 83.8 – 87.1 days, 95.0 – 97.1 days, 100.0 – 103.8 days, 105.0 – 107.1 days, 110.8 – 113.8 days, 120.8 – 122.9 days, 134.6 – 138.3 days, 140.4 – 142.9 days, 145.0 – 147.5 days and 149.6 – 153.3 days. The inlet is closed for a total of 31.3 days, which is equal to 9% of the simulation time. The inlet closes more often compared to the simulation with a river discharge of $5 \text{ m}^3/\text{s}$. However, the closure times are shorter. At the start of the simulation the inlet opens and closes intermittently and migrates at most 180 m in northern direction. The formation of a spit is visible after 108 days. Water levels in the estuary built up 0.75 m due to river flow from the Mfolozi that enters the St Lucia Estuary when the inlet is closed. The inlet behaves as a type 3 inlet that is locationally stable and closes intermittently. At the end of the simulation, after 220 days, the channel towards the St Lucia Estuary closes. The tidal gorge reaches depths of 5.0 m (Figure 5.16), which occur after the inlet breaches and high ebb flows up to $400 \text{ m}^3/\text{s}$ are reached. The cumulative transport along the coast equals $448,000 \text{ m}^3/\text{year}$ at the southern side of the inlet and $353,000 \text{ m}^3/\text{year}$ at the northern side.

The hydrodynamic results are visible in Figure 5.16. The water levels in the estuary vary between -0.10 m up to 0.40 m. The offshore water levels vary between -0.25 m to 0.25 m. The ratio between the water levels in the estuary compared to ocean equals 1.00. Peak flows are varying from 40 to $30 \text{ m}^3/\text{s}$ during flood flows and 60 to $40 \text{ m}^3/\text{s}$ for ebb flows with maxima of approximately $90 \text{ m}^3/\text{s}$. The ebb tidal prism equals $975,000 \text{ m}^3$ and the flood tidal prism equals $337,000 \text{ m}^3$. The P/M ratio is equal to 2.18, which corresponds to an inlet type 3 that is unstable and intermittently closing.

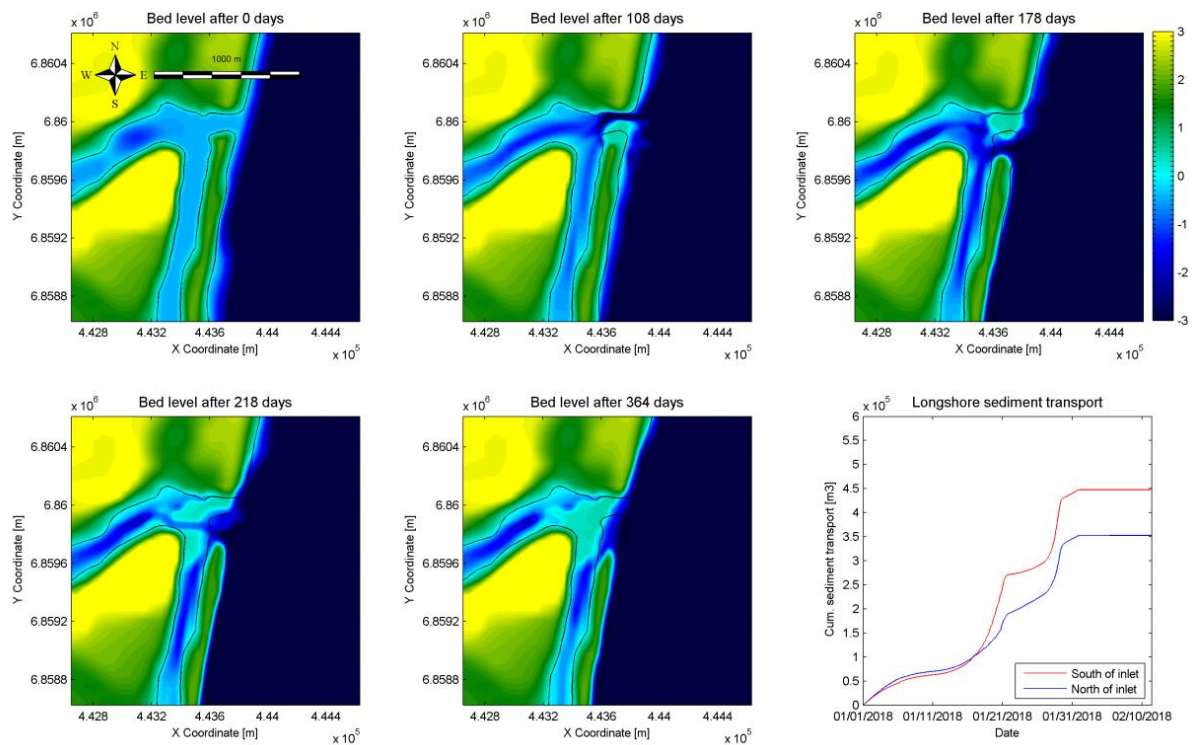


Figure 5.15: Bed level after 0 days, 108 days, 178 days, 218 days, 364 days and cumulative sediment transport along the coast for neap tidal range of 0.5 m

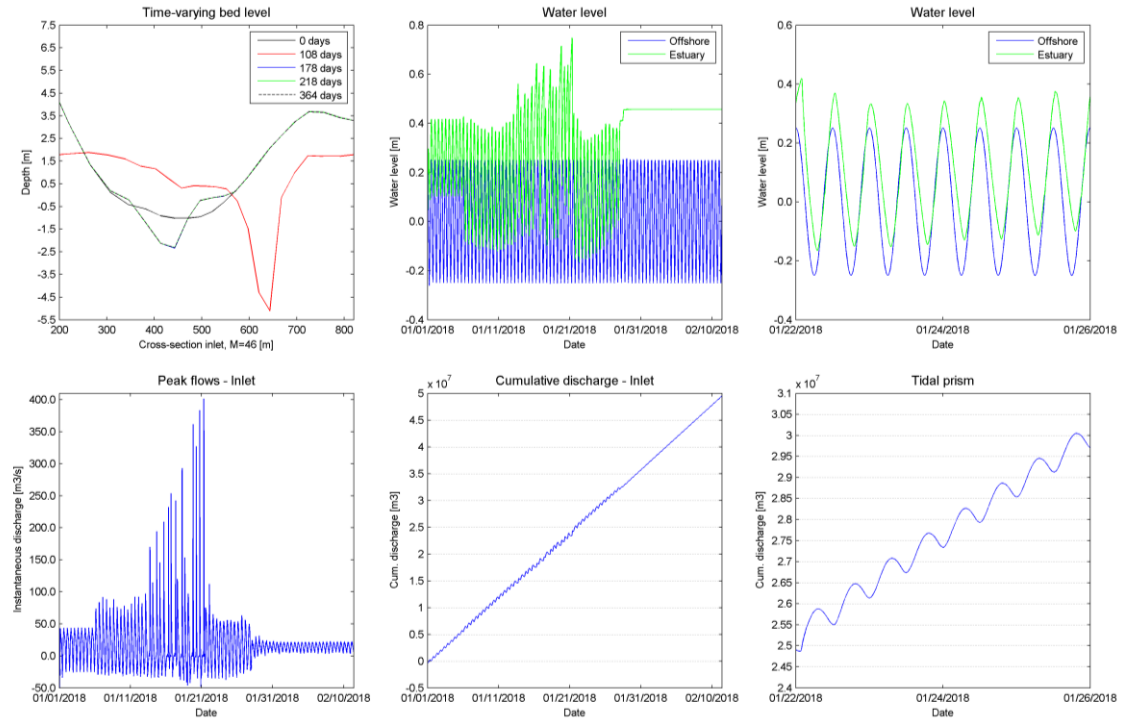


Figure 5.16: Time-varying bed level inlet, water level, detailed water level, peak flows, cumulative discharge through inlet and tidal prism for neap tidal range of 0.5 m

5.1.3.3 Spring tidal range

As in previous simulation the model is simulated with a river discharge of $14 \text{ m}^3/\text{s}$, only now with a spring tidal range of 1.8 m. The morphological evolution is visible in Figure 5.17. The estuary behaves similar as in previous simulation with a river discharge of 2 and $5 \text{ m}^3/\text{s}$. The tidal gorge migrates in northern direction due to the spit that is growing at the updrift side of the inlet and erosion at the downdrift side. The formation of the flood tidal delta is visible with a large tidal flat located next to the dredge spoil island. The inlet does not close in contrast to previous simulation with a river discharge of $5 \text{ m}^3/\text{s}$. The impact of the larger waves in combination with spring tide erodes the inlet and it widens up to 430 m at MSL (Figure 5.18). The longshore transport at the southern side of the inlet equals $524,000 \text{ m}^3/\text{year}$ and at the northern side equals $508,000 \text{ m}^3/\text{year}$.

The hydrodynamic results are given in Figure 5.18. The water levels in the estuary vary between -0.25 m and -0.30 m up to 1.00 m . During periods of high wave action water levels in the estuary rise up to 1.10 m , which is an elevation of 0.20 m compared to oceanic water levels. The offshore water levels vary between -0.90 m to 0.90 m . The ratio between the water levels in the estuary compared to ocean equals 0.72. Peak flows are varying from $150 \text{ m}^3/\text{s}$ during flood flows and $150 \text{ m}^3/\text{s}$ for ebb flows with maxima of $200 \text{ m}^3/\text{s}$. The ebb tidal prism equals $2,180,000 \text{ m}^3$ and the flood tidal prism equals $1,600,000 \text{ m}^3$. The P/M ratio is equal to 3.92, which corresponds to an inlet type 3 that is unstable and intermittently closing.

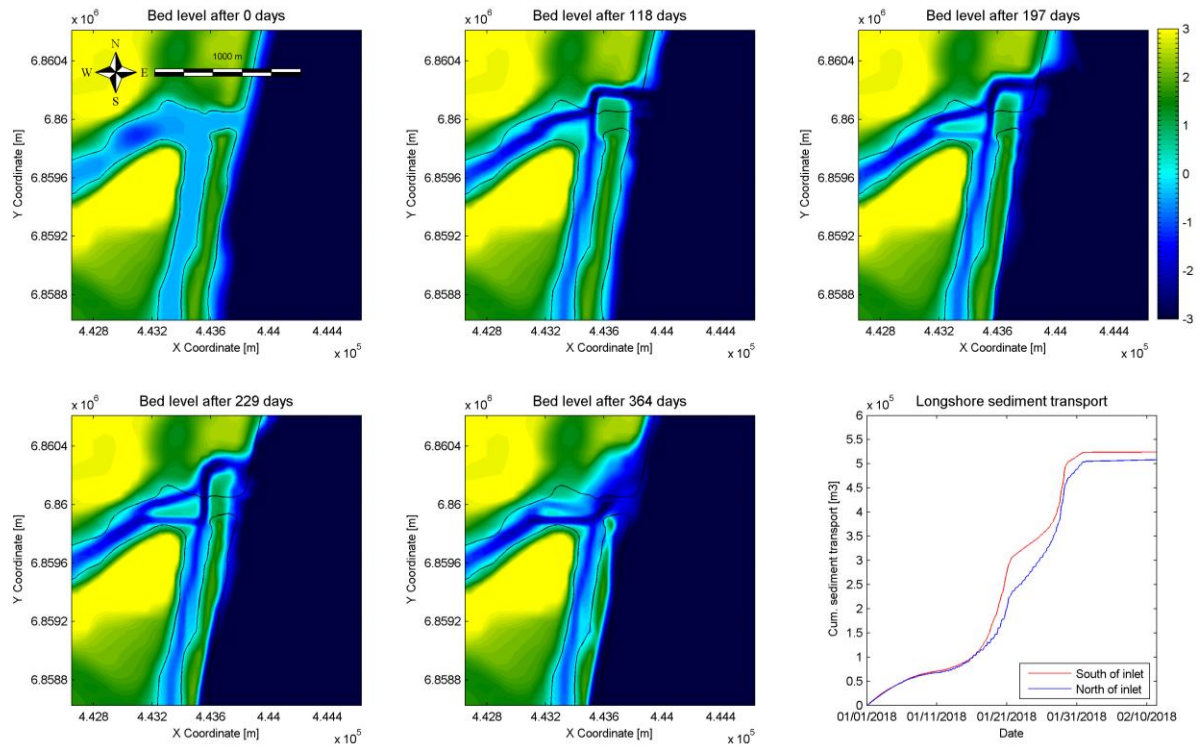


Figure 5.17: Bed level after 0 days, 118 days, 197 days, 229 days, 364 days and cumulative sediment transport along the coast for spring tidal range of 1.8 m

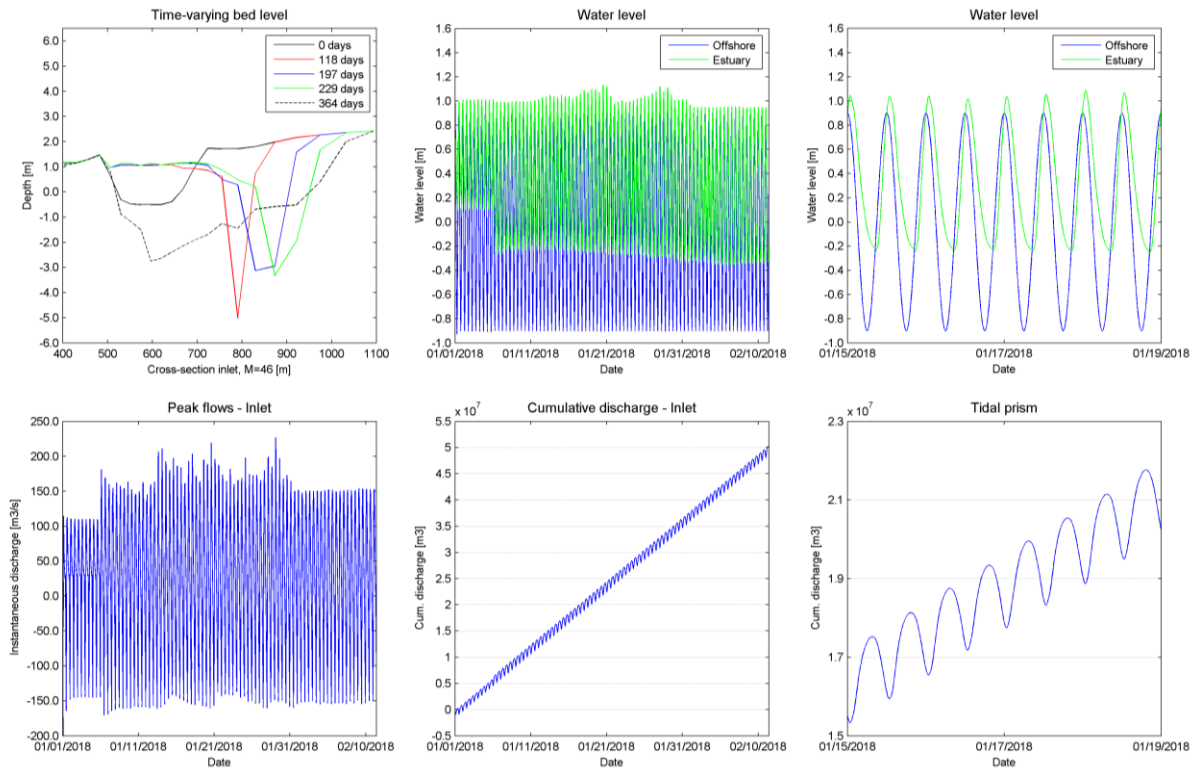


Figure 5.18: Time-varying bed level inlet, water level, detailed water level, peak flows, cumulative discharge through inlet and tidal prism for spring tidal range of 1.8 m

5.1.4 Mfolozi River with discharge of 30 m³/s (Mean Annual Runoff)

5.1.4.1 Mean tidal range

The model is simulated with a river discharge of 30 m³/s from the Mfolozi River. This discharge is equal to a yearly runoff of $946.1 \cdot 10^6$ m³, which is equal to the MAR. In the initial simulation where the discharge from the Mfolozi River was zero the inlet closed after 156 days. In current simulation the inlet does not close. The morphological evolution of the inlet is visible in Figure 5.19. The tidal gorge migrates 290 m in northern direction due to the spit that is growing at the updrift side of the inlet and erosion at the downdrift side. The tidal gorge reaches a maximum depth of 4.4 m (Figure 5.20). The cumulative transport along the coast equals 478,000 m³/year at the southern side of the inlet and 418,000 m³/year at the northern side.

The hydrodynamic results are given in Figure 5.20. The water levels in the estuary vary between -0.25 m to 0.70 m. During periods of high wave action water levels in the estuary rise up to 0.90 m, which is an elevation of 0.25 m compared to oceanic water levels. The offshore water levels vary between -0.65 m to 0.65 m. The ratio between the water levels in the estuary compared to ocean equals 0.73. Peak flows are varying from 90 m³/s for flood flows and 130 m³/s ebb flows. Due to the high river discharge the ebb flows are higher than the flood flows. The ebb tidal prism equals 2,240,000 m³ and the flood tidal prism equals 945,000 m³. This difference is approximately equal to the discharge of the Mfolozi River over one tidal period, which equals 1,296,000 m³. The P/M ratio increases from 3.74 to 4.69. For both cases this corresponds to an inlet type 3 that is unstable and intermittently closing.

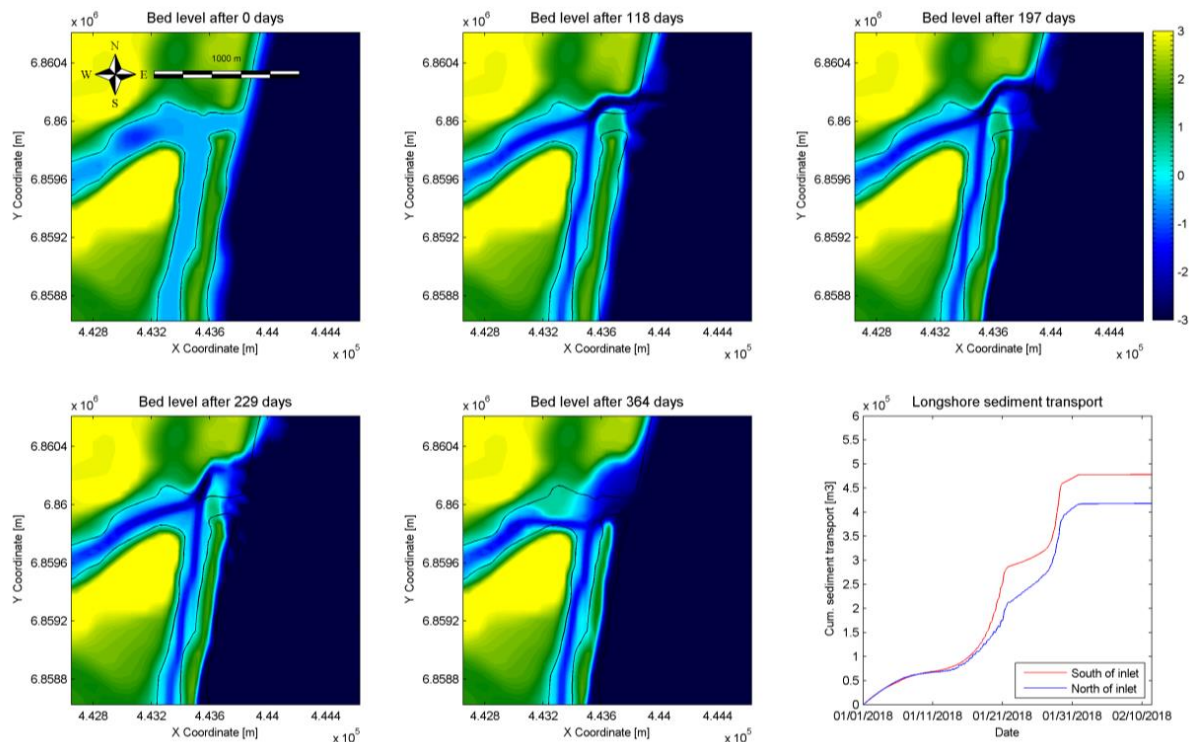


Figure 5.19: Bed level after 0 days, 118 days, 197 days, 229 days, 364 days and cumulative sediment transport along the coast for mean tidal range of 1.3 m

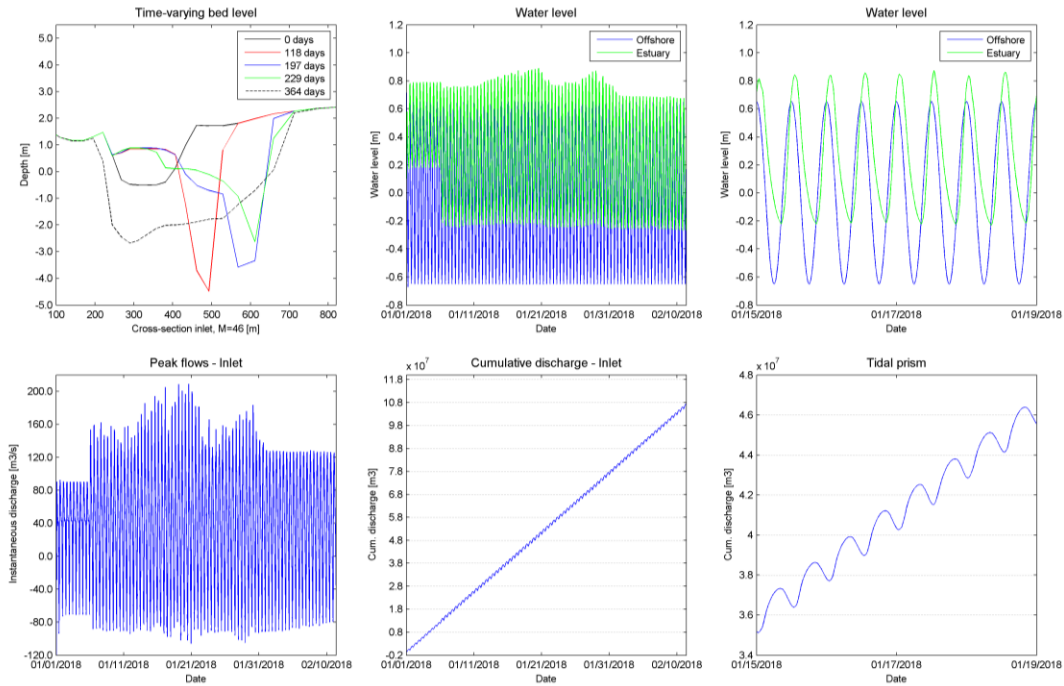


Figure 5.20: Time-varying bed level inlet, water level, detailed water level, peak flows, cumulative discharge through inlet and tidal prism for mean tidal range of 1.3 m

5.1.4.2 Neap tidal range

The morphological evolution of the inlet forced with neap tidal range and a discharge of $30 \text{ m}^3/\text{s}$ is given in Figure 5.21. In previous simulations without river discharge the inlet closed after 22 days. In this simulation the inlet closes 6 times, mainly during ebb periods, in the periods between 89.2 – 92.5 days, 109.6 – 112.1 days, 139.2 – 140.8 days, 144.2 – 145.4 days, 149.2 – 150.8 days and 154.2 – 155.0 days. The inlet is closed for a total of 11.3 days, which is equal to 3% of the simulation time. The closure times are shorter and less often compared to the simulation with a river discharge of $14 \text{ m}^3/\text{s}$. At the start of the simulation the inlet opens and closes intermittently and migrates at most 100 m in northern direction. The formation of a spit is visible after 118 days. Water levels in the estuary built up 0.79 m due to river flow from the Mfolozi that enters the St Lucia Estuary when the inlet is closed. The inlet behaves as a type 3 inlet that is locationally stable and closes intermittently. At the end of the simulation, after 232 days, the channel towards the St Lucia Estuary closes. This closure occurs 12 days later than the simulation with $14 \text{ m}^3/\text{s}$. The tidal gorge reaches depths of 5.5 m (Figure 5.22), which occur after the inlet breaches and high ebb flows up to $350 \text{ m}^3/\text{s}$ are reached. The cumulative transport along the coast equals $465,000 \text{ m}^3/\text{year}$ at the southern side of the inlet and $349,000 \text{ m}^3/\text{year}$ at the northern side.

The hydrodynamic results are visible in Figure 5.22. The water levels in the estuary vary between -0.10 m up to 0.40 m. The offshore water levels vary between -0.25 m to 0.25 m. The ratio between the water levels in the estuary compared to ocean equals 1.00. Peak flows are varying from 15 to $35 \text{ m}^3/\text{s}$ during flood flows and $80 \text{ m}^3/\text{s}$ for ebb flows. The peak flows decrease significantly after the estuary is closed to 20 and $40 \text{ m}^3/\text{s}$. The mouth is completely ebb dominated by the river discharge of the Mfolozi River. The ebb tidal prism equals $1,400,000 \text{ m}^3$ and the flood tidal prism equals $110,000 \text{ m}^3$. The P/M ratio increases from 2.18 to 3.01 and still corresponds to an inlet type 3 that is unstable and intermittently closing.

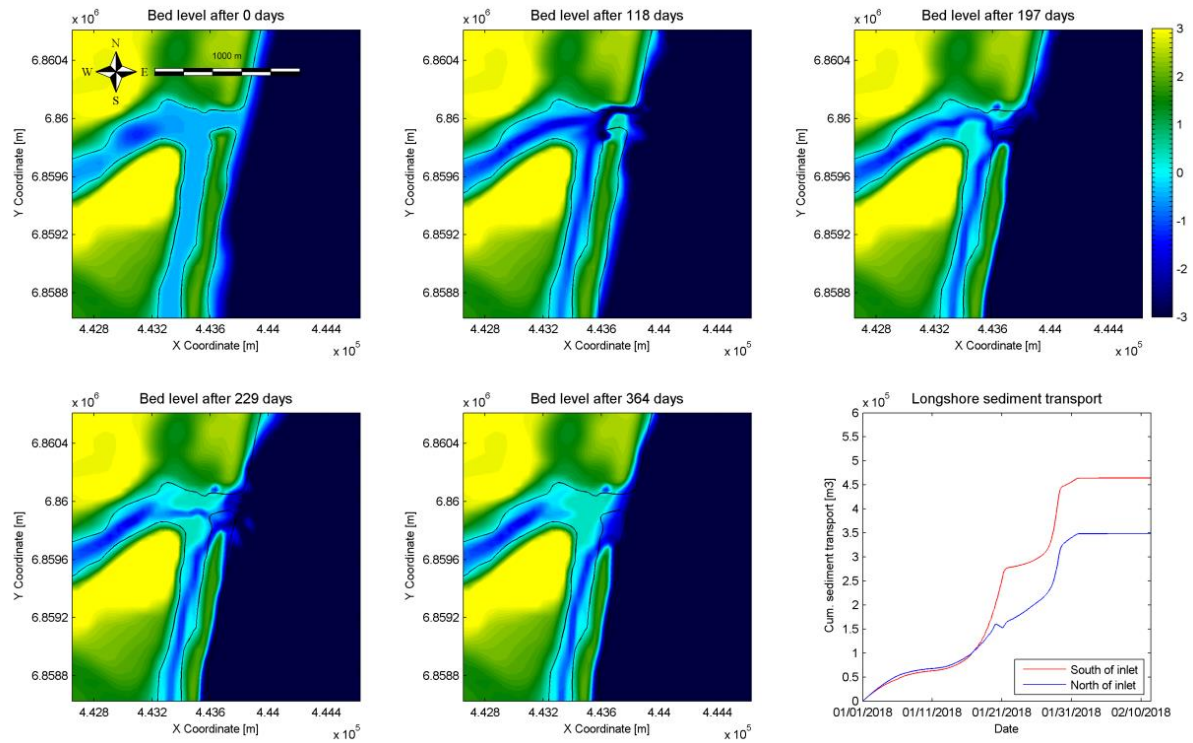


Figure 5.21: Bed level after 0 days, 118 days, 197 days, 229 days, 364 days and cumulative sediment transport along the coast for neap tidal range of 0.5 m

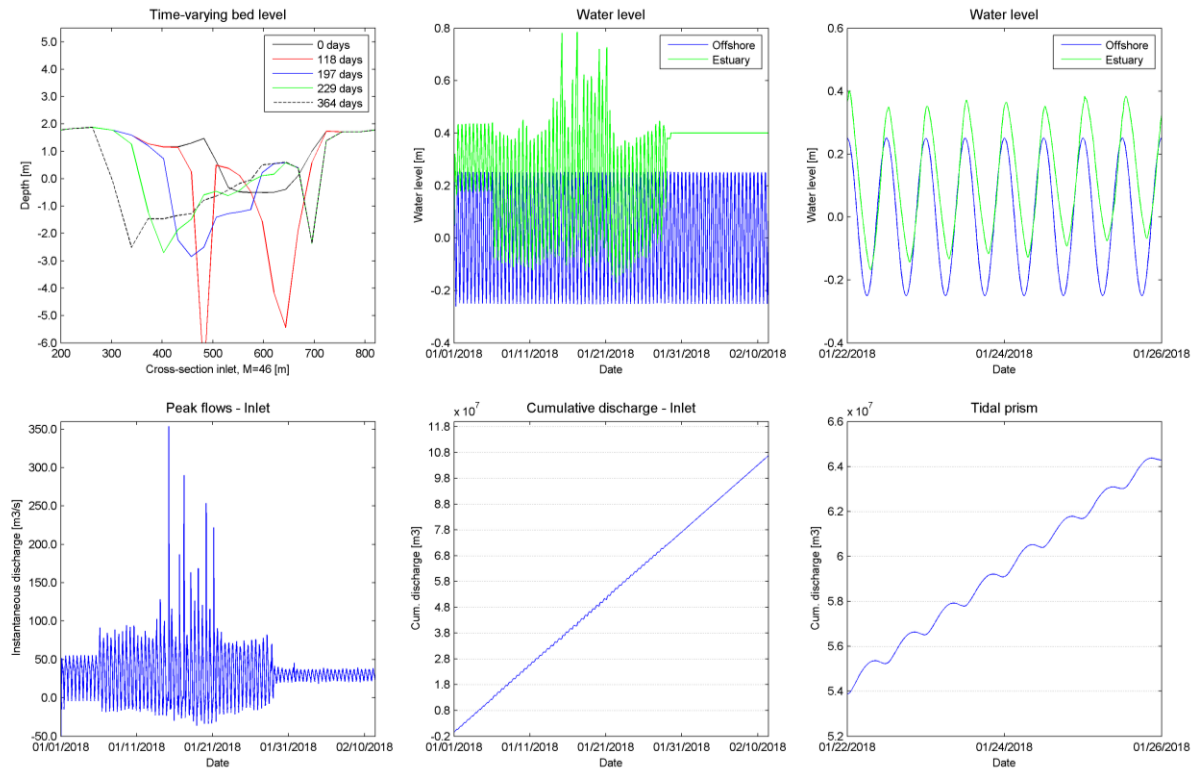


Figure 5.22: Time-varying bed level inlet, water level, detailed water level, peak flows, cumulative discharge through inlet and tidal prism for neap tidal range of 0.5 m

5.1.4.3 Spring tidal range

As in previous simulation the model is simulated with a river discharge of $30 \text{ m}^3/\text{s}$, only now with a spring tidal range of 1.8 m. The morphological evolution is visible in Figure 5.23. The estuary behaves similar as in previous simulation with a river discharge of 2, 5 and $14 \text{ m}^3/\text{s}$. The tidal gorge migrates in northern direction due to the spit that is growing at the updrift side of the inlet and erosion at the downdrift side. The inlet stays open during the complete simulation time. At the end of the simulation the impact of the larger waves in combination with spring tide erodes the inlet and it widens up to 230 m at MSL (Figure 5.24). This is considerably less than the final inlet width of 430 m that corresponds to a river discharge of $14 \text{ m}^3/\text{s}$. Due to the increased river discharge the mouth is more stable. The longshore transport at the southern side of the inlet equals $516,000 \text{ m}^3/\text{year}$ and at the northern side equals $509,000 \text{ m}^3/\text{year}$.

The hydrodynamic results are given in Figure 5.24. The water levels in the estuary vary between -0.25 m and -0.30 m up to 1.00 m. During periods of high wave action water levels in the estuary rise up to 1.15 m, which is an elevation of 0.25 m compared to oceanic water levels. The offshore water levels vary between -0.90 m to 0.90 m. The ratio between the water levels in the estuary compared to ocean equals 0.72. Peak flows are varying from $150 \text{ m}^3/\text{s}$ during flood flows and 190 to $170 \text{ m}^3/\text{s}$ for ebb flows with maxima of $290 \text{ m}^3/\text{s}$. Due to the higher ebb flows the flood tidal delta does not develop as much compared to previous simulations. The ebb tidal prism equals $2,700,000 \text{ m}^3$ and the flood tidal prism equals $1,400,000 \text{ m}^3$. The P/M ratio is increased from 4.16 to 5.23, which corresponds to an inlet type 2/3 that is unstable; migrating or intermittently closing.

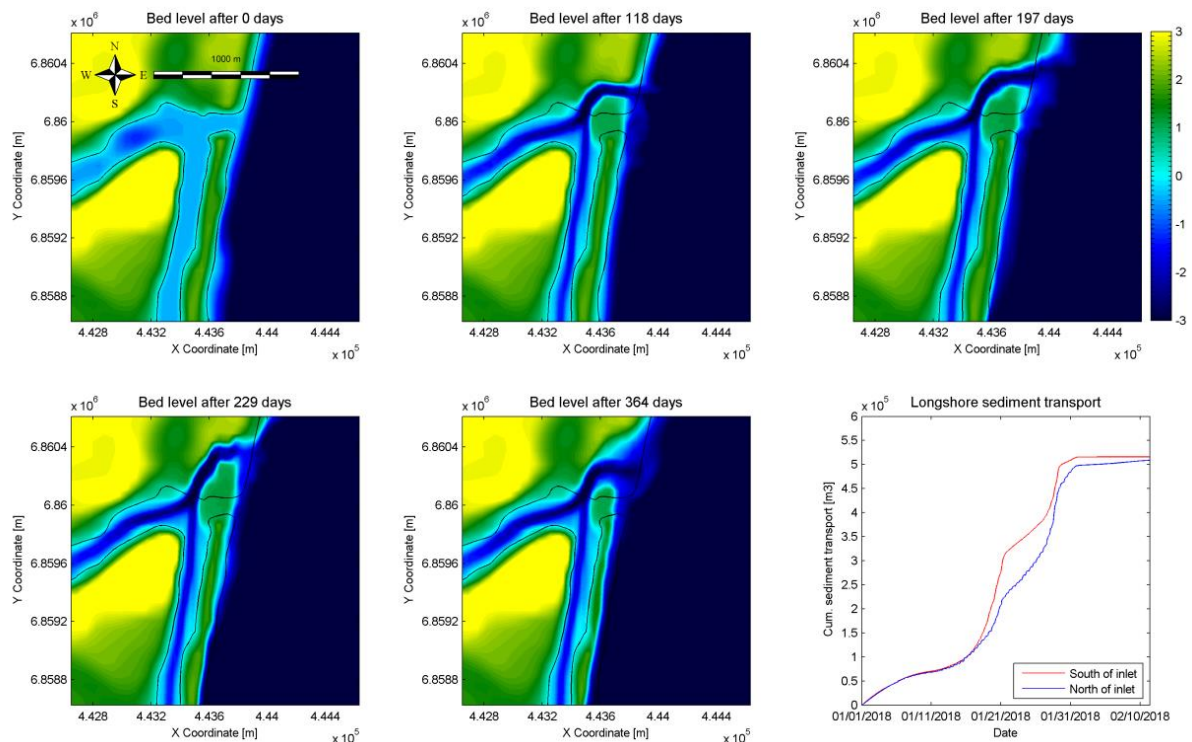


Figure 5.23: Bed level after 0 days, 118 days, 197 days, 229 days, 364 days and cumulative sediment transport along the coast for spring tidal range of 1.8 m

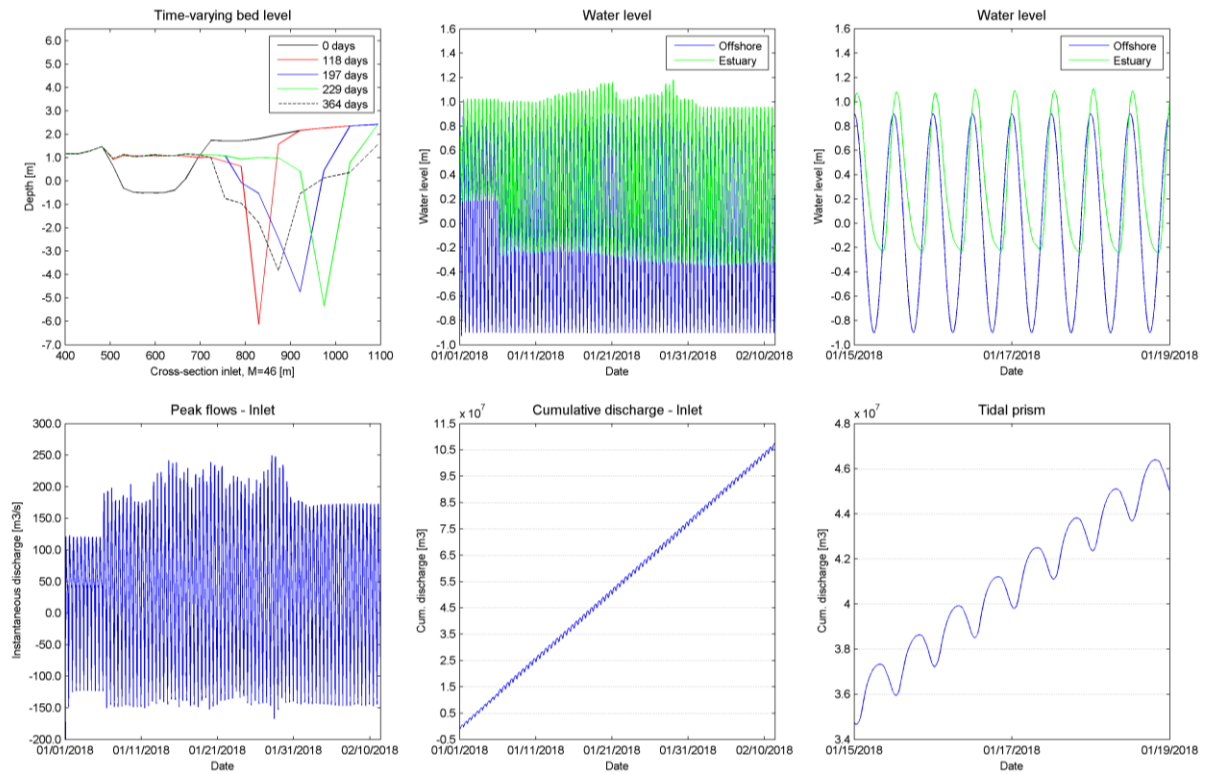


Figure 5.24: Time-varying bed level inlet, water level, detailed water level, peak flows, cumulative discharge through inlet and tidal prism for spring tidal range of 1.8 m

5.2 Analysis scenario A

In previous section the results of different scenarios are presented. An overview of the results is given in Appendix D. The Mfolozi River is reconnected to the estuarine system and varied in discharge from $0 \text{ m}^3/\text{s}$ to $30 \text{ m}^3/\text{s}$. The following four points will be analysed: 1. Morphological development, 2. Closure times, 3. A-P Relationship, 4. Wave dominated system.

5.2.1 Morphological development

The discharge from the Mfolozi River has influence on the morphological development of the system. The inlet behaves in three different ways, namely:

- (1) Locationally stable and intermittently closing inlet, mainly observed when the inlet is forced with a neap tidal range.
- (2) Migrating inlet in northern direction due to spit formation at the updrift side of the inlet and no closure of the mouth. This is mainly visible during spring tidal range where flow velocities through the inlet are large enough to maintain an open mouth. The large tidal range results in more suspended sediments resulting in a migrating inlet. Closure of the inlet might occur which is visible during two simulations; no discharge combined with a mean tidal range and a river discharge of $5 \text{ m}^3/\text{s}$ combined with spring tidal range.
- (3) Migration of the inlet in southern direction. The higher discharges from the Mfolozi River result in more suspended sediments in the water column. As described in chapter 2.5.3 the sediment content increases significantly during autumn and summer. The sediments settle at the northern side of the estuary. Increased ebb flows aided by river flow result in erosion at the updrift side and accretion at the downdrift side of the inlet. The northern part of land evolves in southern direction. This behaviour is explained in more detail in chapter 5.4.1.

All of the observed processes correspond to the behaviour of an unstable inlet. The P/M ratios vary from 1.23 to 5.23. The inlets are classified as type 3 (intermittently closing) and type 2/3 (migrating or intermittently closing) according to Duong (2015).

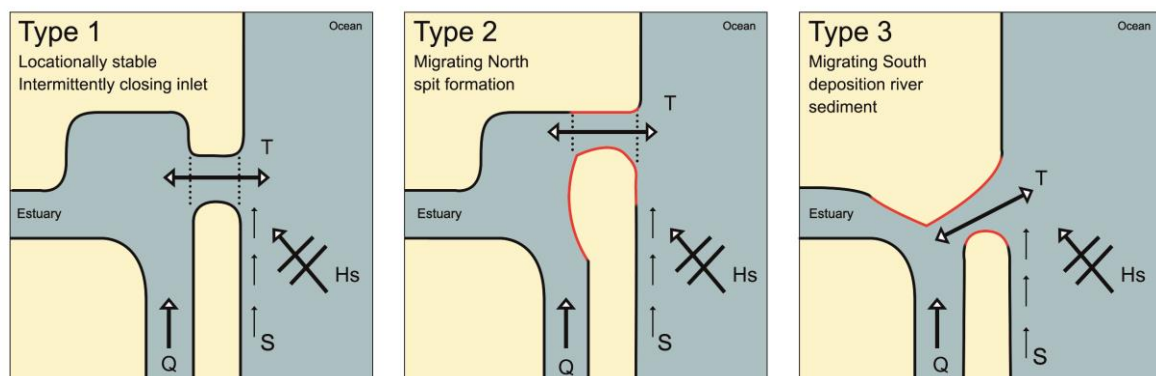


Figure 5.25: Types of morphological development inlet

5.2.2 Closure times

The closure times of the inlet decreases significantly due to re-linkage of the Mfolozi River. Before reconnecting the Mfolozi River the inlet was closed for 50.4% of the time. This is the average closure time of the simulations with neap –, mean –, and spring tidal range equal to 94.0%, 57.1% and 0.0%

respectively. The closure time of the combined simulations is reduced to 11.6%, 6.1%, 3.0% and 1.0% for a corresponding river discharge equal to 2 m³/s, 5 m³/s, 14 m³/s and 30 m³/s.

The inlet mainly closes during neap tidal range. When increasing the river discharge the closure time decreases, but the inlet closes more frequently. The inlet forced with a neap tidal range is closed for 94.0%, 29.1%, 12.9%, 8.6% and 3.1% of the simulation time for a river discharge equal to 0 m³/s, 2 m³/s, 5 m³/s, 14 m³/s and 30 m³/s.

The cross-sectional area of the inlet varying over time is visible in Figure 5.26. The graph shows five different scenarios during mean tidal range where the river discharge is increased from 0 m³/s to 30 m³/s. The cross-section is calculated by integrating the area beneath the bed level from two points closest to MSL (height equal to 0 m). The two points, one above MSL and one below MSL, are interpolated to calculate the average. At both sides of the cross-section this is performed after integration leads to the area of the inlet. The cross-section is retrieved every 12 hours. This does imply that the effect of high tide and low tide are not visible in the graph, however the trend of the cross-sectional evolution is represented. A decrease in cross-section is visible during the first 150 days of the simulation period. During the first period with low wave action the coastline accretes. After this a period of higher wave action starts. This causes an increase in longshore sediment transport. The inlet closes when the river discharge is equal to 0 m³/s and 2 m³/s. The inlet reduced in size to approximately 50 m² after which the inlet closes due to reduced flows in the constricted entrance and increased longshore sediment transport. In case the inlet remains open due to an increase in river discharge a different trend is observed. The higher wave action causes erosion of the inlet, resulting in a cross-section of 460 m² up to 800 m². The closure due to spit formation and an increase in longshore current corresponds to mechanism 1 as described by Ranasinghe et al. (1999). During neap tidal range inlet is locationally stable and the closure corresponds more to mechanism 2; closure due to onshore bar migration.

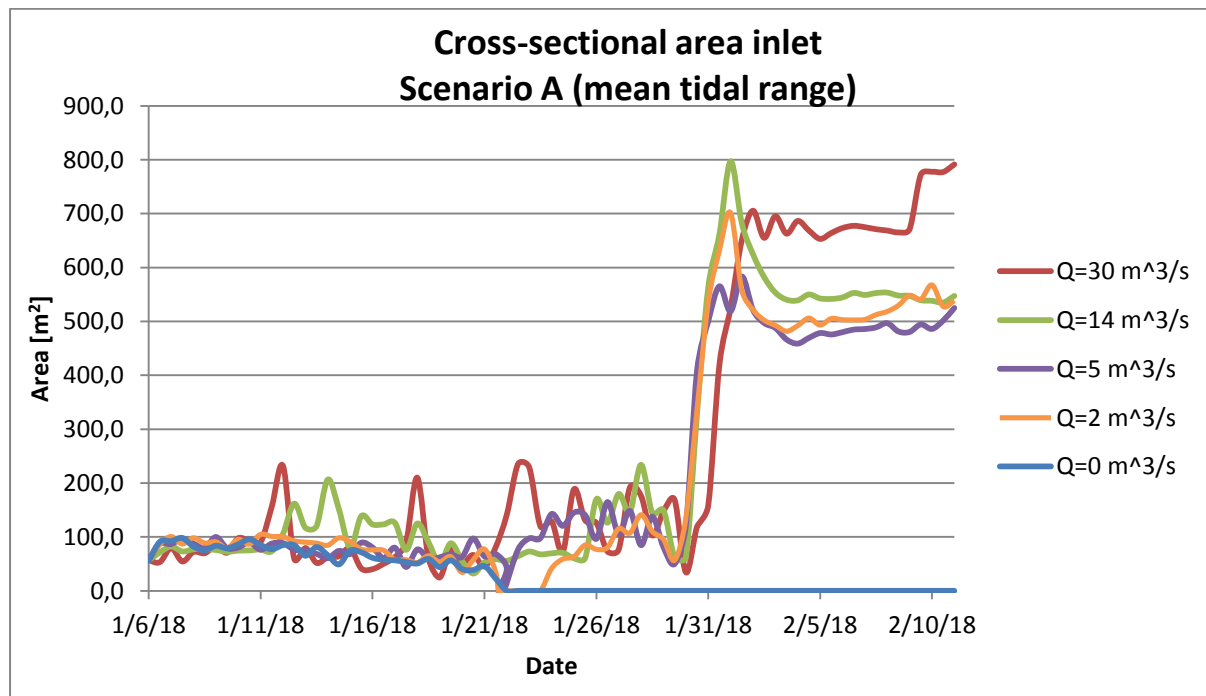


Figure 5.26: Cross-sectional area inlet of scenario A

5.2.3 A-P Relationship

The A-P relationship is explained in chapter 2.7.2 and describes the relation between cross-sectional area of an inlet and tidal prism found by O'Brien (1969). The simulations from scenario A forced with mean tidal range are further investigated regarding the A-P relationship. The average cross-sectional area is calculated for each simulation. The average cross-sectional area is plotted as a function of the tidal prism. In Figure 5.27 the results from scenario A are compared with the findings by O'Brien. It is clearly visible that after re-linkage of the Mfolozi River the inlet is closer to O'Brien's curve that shows the stable equilibrium of an inlet.

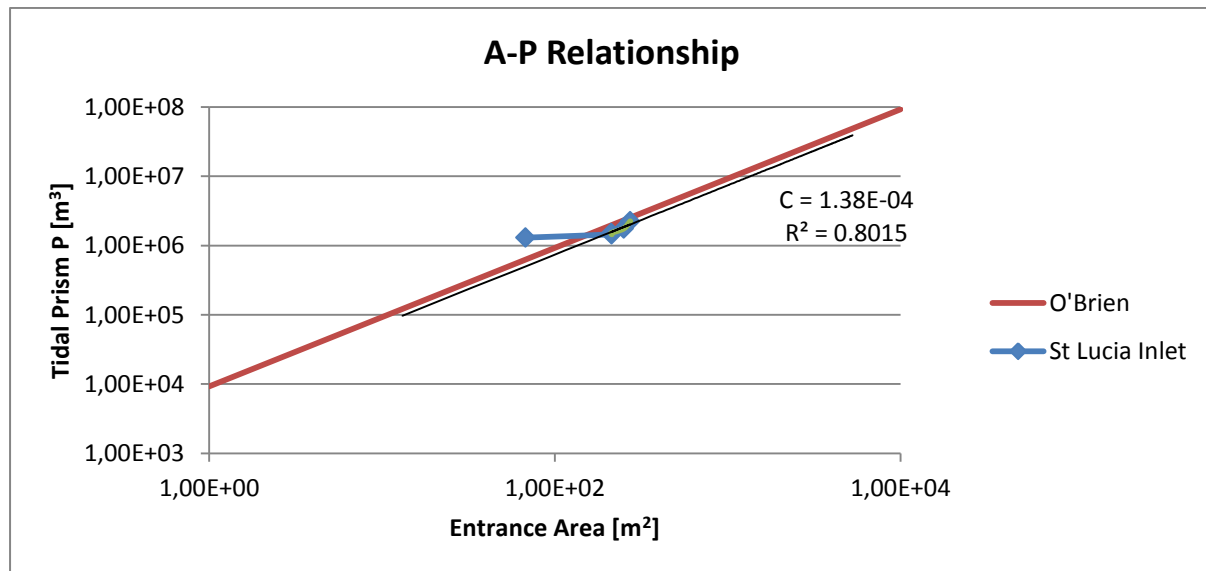


Figure 5.27: A-P Relationship scenario A

The curve given in Figure 5.27 from O'Brien belongs to the data set of 8 non-jettied entrances, where the empirical coefficients are equal to $C = 1.08 \cdot 10^{-4}$ and $q = 1$. After re-linkage of the Mfolozi River the cross-sectional area increases from 67.8 m² to 213.4 m², 212.1 m², 250.4 m² and 273.0 m² corresponding to a river discharge of 0 m³/s, 2 m³/s, 5 m³/s, 14 m³/s and 30 m³/s. The averaged empirical coefficient from the simulations with river flow equals $C = 1.38 \cdot 10^{-4}$, when $q = 1$. The trendline corresponding to the results of scenario A has a coefficient of determination R^2 equal to 0.8015.

The empirical coefficient before re-linking the Mfolozi River equals $C = 5.21 \cdot 10^{-5}$, when $q = 1$. The equilibrium velocity for the Escoffier curve is approximately 0.9 m/s which results in coefficients $C = 7.8 \cdot 10^{-5}$ and $q = 1$. The empirical coefficient belonging to no river discharge is lower than the equilibrium velocity. This indicates the inlet is unstable and is prone to close, due to low velocities in the inlet.

Re-linkage of the Mfolozi River is of major importance in the closure times of the inlet. A winter discharge of 2 m³/s leads to a decrease in total closure time of 50.4% to 11.6%. Although the river discharge in South Africa is highly variable these low flows already make a large difference in the mouth dynamics. The empirical coefficient C is close to the value found by O'Brien and shows the inlet after re-linkage of the Mfolozi River is close to stable equilibrium.

5.2.4 Wave dominant system

Re-linkage of the Mfolozi River does not change the system from a wave dominated to a river dominated system. Hinwood et al. (2012) analysed tidal estuaries to investigate dominance of tidal and fluvial flows which is explained in chapter 2.7.2. It is shown that fluvial dominated inlets have a smaller cross-sectional area around 1 to 10 m². Whereas estuaries dominated by the tide have a cross-section in the order of 100 to 5000 m². The area of the St Lucia inlet is around 60 to 270 m² when averaged and this fits into lower region of the graph that shows tidal dominance. The St Lucia Estuary will have a smaller cross-section during neap tidal range, thus slightly more dominated by river flow. However, the St Lucia inlet will remain more dominated by tidal flows than fluvial flows.

The inlet remains flood dominant for majority of the time; during the winter (2 m³/s) and drought period (5 m³/s) the flood flows are higher than the ebb flows. In the summer season (14 m³/s) the flood flows are approximately equal to the ebb flows. Simulations with the mean annual runoff (30 m³/s) result in higher ebb flows than flood flows. This shows the inlet is only dominated by ebb flows during river floods.

5.3 Scenario B: Dredge spoil removal

In this section the result of the dredge spoil removal on the inlet is investigated. At first the model is simulated without river discharge from the Mfolozi River. Hereafter the discharge of the Mfolozi River is increased and varied from $2 \text{ m}^3/\text{s}$ to $30 \text{ m}^3/\text{s}$ as in previous chapter.

5.3.1 Future state, $Q = 0 \text{ m}^3/\text{s}$ (No river flow)

5.3.1.1 Mean tidal range

The St Lucia Estuary has changed significantly; approximately $1,300,000 \text{ m}^3$ of dredge spoil is removed until a depth of -0.5 MSL . In scenario A, the initial bathymetry, the inlet closes after 156 days when the model is forced with no river discharge and a mean tidal range.

After the dredge spoil is removed the inlet does not close. The morphological evolution of the inlet is visible in Figure 5.29. At first instance two channels are present surrounding the tidal flat in the flood tidal delta. The flood tidal delta develops consisting of multiple tidal flats. After 172 days most of the smaller channels are closed creating a big piece of land that eventually attached to the northern area. The inlet migrates 340 m in southern direction before being severely eroded by high wave action that causes widening of the inlet up to 490 m. In the initial situation, before removing the dredge spoil, the inlet migrates 200 m in northern direction due to the longshore sediment transport before it is closed. The tidal gorge reaches depths of 3.2 m (Figure 5.30). The cumulative transport along the coast equals $465,000 \text{ m}^3/\text{year}$ at the southern side of the inlet and $398,000 \text{ m}^3/\text{year}$ at the northern side.

The hydrodynamic results are given in Figure 5.30. The water levels in the estuary vary between -0.25 m to 0.70 m . During periods of high wave action water levels in the estuary rise up to 0.90 m , which is an elevation of 0.25 m compared to oceanic water levels. The offshore water levels vary between -0.65 m to 0.65 m . The ratio between the water levels in the estuary compared to ocean equals 0.73. Peak flows are varying from 150 to $130 \text{ m}^3/\text{s}$ for flood flows and 120 to $100 \text{ m}^3/\text{s}$ ebb flows. Before the dredge spoil is removed the peak flows are ranging from 110 to $90 \text{ m}^3/\text{s}$ for both flood and ebb flows. The tidal prism equals approximately $1,730,000 \text{ m}^3$, which is an increase of 33.3% compared to the initial situation. This results in an increase of the P/M ratio from 2.70 to 3.72. The inlet stays unstable (intermittently closing) and corresponds to type 3.



Figure 5.28: Photos of dredge spoil removal in St Lucia Estuary

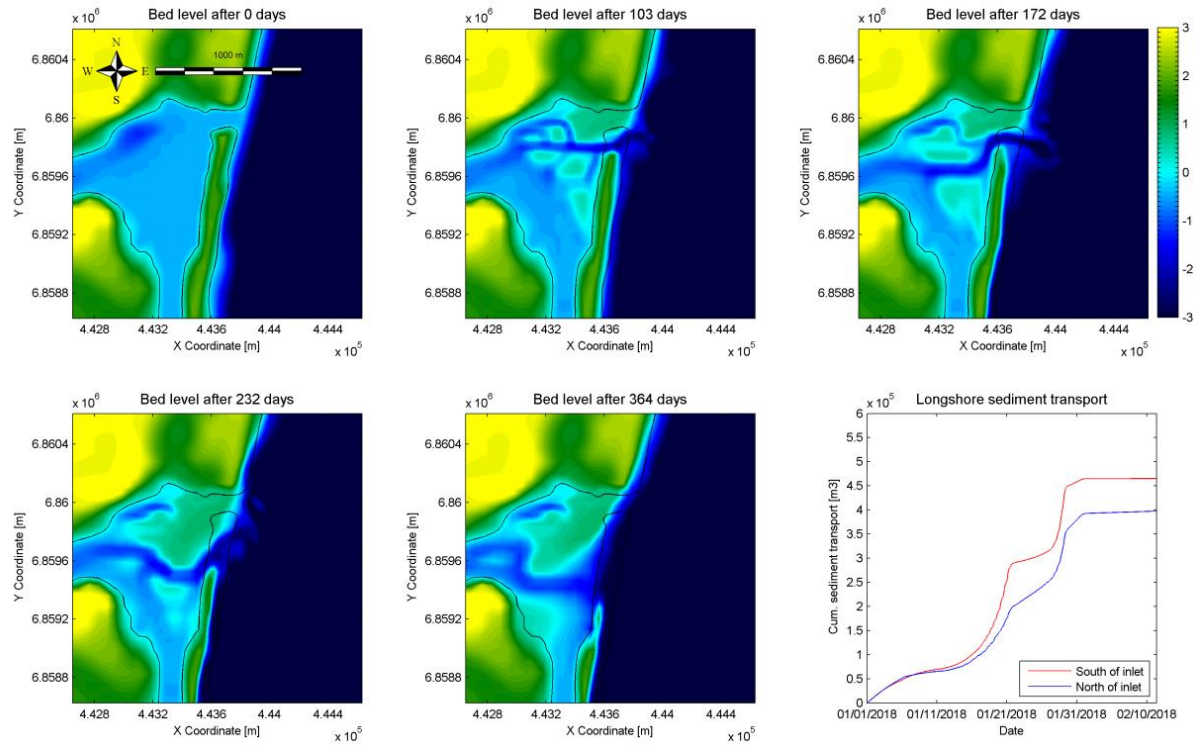


Figure 5.29: Bed level after 0 days, 103 days, 172 days, 232 days, 364 days and cumulative sediment transport along the coast for mean tidal range of 1.3 m

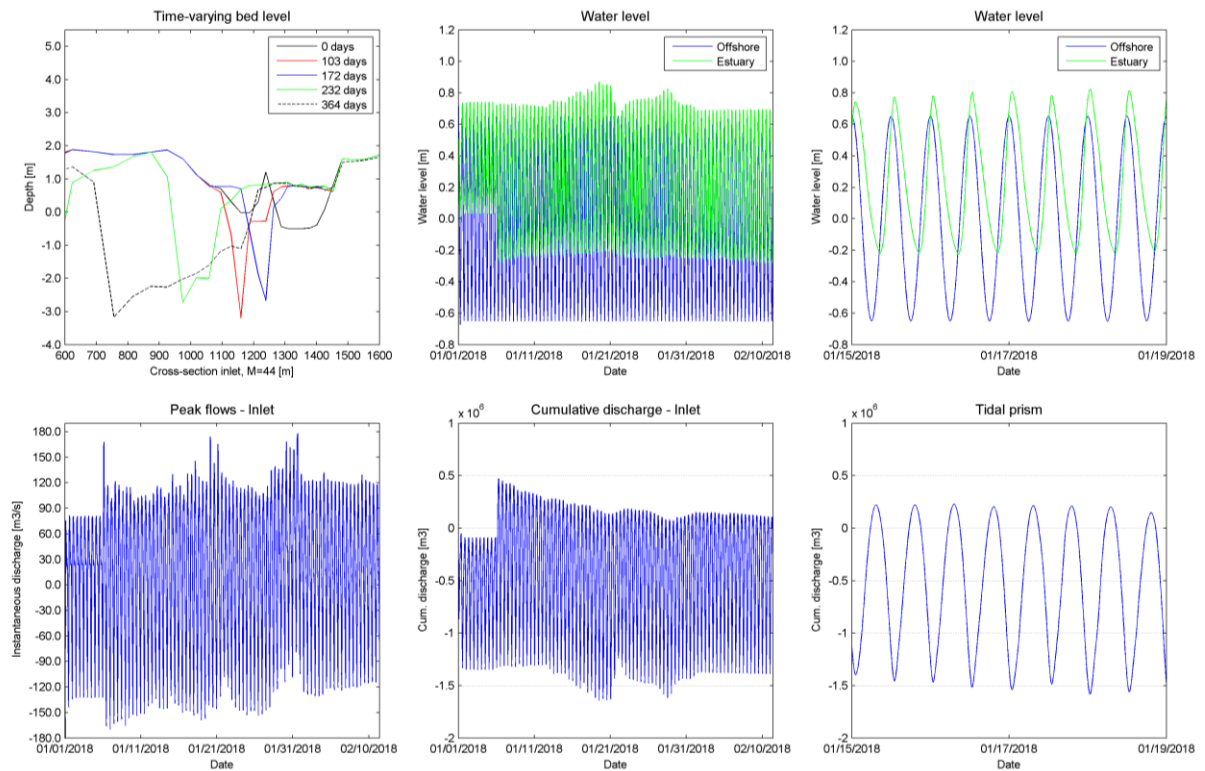


Figure 5.30: Time-varying bed level inlet, water level, detailed water level, peak flows, cumulative discharge through inlet and tidal prism for mean tidal range of 1.3 m

The removal of the dredge spoil has increased the tidal prism and flood dominant character of the estuary. In chapter 4.2.1 one tidal cycle is analysed to show the flood dominant character which is represented by the model. The rising periods are shorter than the falling period and the flood periods are shorter than the ebb periods. Both are properties of flood dominant estuaries.

In Figure 5.31 the water levels in the estuary and peak flows are given for the period from 09/01/2018 18:00 to 10/01/2018 18:00. Besides the tidal prism and sediment transport through the inlet is given. Scenario A and B without river discharge from the Mfolozi River are compared. The low water levels occur at the same time at 20:45. However, the following high water level occurs half an hour earlier compared to the initial situation, at 00:30 instead of 01:00. The low water level occurs at 08:50, which is similar. The rising period decreased by half an hour to 3 hours and 45 minutes and the falling period extended with half an hour to 8 hours and 20 minutes. The flood period starts earlier, 19:20 instead of 19:45, so 20 minutes earlier. The flood duration equals 5 hours and 13 minutes instead of 5 hours and 18 minutes, lasting until 00:33 when the next slack water period starts. After this the ebb period lasts until 07:23, leading to a total duration of 6 hours and 50 minutes. The flood period is 5 minutes shorter compared to scenario A and the ebb period lasts 7 minutes longer. The time of slack water, the change from the ebb period to the flood period, occurs even earlier before reaching low water. These are all properties indicating the estuary got a more flood dominant character due to the removal of the dredge spoil.

Besides the water levels and peak flows one can observe the tidal prism and sediment transport through the inlet in Figure 5.31. The tidal prism increased in magnitude mainly during the flood period. This influences the import of sediments into the estuary, which increased by a factor of 2.7 from 92,000 m³ to 247,000 m³.

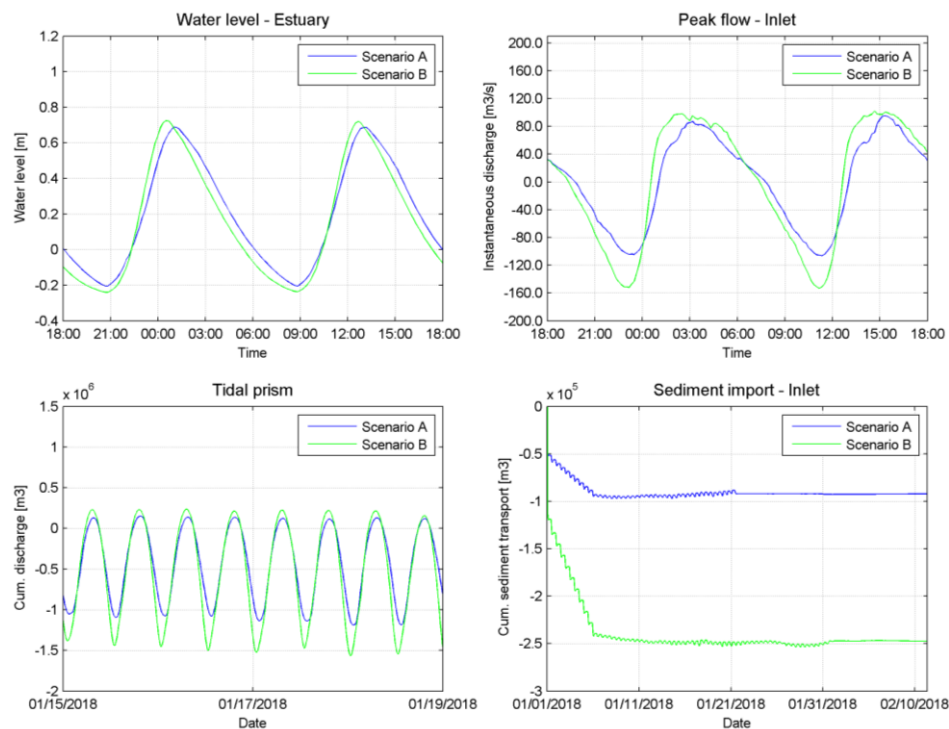


Figure 5.31: Water level and peak flows during two tidal cycles from 9/1/2018 18:00 to 10/1/2018 18:00, tidal prism from 15/1 to 19/1/18 and sediment import through inlet

5.3.1.2 Neap tidal range

The inlet is forced with a neap tidal range of 0.5 m and a time-varying wave climate. The morphological evolution of the estuary after removal of the dredge spoil is given in Figure 5.32. The estuary behaves similar as before and still closes for the majority of the simulation. After 33 days a spit is formed at the downdrift side of the inlet due to sediment bypassing. The tidal gorge reaches a depth of 2.2 m (Figure 5.33). The cumulative longshore sediment transport equals 470,000 m³/year at the southern side of the inlet and 374,000 m³/year at the northern side of the inlet. After 40 days the inlet is closed completely and until approximately 150 days the coastline accretes. The inlet closes 18 days later compared to scenario A. The water levels after closure decreased from 0.35 to 0.20 m. This is because there is more space to accommodate the water. The higher waves during the summer season erode the beach, but the inlet remains closed with a berm height of 0.2 m above MSL.

The hydrodynamic results are given in Figure 5.33. The water levels in the estuary range from -0.10 m to 0.30 m. Offshore the water levels range from -0.25 m to 0.25 m. The ratio between the oceanic tidal range and estuarine tidal range equals 0.80. Peak flows are varying from 50 m³/s during flood flows and 50 to 70 m³/s during ebb flows. The peak flows increased due to the dredge spoil removal, which is one of the reasons the inlet closes at a later stage. The tidal prism equals approximately 760,000 m³ and increased by 31% from 580,000. The P/M ratio increased from 1.23 to 1.62. The inlet remains unstable (intermittently closing) and corresponds to inlet type 3.

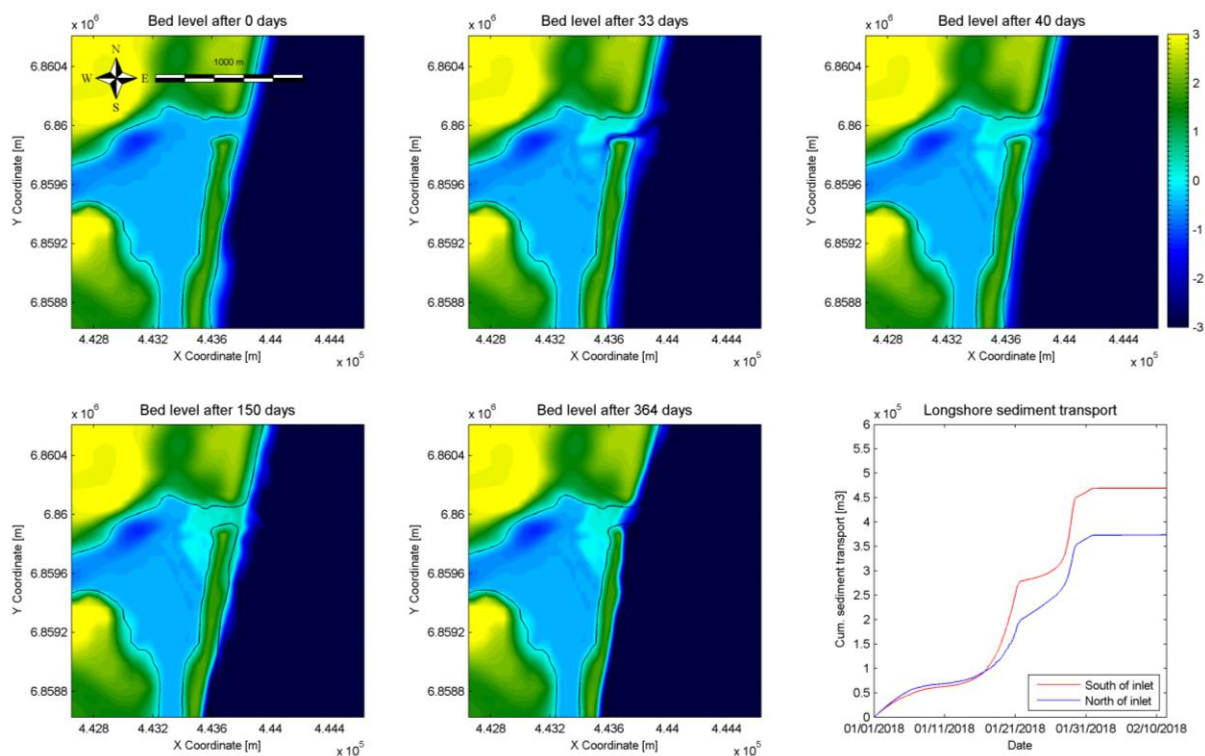


Figure 5.32: Bed level after 0 days, 33 days, 40 days, 150 days, 364 days and cumulative sediment transport along the coast for neap tidal range of 0.5 m

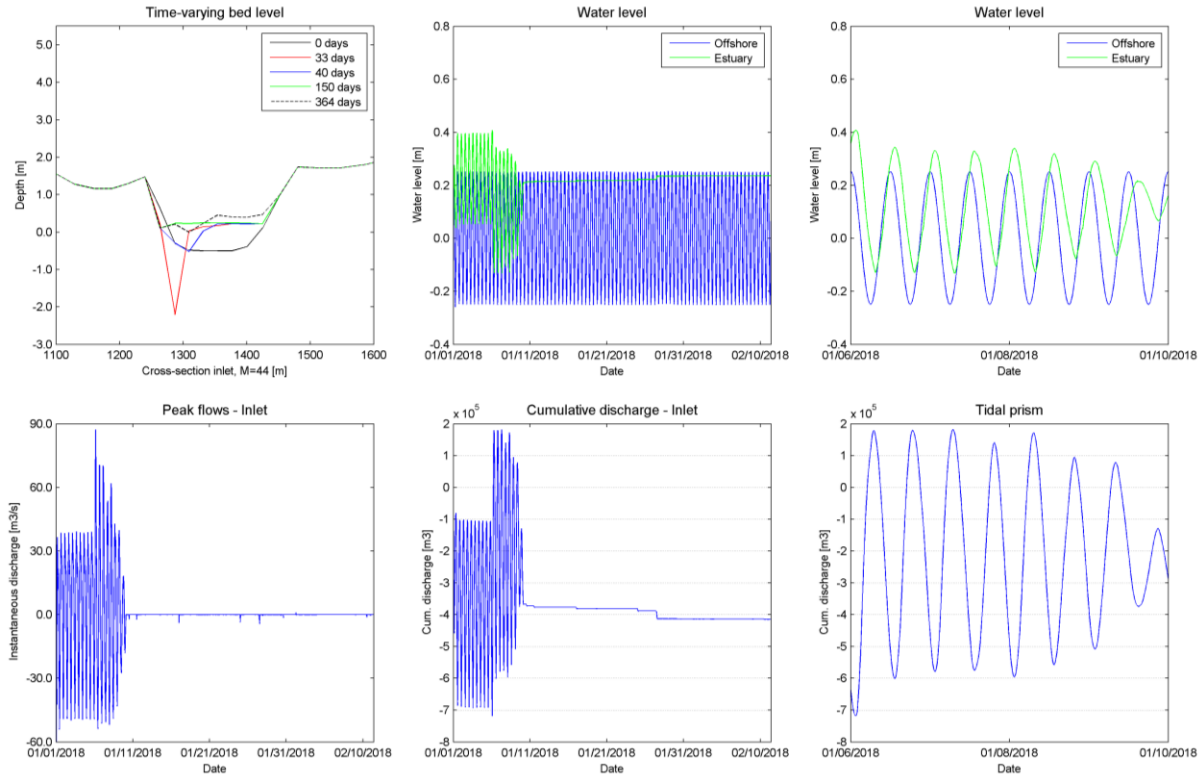


Figure 5.33: Time-varying bed level inlet, water level, detailed water level, peak flows, cumulative discharge through inlet and tidal prism for neap tidal range of 0.5 m

5.3.1.3 Spring tidal range

The morphological evolution of the inlet forced with spring tidal range and the dredge spoil removed is given in Figure 5.34. The simulation behaves similar to the case where the dredge spoil was still present. In both simulations a spit is formed at the updrift side of the inlet and large quantities of sediments are imported in the estuary. The formation of the flood tidal delta is larger when the dredge spoil is removed. Several tidal flats are visible. The inlet nearly closes after 153 days during slack water. The tidal gorge is very narrow, but remains open due to the high peak flows. After 247 days a new opening is formed and the previous inlet closes. This phenomenon of inlet migration and spit breaching is described by Davis and FitzGerald (2004). At the end of the simulation the high wave action causes the inlet to erode and widen up to approximately 460 m (Figure 5.35). The cumulative longshore sediment transport is 520,000 m³/year at the southern side of the inlet and equal to 490,000 m³/year at the northern side of the inlet.

The hydrodynamic results are given in Figure 5.35. The water levels in the estuary vary between -0.25 m to 0.95 m. During periods of high wave action water levels in the estuary reach 1.15 m. This setup of 0.20 m is caused by radiation stress due to wave breaking. The offshore water levels vary between -0.90 m to 0.90 m. The ratio between the water levels in the estuary compared to ocean equals 0.67. Peak flows are varying from 220 to 180 m³/s during flood flows and 180 m³/s for ebb flows. The tidal prism equals 2,240,000 m³. The P/M ratio is equal to 4.31, which corresponds to an inlet type 3 that is unstable and intermittently closing.

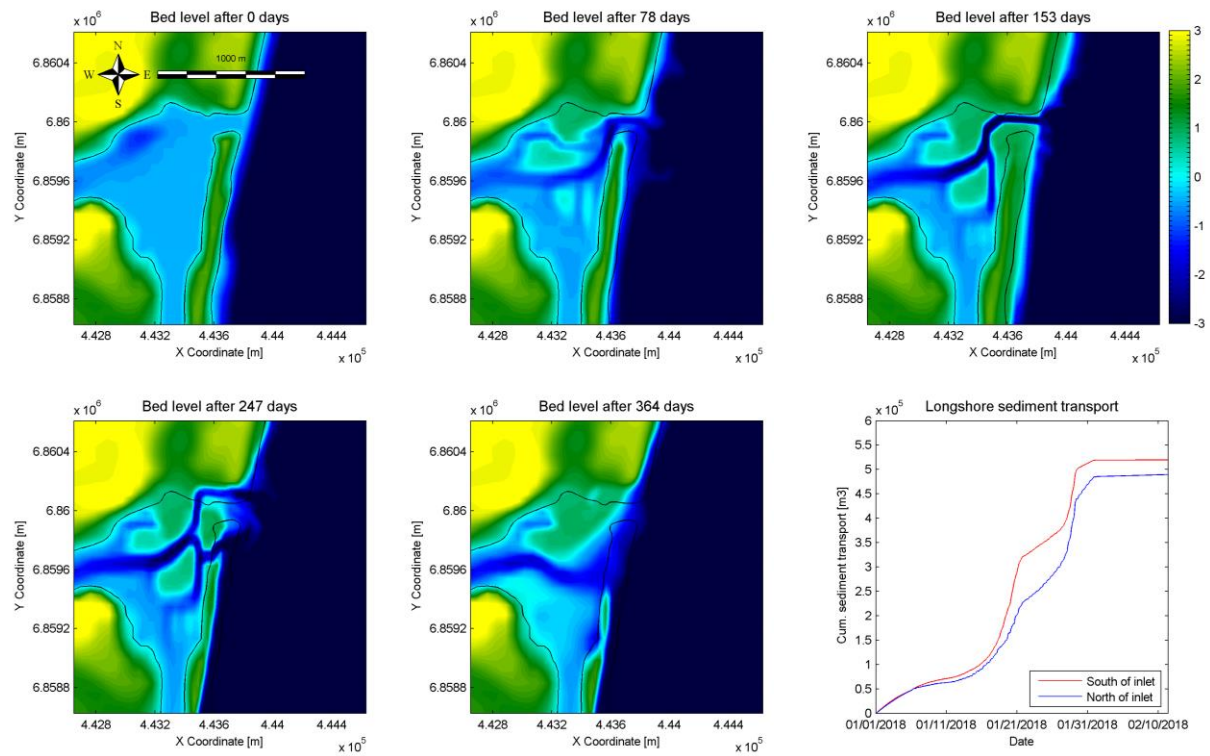


Figure 5.34: Bed level after 0 days, 78 days, 153 days, 247 days, 364 days and cumulative sediment transport along the coast for spring tidal range of 1.8 m

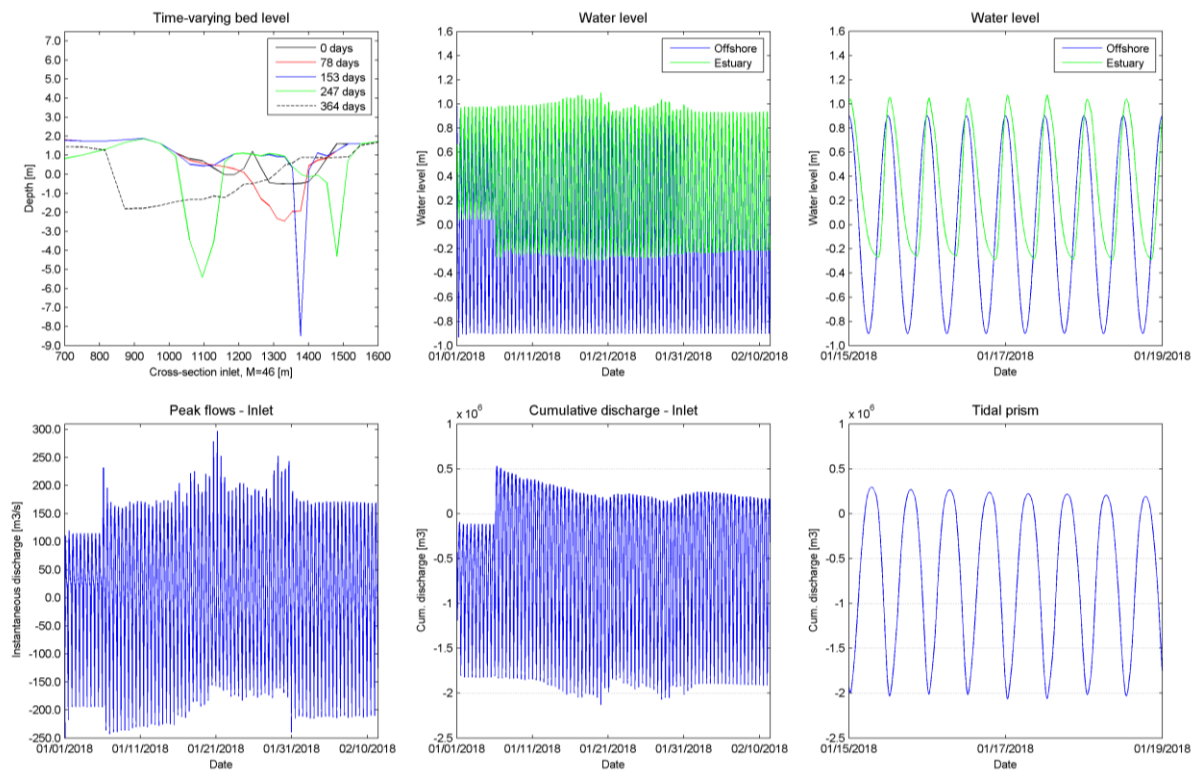


Figure 5.35: Time-varying bed level inlet, water level, detailed water level, peak flows, cumulative discharge through inlet and tidal prism for spring tidal range of 1.8 m

5.3.2 Future state, $Q = 2 \text{ m}^3/\text{s}$ (Winter)

5.3.2.1 Mean tidal range

The model is simulated with a river discharge of $2 \text{ m}^3/\text{s}$ from the Mfolozi River. This discharge is equal to a yearly runoff of $63.1 \cdot 10^6 \text{ m}^3$, which is 7% of the MAR. In previous simulation where the dredge spoil was still present and the river discharge was equal to $2 \text{ m}^3/\text{s}$ the inlet closed for a total period of 21 days. Removal of the dredge spoil prevents closure of the inlet. The morphological evolution of the inlet is visible in Figure 5.36. At first instance two channels are present surrounding the tidal flat in the flood tidal delta. The flood tidal delta develops consisting of multiple tidal flats. The tidal gorge migrates 450 m in southern direction due to the spit that is growing at the downdrift side of the inlet and erosion at the updrift side. The inlet widens drastically after being eroded by high wave action lasting from 208 – 264 days. The tidal gorge reaches a depth of 3.0 m and a width of 540 m (Figure 5.2). This is wider than previous simulation where a width of 400 m was reached. The cumulative transport along the coast equals $468,000 \text{ m}^3/\text{year}$ at the southern side of the inlet and $383,000 \text{ m}^3/\text{year}$ at the northern side.

The hydrodynamic results are given in Figure 5.37. The water levels in the estuary vary between -0.25 m to 0.70 m. During periods of high wave action water levels in the estuary rise up to 0.90 m, which is an elevation of 0.25 m compared to oceanic water levels. The offshore water levels vary between -0.65 m to 0.65 m. The ratio between the water levels in the estuary compared to ocean equals 0.73. Peak flows are varying from 120 to $150 \text{ m}^3/\text{s}$ during both flood flows and ebb flows. Due to the river discharge the tidal prism during ebb tide differs from the tidal prism during flood tide. The ebb tidal prism equals $1,720,000 \text{ m}^3$ and the flood tidal prism equals $1,640,000 \text{ m}^3$. This difference is almost equal to the discharge of the Mfolozi River over one tidal period, which equals $86,400 \text{ m}^3$. The P/M ratio is equal to 3.68, which corresponds to an inlet type 3 that is unstable and intermittently closing.

The tidal prism increased with 19% compared to the simulation where the dredge spoil was still present combined with a river discharge of $2 \text{ m}^3/\text{s}$. The inlet stays open for the complete simulation in contrast to the closure time of 21 days. The increase in tidal prism due to the dredge spoil removal is one factor behind the mouth not closing. The P/M ratio increased from 3.07 to 3.68 due to the dredge spoil being removed.

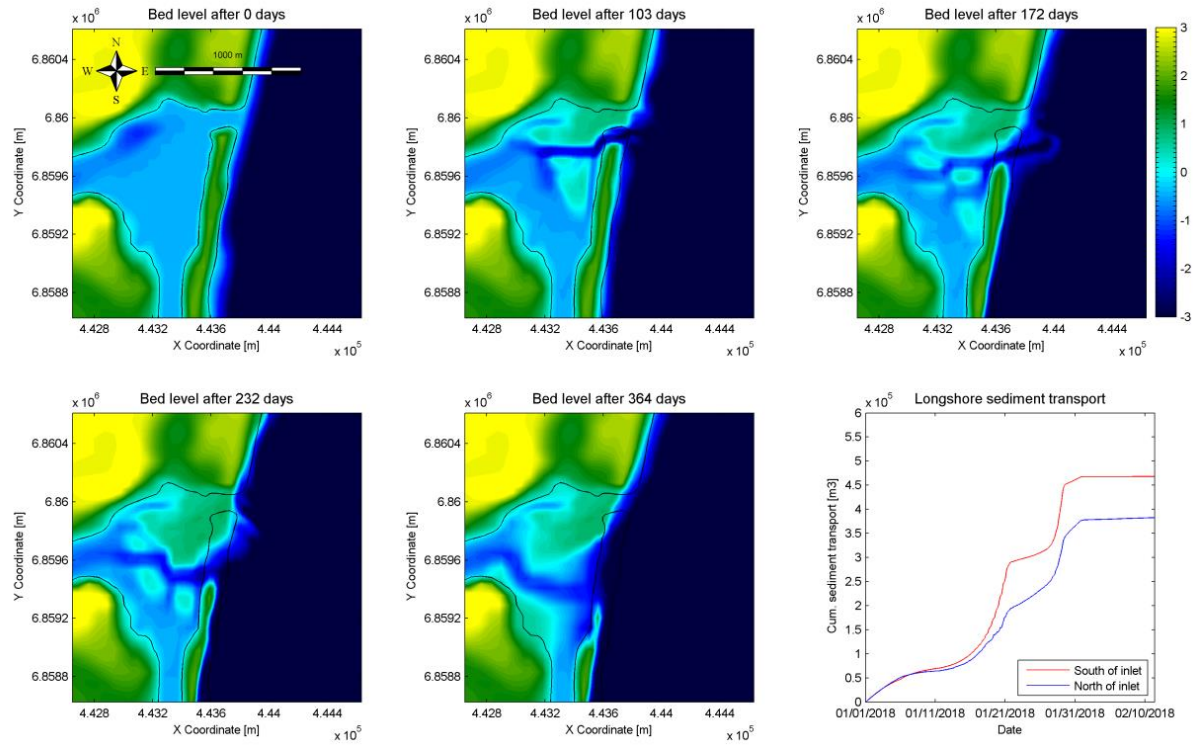


Figure 5.36: Bed level after 0 days, 103 days, 172 days, 232 days, 364 days and cumulative sediment transport along the coast for mean tidal range of 1.30 m

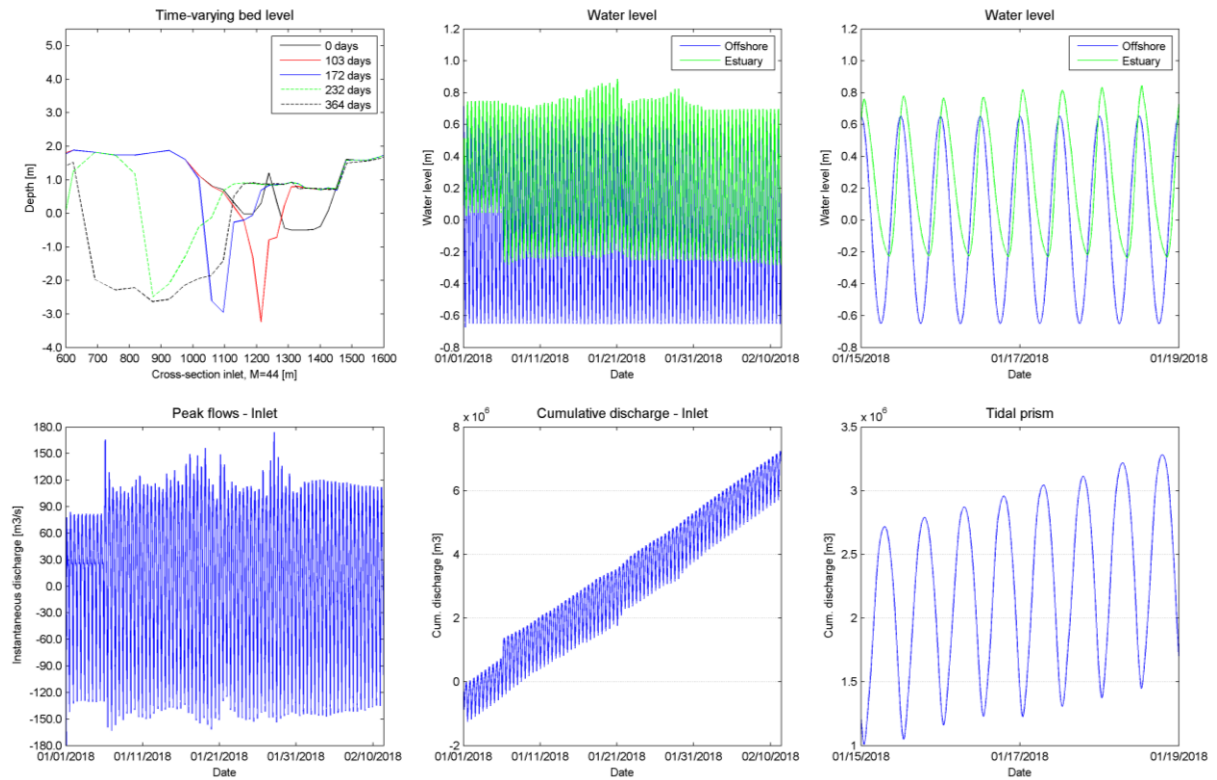


Figure 5.37: Time-varying bed level inlet, water level, detailed water level, peak flows, cumulative discharge through inlet and tidal prism for mean tidal range of 1.30 m

5.3.2.2 Neap tidal range

The morphological evolution of the inlet forced with neap tidal range, dredge spoil removed and a discharge of $2 \text{ m}^3/\text{s}$ is given in Figure 5.38. In previous simulations where the dredge spoil was still present the inlet closed for a total of 105.9 days in four periods. After removing the dredge spoil the inlet again closes four periods around similar times. The mouth closes from 50.4 – 76.3 days, 80.8 – 114.6 days, 125.4 – 162.9 days and 225.0 – 251.3 days. This results in a total closure time of 123.3 days, which is 17.5 days longer than before the dredge spoil is removed.

The inlet shows similar behaviour as before the dredge spoil is removed. The inlet does not migrate a lot and import of sediments cause intermittent closure of the mouth. At the end of the simulation the inlet has migrated 180 m in southern direction. The tidal gorge varies in depth; from a final depth of 1.5 m up to 9.0 m after the inlet is breached (Figure 5.39). The cumulative transport along the coast equals $462,000 \text{ m}^3/\text{year}$ at the southern side of the inlet and $359,000 \text{ m}^3/\text{year}$ at the northern side.

The hydrodynamic results are given in Figure 5.39. The water levels in the estuary vary between -0.10 m to 0.35 m . The water levels in the estuary reach 0.75 m while the inlet is closed and water from the Mfolozi River is flowing into the estuary. The offshore water levels vary between -0.25 m to 0.25 m . The ratio between the water levels in the estuary compared to ocean equals 0.90 . Peak flows are varying from $35 \text{ m}^3/\text{s}$ during flood flows and 50 to $35 \text{ m}^3/\text{s}$ for ebb flows. When the inlet breaches peak flows up to $130 \text{ m}^3/\text{s}$ are reached. The ebb tidal prism equals approximately $736,000 \text{ m}^3$ and the flood tidal prism equals $641,000 \text{ m}^3$. The P/M ratio is equal to 1.59 , which corresponds to an inlet type 3 that is unstable and intermittently closing.

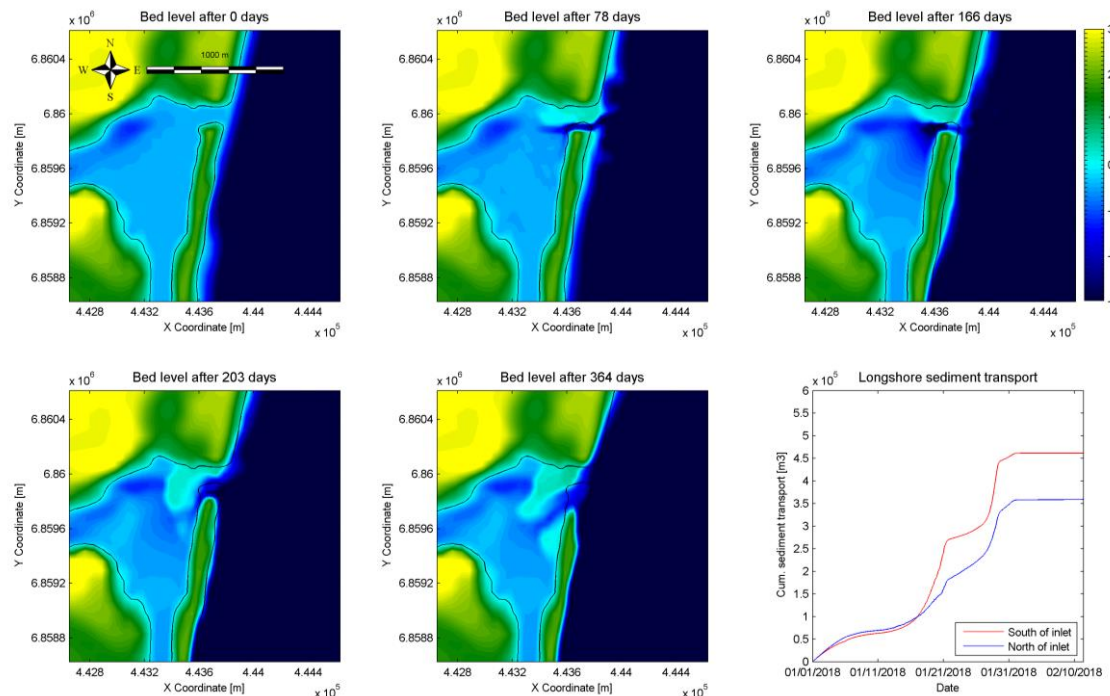


Figure 5.38: Bed level after 0 days, 78 days, 166 days, 203 days, 364 days and cumulative sediment transport along the coast for neap tidal range of 0.50 m

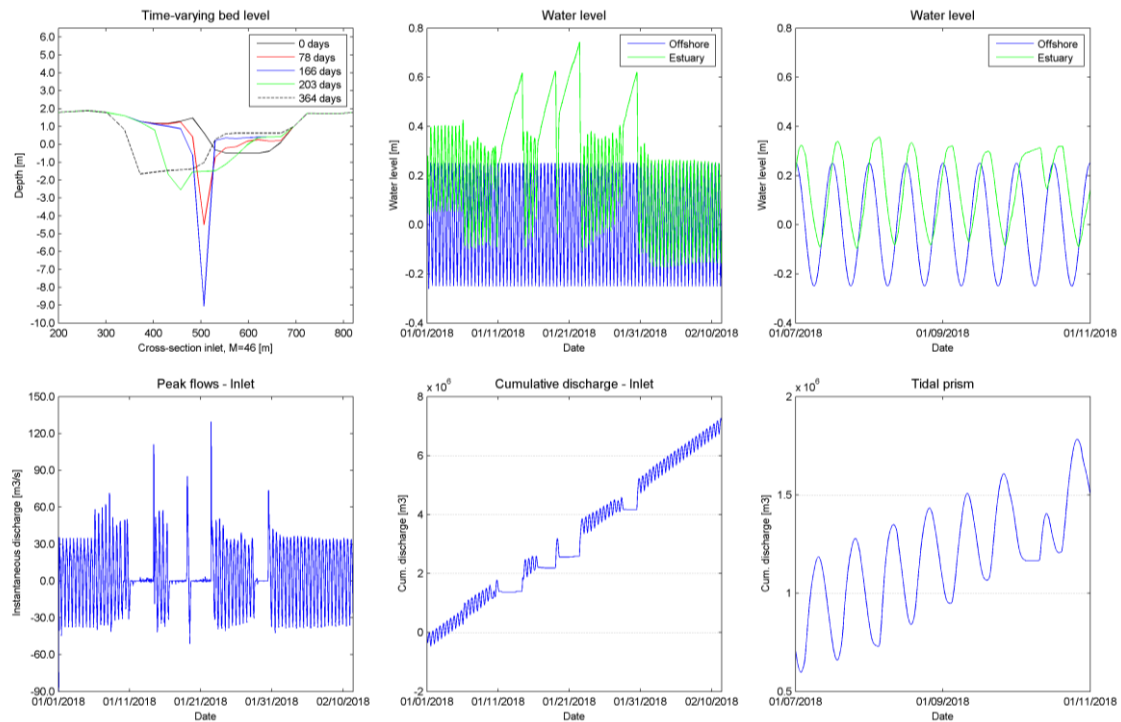


Figure 5.39: Time-varying bed level inlet, water level, detailed water level, peak flows, cumulative discharge through inlet and tidal prism for neap tidal range of 0.50 m

5.3.2.3 Spring tidal range

The morphological evolution of the inlet forced with spring tidal range, dredge spoil removed and a discharge of $2 \text{ m}^3/\text{s}$ is given in Figure 5.40. The simulation behaves similar to the case where the dredge spoil was still present. In both simulations a spit is formed at the updrift side of the inlet and large quantities of sediments are imported in the estuary. The formation of the flood tidal delta is more when the dredge spoil is removed. Several tidal flats are visible. After 247 days a new opening is formed and the previous inlet closes. This is similar as in the simulation where the river discharge equals zero and the dredge spoil is removed. This phenomenon of inlet migration and spit breaching is described by Davis and FitzGerald (2004). At the end of the simulation the high wave action causes the inlet to erode and widen drastically up to 670 m (Figure 5.41). The cumulative longshore sediment transport is $539,000 \text{ m}^3/\text{year}$ at the southern side of the inlet and equal to $496,000 \text{ m}^3/\text{year}$ at the northern side of the inlet.

The hydrodynamic results are given in Figure 5.41. The water levels in the estuary vary between -0.25 m to 0.95 m . During periods of high wave action water levels in the estuary reach 1.15 m . This setup of 0.20 m is caused by radiation stress due to wave breaking. The offshore water levels vary between -0.90 m to 0.90 m . The ratio between the water levels in the estuary compared to ocean equals 0.67 . Peak flows are 180 to 240 during flood flows and varying from $180 \text{ m}^3/\text{s}$ for ebb flows. The ebb tidal prism equals $2,390,000 \text{ m}^3$ and the flood tidal prism equals $2,320,000 \text{ m}^3$. The P/M ratio is equal to 4.43 , which corresponds to an inlet type 3 that is unstable and intermittently closing.

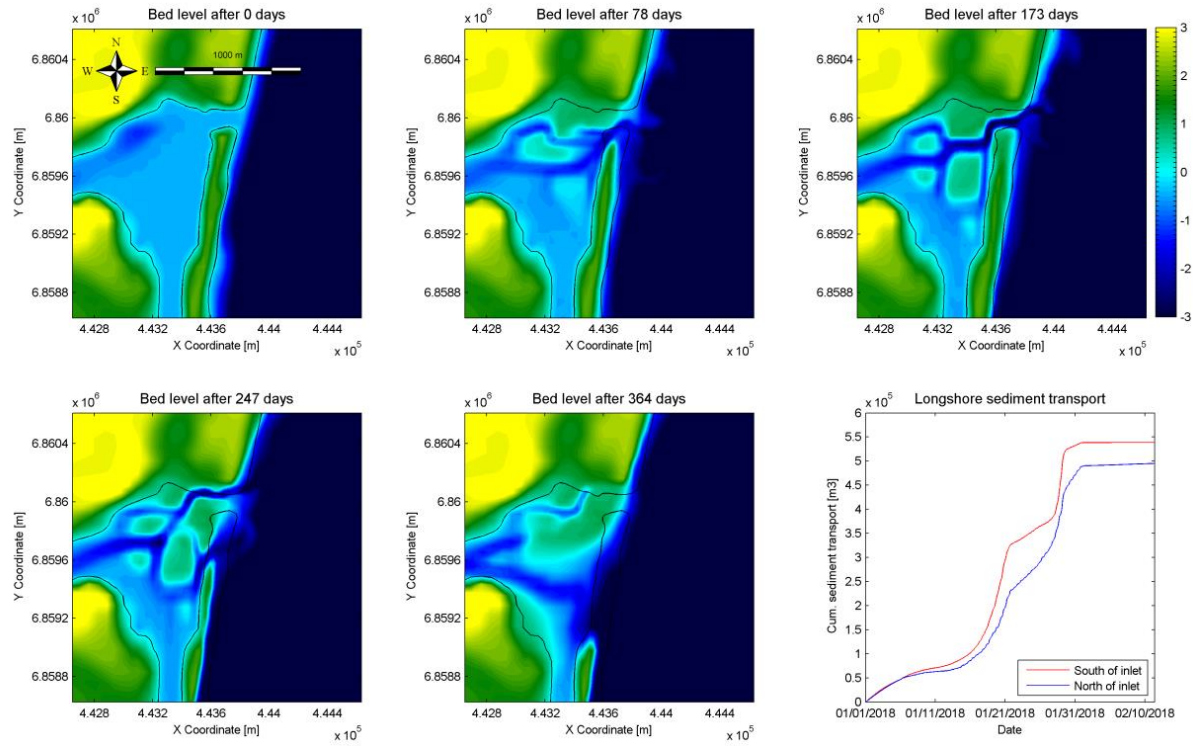


Figure 5.40: Bed level after 0 days, 78 days, 173 days, 247 days, 364 days and cumulative sediment transport along the coast for spring tidal range of 1.80 m

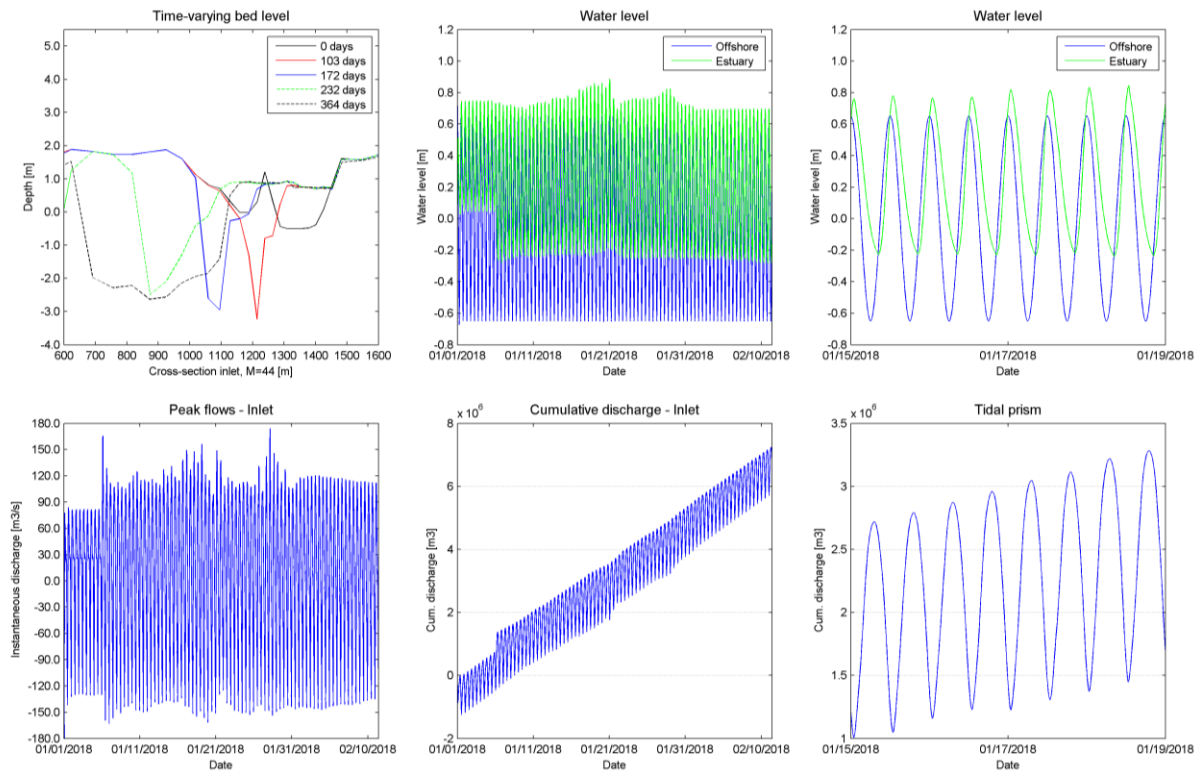


Figure 5.41: Time-varying bed level inlet, water level, detailed water level, peak flows, cumulative discharge through inlet and tidal prism for spring tidal range of 1.80 m

5.3.3 Future state, $Q = 5 \text{ m}^3/\text{s}$ (Drought)

5.3.3.1 Mean tidal range

The model is simulated with a river discharge of $5 \text{ m}^3/\text{s}$ from the Mfolozi River. This discharge is equal to a yearly runoff of $157.7 \cdot 10^6 \text{ m}^3$, which is 17% of the MAR. Before removing the dredge spoil the inlet closed twice for a total duration of 5 days when the Mfolozi River discharge is increased to $5 \text{ m}^3/\text{s}$. After dredge spoil removal the inlet remains closed once between 155.4 and 166.3 days, leading to a total closure time of 10.8 days. The morphological evolution of the inlet is visible in Figure 5.42. The estuary imports a lot of sediments and the development of a flood tidal delta is visible in the first period. After reopening there is one main channel left towards the St Lucia Estuary. Most of the land that has been removed is imported again in the estuary. The inlet widens up to 600 m due to high wave action and migrates approximately 500 m in southward direction with respect to its starting position. The tidal gorge reaches a maximum depth of 3.3 m (Figure 5.43). The cumulative transport along the coast equals $463,000 \text{ m}^3/\text{year}$ at the southern side of the inlet and $386,000 \text{ m}^3/\text{year}$ at the northern side.

The hydrodynamic results are given in Figure 5.43. The water levels in the estuary vary between -0.25 m to 0.70 m . During periods of high wave action water levels in the estuary rise up to 0.88 m , which is an elevation of 0.23 m compared to oceanic water levels. The offshore water levels vary between -0.65 m to 0.65 m . The ratio between the water levels in the estuary compared to ocean equals 0.73. Peak flows are varying from 150 to $130 \text{ m}^3/\text{s}$ for both flood – and ebb flows. The ebb tidal prism equals $1,990,000 \text{ m}^3$ and the flood tidal prism equals $1,720,000 \text{ m}^3$. This difference is approximately equal to the discharge of the Mfolozi River over one tidal period, which equals $216,000 \text{ m}^3$. The P/M ratio increased to 4.30 from 3.25, which corresponds to an inlet type 3 that is unstable and intermittently closing.

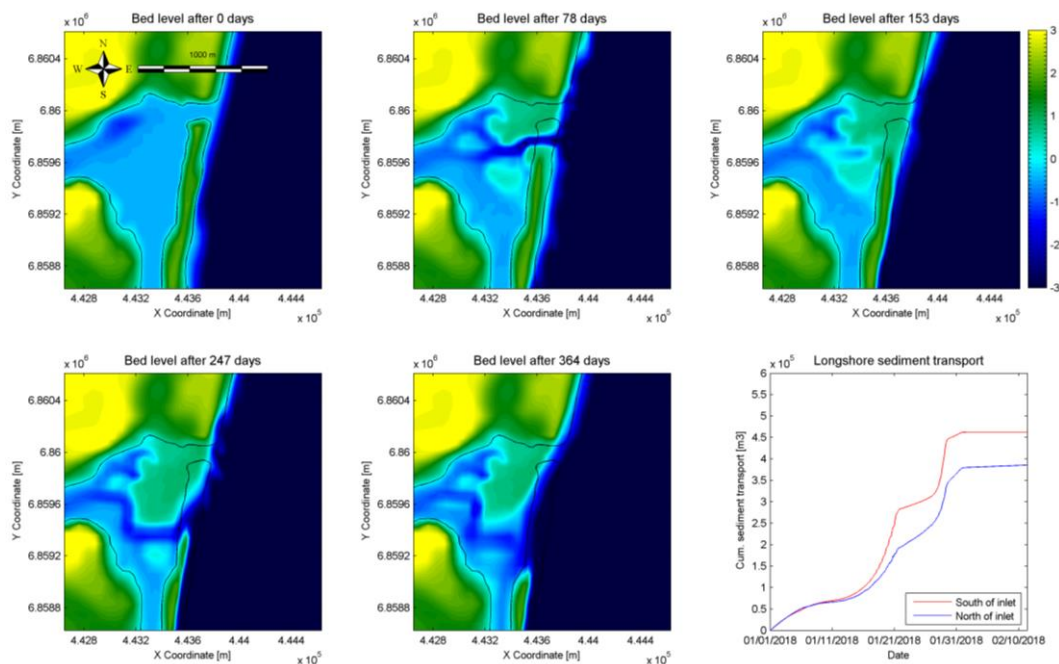


Figure 5.42: Bed level after 0 days, 78 days, 153 days, 247 days, 364 days and cumulative sediment transport along the coast for mean tidal range of 1.30 m

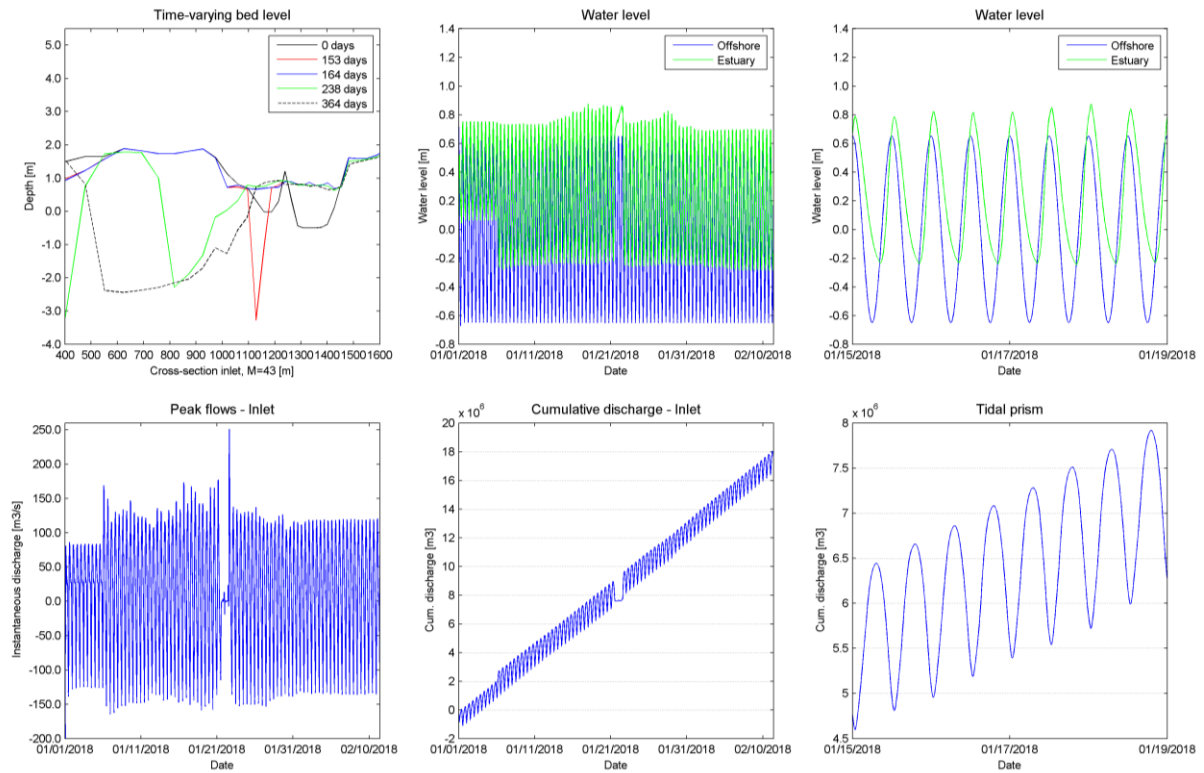


Figure 5.43: Time-varying bed level inlet, water level, detailed water level, peak flows, cumulative discharge through inlet and tidal prism for mean tidal range of 1.30 m

5.3.3.2 Neap tidal range

The morphological evolution of the inlet forced with neap tidal range and a discharge of $5 \text{ m}^3/\text{s}$ is given in Figure 5.44. In previous simulation with dredge spoil still present the inlet closed 9 times for a total of 46.8 days. The estuary behaves similar before and after removing the dredge spoil. The inlet still closes 9 times from 65.4 – 75.8 days, 80.0 – 81.3 days, 84.6 – 87.1 days, 90.4 – 100.8 days, 110.4 – 111.3 days, 115.4 – 126.7 days, 134.6 – 143.8 days, 145.4 – 157.5 days and from 230.4 – 232.1 days. The inlet is closed for a total duration of 59.6 days, which is an increase of 12.8 days. Water levels in the estuary built up 0.75 m due to river flow from the Mfolozi that enters the St Lucia Estuary when the inlet is closed. The inlet behaves as a type 3 inlet that is locationally stable and closes intermittently. Due to the dredge spoil removal the channel towards the St Lucia Estuary stays open, whereas before the channel was prone to close. The cumulative transport along the coast equals $468,000 \text{ m}^3/\text{year}$ at the southern side of the inlet and $380,000 \text{ m}^3/\text{year}$ at the northern side.

The hydrodynamic results are visible in Figure 5.45. The water levels in the estuary vary between -0.15 m up to 0.35 m . The offshore water levels vary between -0.25 m to 0.25 m . The ratio between the water levels in the estuary compared to ocean equals 1.00. Peak flows are varying from $40 \text{ m}^3/\text{s}$ during both flood flows and ebb flows with maxima of approximately $650 \text{ m}^3/\text{s}$. These high discharges are reached after the inlet breaches and water from the estuary flushes out to the ocean. The ebb tidal prism equals $880,000 \text{ m}^3$ and the flood tidal prism equals $680,000 \text{ m}^3$. The P/M ratio increased from 1.54 to 1.88. The inlet still corresponds to an inlet type 3 that is unstable and intermittently closing.

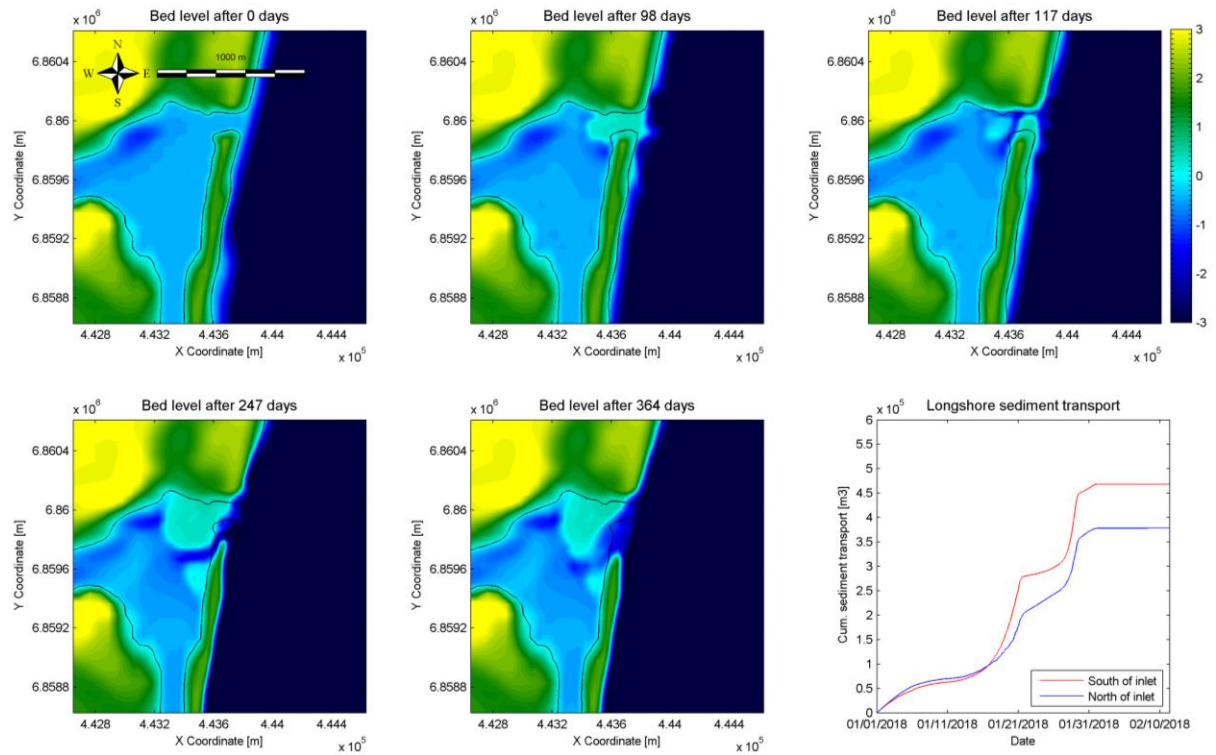


Figure 5.44: Bed level after 0 days, 98 days, 117 days, 247 days, 364 days and cumulative sediment transport along the coast for neap tidal range of 0.50 m

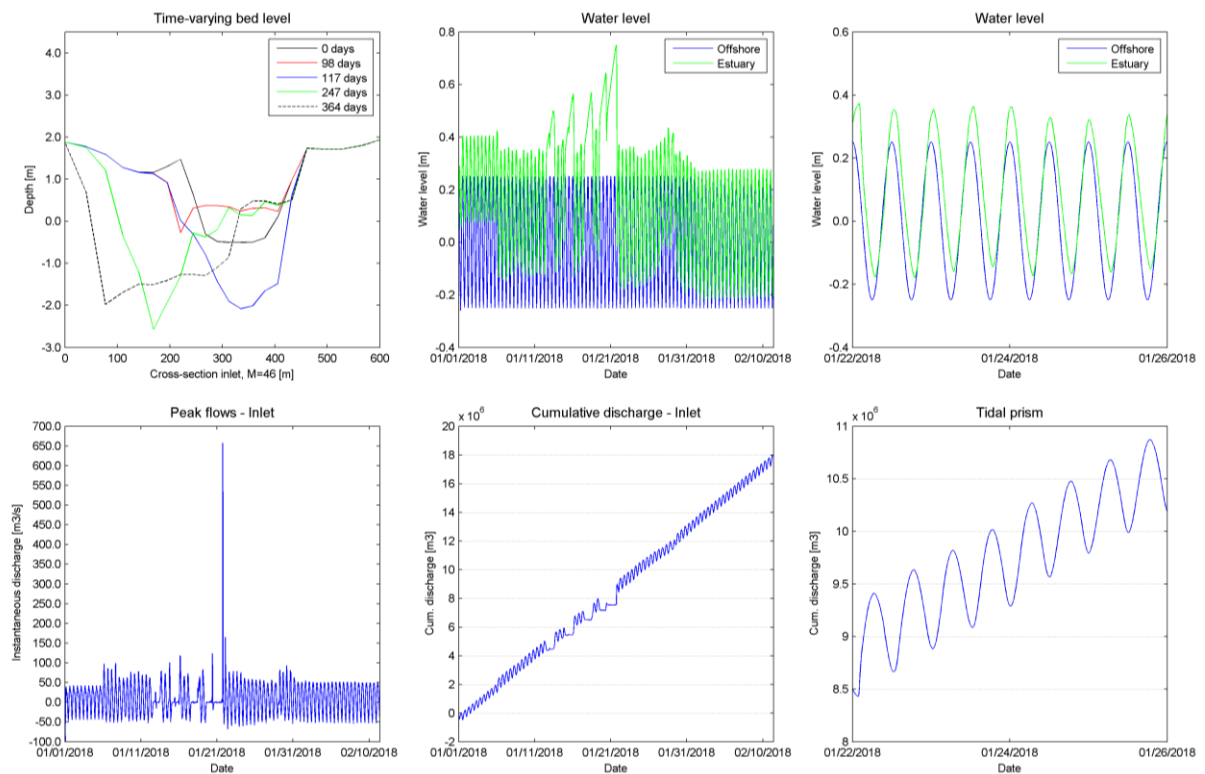


Figure 5.45: Time-varying bed level inlet, water level, detailed water level, peak flows, cumulative discharge through inlet and tidal prism for neap tidal range of 0.50 m

5.3.3.3 Spring tidal range

As in previous simulation the model is simulated with a river discharge of $5 \text{ m}^3/\text{s}$, only now with a spring tidal range of 1.8 m. The morphological evolution is visible in Figure 5.46. The estuary behaves similar as in previous simulation with a river discharge of $2 \text{ m}^3/\text{s}$. However fewer tidal flats are present and there are two main channels into the St Lucia Estuary and the Mfolozi River. The tidal flat forms onto the land of dredge spoil. The inlet does not close in contrast to previous simulation where the dredge spoil was still present the inlet closed for a period of 15 days. The impact of the larger waves in combination with spring tide erodes the inlet and it widens up to 580 m at MSL (Figure 5.47). The longshore transport at the southern side of the inlet equals $518,000 \text{ m}^3/\text{year}$ and at the northern side equals $479,000 \text{ m}^3/\text{year}$.

The hydrodynamic results are given in Figure 5.47. The water levels in the estuary vary between -0.25 m and -0.30 m up to 1.00 m . During periods of high wave action water levels in the estuary rise up to 1.15 m , which is an elevation of 0.25 m compared to oceanic water levels. The offshore water levels vary between -0.90 m to 0.90 m . The ratio between the water levels in the estuary compared to ocean equals 0.69. Peak flows are varying from 240 to $220 \text{ m}^3/\text{s}$ during flood flows and $200 \text{ m}^3/\text{s}$ for ebb flows. The ebb tidal prism equals $2,400,000 \text{ m}^3$ and the flood tidal prism equals $2,170,000 \text{ m}^3$. The P/M ratio increased to 4.63 from 3.92, which corresponds to an inlet type 3 that is unstable and intermittently closing.

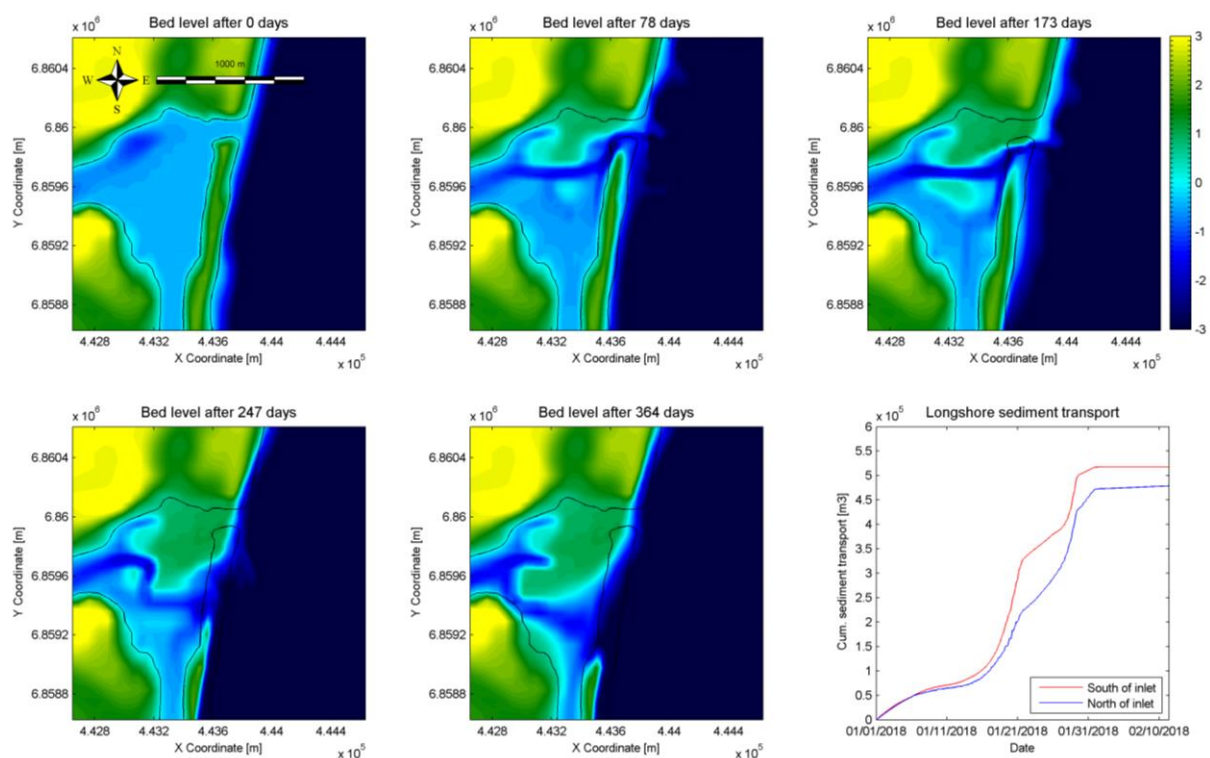


Figure 5.46: Bed level after 0 days, 78 days, 173 days, 247 days, 364 days and cumulative sediment transport along the coast for spring tidal range of 1.80 m

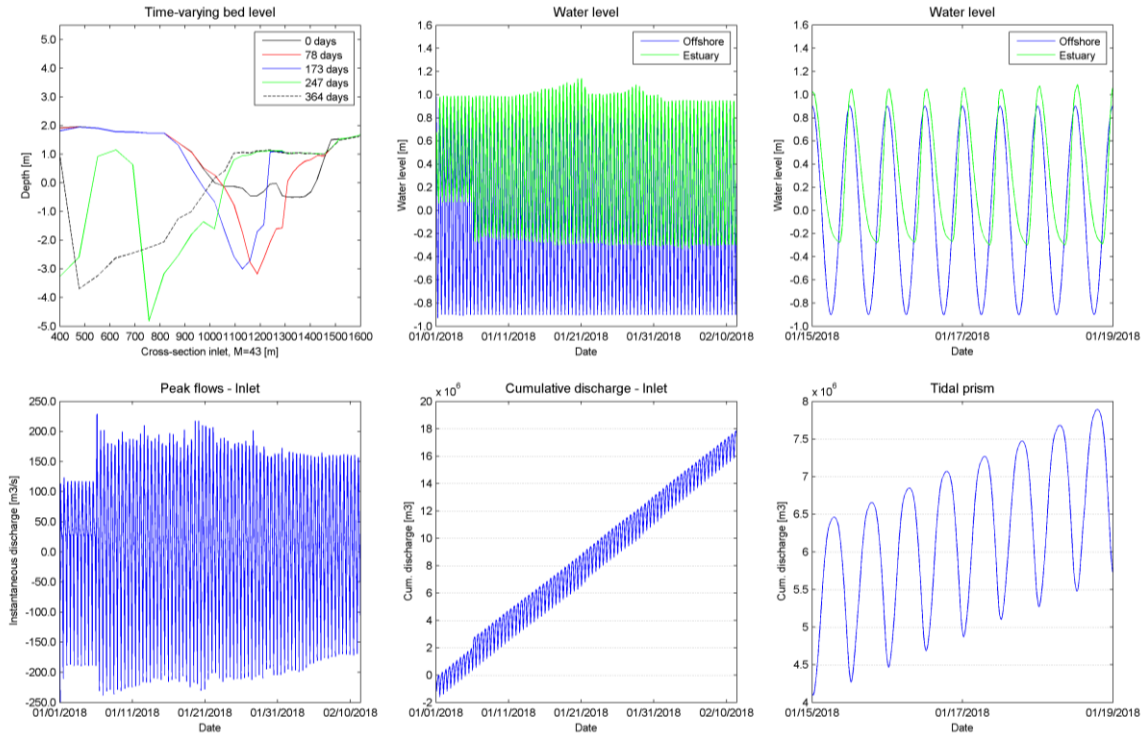


Figure 5.47: Time-varying bed level inlet, water level, detailed water level, peak flows, cumulative discharge through inlet and tidal prism for spring tidal range of 1.80 m

5.3.4 Future state, $Q = 14 \text{ m}^3/\text{s}$ (Summer)

5.3.4.1 Mean tidal range

The model is simulated with a river discharge of $14 \text{ m}^3/\text{s}$ from the Mfolozi River. This discharge is equal to a yearly runoff of $441.5 \cdot 10^6 \text{ m}^3$, which is 47% of the MAR. Before removing the dredge spoil the inlet closed for a duration of 1.3 days from 150.4 to 151.7 days. After the dredge spoil is removed the inlet does not close. The morphological evolution of the inlet is visible in Figure 5.48. The estuary imports sediments and the development of tidal flats in the flood tidal delta is visible. Two channels surround the tidal flat. Accretion of the northern channel causes the tidal gorge to migrate in southern direction. The tidal gorge migrates approximately 550 m in southern direction. At the end of the simulation time the high wave action cause widening of the inlet up to 640 m. The tidal gorge reaches depths of 4.3 m (Figure 5.49). The cumulative transport along the coast equals $463,000 \text{ m}^3/\text{year}$ at the southern side of the inlet and $406,000 \text{ m}^3/\text{year}$ at the northern side.

The hydrodynamic results are given in Figure 5.49. The water levels in the estuary vary between -0.25 m to 0.70 m . During periods of high wave action water levels in the estuary rise up to 0.90 m , which is an elevation of 0.25 m compared to oceanic water levels. The offshore water levels vary between -0.65 m to 0.65 m . The ratio between the water levels in the estuary compared to ocean equals 0.73. Peak flows are varying from $150 \text{ m}^3/\text{s}$ for flood flows and ebb flows. Due to elevated water levels the peak discharges increase up to $200 \text{ m}^3/\text{s}$ during ebb flows. The ebb tidal prism equals $2,150,000 \text{ m}^3$ and the flood tidal prism equals $1,590,000 \text{ m}^3$. This difference is approximately equal to the discharge of the Mfolozi River over one tidal period, which equals $604,800 \text{ m}^3$. The P/M ratio is increased from 3.74 to 4.64. The inlet remains an unstable and intermittently closing inlet that corresponds to an inlet type 3.

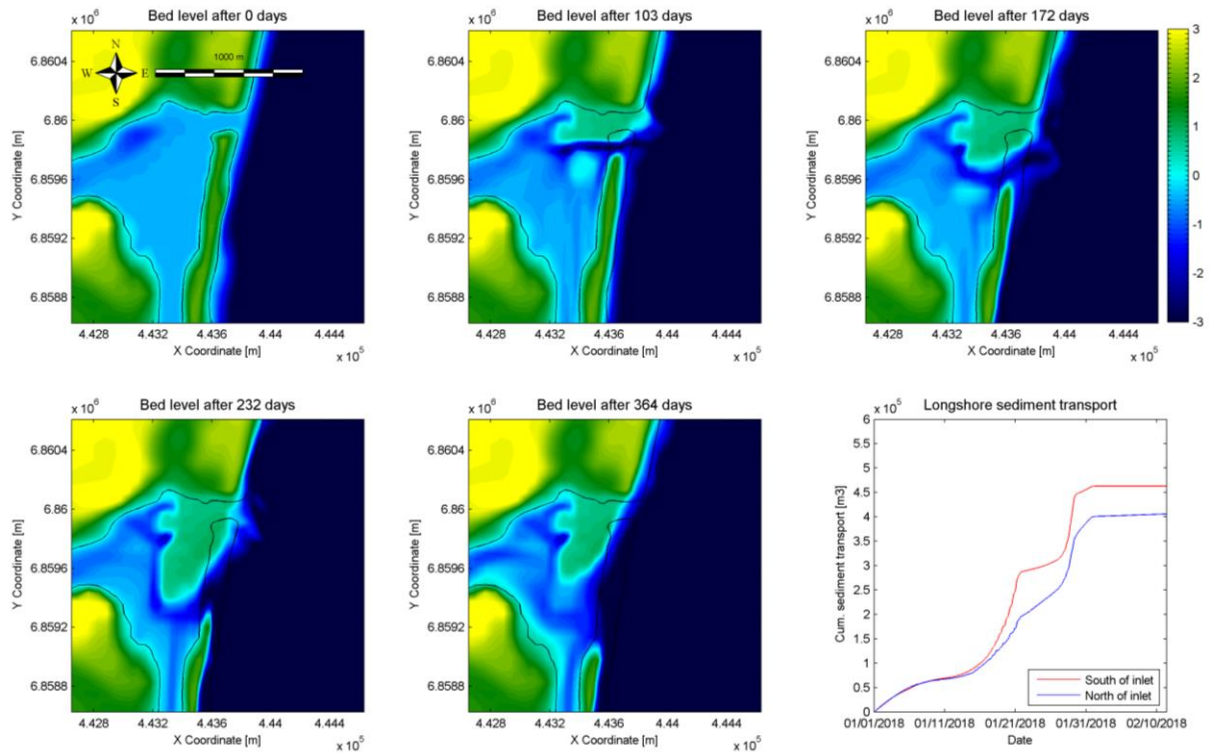


Figure 5.48: Bed level after 0 days, 103 days, 172 days, 232 days, 364 days and cumulative sediment transport along the coast for mean tidal range of 1.30 m

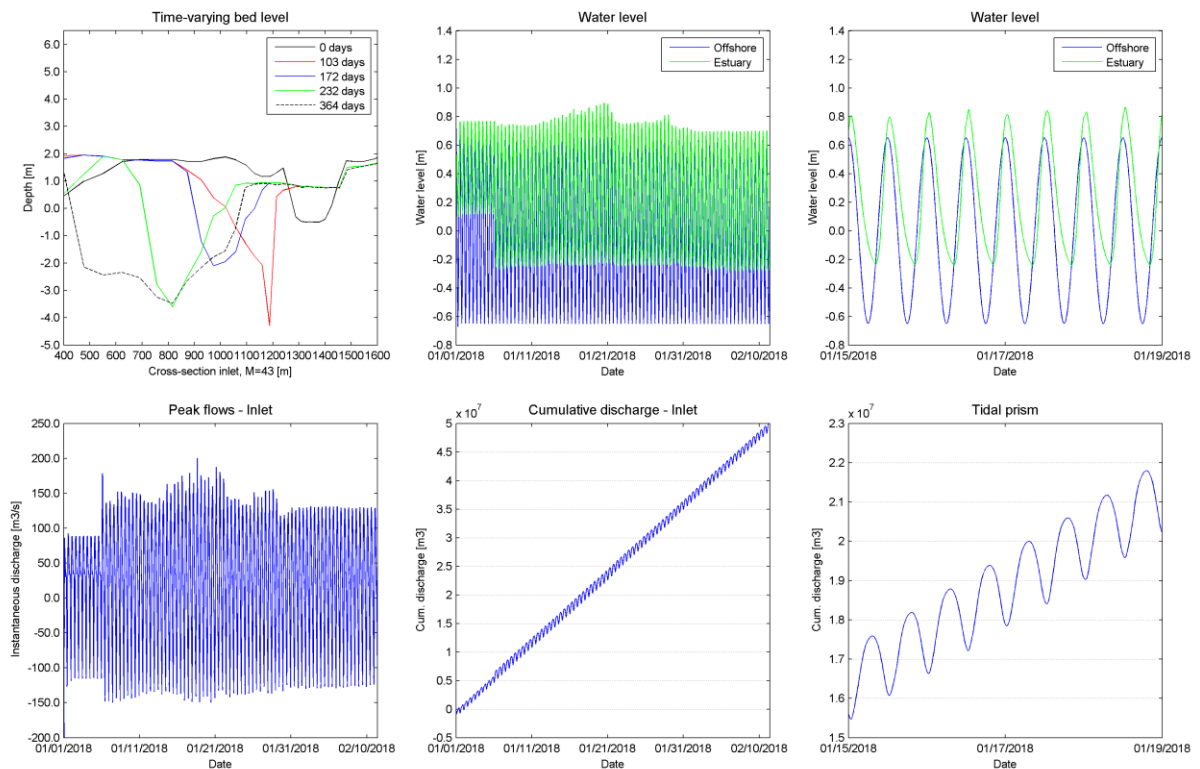


Figure 5.49: Time-varying bed level inlet, water level, detailed water level, peak flows, cumulative discharge through inlet and tidal prism for mean tidal range of 1.30 m

5.3.4.2 Neap tidal range

The morphological evolution of the inlet forced with neap tidal range and a discharge of $14 \text{ m}^3/\text{s}$ is given in Figure 5.50. In previous simulation with dredge spoil still present the inlet closed 11 times for a total of 31.3 days. After 220 days the channel towards the St Lucia Estuary closes, the dredge spoil island attaches to the northern part. The estuary behaves differently after the dredge spoil is removed. The inlet closes 9 times from 75.4 – 76.7 days, 80.4 – 82.5 days, 85.4 – 87.5 days, 90.8 – 91.7 days, 105.4 – 107.1 days, 125.4 – 128.3 days, 133.3 – 137.1 days, 145.0 – 148.8 days and from 155.0 – 155.8 days. The inlet is closed for a total duration of 19.2 days, which is a decrease of 12.1 days. After the inlet reopens the estuary starts importing a lot of sediments creating a large piece of land extending from the northern side. The connection to the St Lucia Estuary remains open. A longer simulation time is necessary to see if the inlet will eventually close. The cumulative transport along the coast equals $467,000 \text{ m}^3/\text{year}$ at the southern side of the inlet and $369,000 \text{ m}^3/\text{year}$ at the northern side.

The hydrodynamic results are visible in Figure 5.51. The water levels in the estuary vary between -0.15 m up to 0.35 m . The offshore water levels vary between -0.25 m to 0.25 m . The ratio between the water levels in the estuary compared to ocean equals 1.00. Peak flows are varying from $40 \text{ m}^3/\text{s}$ during flood flows and $60 \text{ m}^3/\text{s}$ for ebb flows with maxima of $960 \text{ m}^3/\text{s}$. These high discharges are reached after the inlet breaches and water from the estuary flushes out to the ocean. The ebb tidal prism equals $1,100,000 \text{ m}^3$ and the flood tidal prism equals $490,000 \text{ m}^3$. The P/M ratio is increased from 2.18 to 2.36. The inlet still corresponds to an inlet type 3 that is unstable and intermittently closing.

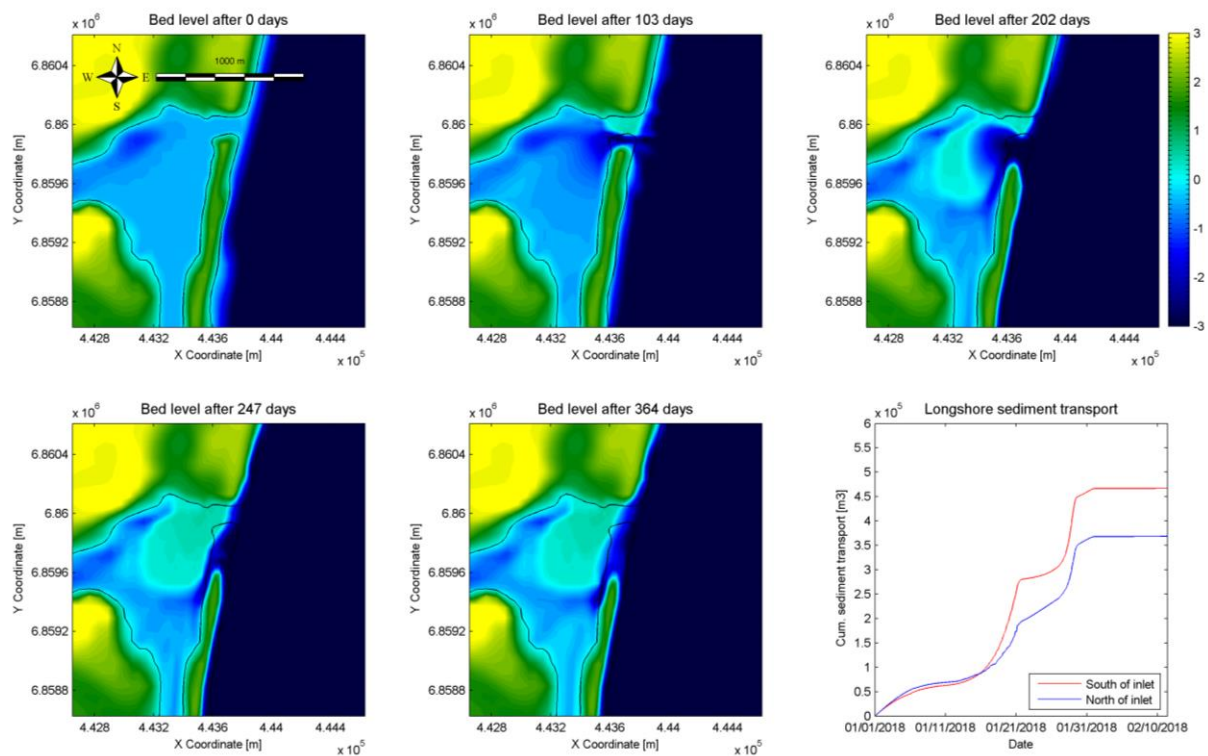


Figure 5.50: Bed level after 0 days, 103 days, 202 days, 247 days, 364 days and cumulative sediment transport along the coast for neap tidal range of 0.50 m

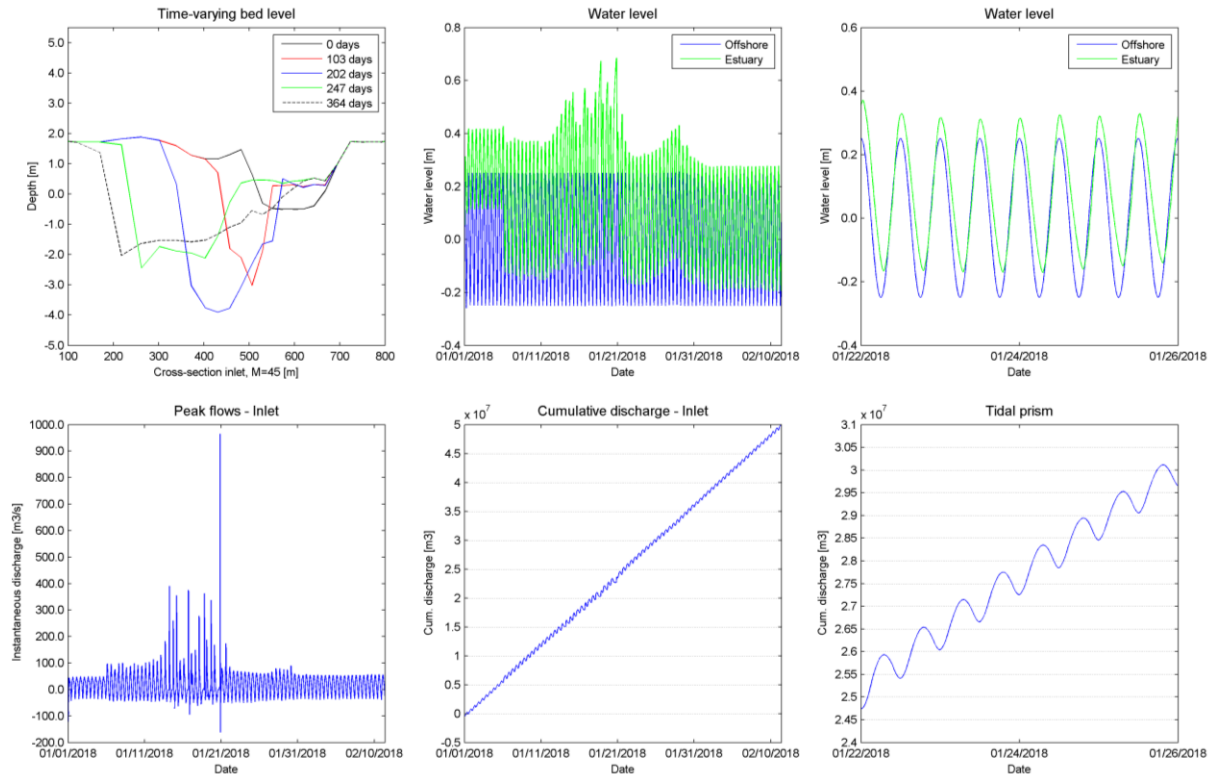


Figure 5.51: Time-varying bed level inlet, water level, detailed water level, peak flows, cumulative discharge through inlet and tidal prism for neap tidal range of 0.50 m

5.3.4.3 Spring tidal range

As in previous simulation the model is simulated with a river discharge of $14 \text{ m}^3/\text{s}$, only now with a spring tidal range of 1.8 m. The morphological evolution is visible in Figure 5.52. The estuary behaves similar as the simulation forced with mean tidal range. The tidal flats are large due to the higher discharges that import and export sediments. The tidal flats are surrounded by two channels of which the northern channel silts up and closes. This repeats itself and causes the extension of land from the northern side into the estuary. Before removing the dredge spoil the tidal gorge migrates in northern direction due to spit formation instead of migrating in southern direction. The impact of the larger waves in combination with spring tide erodes the inlet and it widens up to 600 m at MSL (Figure 5.53). The longshore transport at the southern side of the inlet equals $502,000 \text{ m}^3/\text{year}$ and at the northern side equals $468,000 \text{ m}^3/\text{year}$.

The hydrodynamic results are given in Figure 5.53. The water levels in the estuary vary between -0.25 m and -0.30 m up to 1.00 m . During periods of high wave action water levels in the estuary rise up to 1.15 m , which is an elevation of 0.25 m compared to oceanic water levels. The offshore water levels vary between -0.90 m to 0.90 m . The ratio between the water levels in the estuary compared to ocean equals 0.69 . Peak flows are varying from 220 to $200 \text{ m}^3/\text{s}$ during flood flows and $200 \text{ m}^3/\text{s}$ for ebb flows. The ebb tidal prism equals $2,720,000 \text{ m}^3$ and the flood tidal prism equals $2,120,000 \text{ m}^3$. The P/M ratio increased to 4.16 from 5.42 . This changes the inlet type from 3 to $2/3$ which corresponds to an inlet type that is unstable; migrating or intermittently closing.

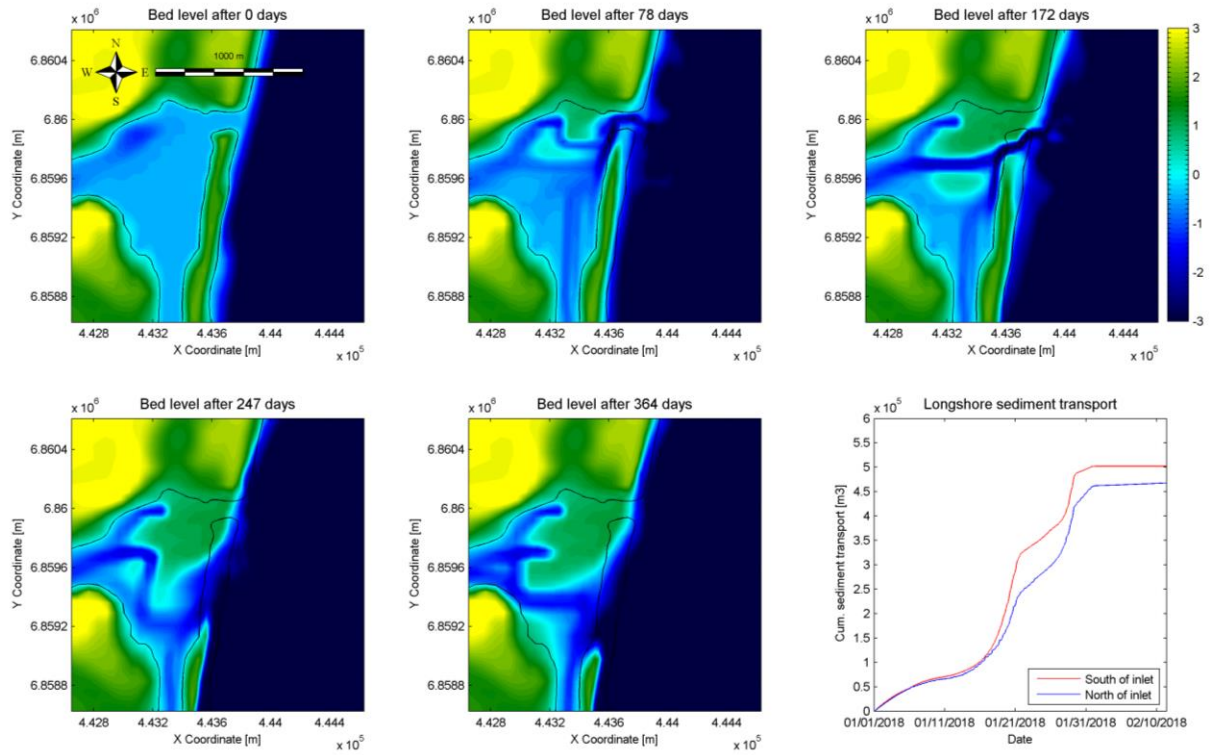


Figure 5.52: Bed level after 0 days, 78 days, 172 days, 247 days, 364 days and cumulative sediment transport along the coast for spring tidal range of 1.80 m

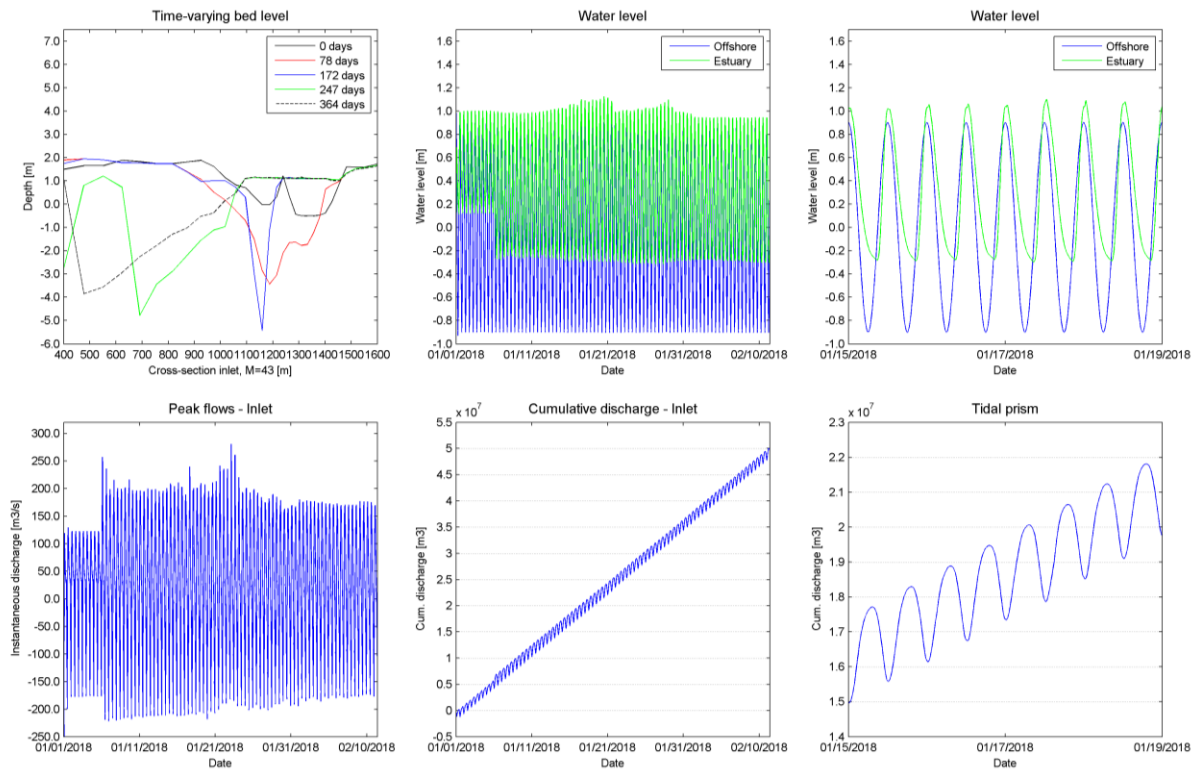


Figure 5.53: Time-varying bed level inlet, water level, detailed water level, peak flows, cumulative discharge through inlet and tidal prism for spring tidal range of 1.80 m

5.3.5 Future state, $Q = 30 \text{ m}^3/\text{s}$ (MAR)

5.3.5.1 Mean tidal range

The model is simulated with a river discharge of $30 \text{ m}^3/\text{s}$ from the Mfolozi River. This discharge is equal to a yearly runoff of $946.1 \cdot 10^6 \text{ m}^3$, which is equal to the MAR. Before removing the dredge spoil the inlet does not close. The inlet migrates northwards due to spit formation at the updrift side of the inlet. After removing the dredge spoil the inlet remains open for the complete simulation. The morphological evolution of the inlet, visible in Figure 5.54, is different than before dredge spoil removal. The inlet imports more sediments and land forms from the northern side into the estuary, leading to migration of the tidal gorge in southern direction. The tidal gorge reaches depths of 3.5 m (Figure 5.55). The cumulative transport along the coast equals $459,000 \text{ m}^3/\text{year}$ at the southern side of the inlet and $405,000 \text{ m}^3/\text{year}$ at the northern side.

The hydrodynamic results are given in Figure 5.55. The water levels in the estuary vary between -0.25 m to 0.70 m . During periods of high wave action water levels in the estuary rise up to 0.93 m , which is an elevation of 0.28 m compared to oceanic water levels. The offshore water levels vary between -0.65 m to 0.65 m . The ratio between the water levels in the estuary compared to ocean equals 0.73 . Peak flows are varying from $130 \text{ m}^3/\text{s}$ for flood flows and $180 \text{ m}^3/\text{s}$ for ebb flows. Due to the high river discharge the ebb flows are higher than the flood flows. The ebb tidal prism equals $2,650,000 \text{ m}^3$ and the flood tidal prism equals $1,350,000 \text{ m}^3$. This difference is approximately equal to the discharge of the Mfolozi River over one tidal period, which equals $1,296,000 \text{ m}^3$. The P/M ratio increased to 5.77 from 4.69 . This changes the inlet type from 3 to $2/3$ which corresponds to an inlet type that is unstable; migrating or intermittently closing.

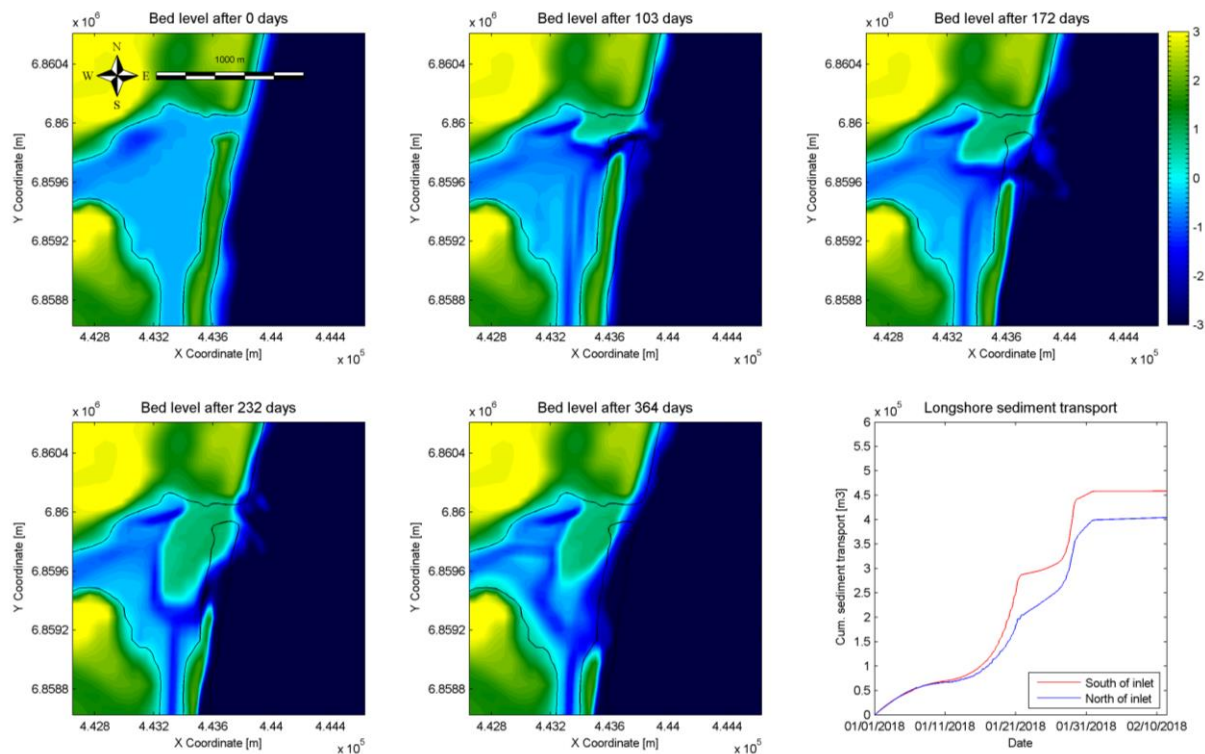


Figure 5.54: Bed level after 0 days, 103 days, 172 days, 232 days, 364 days and cumulative sediment transport along the coast for mean tidal range of 1.30 m

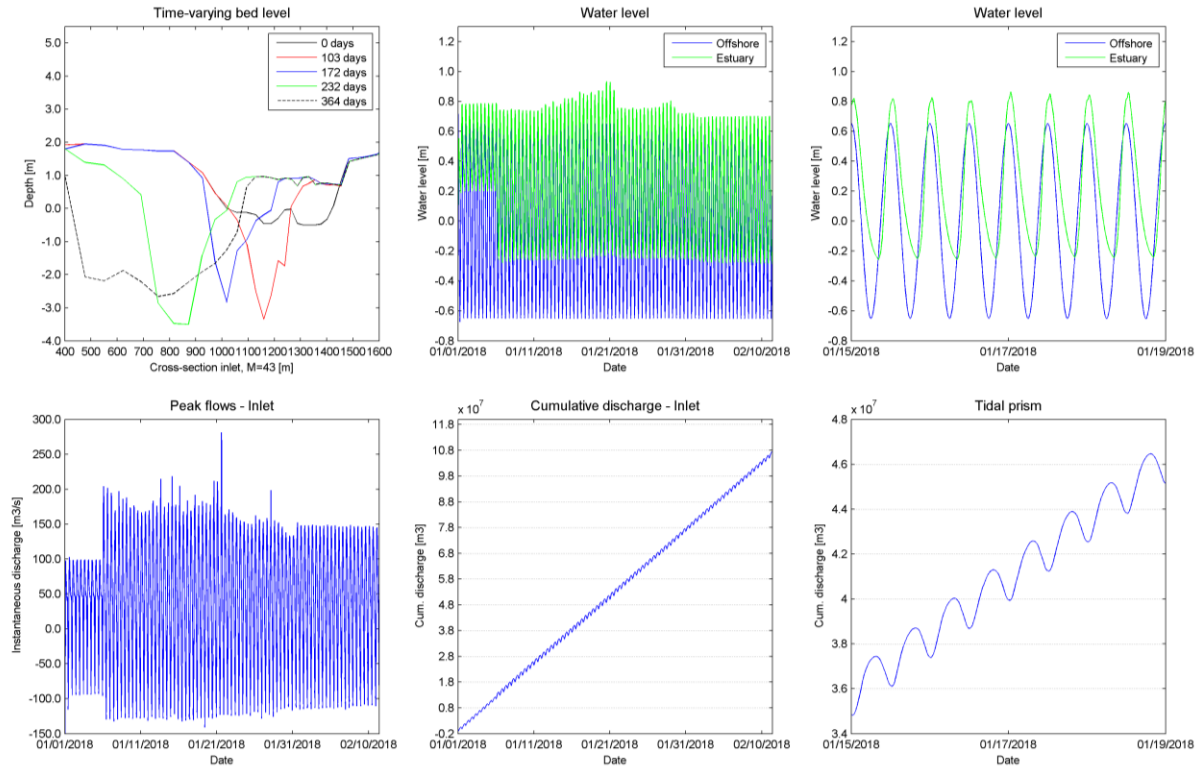


Figure 5.55: Time-varying bed level inlet, water level, detailed water level, peak flows, cumulative discharge through inlet and tidal prism for mean tidal range of 1.30 m

5.3.5.2 Neap tidal range

The morphological evolution of the inlet forced with neap tidal range and a discharge of $30 \text{ m}^3/\text{s}$ is given in Figure 5.56. In previous simulation before removing the dredge spoil the inlet closed 6 times, mainly during ebb periods, for a total of 11.3 days. After removing the dredge spoil the inlet closes 11 times for a total duration of 14.2 days. The inlet closes from 94.2 – 95.4 days, 99.6 – 101.7 days, 113.8 – 115.4 days, 119.6 – 120.0 days, 125.0 – 125.8 days, 129.2 – 130.8 days, 135.0 – 135.4 days, 139.6 – 141.7 days, 145.4 – 146.3 days, 150.0 – 152.5 days and from 155.4 – 155.8 days. The closure times are shorter, but more often compared to the simulation before dredge spoil removal. The inlet behaves similar as when forced with a river discharge of $14 \text{ m}^3/\text{s}$, the inlet opens and closes intermittently and is locationally stable. The formation of a spit is visible after 103 days. After 202 days the inlet imports a lot of sediments and land formation from the northern side is visible. The connection with the St Lucia Estuary remains present in contrast to the simulation where the dredge spoil is still present. The cumulative transport along the coast equals $468,000 \text{ m}^3/\text{year}$ at the southern side of the inlet and $371,000 \text{ m}^3/\text{year}$ at the northern side.

The hydrodynamic results are visible in Figure 5.57. The water levels in the estuary vary between -0.10 m up to 0.35 m . The offshore water levels vary between -0.25 m to 0.25 m . The ratio between the water levels in the estuary compared to ocean equals 0.90. Peak flows are varying from $30 \text{ m}^3/\text{s}$ during flood flows and $80 \text{ m}^3/\text{s}$ for ebb flows. The ebb tidal prism equals $1,550,000 \text{ m}^3$ and the flood tidal prism equals $260,000 \text{ m}^3$. The P/M ratio increased to 3.31 from 3.01. The inlet type remains 3 which corresponds to an inlet that is unstable and intermittently closing

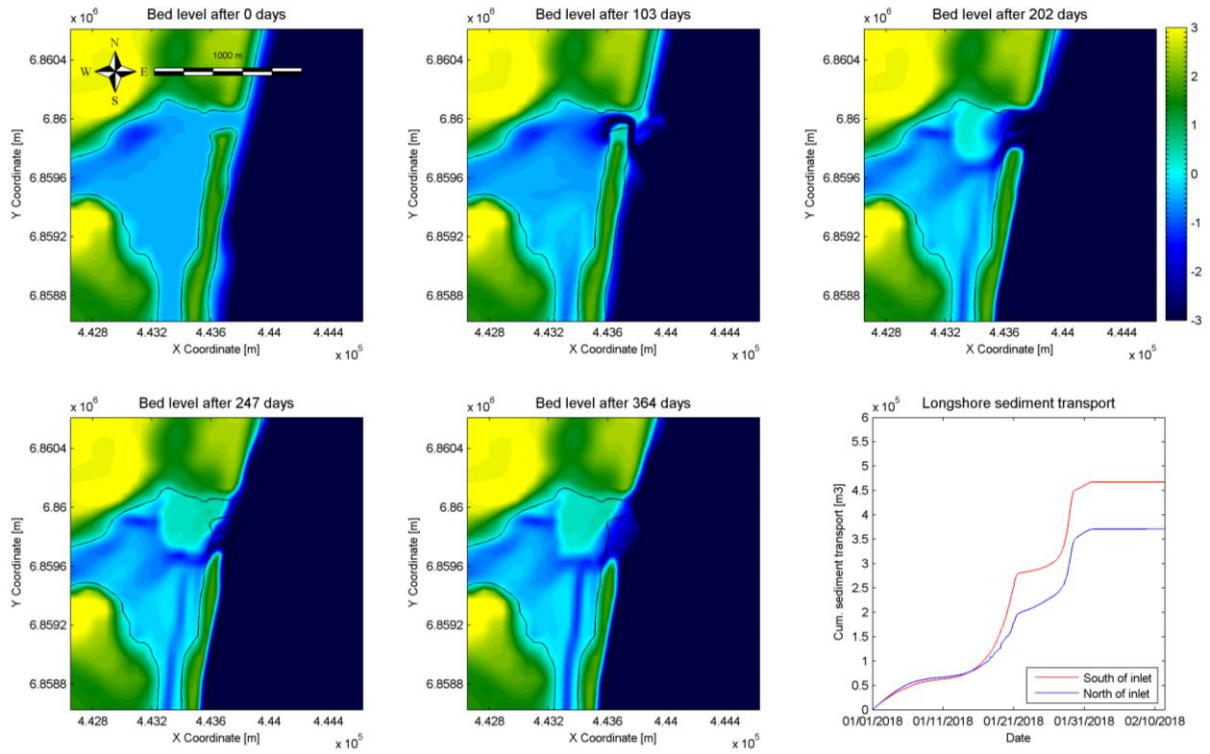


Figure 5.56: Bed level after 0 days, 103 days, 202 days, 247 days, 364 days and cumulative sediment transport along the coast for neap tidal range of 0.50 m

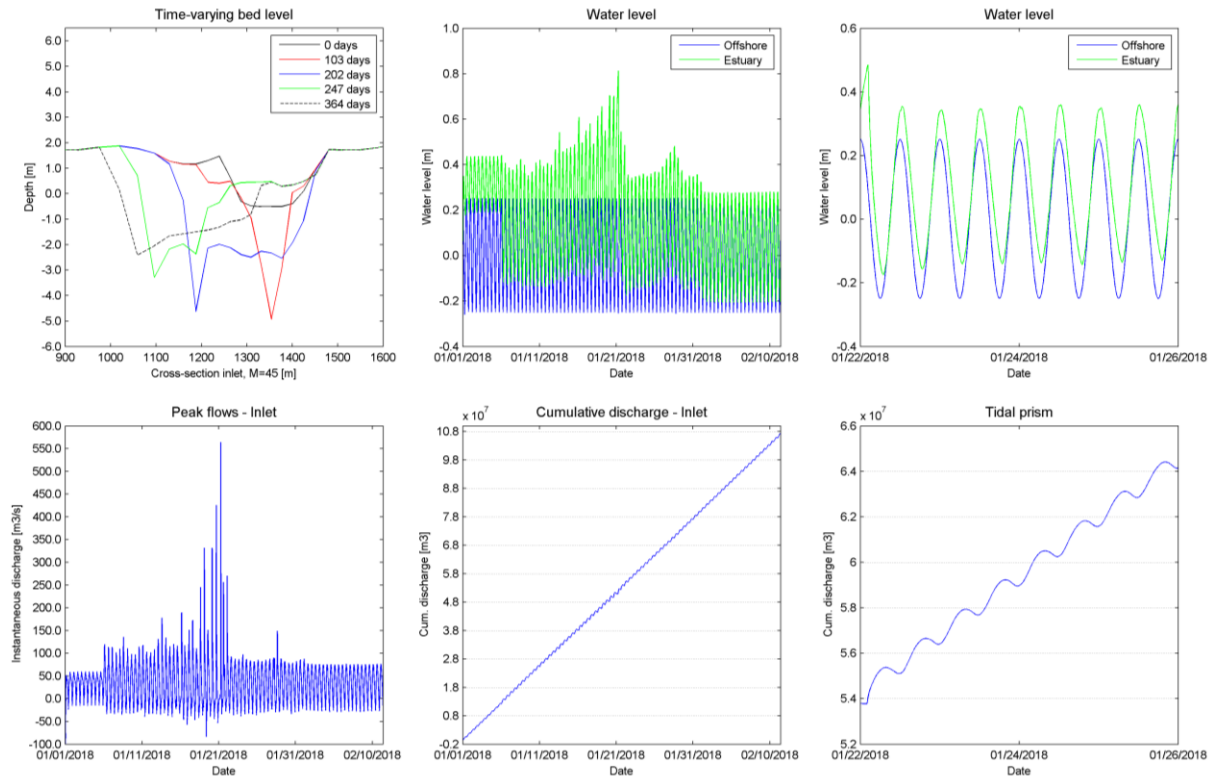


Figure 5.57: Time-varying bed level inlet, water level, detailed water level, peak flows, cumulative discharge through inlet and tidal prism for neap tidal range of 0.50 m

5.3.5.3 Spring tidal range

As in previous simulation the model is simulated with a river discharge of $30 \text{ m}^3/\text{s}$, only now with a spring tidal range of 1.8 m. The morphological evolution is visible in Figure 5.58. The estuary behaves similar as in previous simulation with a river discharge of $14 \text{ m}^3/\text{s}$. At the start of the simulation tidal flats are formed in the flood tidal delta. The tidal flats are surrounded by two channels of which the northern channel silts up and closes. This repeats itself and causes the extension of land from the northern side into the estuary. Before removing the dredge spoil the tidal gorge migrates in northern direction due to spit formation instead of migrating in southern direction. The impact of the larger waves in combination with spring tide erodes the inlet and it widens up to 600 m at MSL (Figure 5.59). The longshore transport at the southern side of the inlet equals $514,000 \text{ m}^3/\text{year}$ and at the northern side equals $458,000 \text{ m}^3/\text{year}$.

The hydrodynamic results are given in Figure 5.59. The water levels in the estuary vary between -0.25 m and -0.30 m up to 1.00 m . During periods of high wave action water levels in the estuary rise up to 1.20 m , which is an elevation of 0.30 m compared to oceanic water levels. The offshore water levels vary between -0.90 m to 0.90 m . The ratio between the water levels in the estuary compared to ocean equals 0.72. Peak flows are varying from $200 \text{ m}^3/\text{s}$ during flood flows and $220 \text{ m}^3/\text{s}$ for ebb flows with maxima of $360 \text{ m}^3/\text{s}$. The ebb tidal prism equals $3,150,000 \text{ m}^3$ and the flood tidal prism equals $1,900,000 \text{ m}^3$. The P/M ratio is increased from 5.23 to 6.13. The inlet remains an unstable inlet; migrating or intermittently closing, which corresponds to an inlet type 2/3.

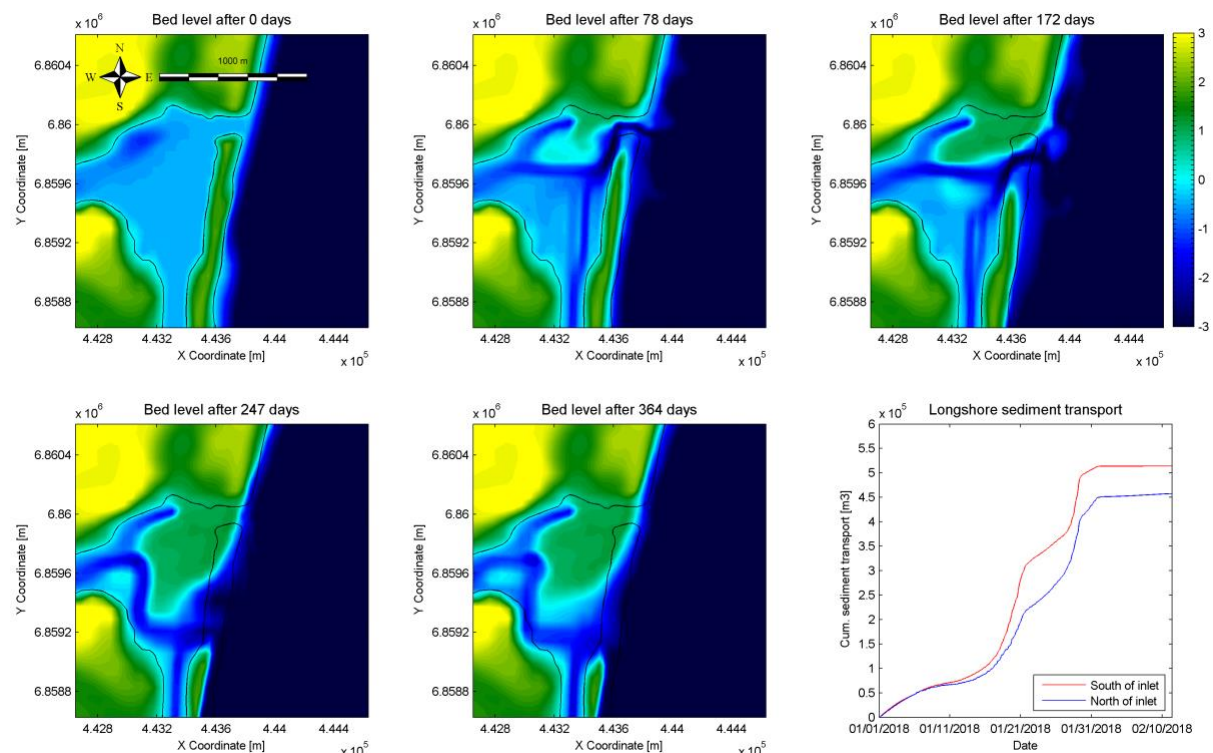


Figure 5.58: Bed level after 0 days, 78 days, 172 days, 247 days, 364 days and cumulative sediment transport along the coast for spring tidal range of 1.80 m

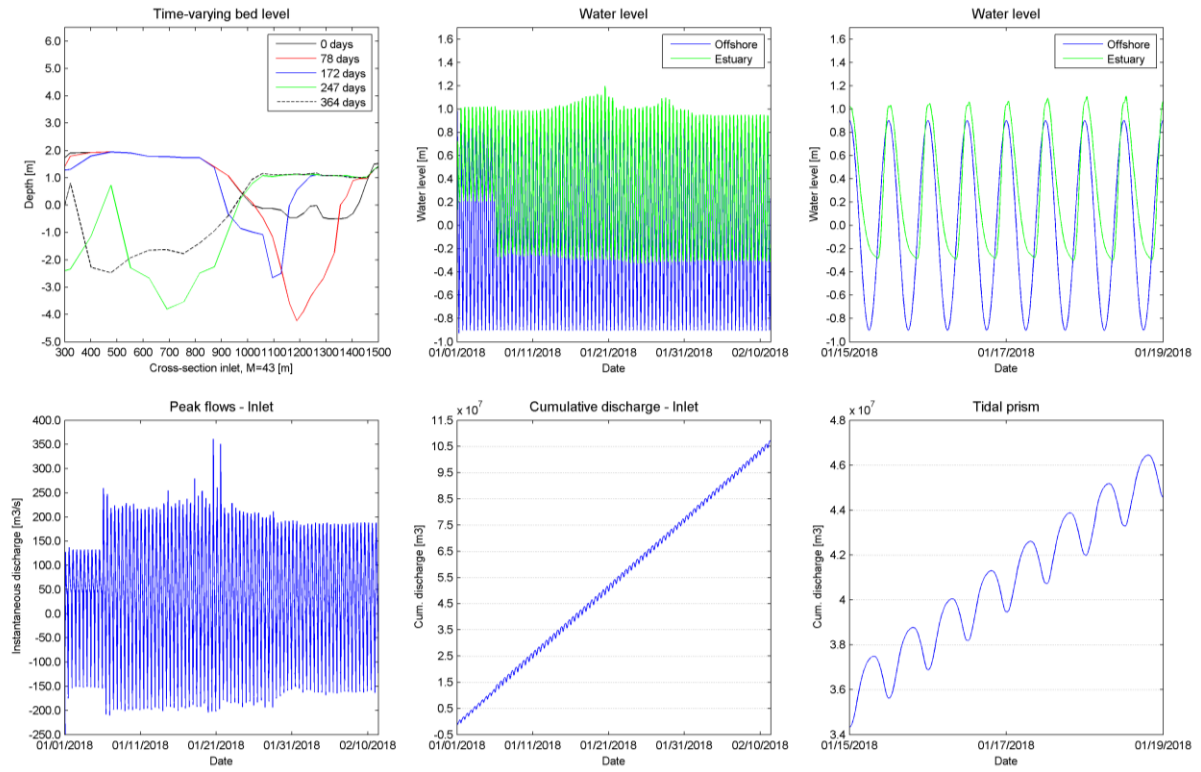


Figure 5.59: Time-varying bed level inlet, water level, detailed water level, peak flows, cumulative discharge through inlet and tidal prism for spring tidal range of 1.80 m

5.4 Analysis scenario B

The results from the scenario B, the dredge spoil removal, were presented in previous chapter. An overview from the results combined with scenario A is given in appendix D. The following three points will be analysed: 1. Morphological development, 2. Closure times, 3. A-P Relationship.

5.4.1 Morphological development

The removal of 1,300,000 m³ of dredge spoil from the estuary into the ocean has limited effect on the morphological development of the system. The inlet behaves in three different ways, namely:

- (1) Locationally stable and intermittently closing inlet, mainly observed when the inlet is forced with a neap tidal range and no river discharge.
- (2) Migrating inlet in northern direction due to spit formation at the updrift side of the inlet and eventually spit breaching. This is visible during two simulations; a discharge of 0 m³/s and a discharge of 2 m³/s, both combined with spring tidal range.
- (3) Migration of the inlet in southern direction. The higher discharges from the Mfolozi River result in more suspended sediments in the water column. As described in chapter 2.5.3 the sediment content increases significantly during autumn and summer. A combination of increased ebb flows aided by river flow results in erosion at the updrift side and accretion at the downdrift side of the inlet. The northern part of land evolves in southern direction. The inlet might close due to a decrease in cross-sectional area and higher wave action resulting in increased longshore sediment transport. This behaviour is visible in the simulation with a discharge of 5 m³/s combined with a mean tidal range.

The morphological development of scenario B corresponds to the behaviour observed in scenario A. The first behaviour is observed both during neap tidal range. The second behaviour of scenario B corresponds to behaviour 2 from scenario A. The inlet does not close when the tidal gorge migrates in northern direction and spit breaching occurs. This mainly happens during spring tidal range combined with a limited river flow. The 3rd behaviour is visible in majority of the simulations and occurs when either tidal flows or the river discharge is increased. This behaviour corresponds to behaviour 3 in scenario A.

The inlet behaviour remains unstable; it closes intermittently or migrates along the coast. The P/M ratios vary from 1.62 to 6.13 and can be classified as an inlet type 3 and type 2/3. The behaviour observed in the simulations corresponds to classification type found in literature.

The third morphological behaviour that is observed, migration of the inlet in southern direction, might not be expected to occur. Generally the inlet has a tendency to migrate in the same direction as the longshore sediment transport. Similar behaviour is observed at the Keurbooms Inlet in South Africa and has been investigated by Reddering (1983). At the Keursboom Inlet a similar wave climate is present as at the St Lucia inlet. The migration of the Keurbooms Inlet is mainly caused by deposition of sediment at the northern margin due to a combined process of tide and wave accretion of sediment, while the southern margin is eroded by ebb currents during spring tide, aided by freshwater floods. According to Reddering the tidal currents are of vital importance in redistributing sediments into the flood channel deposits on the downdrift side of the inlet. Migration in the direction of longshore drift due to spit formation, deposition at the updrift side and erosion at the downdrift side, could proceed with less tidal action as sediments are eroded from the beach. As

visible in Figure 5.60 the sediment transport caused by the flooding tide stretches across the entire inlet, while the ebbing tide erodes a deeper channel at the southern side. At the Keurbooms Inlet during ebbing tide a flow separation cell extends from the edge of the barrier into the inlet, which causes sand transport into the quiet water zone next to the northern inlet margin. The flood channel at the northern side of the inlet forms a platform for sand accretion during the succeeding flooding tide and by wave action. This causes the inlet to migrate in southern direction. The same behaviour is observed in the computed St Lucia inlet. The third behaviour is mainly observed when either the tidal exchange or the river discharge is increased.

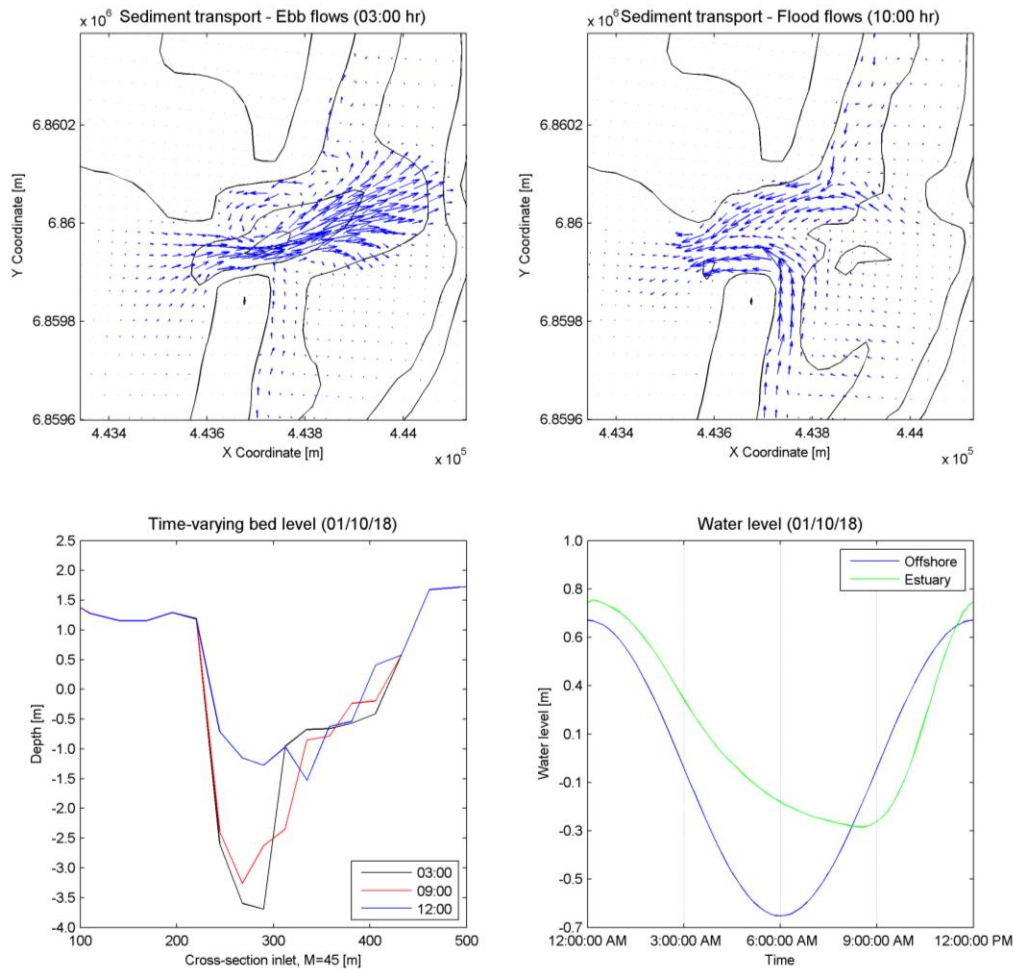


Figure 5.60: Sediment transport through the inlet during ebb – and flood flows, time-varying bed level and water levels on 01/10/2018

5.4.2 Closure times

The closure times of the inlet do not change significantly due to the dredge spoil removal and are almost the same as in previous scenario, after re-linkage of the Mfolozi River. The closure times of both scenarios are given in Figure 5.61. The inlet mainly closes during neap tidal range as flow velocities are still below equilibrium velocities. After removal of the dredge spoil the inlet is closed for 89% (94%), 33.9% (29.1%), 16.4% (12.9%), 5.3% (8.6%) and 3.9% (3.1%) of the simulation time when forced with a neap tidal range. The values in between brackets are the closure times that belong to scenario A. This variation is negligible and the area of dredge spoil removal is too small in order to have effect on the closure times of the inlet.

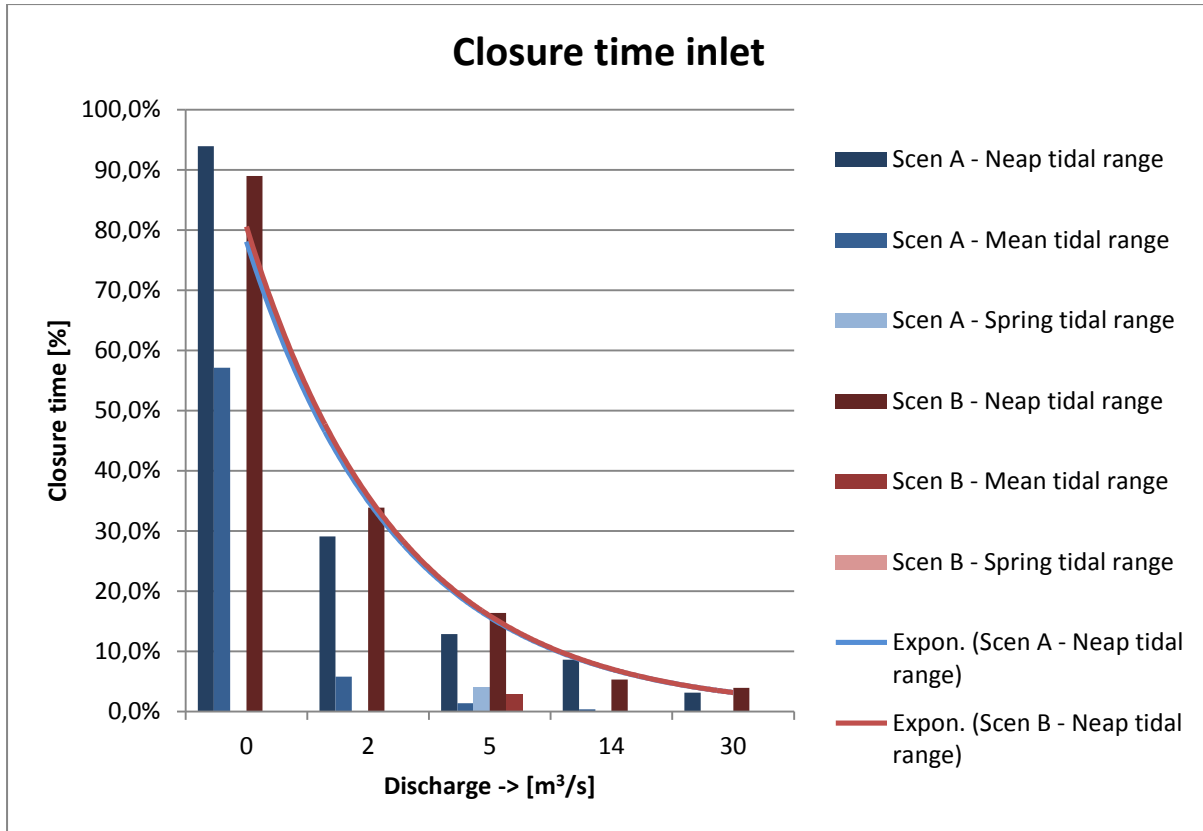


Figure 5.61: Comparison closure times inlet

The cross-sectional area varying over time is visible in Figure 5.62. The graph shows five different scenarios during mean tidal range where the river discharge is increased from 0 m³/s to 30 m³/s. The cross-sectional development has the same trend as in scenario A and is derived in similar way. As in previous scenario the cross-sectional area of the inlet decreases slightly during the first 150 days. The higher wave action causes an increase in longshore sediment transport and leads to a decrease in inlet cross-section. The cross-sectional area of the inlet increased from 60-70 m² in scenario A to approximately 150 m² in scenario B during the first 150 days. Similar to scenario A the higher wave action causes erosion of the inlet, resulting in a cross-section of 700 m² up to 1400 m². The cross-sectional area increased by a factor 2 compared to scenario A.

5.4.3 A-P Relationship

The simulations from scenario B forced with mean tidal range are further investigated regarding the A-P relationship. In Figure 5.63 the results from scenario B are compared with the findings by O'Brien and the simulations from scenario A. The results from scenario B are further from the stable equilibrium defined by O'Brien's curve. It shows that the removal of the dredge spoil does not create a system that is in equilibrium.

After dredge spoil removal the average cross-sectional area increases to 333.8 m², 335.5 m², 422.7 m², 526.4 m² and 470.3 m² corresponding to a river discharge of 0 m³/s, 2 m³/s, 5 m³/s, 14 m³/s and 30 m³/s. The averaged empirical coefficient from the simulations after dredge spoil removal equals $C = 2.06 \cdot 10^{-4}$, when $q = 1$. This value deviates a lot more from the value found by O'Brien: $C = 1.08 \cdot 10^{-4}$ and the value corresponding to scenario A: $C = 1.38 \cdot 10^{-4}$. The trendline corresponding

to the results of scenario B has a coefficient of determination R^2 equal to 0.4477. The R^2 value is relatively low, which can be explained by the fact different simulations are combined where the river flows are varied. All empirical coefficients are higher than $C = 7.8 \cdot 10^{-5}$ with $q = 1$, which corresponds to the equilibrium velocity for the Escoffier curve. According to the Escoffier curve the inlet is prone to close when the area is smaller than 135 m^2 up to 207 m^2 depending on tidal prism. During periods of low wave action these cross-sections are present and the inlet can close, which is visible in the simulation with a river discharge of $5 \text{ m}^3/\text{s}$.

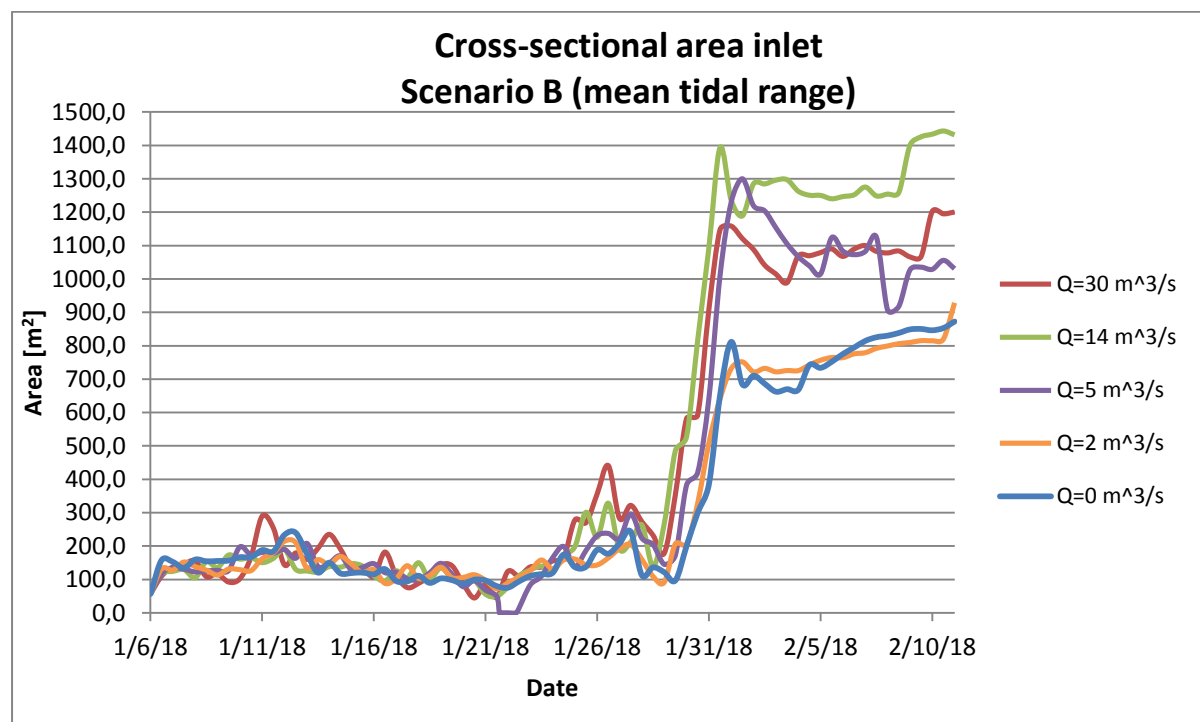


Figure 5.62: Cross-sectional area inlet of scenario B

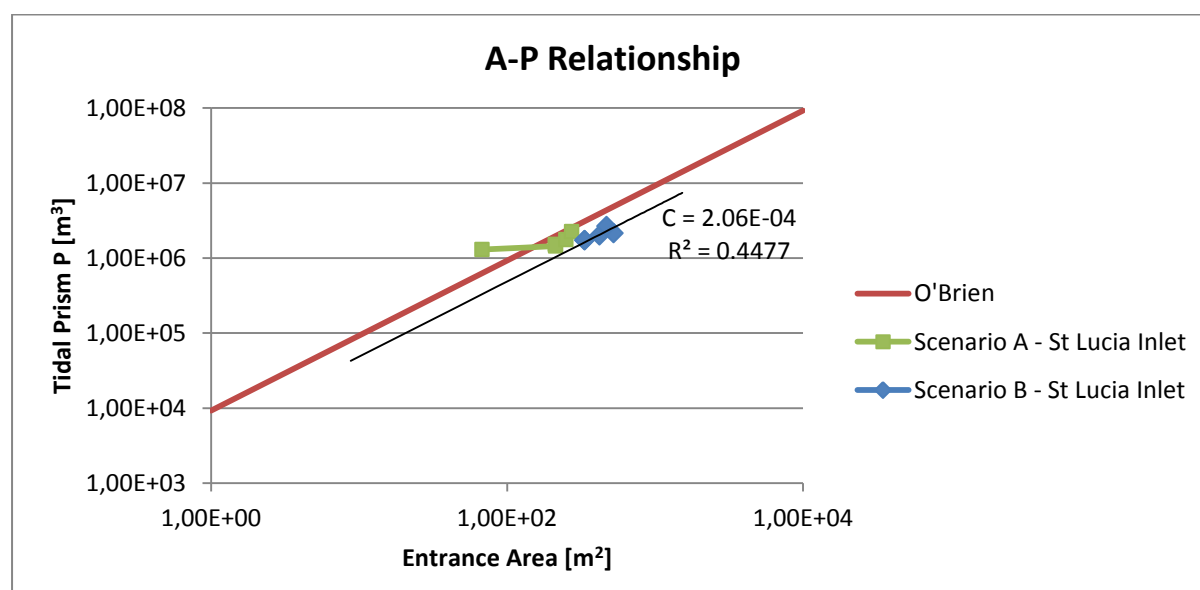


Figure 5.63: Comparison A-P Relationship scenario A and B

6 Discussion

In this chapter the strengths and weaknesses of the methods and data used in this report are discussed. Three parts of the report are discussed: 1. Delft3D model setup, 2. Forcing of the model, 3. Process-based model.

6.1 Delft3D model setup

The process-based program Delft3D is used to simulate the effects of re-linkage of the Mfolozi River and the removal of the dredge spoil from the estuary. The model has been calibrated to approach real life observations and reproduce measurements from literature.

The model consists of a flow grid nested in a larger wave grid. The flow grid and wave grid have different bathymetric data, which is explained in chapter 3.2.1. The flow grid does not cover the complete area of the St Lucia System; the lakes and approximately three quarters of the Narrows are not included in the model. It is chosen to limit the size of the flow grid in order to reduce the computation time. The bathymetry of the estuary is adjusted to reproduce the tidal prism measurements through the mouth. A larger flow grid might result in a more realistic model, however by adjusting the bathymetry the model is calibrated and reproduces field measurements. The restricted area plays a role when looking at a wider variety of studies. The model will get more complex if the area is enlarged. However, other studies can be investigated with respect to water quality, silt content, water levels in the St Lucia Lakes or the effects of cyclones and flooding on the area. In case a larger model is used it is also possible to incorporate evaporation, precipitation and groundwater flows.

6.2 Forcing of the model

6.2.1 Wave climate

The model is forced with a reduced wave climate. The reduced wave climate is obtained by manual selection of 10 wave conditions that have equal contribution to the total sediment transport. A reduced wave climate instead of a simulation with brute forcing is used in order to reduce computation time of the model. The wave conditions in the reduced wave climate are ordered from low to high and low wave heights again. The sequencing of wave heights has a large effect on the morphological development, as explained in chapter 4.2.1 and appendix C.2. In order to investigate the closure times of the inlet it is chosen to start with a period of low wave action which has relatively less influence on the morphology. If the simulation would start with higher waves the inlet widens and does not close again during the simulation time, because the coast needs time to recover. Longer simulation times are necessary in order to study the effect of a different wave sequencing on the closure times and morphological development of the inlet.

6.2.2 River flow

Besides the wave climate another important parameter is the river discharge. The river flow is varied from 0 m³/s to 30 m³/s covering all seasons. This gives a good indication of the possible ways the St Lucia Estuary can develop. In the simulations the river discharge is kept constant for the complete duration. In reality the river discharge would vary more over time and experience more extreme discharges. For future research it is important to study the effect of flood flows on the inlet. The

flood flows will have effect on the opening times of the inlet. In reality there will be more extremes, longer periods of droughts and larger river discharges with a smaller frequency of occurrence. The study of a flooding gives more insight into the recovery of the beach. The importance of the flood flows is also visible on the seasonal distribution of river flow. The mean annual runoff equals $30 \text{ m}^3/\text{s}$ while all average seasonal flows are well below this value; the average winter discharge equals $2 \text{ m}^3/\text{s}$ and the average summer discharge equals $14 \text{ m}^3/\text{s}$. Severe floods might affect the dredge spoil and can alter the system drastically. More research of the impact of these extreme events will give more insight in the behaviour of the system.

The river flow is only modelled from the Mfolozi side in order to compare this to the initial situation. In reality there will also be river flow from the Narrows, up north from the St Lucia Estuary, which will alter the morphological behaviour. Currently the inlet migrates in southern direction towards the Mfolozi River when the discharge is increased. The updrift side of the inlet erodes due to the river flow. The inlet is expected to be more locationally stable in case there is river flow from the St Lucia Estuary.

The river flow also affects the built up of water levels in the estuary while the inlet is closed. The highest water level reached in the simulations equals 1.3 m above MSL. This is in scenario A when simulated with spring tidal range and a river discharge of $5 \text{ m}^3/\text{s}$. Previous research by Huizinga & Niekerk (2005) showed water levels reached approximately 3 to 3.5 m above MSL before the St Lucia mouth would breach. However, this source is from a symposium and it is not sure how these elevated water levels are computed. Several factors affect the breaching of an inlet and it is not known if Delft3D reproduces the failure mechanisms of a dike in a realistic manner. The breaching height can differ due to the model complexity, the formation of a higher berm, vegetation which starts growing on the berm, a wider coast due to more accretion. Further research is necessary in order to investigate the height at which the St Lucia inlet will breach. The time breaching occurs has significant effect on the closure times of the inlet.

6.3 Process-based model

Delft3D is used to evaluate the effect of re-linking the Mfolozi River and removal of dredge spoil from the estuary on the St Lucia inlet. The model is calibrated on longshore sediment transport and morphological evolution of the inlet. Several factors of Delft3D are adjusted to calibrate the model of which the most important are the current related transport factors and wave related factors. The current related factor mainly influences the longshore sediment transport, while the wave related factor influences cross-shore sediment transport.

The factors influencing the morphological development of the model are discussed. For certain factors the sensitivity in results is relatively high. In chapter 3.3 the gross longshore sediment transport is calculated with transport formulae from literature. The results are in the order of 5-6 times higher compared to results from Delft3D. The current related factor is set to 20 in Delft3D, which is relatively high. It could be that Delft3D does not reproduce the energetic wave climate of South Africa in a correct way. The average longshore sediment transport along the Dutch coast is approximately $125,000 \text{ m}^3/\text{year}$ (Rijn L. v., 1997), which is significantly less compared to the $800,000 \text{ m}^3/\text{year}$ measured at Richards Bay. The Kamphuis formula is used for the calculation of the gross longshore sediment transport while The Van Rijn formula is used in Delft3D. The use different

transport formula could cause a difference in observed longshore sediment transport. Changing the morfac from 10 to 20 in Delft3D affects the longshore sediment transport largely resulting in a decrease from approximately 500,000 m³/year to 250,000 m³/year. The cumulative longshore sediment transport is halved. Normally changing the morfac should have negligible influence in the results. The lower longshore sediment transport in the simulation with higher morfac can be explained by the fact more erosion occurs at the start of the simulation that changes the cross-shore profile in the surf zone; it is steeper and approximately 2 m lower. The variation can be due to the complexity of the model. Further research is necessary to investigate the dependencies of different longshore sediment transport formulae on the model results.

The wave related factor has a lot of influence on the closure time of the inlet. The factor is calibrated to reproduce the observed morphological behaviour of the St Lucia inlet in reality and to keep an equilibrium beach width. It is however questioned how realistic Delft3D can model morphological evolution in cross-shore direction. Slightly varying the wave related factor from 0.31 to 0.25 changes the inlet to an open inlet, while increasing the factor from 0.31 to 0.40 increases the closure time up to 35 days. The results are quite sensitive and have large effect on the results. This can also cause the difference found in breaching height of the St Lucia inlet. In case the wave related factor is increased, the inlet will close sooner and the berm will increase in height. This will result in longer closure times and breaching heights will increase. The sensitivity to the morphological factors in Delft3D needs further research.

However, the model results do show it is possible to simulate the closure of an inlet with physical processes described in literature. Both closure mechanisms described by Ranasinghe et al. (1999) are observed. Spit migration leading to closure due to the high longshore sediment transport is reproduced as well as closure due to onshore bar migration. The model is able to simulate accretion during low wave action and erosion during high wave action. These findings are positive and lead to more realistic simulations.

Even though varying the factors used in the setup of Delft3D leads to variations in results, the conclusions in this report can be regarded as useful. This is because different scenarios are compared to each other. The scenarios are simulated with the same process-based model and only varied in either river discharge or bathymetry. All of the scenarios will have approximately the same prediction error. The influence of the errors caused by the model is minimized due to relative comparison of the simulations.

7 Conclusion

In this chapter the final conclusions of the report are discussed. The conclusions are based on the findings from this study and provide an answer to the research questions. The main goal of this thesis was determining the effects of re-linkage of the Mfolozi River and removal of the dredge spoil. The following main research question was formulated:

“What is the effect of relinking the Mfolozi River and removal of the dredge spoil on the morphodynamic behaviour of the inlet?”.

In order to answer this main question, the following four sub-questions are addressed:

1. What is the influence of the different interventions on the closure times of the inlet?
2. What is the exact transition point at which the St Lucia mouth will close or stay open?
3. Is there a significant change in morphological development after removal of the dredge spoil compared to the initial situation?
4. Is the inlet after re-linkage of the Mfolozi River dominated by tidal or fluvial flows?

The morphodynamic behaviour of the St Lucia inlet has been investigated in this thesis. The closure of the mouth is reproduced and the predicted morphological development corresponds to real life observations. The four sub-questions will be answered in the following subsections. The conclusions from the sub-questions give answer to the main research question.

7.1 Closure time of the inlet

The drought period ranging from 2002 has drastically affected the St Lucia System as a whole with the desiccation of 90% of the lakes, reaching the all-time low. Breaching of the inlet occurred in March 2007 due to Cyclone Gamede. Natural closure of the mouth occurred six months later during neap tidal range. The simulations from Delft3D show similar results with closure of the mouth after 22 and 156 days when forced by neap – and mean tidal range respectively. The re-linkage of the Mfolozi River and removal of the dredge spoil leads to the following conclusions:

- Re-linkage of the Mfolozi River reduces the closure times of the inlet drastically. When the simulations from neap –, mean – and spring tidal range are combined the inlet is closed for 50.4% with no river flow. The high wave action results in closure of the inlet. During the winter ($2 \text{ m}^3/\text{s}$), drought ($5 \text{ m}^3/\text{s}$) and summer period ($14 \text{ m}^3/\text{s}$) the river flow reduces the closure times significantly to 11.6%, 6.1% and 3.0% respectively. The MAR ($30 \text{ m}^3/\text{s}$) results in a closure time of 1%.
- The removal of dredge spoil in the estuary has limited effect on the closure time of the inlet. Due to the increased accommodation space in the estuary the tidal prism and peak flows through the inlet increase. This however is too small in order to have an effect. The averaged closure time decreases from 50.4% to 29.7% when river flow is zero. Once river flow enters the system the closure times barely change. It can be concluded that the removal of $1,300,000 \text{ m}^3$ of dredge spoil from the estuary does not have a positive influence with respect to opening times of the St Lucia inlet.

7.2 Exact transition point inlet

The cross-sectional area of the inlet is analysed during mean tidal range with varying river flow. It is concluded that there is no exact transition point of inlet closure, but a clear trend is visible in all scenarios. During the first 150 days low wave action causes the cross-sectional area of the inlet to decrease slightly. The smaller waves lead to a net onshore sediment transport in cross-shore direction. The first period of high wave action starts subsequently. The higher waves cause an increase in longshore sediment transport and suspended sediments in the water column. Spit formation causes the inlet to close in several occasions, visible after 160 days. In case the inlet remains open the larger waves erode the coast and lead to widening of the inlet.

The cross-sectional area in scenario B, after dredge spoil removal, is slightly higher compared to scenario A. In the first period the inlet cross-section ranges from 50 to 100 m² in scenario A and approximately 150 m² in scenario B. In case the inlet does not close or reopens again it widens up to 460 to 800 m² in scenario A and 700 to 1400 m² in scenario B. The removal of dredge spoil leads to a temporary increase in cross-sectional area, but as a similar trend is observed as in scenario A it is assumed that in future the estuary will silt up again leading to a decreasing cross-sectional area of the inlet. The observed morphological behaviour correspond to literature. According to the Escoffier curve the inlet is prone to close when flow velocities reach below the equilibrium velocity of 0.9 m/s. The corresponding cross-sectional area at which the inlet closes ranges from 113 m² up to 207 m² depending on tidal prism. During periods of low wave action these cross-sections are present and the inlet can close.

7.3 Morphological development

The morphological development of the St Lucia Estuary is analysed for the initial situation, after re-linkage of the Mfolozi River and after dredge spoil removal. A total of 30 simulations are obtained by varying the river discharge and tidal range. There is no significant change in morphological development after and before removal of the dredge spoil. The following three main types of behaviour are observed:

- (1) Locationally stable and intermittently closing inlet, mainly observed when the inlet is forced with a neap tidal range.
- (2) Migrating inlet in northern direction due to spit formation at the updrift side and erosion at the downdrift side of the inlet. The inlet might show closure, maintain open or show spit breaching.
- (3) Migration of the inlet in southern direction. The higher discharges from the Mfolozi River result in more suspended sediments in the water column, which are deposited in the estuary. A combination of increased ebbing tides aided by river flow results in erosion at the updrift side and accretion at the downdrift side of the inlet. Flow separation during ebbing tide causes sand transport into the quiet water zone at the northern side of the inlet. During the succeeding flooding tide accretion occurs in the flood channel, causing the inlet to migrate in southern direction.

Depending on the tidal range and wave conditions one or another process is observed. In general an increase in tidal range changes the process from 1 to 2 and an increase in river discharge from 2 to 3. A schematisation of the different types of morphological behaviour is given in Figure 7.1.

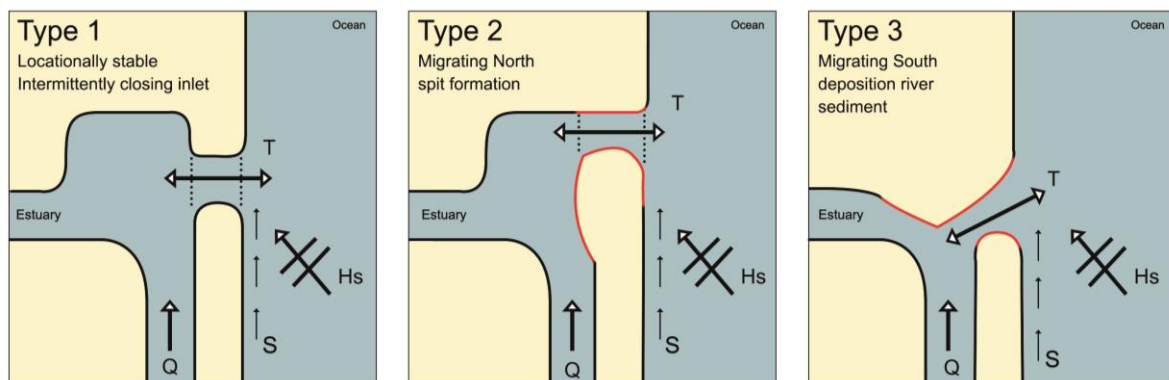


Figure 7.1: Types of morphological development inlet

The different types of morphological development of the inlet correspond to the behaviour of an unstable inlet. The P/M ratios vary from 1.23 to 5.23 in scenario A and barely increase in scenario B ranging from 1.62 to 6.13. The inlet remains classified as type 3 or type 2/3. It can be concluded that the change in morphological development due to the dredge spoil removal is small. The tidal prism increases slightly leading to higher flows through the inlet and occasionally changing the observed behaviour. The inlet type remains unstable; intermittently closing or migrating.

Before removal of the dredge spoil the St Lucia estuary is closer to the stable equilibrium. This can be concluded from analyses of the A-P Relationship by O'Brien. The empirical coefficient C after re-linkage of the Mfolozi River (scenario A) is closer to the value of O'Brien, whereas after the removal of the dredge spoil (scenario B) this value deviates a lot more.

Due to the removal of dredge spoil the estuary becomes more flood dominated which is visible during the simulations with no river discharge. The tidal prism increased in magnitude mainly during the flood period. This influences the import of sediments into the estuary, which increased by a factor of 2.7 from 92,000 m³ to 247,000 m³. The rising periods become even shorter than the falling period. The same holds for the flood periods that become shorter than the ebb periods. Both are properties of flood dominant estuaries.

7.4 Wave dominated system

The coast along St Lucia experiences a highly energetic wave climate. Delta's can be classified as river dominated, tidal dominated or wave dominated. Re-linkage of the Mfolozi River does not change the system to a more river dominated system.

Tidal estuaries can be dominated by tidal or fluvial flows as described by Hinwood et al. (2012). These observations showed fluvial dominated inlets have a smaller cross-sectional area around 1 to 10 m². Whereas estuaries dominated by the tide have a cross-section in the order of 100 to 5000 m². The area of the St Lucia inlet is around 60 to 270 m² during mean tidal range. This shows the St Lucia inlet is more dominated by tidal flows than fluvial flows.

When looking at the peak flows through the inlet a transition is visible at a river discharge equal to 14 m/s, which is the average discharge during summer periods. This shows flood flows are higher or equal to the ebb flows in almost all seasons. Only during simulations with the mean annual runoff the ebb flows through the inlet are higher than the flood flows.

8 Recommendations

In this chapter recommendations are given for future research. The recommendations cover both the limitations of this study and suggestions for future research due to new findings. Finally, advice for future management of the St Lucia estuary is given.

8.1 Further research

In this thesis the effect of re-linkage of the Mfolozi River and dredge spoil removal on the inlet have been investigated. This has been done by simulating various scenarios forced with a reduced wave climate and varying river flow.

For future research it is possible to optimize the model or investigate a wider variety of studies:

- Enlarge the model to include the St Lucia Lakes and larger part of the Mfolozi River. Incorporating a larger part of the St Lucia System will lead to a more realistic model and gives the possibility to look at a wider variety of studies. Studies can be investigated with respect to water quality, silt content and water levels in the St Lucia Lakes.
- Investigate the effect of the river flow from the Narrows. The river flow from a different direction will alter the morphological behaviour of the inlet. For future research it might be possible to make a model that incorporates the complete hydrological cycle; evaporation, precipitation, groundwater flows and river discharge towards or from the Narrows depending on St Lucia Lake water levels.
- Investigate the failure mechanisms and breaching height of the St Lucia inlet. Examine the capability of Delft3D with respect to reproducing failure mechanisms found in literature; overtopping, piping, erosion or sliding of the dike, etc. The breaching height can differ due to the model complexity, the formation of a higher berm, vegetation which starts growing on the berm, a wider coast due to more accretion. It is possible to study the relative importance of these factors with respect to the breaching height of the inlet.
- A couple of morphological factors need extra research to investigate the sensitivity of the model. The research in this thesis does simulate physical processes that are described in literature. However, varying factors such as the morfac, wave related factor and current related factor leads to relatively large variation in results.
- Modelling of flood flows from the Mfolozi River and the effect on the St Lucia Estuary. Flood flows have a large effect on the estuary and can alter the system drastically. The effect of flooding on the dredge spoil should be investigated. The dredge spoil might be removed naturally due to these extreme events such as floods caused by cyclones with severe rainfall. The impact of these extreme events will give more insight in the behaviour of the system.

8.2 Suggestion management

The St Lucia System has gone through many changes in the last century. Over the years park authorities changed and so did their policy on the iSimangaliso Wetland Park. The current restoration project has a large influence on the system. It can be concluded that re-linkage of the Mfolozi River has a large effect on the closure times of the inlet. The inlet remains open for majority of the time leading to a connection between the St Lucia Estuary and the Indian Ocean. This makes

the St Lucia Estuary and Lake System a breeding ground for many marine species as it was before. The removal of dredge spoil however does not seem to be very effective. The closure times of the inlet barely change and the inlet re-imports most of the sediments. It is suggested to limit the amount of dredge spoil removal, because the estuary will return to its equilibrium state.

There have been plans to remove a larger part of dredge spoil as shown in Figure 8.1. Besides the 1,300,000 m³ of dredge spoil, covering approximately section A and B, that has been removed in the period from January 2017 until June 2017 plans were made to remove section C and D as well. As shown in this report removing of the dredge spoil enhances the flood dominant behaviour of the system. Removing a larger part of the dredge spoil will increase the tidal prism and the flood flows through the inlet. Once the inlet breaches most of the sediments will be re-imported into the estuary. The flood flows are higher than the ebb flows in all seasons except for the summer period where they are approximately equal. This means only during flooding after severe rainfall ebb flows will be dominant leading to an export of sediment and flushing of the basin. It is suggested not to remove the other sections of dredge spoil. However, the connection with the Mfolozi River is very important and should be maintained.



Figure 8.1: Plans future dredge spoil removal St Lucia Estuary (iSimangaliso, 2016)

Bibliography

- AOC Geomatics. (2013). *LIDAR Aerial Survey, St. Lucia, Kwa-Zulu Natal, South Africa*. iSimangaliso Wetland Park Authority.
- Boothroyd, J. (1985). Tidal inlets and tidal basins. In R. Davis, *Coastal sedimentary Environments* (pp. 445-532). New York: Springer-Verlag.
- Bosboom, J., & Stive, M. (2015). *Coastal Dynamics I, letcure notes CIE4305*. Delft: VSSD.
- Chrystal, C., & Stretch, D. (2014). *Tidal Flows and Inlet Dynamics of the St Lucia/Mfolozi Estuarine System, South Africa*. Preprint submitted to Estuarine Coastal and Shelf Science.
- Clark, B., Turpie, J., Gorgens, A., Basson, G., Stretch, D., & Geldenhuys, M. (2014). *Analysis of alternatives for the rehabilitation of the Lake St Lucia estuarine system*. Anchor Environmental Consultants.
- Corbella, S., & Stretch, D. (2012a). *Shoreline recovery from storms on the east coast of Southern Africa*. Natural Hazards and Earth Sciences.
- Corbella, S., & Stretch, D. (2012b). The wave climate on the KwaZulu-Natal coast of South Africa. *Journal of the South African Institution of Civil Engineering*, 54, 45-54.
- Corbella, S., & Stretch, D. (2014). Directional wave spectra on the east coast of South Africa. *Journal of the South African Institution of Civil Engineering*, 53-64.
- Corbella, S., Pringle, J., & Stretch, D. (2015). Assimilation of ocean wave spectra and atmospheric circulation patterns. *Coastal Engineering*, 1-10.
- Davis, R., & FitzGerald, D. (2004). *Beaches and Coasts*. Blackwell Publishing.
- Davis, R., & Hayes, M. (1984). What is a wave dominated coast? *Marine Geology*, 60, 313-329.
- Deltares. (2009). *Delft3D-Wave User Manual*. Delft: Deltares.
- Duong, T. (2015). *Climate change impacts on the stability of small tidal inlets*. Delft: TU Delft.
- Environmental Mapping & Surveying. (2014). *Lidar & Bathymetric Survey of St Lucia Beach Barrier & Adjoining Offshore Area September 2014*. iSimangaliso Wetland Park Authority.
- Escoffier, F. (1940). The stability of tidal inlets. *Shore and Beach*(8), 111-114.
- Google Earth. (2017). 7.1.8.3036.
- Guo, L., Wegen, M. v., Roelvink, D., & Wang, Z. (2015). Long-term, process-based morphodynamic modeling of a fluvio-deltaic system. *Continental Shelf Research*, 95-111.
- Hayes, M. (1979). Barrier island morphology as a function of tidal and wave regime. In S. Leatherman, *Barrier Islands* (pp. 1-27). New York: Academic Press.
- Heerden, I. V., & Swart, D. (1986). *An assessment of past and present geomorpological and sedimentary processes operative in the St Lucia Estuary and environs*. Stellenbosch: CSIR Research Report 569.

- Hinwood, J., McLean, E., & Wilson, B. (2012). Non-linear dynamics and attractors for the entrance state of a tidal estuary. *Coastal Engineering*, 61, 20-26.
- Horrevoets, A., Savenije, H., Schuurman, J., & Graas, S. (2004). The influence of river discharge on tidal damping in alluvial estuaries. *Journal of Hydrology*, 213-228.
- Huizinga, P., & Niekerk, L. v. (2005). *The physical processes driving the St Lucia system*. Durban: Presentation at the South African Marine Science Symposium, 4-7 July 2005.
- iSimangaliso. (2016, April 29). *isimangaliso.com*. Retrieved January 19, 2017, from Update on work to remove dredge spoil from the Lake St Lucia Estuary mouth:
<http://isimangaliso.com/newsflash/update-work-remove-dredge-spoil-lake-st-lucia-estuary-mouth/>
- iSimangaliso. (2016, July 19). *traveller24.news24.com*. Retrieved January 20, 2017, from iSimangaliso Then and Now pic shows dramatic conservation efforts:
<http://traveller24.news24.com/Explore/Green/isimangaliso-then-and-now-pic-shows-dramatic-conservation-efforts-20160719>
- iSimangaliso. (2017, January 10). *isimangaliso.com*. Retrieved January 19, 2017, from iSimangaliso: The restoration of Africa's largest estuarine lake receives a boost:
<http://isimangaliso.com/newsflash/isimangaliso-the-restoration-of-africas-largest-estuarine-lake-receives-a-boost/>
- Jarrett, J. (1976). *Tidal Prism - Inlet Area Relationships*. Fort Belvoir, VA, USA: U.S. Army Engineer Waterways Experiment Station.
- Kamphuis, J. (1991). Alongshore sediment transport rate. *Journal of Waterway, Port, Coastal and Ocean Engineering*, 117, 624-640.
- Kriel, J. (1966). *Report of the commission of inquiry into the alleged threat to plant and animal life in St Lucia Lake*. Pretoria: Government Printer.
- Lawrie, R., & Stretch, D. (2011a). Occurrence and persistence of water level/salinity states and the ecological impacts for St Lucia estuarine lake, South Africa. *Estuarine, Coastal and Shelf Science*, 67-76.
- Lawrie, R., & Stretch, D. (2011b). Anthropogenic impacts on the water and salt budgets of St Lucia estuarine lake: an evaluation using simulations of historical scenarios. *Estuarine Coastal and Shelf Science* 93, 58-67.
- Lawrie, R., Chrystal, C., & Stretch, D. (2011c). On the Role of the Mfolozi in the Functioning of St Lucia: Water Balance and Hydrodynamics. In G. Bate, A. Whitfield, & A. Forbes, *A review of studies on the Mfolozi Estuary and associated flood plain, with emphasis on information required by management for future reconnection of the river to the St Lucia System* (WRC Report No. KV 255/10 ed., pp. 99-109). Gezina, South Africa.
- Lesser, G., Roelvink, J., Meganck, R., Vriend, H. d., Stelling, G., Stive, M., . . . Gelfenbaum, G. (2009). *An Approach to Medium-term Coastal Morphological Modelling*. PhD Thesis, Delft.
- Moerland, V. (2013). *A parametric study concerning estuary mouth dynamics and inlet closure*. Delft: TU Delft.

- Niekerk, L. v., & Huizinga, P. (2011). Key role of the Mfolozi River in the greater St Lucia water requirements and preliminary health assessment for the system. In G. Bate, A. Whitfield, & A. Forbes, *A review of studies on the Mfolozi flood plain, with emphasis on information required by management for future reconnection of the river to the St Lucia* (pp. 118-137). Pretoria, South Africa: Water Research Commission Report KV 255/10.
- O'Brien, M. (1931). Estuary and tidal prisms related to entrance areas. *Civil Engineering*, 1, 738-739.
- O'Brien, M. (1969). Equilibrium flow areas of inlets on sandy coasts. *Waterways and harbors division*, 95, 43-52.
- Olij, D. (2015). *Wave climate reduction for medium term process based morphodynamic simulations*. Delft: TU Delft.
- Perissinotto, R., Stretch, D., & Taylor, R. (2013). *Ecology and Conservation of Estuarine Ecosystem*. Barcelona: Cambridge University Press.
- Ranasinghe, R., & Pattiaratchi, C. (1998). Flushing Characteristics of a Seasonally-Open Tidal Inlet: A Numerical Study. *Journal of Coastal Research*, 1405-1421.
- Ranasinghe, R., Pattiaratchi, C., & Masselink, G. (1999). A morphodynamic model to simulate the seasonal closure of tidal inlets. *Coastal Engineering*, 37(1), 1-36.
- Reddering, J. (1983). An inlet sequence produced by migration of a small microtidal inlet against longshore drift: the Keurbooms Inlet, South Africa. *Sedimentology*, 30, 201-218.
- Rijn, L. v. (1997). Sediment transport and budget of the central coastal zone of Holland. *Coastal Engineering*, 32, 61-90.
- Rijn, L. v. (2002). *Longshore Sand Transport*. LVRS-Consultancy. Retrieved from <http://www.leovanrijn-sediment.com/papers/P3-2002a.pdf>
- Rijn, L. v. (2013). *A Simple General Expression for Longshore Transport of Sand, Gravel and Shingle*. LVRS-Consultancy.
- SANHO. (2017). *Ocean Rhythm*. Retrieved from South African Tide Tables: <http://www.satides.co.za/>
- Schoonees, J. (2000). Annual variation in the net longshore sediment transport rate. *Coastal Engineering*, 141-160.
- Schumann, E. (2013). Sea level variability in South African estuaries. *South African Journal of Science*, 109, 7. Retrieved from <http://sajs.co.za/sea-level-variability-south-african-estuaries/eckart-h-schumann>
- Sobrevila, C. (2017). *South Africa - Development, Empowerment and Conservation in the Greater St Lucia Wetland Park and Surrounding Region*. Washington, D.C.: World Bank Group. Retrieved from <http://documents.worldbank.org/curated/en/818111486589103482/South-Africa-Development-Empowerment-and-Conservation-in-the-Greater-St-Lucia-Wetland-Park-and-Surrounding-Region-P086528-Implementation-Status-Results-Report-Sequence-12>
- Stability of Tidal Inlets: Theory and Engineering (Developments in geotechnical engineering)*. (1978). Amsterdam: Elsevier Scientific Publishing Company.

- Stretch, D., & Zietsman, I. (2015). The Hydrodynamics of Mhlanga & Mdloti Estuaries: flows, residence times, water levels & mouth dynamics.
- Taylor, R. (1993). *Proceedings of the workshop on water requirements for Lake St. Lucia, organised by the St. Lucia Ecological and Technical Committee (SCADCO)*. Pretoria: Department of Environmental Affairs.
- Times Live. (2016, June 07). *Times Live*. Retrieved from <http://www.timeslive.co.za/scitech/2016/06/07/This-is-how-the-drought-has-drained-Lake-St-Lucia-Pictures>
- Turpie, J., Adams, J., Joubert, A., Harrison, T., Colloty, B., Maree, R., . . . Niekerk, L. v. (2002, April 2). Assessment of the conservation priority status of South African estuaries for use in management and water allocation. *Water SA*, 28.
- Walstra, D., Ruessink, G., Hoekstra, R., & Tonnon, P. (2013). Input reduction for long-term morphodynamic simulations. *Coastal Engineering*, 77, 57-70.
- Whitfield, A., & Taylor, R. (2009). A review of the importance of freshwater inflow to the future conservation of Lake St Lucia. *Aquatic Conservation Marine and Freshwater Ecosystems*, 838-848.
- Wright, C., & Mason, T. (1990). Sedimentary environment and facies of St Lucia Estuary Mouth, Zululand, South Africa. *Journal of African Earth Sciences*, 11, 411-420.

Appendices

Contents

A. Theoretical background	2
A.1. Delta classification	2
A.2. Tidal delta morphology	3
A.3. Bruun criteria for inlet stability	5
B. Wave climate reduction	6
B.1. Reduced wave climate	6
B.2. Sensitivity analysis morphological acceleration factor	8
C. Calibration	10
C.1. Tide only	10
C.2. Time-varying wave climate	12
D. Results	14
D.1. Overview results scenario A and B	14
E. Photos site visit St Lucia Estuary	15
E.1. Site visit 15 th of March 2017	15
E.2. Site visit 18 th of May 2017	16
F. List of symbols	17

A. Theoretical background

A.1. Delta classification

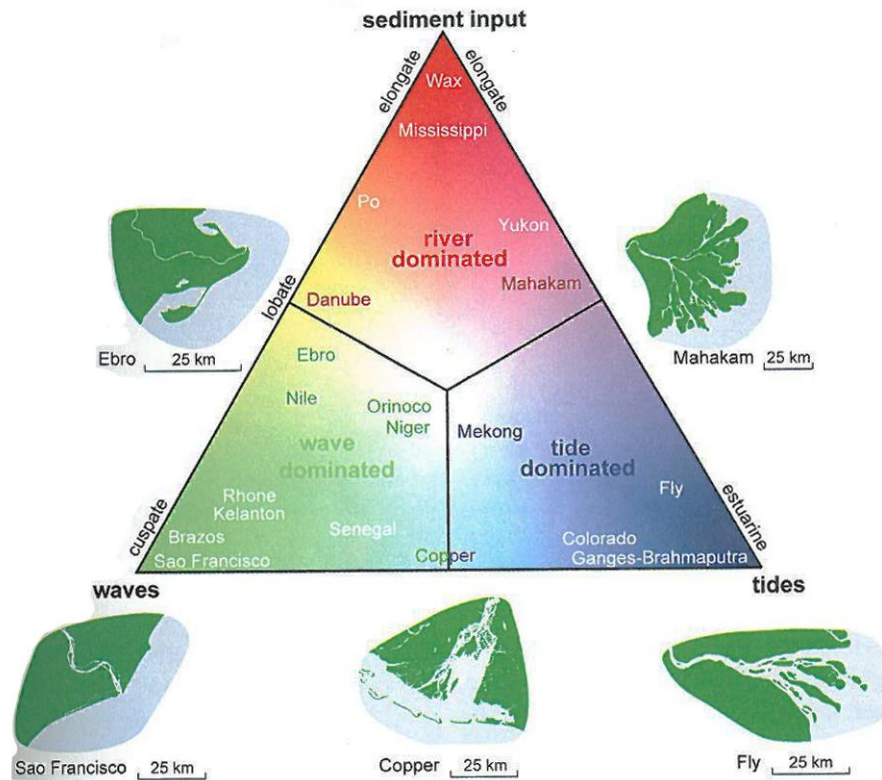


Figure A.1: Classification of deltas. Colours represent the relative influence of waves (green), tides (blue) and fluvial sediment input (red) (Bosboom & Stive, 2015)

Deltas can be classified in three groups depending on local climate. The formation of a delta depends on the interaction between river flow and sediment supply on one side and the distribution of river sediment by waves and tidal currents on the other side. The influence of these three major factors determines the development on the morphological structure. In general deltas can be distinguished between river-dominated, tide-dominated and wave dominated.

A.2. Tidal delta morphology

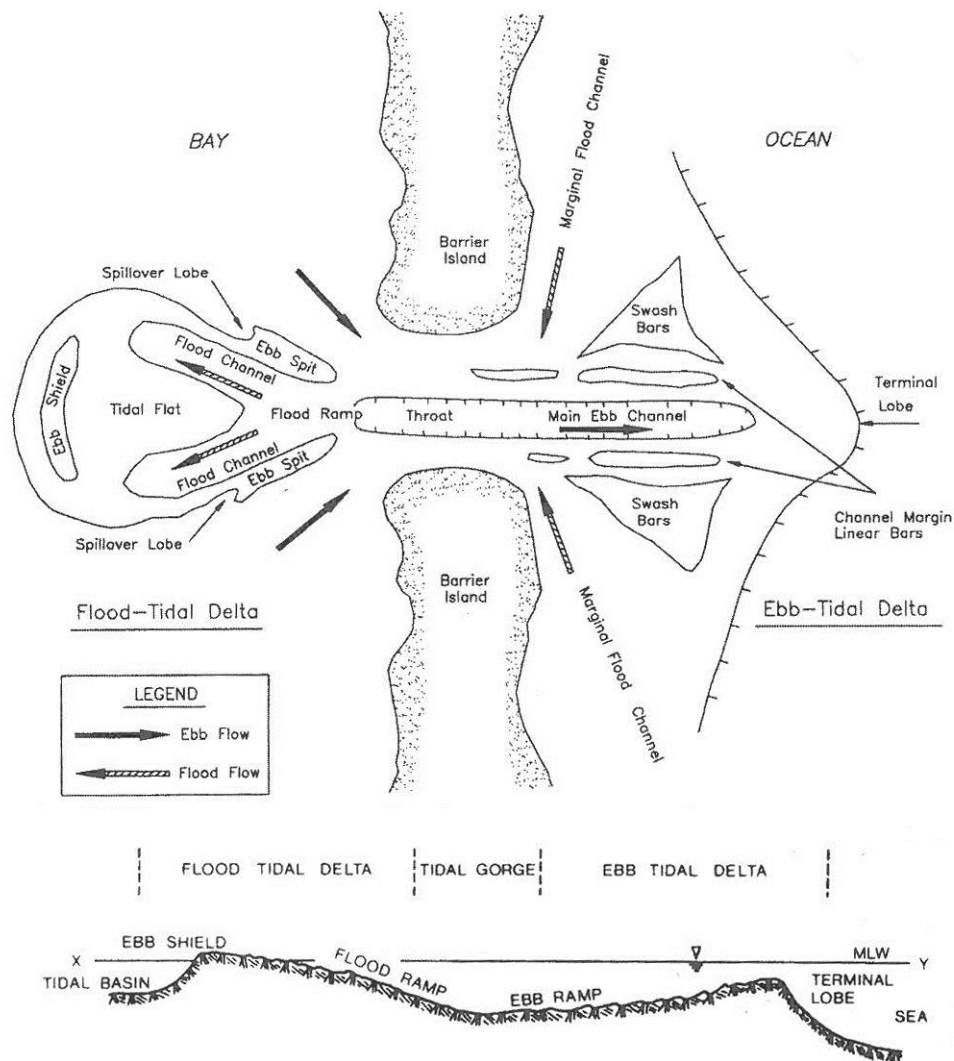


Figure A.2: Morphological elements of a tidal inlet (Bosboom & Stive, 2015)

The tidal delta consists of three main morphological elements: ebb tidal delta, tidal gorge and the flood tidal delta. Boothroyd et al. (1985) discerned the ebb tidal delta and flood tidal delta in several elements.

The ebb tidal delta includes:

- **Marginal flood channels.** During flood tide the currents are entering the inlet through these channels. Marginal in the context of marginal flood channels is used to indicate the position of the channels.
- **Main ebb channel.** The ebb currents are exiting the inlet through this channel.
- **Channel margin linear bars.** These bars flank the ebb tidal channel and are built up from deposits as a result of the interaction of flood- and ebb-tidal currents with wave-generated currents.

- **Terminal lobe.** A rather steep seaward-sloping body of sand that forms at the outer end of the ebb-tidal delta.
- **Swash platforms and bars.** The main ebb channel is flanked by swash platforms, which are broad sheets of sand. These are built up by swash action of waves.

The flood tidal delta includes:

- **Flood ramp.** A sand body sloping upward ending at the ebb shield. The ebb shield is the most elevated outer edge of the flood-tidal delta.
- **Flood channels.** During flood periods the currents flow over the flood ramp and continue in the flood channels.
- **Ebb shield.** The ebb shield is the flood-tidal deltas equivalent of the terminal lobe from the ebb-tidal delta. It helps to divert ebb-currents along the margins of the flood-tidal delta.
- **Ebb spits.** Ebb currents transport sediments from the ebb shields creating ebb spits.
- **Spillover lobes.** Ebb spits can be breach by ebb currents which creates spillover lobes.

A.3. Bruun criteria for inlet stability

Table A.1: Bruun criteria for inlet stability

$r = P / M_{tot}$	Inlet stability condition
> 150	<i>Good</i> – These inlets are mainly tide-dominated and reasonably stable. There is good flushing and little or no ocean bar forming.
100 – 150	<i>Fair</i> – Inlets have a mix of bar-by-passing and flow-by-passing. Entrance has low ocean bars. There is a mixed energy climate of tide and waves.
50 – 100	<i>Fair to poor</i> – Inlet is mainly bar-by-passing and unstable. The entrance is wider with higher ocean bars.
20 – 50	<i>Poor</i> – Inlet becomes unstable with non-overflow channels. The inlet is mainly wave-dominated, which results in a wide entrance and shallow ocean bars. Navigation will be difficult and probably requires dredging or jetties in order to keep navigable depths.
< 20	<i>Unstable</i> – The entrance becomes unstable. There is no permanent inlet, but rather overflow channels. The inlet might close by deposition of sediment in the channel during a storm event. The small ebb current velocities will not be high enough to maintain an open inlet during storm events.

B. Wave climate reduction

B.1 Reduced wave climate

The reduced wave climate is used to reduce computation time of the simulation but to approach the real wave climate. In Figure B.1 the reduced wave climate is given for the St Lucia Estuary. The first figure shows the wave angle with respect to true North and the second figure, Figure B.2, shows the wave angle with respect to the coastline. Wave from 150 and 160 degrees with respect to true north generate the largest fraction of the total sediment transport along the coast. Incoming waves from 90 degrees with respect to the coastline do not generate any longshore transport, but only cross-shore transport. The wave data is derived from measurements at Richards Bay. It is assumed similar waves occur in the region of St Lucia.

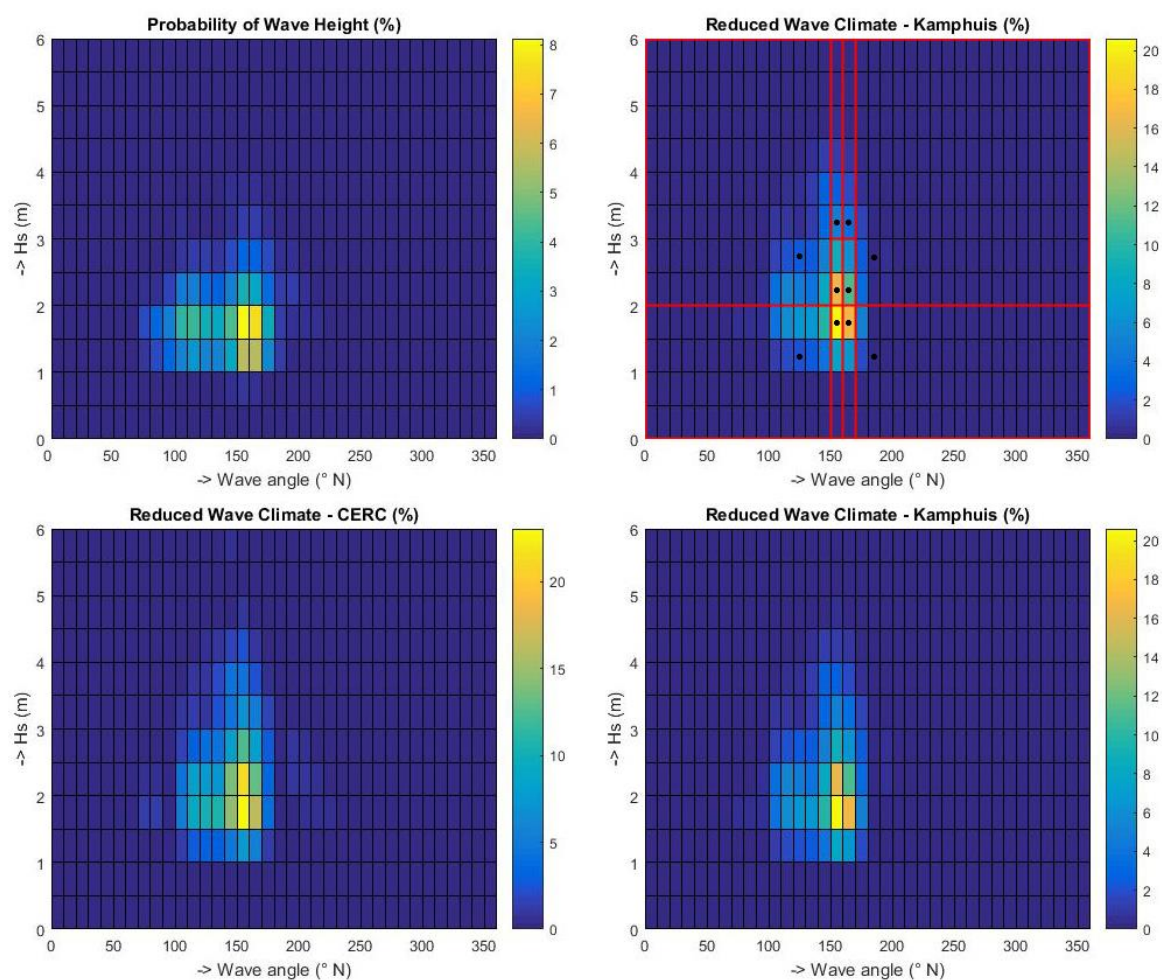


Figure B.1: Probability of wave height (upper left), reduced wave climate (upper right) and sediment transport contribution (bottom)

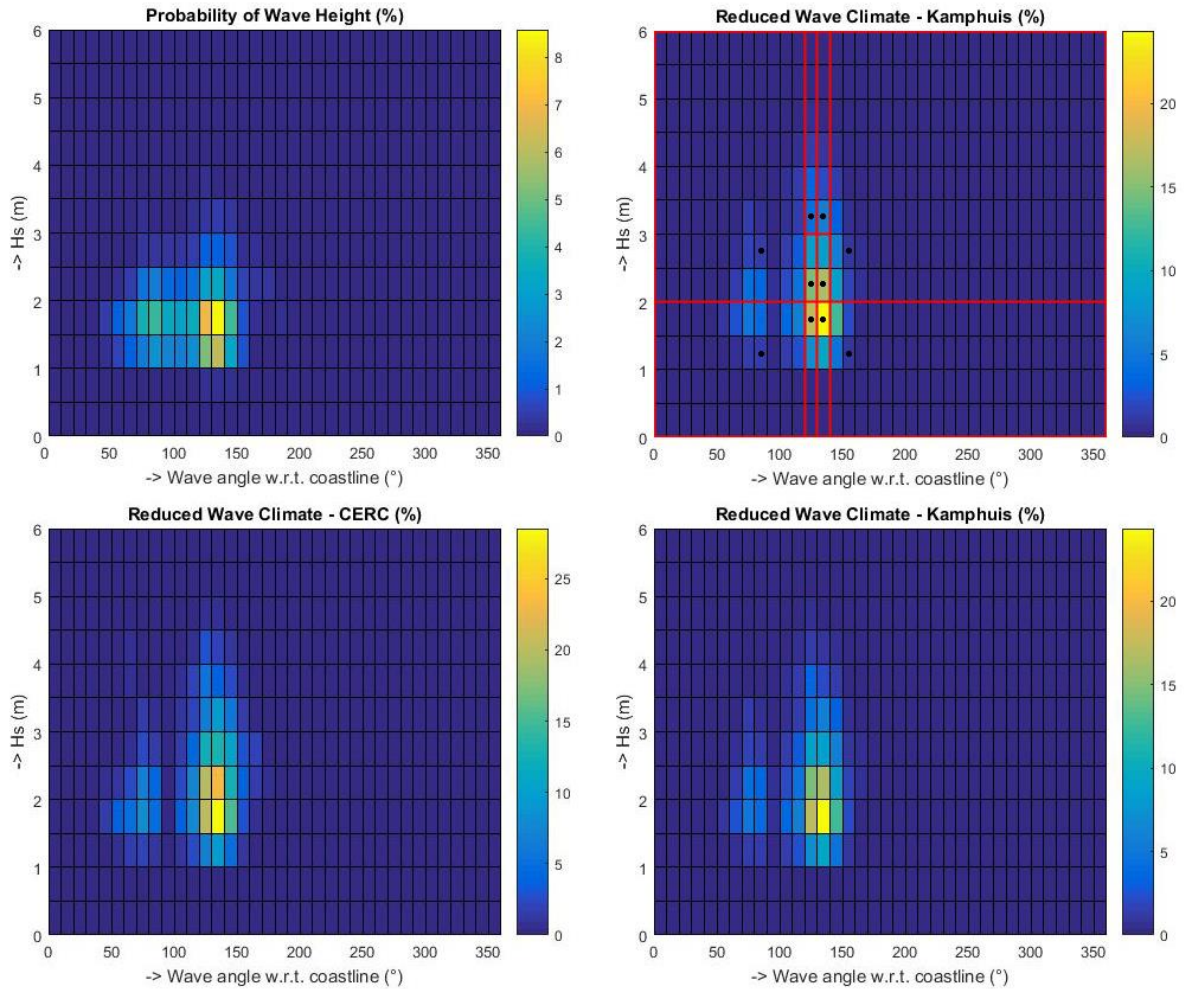


Figure B.2: Reduced wave climate w.r.t coastline

The model is forced with 10 wave conditions shown in Table B.1. The total simulation time equals 36.4 days plus 5 days of spin-up time. The morphological acceleration factor (morfac) is used to simulate different time-scales between hydrodynamic and morphological developments. The factor simply multiplies sediment fluxes to and from the bed by a constant factor, thereby extending the morphological time step as described by Lesser et al. (2009). The morfac is kept constant at a value of 10 while the wave conditions are varied. The reduced wave climate is given in Table 3.1. The morphological duration equals 364 days. In Table B.2 the percentage of occurrence per wave conditions from the reduced wave climate and from the wave climate at Richards Bay is given. The reduced wave climate has similar probabilities of occurrence as the original wave data from Richards Bay.

Table B.1: Reduced wave climate

Season	Wave condition	Hs (m)	Tp (s)	Dir [°]	Duration Simulation [days]	Morfac [-]	Duration Reality [days]	Probability of occurrence [%]
Summer (Nov – Mar)	1	1.5	11	160	5	10	50	13.7
	2	1.0	11	120	10	10	100	27.5
	3	2.5	11	120	0.8	10	8	2.2
Autumn (Apr – May)	4	1.5	11	150	5	10	50	13.7
	5	2.0	11	150	2	10	20	5.5
	6	3.0	11	150	0.4	10	4	1.1
Winter (Jun – Aug)	7	3.0	11	160	0.4	10	4	1.1
	8	2.0	11	160	2	10	20	5.5
	9	2.5	11	180	0.8	10	8	2.2
Spring (Sep – Oct)								
Summer	10	1.0	11	180	10	10	100	27.5

Table B.2: Probability of occurrence

Hs (m)	Reduced Wave Climate	Original Wave Climate
0 – 1.5	54.9 %	54.5 %
1.5 – 2.0	27.5 %	29.9 %
2.0 – 2.5	11.0 %	10.3 %
2.5 – 3.0	4.4 %	3.4 %
3.0 >	2.2 %	1.9 %

B.2. Sensitivity analysis morphological acceleration factor

A simulation is made with a larger morfac in order to reduce the computation time and in order to investigate the sensitivity of the model. The morphological acceleration factor is changed from 10 to 20, visible in Table B.3. The simulation time reduces from 41 days to 23 days. A sensitivity analysis done by Olij (2015) showed differences between a morfac of 6.5 to 13 are small, but when increased to 26 large differences are observed. These observations correspond to results of this model; when the morfac is increased from 10 to 20 the morphodynamic behaviour of the coast is largely affected.

The morfac can be varied in time. A lower morfac increases the reliability of the results. However, the computation time increases as well when a lower morfac is used. This gives the possibility to use a lower morfac during high wave conditions and a higher morfac during low wave conditions. The effects have been investigated, but the morfac changes in one step while the wave height increases linearly. This results in an overestimation of the longshore sediment transport. It is chosen to use a single value for the morphological acceleration factor.

Table B.3: Different morphological factors reduced wave climate

Season	Wave condition	Hs (m)	Morfac [-]	New morfac [-]
Summer (Nov – Mar)	1	1.5	10	20
	2	1.0	10	20
	3	2.5	10	20
Autumn (Apr – May)	4	1.5	10	20
	5	2.0	10	20
	6	3.0	10	20
Winter (Jun – Aug)	7	3.0	10	20
	8	2.0	10	20
Spring (Sep – Oct)	9	2.5	10	20
Summer	10	1.0	10	20

The model is simulated with a mean tidal range of 1.3 m and a varying wave climate. The inlet with a morfac of 10 closes after 156 days. When the morfac is increased this reduces considerably and the inlet closes after 70 days. In March 2007 the St Lucia inlet closed naturally after 175 days after being breached by Cyclone Gamede. After closure accretion along the coast is visible until 150 days after which the larger waves start eroding the coast. The change in bed level is visible in Figure B.3. The cumulative longshore transport differs considerably between the simulation with a morfac of 10 and morfac of 20, as it is equal to 482,000 m³/year and 250,000 m³/year respectively. The model will be simulated with a maximum morfac of 10 as this represents reality better.

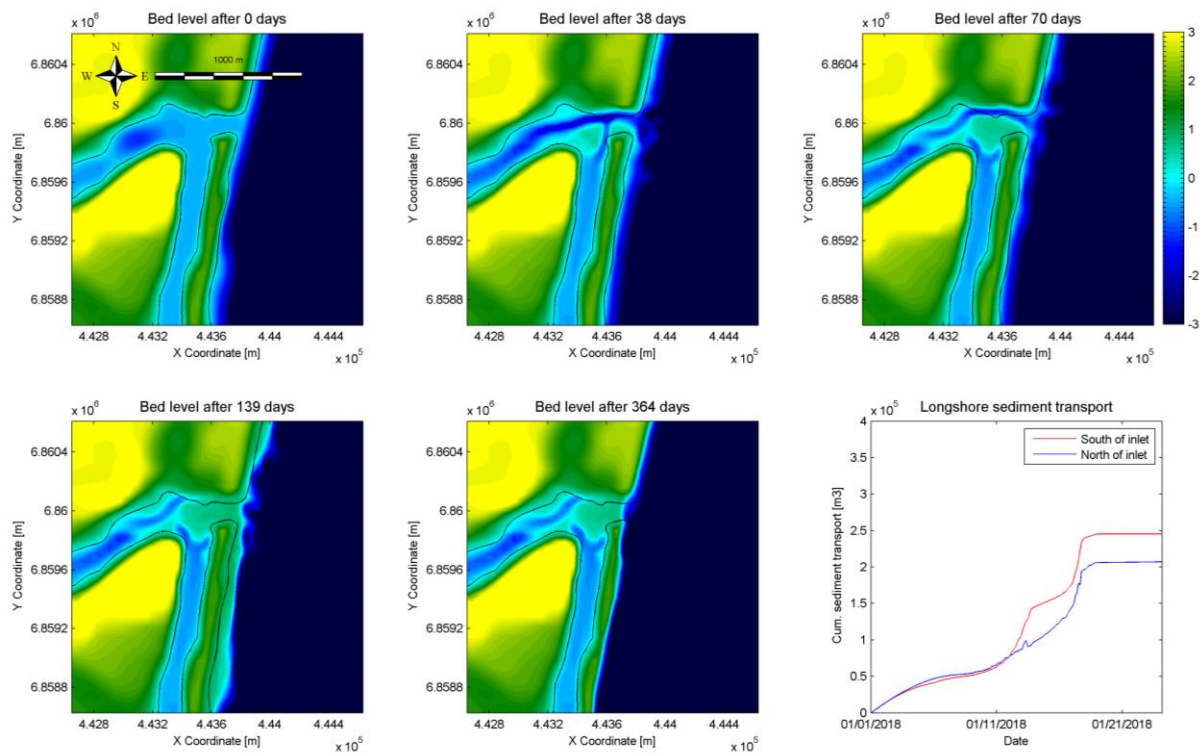


Figure B.3: Bed level change after 0 days, 18 days, 70 days, 72 days, 364 days and cumulative sediment transport along the coast

C. Calibration

The model is calibrated in two stages. At first the model is forced with tide only. This is used to calibrate the peak flows and tidal prism in the inlet. After this the model will be simulated with a time-varying wave climate to calibrate the longshore sediment transport and morphological behaviour. The wave related factor from Delft3D is used to calibrate the morphological behaviour qualitatively.

C.1. Tide only

In Figure C.1 the peak flows corresponding to a mean-, spring- and neap tidal range are given. Chézy values are varied between 40 and 60 $\text{m}^{1/2}/\text{s}$. Slight variation in peak flows are observed in the order of 5 - 10 m^3/s . The bed roughness influences the flow velocities through the inlet. A higher Chézy value results in higher peak flows for both flood- and ebb currents. The peak flows from literature show a lot of variation. The large difference between flood - and ebb flows is due to measurements in dry periods. Water is accumulated in the St Lucia Lakes, which explains the net volume of water that is imported in the system. A Chézy value of 50 $\text{m}^{1/2}/\text{s}$ approaches field measurements most accurately.

Table C.1: Peak flood flows

Chézy value	Neap tidal range [m^3/s]	Mean tidal range [m^3/s]	Spring tidal range [m^3/s]
40	37	113	172
50	41	122	186
60	44	131	200
Literature	50	60 – 100	130 – 190

Table C.2: Peak ebb flows

Chézy value	Neap tidal range [m^3/s]	Mean tidal range [m^3/s]	Spring tidal range [m^3/s]
40	30	90	134
50	34	96	141
60	36	100	147
Literature	25	25 – 30	70 – 150

The model reproduces the flood dominant behaviour of the St Lucia Estuary, which can be observed from the shorter rising water levels (flood period) and longer falling water levels (ebb period). In literature ratios of estuary tidal range over sea tidal range are found in the order of 0.22 to 0.52. Simulations with a Chézy value of 50 $\text{m}^{1/2}/\text{s}$ result in a ratio of 0.72 during mean tidal range.

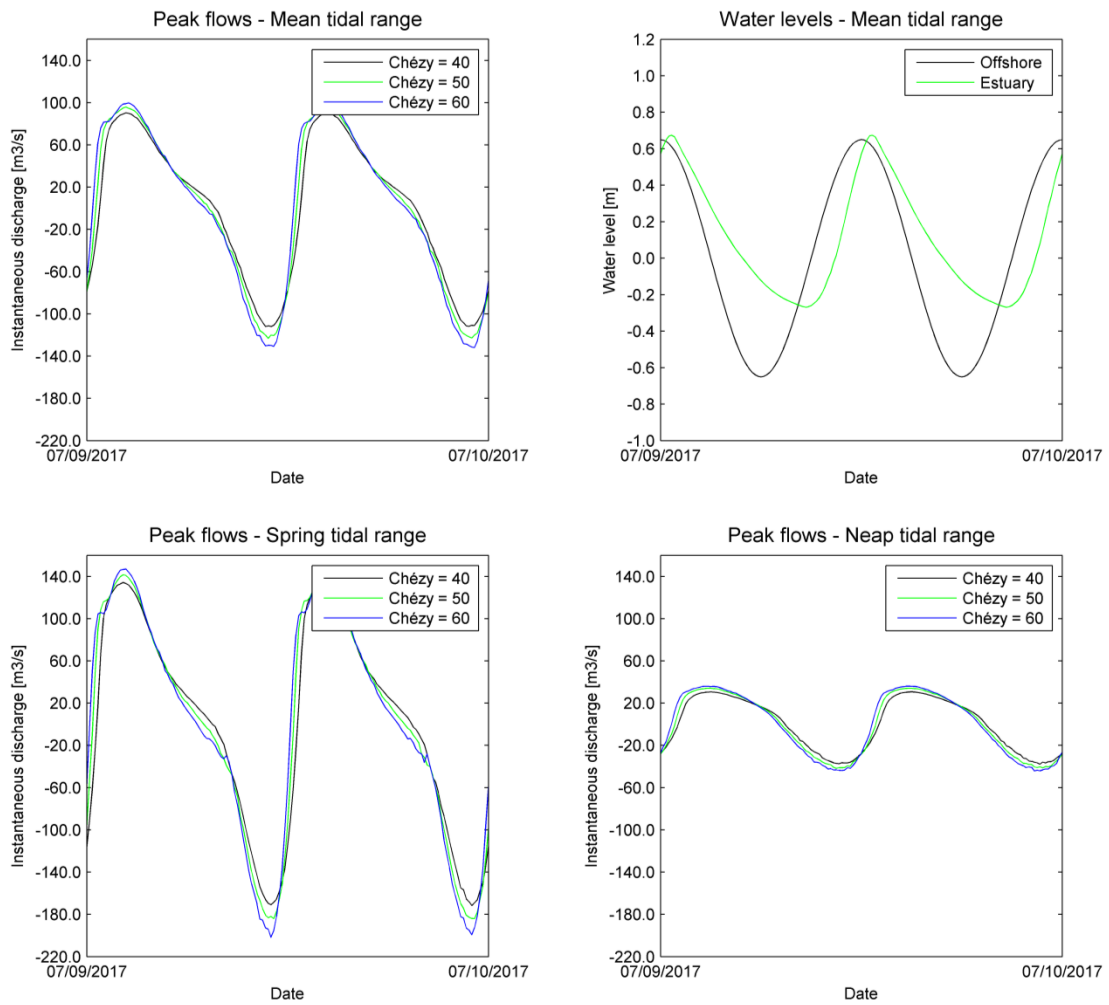


Figure C.1: Calibration tide

C.2. Time-varying wave climate

The model is forced with a time-varying wave climate and a mean tidal range of 1.3 m. The time-varying wave climate is described in chapter 3.3. The wave climate starts with smaller wave heights for the duration of 150 days after larger waves start occurring. The inlet closes after 156 days. The larger waves erode the coast; however, no breaching of the barrier occurs. The cumulative longshore transport in this simulation is 482,000 m³/year.

In this simulation the wave climate is changed to test the sensitivity of the model. The model is forced with larger waves in the beginning of the simulation after smaller waves will restore the beach. The wave climate is given in Table C.3.

Table C.3: Changed reduced wave climate

Wave condition	Hs (m)	Tp (s)	Dir [°]	Duration Simulation [days]	Morfac [-]	Duration Reality [days]	Probability of occurrence [%]
1	1.5	11	160	5	10	50	13.7
2	2.0	11	150	2	10	20	5.5
3	3.0	11	150	0.4	10	4	1.1
4	3.0	11	160	0.4	10	4	1.1
5	2.0	11	160	2	10	20	5.5
6	2.5	11	180	0.8	10	8	2.2
7	1.0	11	180	10	10	100	27.5
8	1.0	11	120	10	10	100	27.5
9	2.5	11	120	0.8	10	8	2.2
10	1.5	11	150	5	10	50	13.7

The morphological evolution of the inlet is given in Figure C.2. The inlet response is different due to the changed wave climate. In the first few days, after 58 days, the development of the flood tidal delta is visible. The inlet is locationally stable in the first 100 days. From here on the period of high wave action starts with significant wave heights up to 3.0 m. This is causing severe erosion and the inlet widens from 50 m to 220 m. After this period the coast recovers for 200 days during smaller wave heights of 1.0 m. The estuary imports sediments and accretion in the estuary is visible. In the last few days of the simulation the inlet widens slightly again, maintaining an open inlet for the whole simulation. The cumulative sediment transport equals 585,000 m³/year, which is higher than the original wave climate that equals 482,000 m³/year. The high wave action in the beginning of the simulation is the main reason for the inlet to be open for the complete year.

The wave related factor from Delft3D is set to 0.31 to maintain an equilibrium beach width. This results in a stable beach over the whole simulation and no unrealistic accretion or erosion. The wave related factor is changed to 0.25 and 0.40 to show the effect of this parameter. This is visible in Figure C.3. The simulation with a wave related factor equal to 0.25 shows less accretion and significant erosion during higher wave action. The inlet closes for a small period but remains open for majority of the simulation. An increase of the wave related factor to 0.40 shows more accretion and widening of the beach. The wave related factor results in erosion or accretion from a specific wave height. The closure of the inlet occurs after 120 days when f_{wave} equals 0.40 and does not close when f_{wave} equals 0.25.

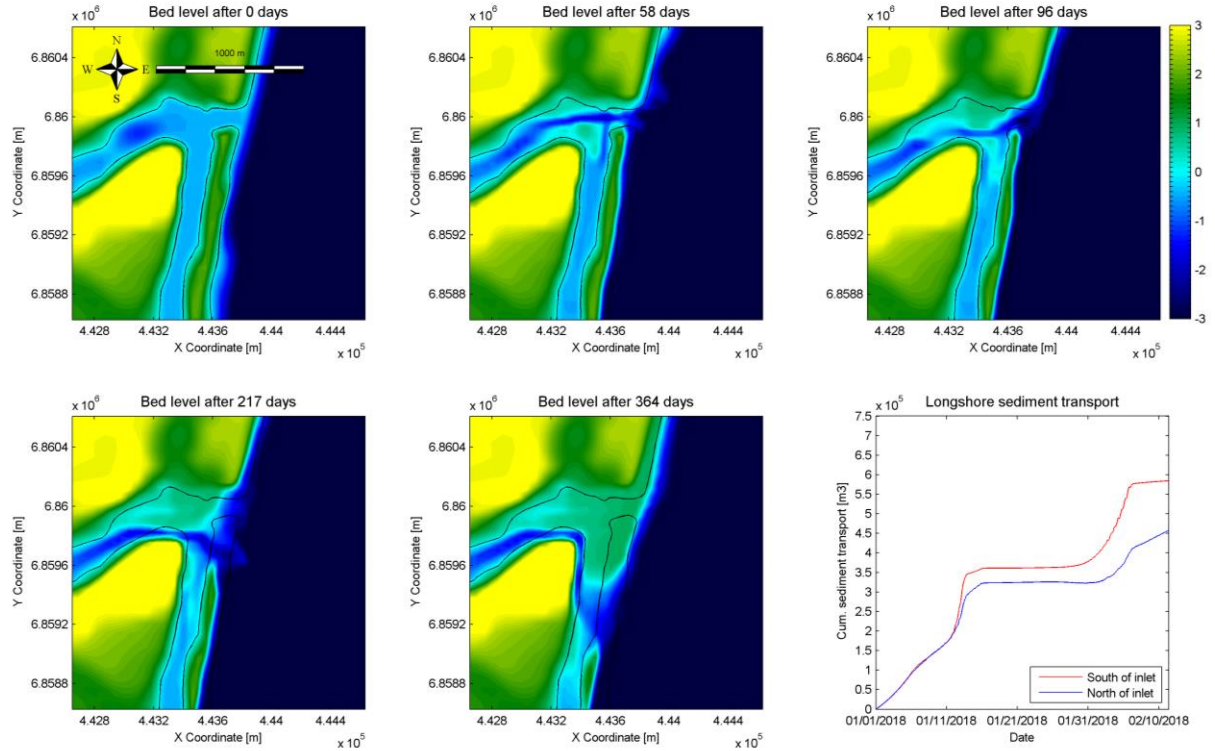


Figure C.2: Bed level change after 0 days, 58 days, 96 days, 217 days, 364 days and cumulative sediment transport along the coast for mean tidal range of 1.3 m

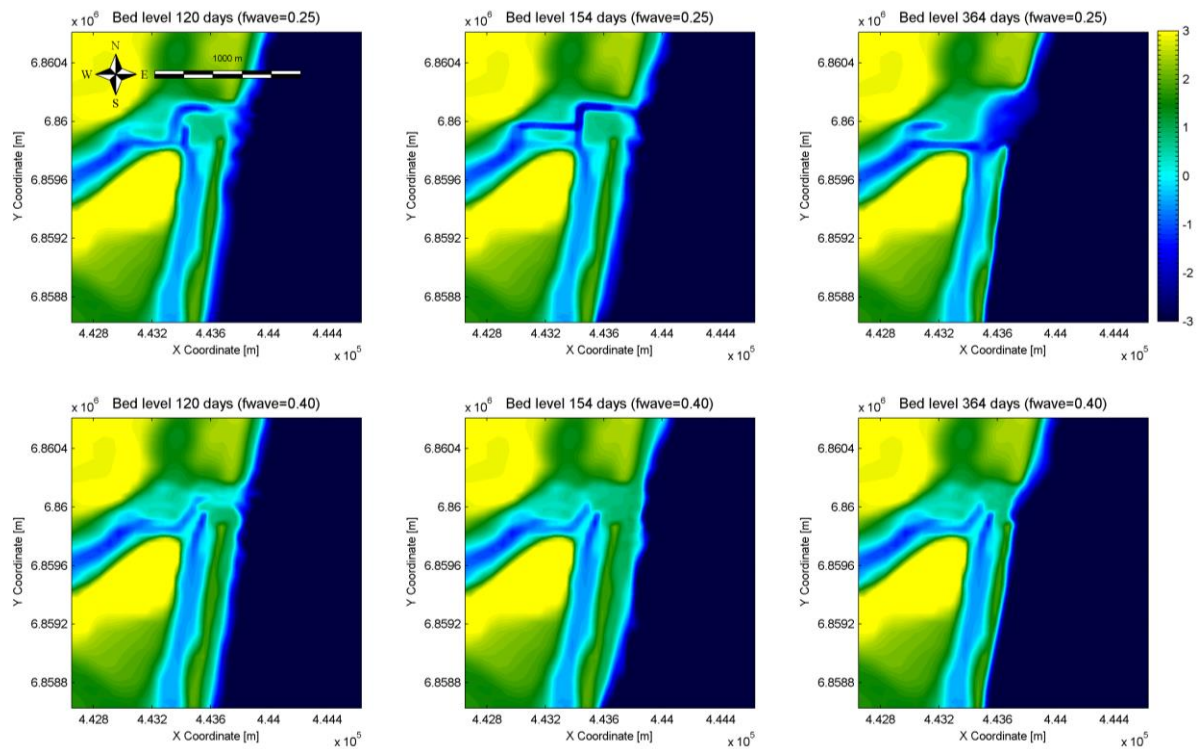


Figure C.3: Comparison bed level change for wave related factor 0.25 and 0.40 for mean tidal range of 1.3 m

D. Results

D.1 Overview results scenario A and B

In Figure D.1 an overview of the results from scenario A and B is given. The different scenarios are shown with neap –, mean –, spring tidal range and varying river flow. The tidal prism, cumulative longshore sediment transport, P/M ratio and inlet type is given for each scenario. The closure time is given for the duration of the simulation or the frequency when the inlet closes more than once. In the column next to this the increase in tidal prism is given. In scenario A this increase is with respect to the initial situation, whereas in scenario B the tidal prism is compared to the same simulation in Scenario A. Finally the total closure time is given in days and percentage of the simulation time. At the left column beneath the discharge the averaged closure times of each scenario is given; the closure time from the simulation with neap –, mean – and spring tidal range are combined.

Scenario A	Tide	Tidal Prism (P)	Cum. longshore transport (M)	P/M ratio	Inlet type	closure time	Incr P%	total days closed	
Q=0	Neap: 0.5 m	5,80E+05	472.000,0	1,23	3	22-364		342,0	94,0%
50,4%	Mean: 1.3 m	1,30E+06	482.000,0	2,70	3	156-364		208,0	57,1%
	Spring: 1.8 m	1,75E+06	515.000,0	3,40	3	0		0,0	0,0%
Q=2	Neap: 0.5 m	6,20E+05	466.000,0	1,33	3	4 times	7%	105,9	29,1%
11,6%	Mean: 1.3 m	1,45E+06	473.000,0	3,07	3	155-176	12%	21,0	5,8%
	Spring: 1.8 m	2,01E+06	542.000,0	3,71	3	0	15%	0,0	0,0%
Q=5	Neap: 0.5 m	7,20E+05	468.000,0	1,54	3	9 times	24%	46,8	12,9%
6,1%	Mean: 1.3 m	1,52E+06	467.000,0	3,25	3	2 times	17%	5,0	1,4%
	Spring: 1.8 m	1,93E+06	558.000,0	3,46	3	151-166	10%	15,0	4,1%
Q=14	Neap: 0.5 m	9,75E+05	448.000,0	2,18	3	11 times	68%	31,3	8,6%
3,0%	Mean: 1.3 m	1,76E+06	470.000,0	3,74	3	151-152	35%	1,3	0,4%
	Spring: 1.8 m	2,18E+06	524.000,0	4,16	3	0	25%	0,0	0,0%
Q=30	Neap: 0.5 m	1,40E+06	465.000,0	3,01	3	6 times	141%	11,3	3,1%
1,0%	Mean: 1.3 m	2,24E+06	478.000,0	4,69	3	0	72%	0,0	0,0%
	Spring: 1.8 m	2,70E+06	516.000,0	5,23	2/3	0	54%	0,0	0,0%
Scenario B	Tide	Tidal Prism (P)	Cum. longshore transport (M)	P/M ratio	Inlet type	closure time	Incr P%	total days closed	
Q=0	Neap: 0.5 m	7,60E+05	470.000,0	1,62	3	40-364	31%	324,0	89,0%
29,7%	Mean: 1.3 m	1,73E+06	465.000,0	3,72	3	0	33%	0,0	0,0%
	Spring: 1.8 m	2,24E+06	520.000,0	4,31	3	0	28%	0,0	0,0%
Q=2	Neap: 0.5 m	7,36E+05	462.000,0	1,59	3	4 times	19%	123,3	33,9%
11,3%	Mean: 1.3 m	1,72E+06	468.000,0	3,68	3	0	19%	0,0	0,0%
	Spring: 1.8 m	2,39E+06	539.000,0	4,43	3	0	19%	0,0	0,0%
Q=5	Neap: 0.5 m	8,80E+05	468.000,0	1,88	3	9 times	22%	59,6	16,4%
6,4%	Mean: 1.3 m	1,99E+06	463.000,0	4,30	3	155-166	31%	10,8	3,0%
	Spring: 1.8 m	2,40E+06	518.000,0	4,63	3	0	24%	0,0	0,0%
Q=14	Neap: 0.5 m	1,10E+06	467.000,0	2,36	3	9 times	13%	19,2	5,3%
1,8%	Mean: 1.3 m	2,15E+06	463.000,0	4,64	3	0	22%	0,0	0,0%
	Spring: 1.8 m	2,72E+06	502.000,0	5,42	2/3	0	25%	0,0	0,0%
Q=30	Neap: 0.5 m	1,55E+06	468.000,0	3,31	3	11 times	11%	14,2	3,9%
1,3%	Mean: 1.3 m	2,65E+06	459.000,0	5,77	2/3	0	18%	0,0	0,0%
	Spring: 1.8 m	3,15E+06	514.000,0	6,13	2/3	0	17%	0,0	0,0%

Figure D.1: Overview results scenario A and B

E. Photos site visit St Lucia Estuary

E.1. Site visit 15th of March 2017

During the site visit on the 15th of March 2017 Mike Udal from MBB Consulting Engineers showed the area where the dredge spoil is removed. A total 1.3 million m³ of dredge spoil will be removed and moved to the surf zone.

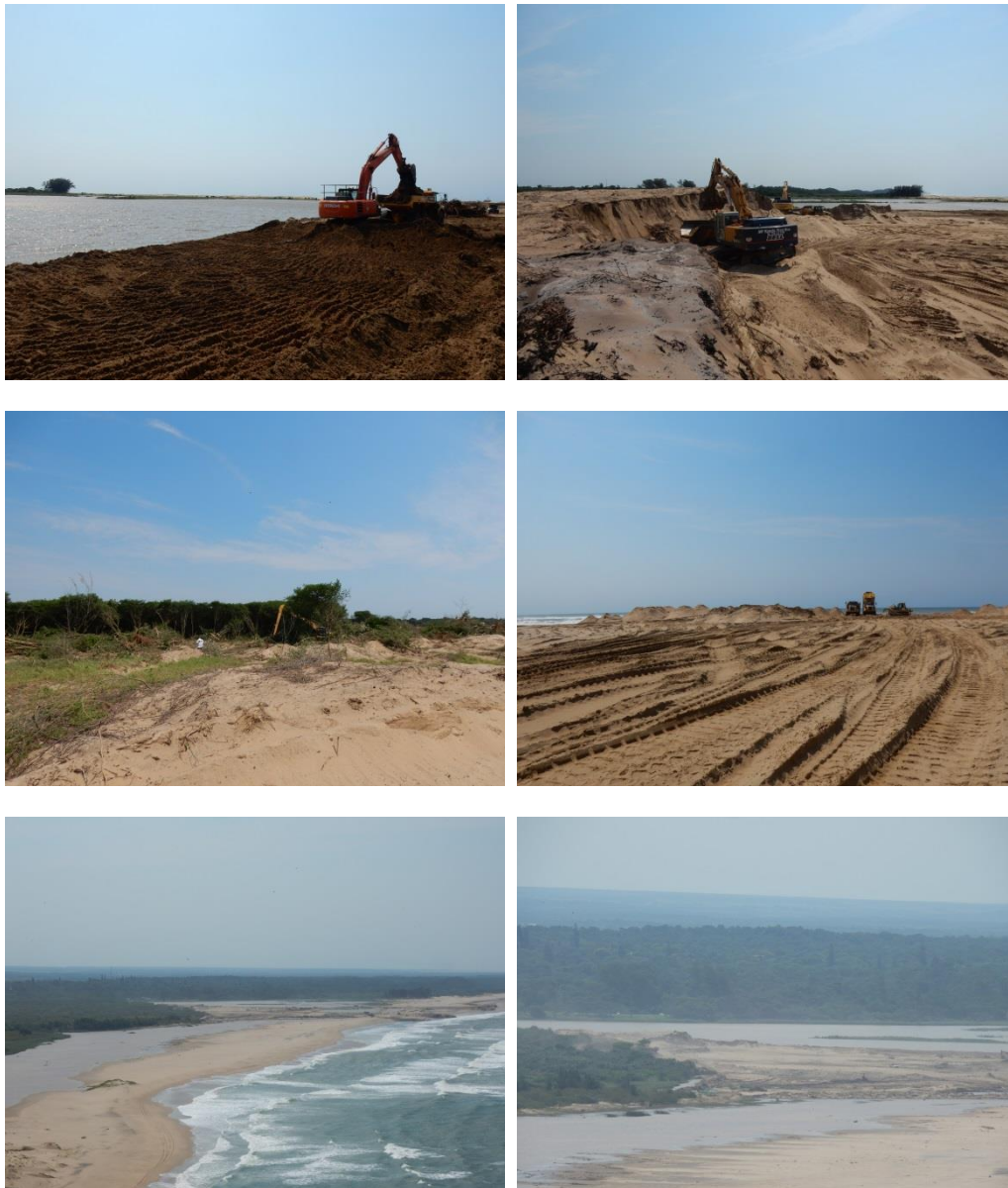


Figure E.1: Photos made during field visit 15/03/2017; from left to right: dredge spoil removal from 12m+MSL to MSL (a), land removal equipment (b), removal of vegetation (c), piles of dredge spoil at surf zone (d), overview of Mfolozi River and St Lucia Estuary (e), area of dredge spoil removal (f).

E.2. Site visit 18th of May 2017

During the site visit on the 18th of May the removal of dredge spoil was almost finished. A barrier between the Mfolozi River and the St Lucia Estuary was still present. Due to this water from the Mfolozi River entered the St Lucia Estuary through the back channel. The water levels were a lot higher compared to last visit mainly because of the severe rainfall. During the weekend of the 13th and 14th of May approximately 300 mm of rain has fallen in the area of KwaZulu-Natal.

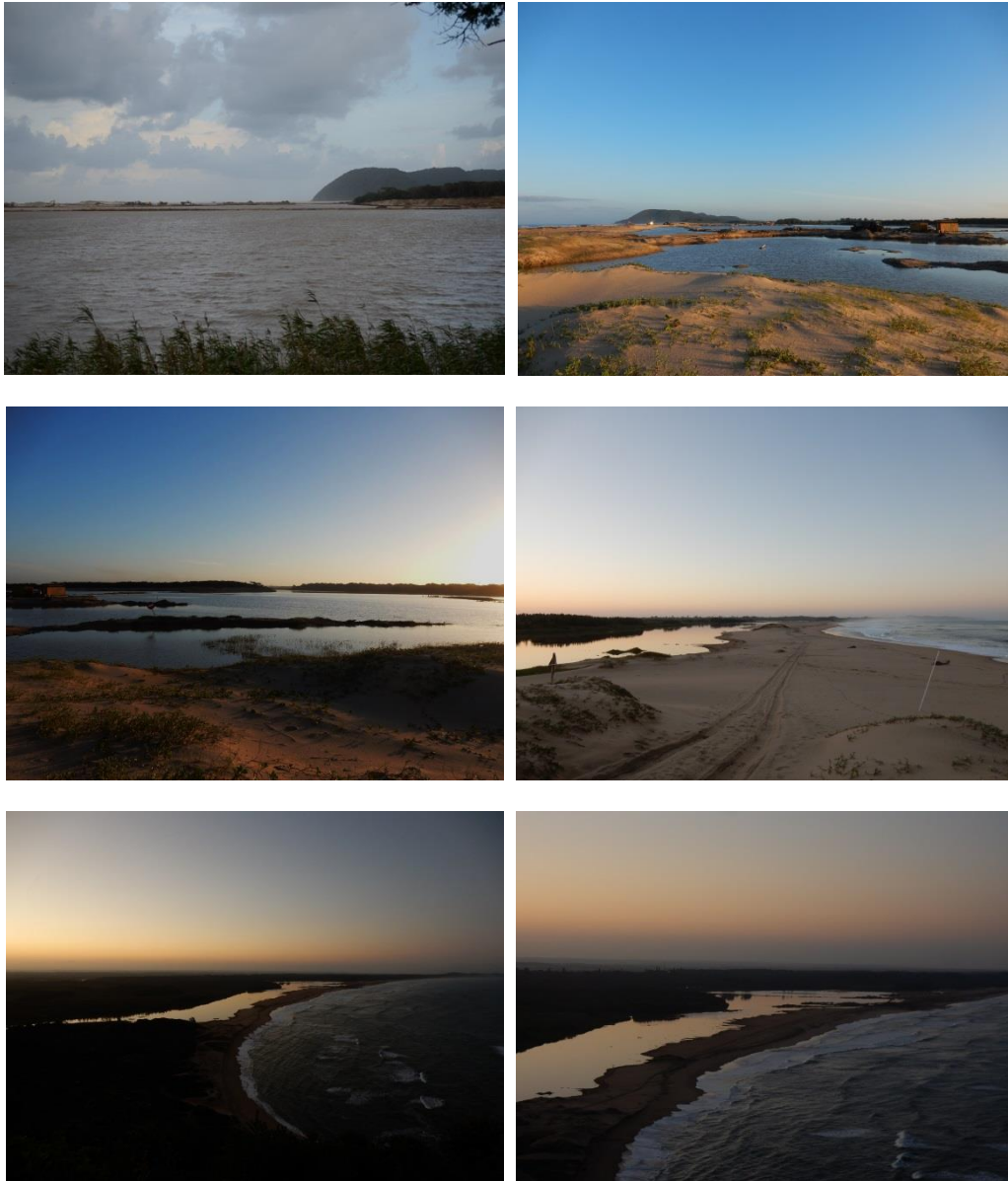


Figure E.2: Photos made during field visit 18/05/2017; from left to right: view from St Lucia Jetty (a), dredge spoil removal (b), view on St Lucia Estuary which used to be land up to +12 m elevation (c), Mfolozi River and Indian Ocean (d), overview of Mfolozi River and St Lucia Estuary (e), area of dredge spoil removal (f).

F. List of symbols

A_{eq}	minimum cross-sectional area of entrance channel measured below mean sea level [m^2]
C	Chézy value [$m^{1/2}/s$]
C	empirical coefficient [-]
E	East
H_s	significant wave height [m]
H	water depth [m]
L_0	wave length [m]
M_{tot}	total annual littoral drift [$m^3/year$]
N	North
P	tidal prism [m^3]
Q_r	river discharge [m^3/s]
Q_t	total sediment transport [dry mass in kg/s]
R^2	coefficient of determination [-]
S	sediment transport
S	South
T_p	peak period [s]
T	Tide, M2 constituent
W	West
cm	centimetre
c_0	deep water phase velocity [m/s]
d_{50}	median particle size in surf zone [m]
g	gravitational acceleration [m^2/s]
kg	kilogram
km	kilometre
l	litre
m	metre
mg	milligram
p	porosity factor [-]
q	empirical coefficient [-]
r	Brun ratio [-]
s	second
v	velocity [m/s]
Δx	grid size [m]
Δt	time step [s]
°	degrees
'	minutes

Greek symbols

ε	phase lag
ρ_s	sediment density [kg/m^3]
θ	incoming wave direction [$^\circ$]
γ	breaker index [-]
μm	micrometer
π	pi
$\tan\beta$	beach slope [-]

Abbreviations

CFL	courant number
hat	highest tidal values predictable over an 19 year cycle
hatoy	highest tide values predicted for one specific year (not over the 19 period)
lat	lowest tidal values predictable over an 19 year cycle
latoy	lowest tide values predicted for one specific year (not over the 19 period)
MAR	mean annual runoff
MSL	mean sea level
Morfac	Morphological Acceleration Factor
mhws	mean (or average) high values predicted for spring tides over an 19 year period
mhwn	mean (or average) high values predicted for neap tides over an 19 year period
ml	mean (or average) tidal level predicted over an 19 year cycle
mlwn	mean (or average) low values predicted for neap tides over an 19 year period
mlws	mean (or average) low values predicted for spring tides over an 19 year period
STI	small tidal inlet
TOCE	temporary open/ closed estuary